



DEPARTAMENTO DE QUÍMICA ORGÁNICA

FACULTAD DE QUÍMICA

UNIVERSIDAD DE SEVILLA

**SYNTHESIS OF NEW NAMPT INHIBITORS AS POTENTIAL
ANTI-CANCER DRUGS.**

AN APPROACH TO ANTIBODY-DRUG CONJUGATES

SIMONE FRATTA

SEVILLA 2022



DEPARTAMENTO DE QUÍMICA ORGÁNICA

FACULTAD DE QUÍMICA

UNIVERSIDAD DE SEVILLA

**SYNTHESIS OF NEW NAMPT INHIBITORS AS POTENTIAL
ANTI-CANCER DRUGS.
AN APPROACH TO ANTIBODY-DRUG CONJUGATES**

Memoria presentada por el Licenciado Simone Fratta para optar al grado de Doctor
en Química

Sevilla 2022



DEPARTAMENTO DE QUÍMICA ORGÁNICA

FACULTAD DE QUÍMICA

UNIVERSIDAD DE SEVILLA

**SYNTHESIS OF NEW NAMPT INHIBITORS AS POTENTIAL
ANTI-CANCER DRUGS.**

AN APPROACH TO ANTIBODY-DRUG CONJUGATES

Vº Bº de los Directores de la Tesis

Fdo. Dra. Inmaculada
Robina Ramírez

Universidad de Sevilla

Fdo. Dra. Ana Teresa
Carmona Asenjo

Universidad de Sevilla

Fdo. Dr. Antonio J.
Moreno Vargas

Universidad de Sevilla

AKNOWLEDGMENTS

I would like to thank Prof. Inmaculada Robina, Prof. Ana T. Carmona, and Prof. Antonio J. Moreno Vargas for supporting and supervising me during my PhD. I would like to extend my gratitude to the European Union, specifically to European Community's H2020-MSCA-ITN-2018 call. Action, MSCA-ITN-ETN. (European Training Networks) for funding the project INTEGRATA (Project: H2020-813284). The INTEGRATA project ("Integrating Chemical and Biological approaches to target NAD production and signaling in cancer integrating chemical and biological approaches to target NAD production and signaling in cancer") is a training network that has gathered an excellent multidisciplinary team which has been very helpful in my formation. I thank, Dr. Caffa, Dr. Piacente, Dr. Benzi, Dr. Del Rio, Dr. Hechler, Prof. Aimable, Prof. Duchosal, Prof. Nencioni and Prof. Bruzzone for their mentorship during my secondments. I also thank the other ITN fellows, Jorge, Paulina, and Pablo. I would like to thank my lab mates, Enrique, Macarena, Carlos, and Alex at the Department of Organic Chemistry for a cherished time spent together. My appreciation also goes out to my mother, my brother, my family, and my friends Matteo, Amedeo, Carlotta, Alice and Federico for their encouragement and support throughout my studies. A special thanks to Irene, for being my home and my inspiring muse. Finally, I would like to dedicate this PhD thesis and the rest of my career to my lovely dad.

TABLE OF CONTENTS

ABBREVIATIONS	15
SUMMARY.....	20
1. SYNTHESIS AND STRUCTURE-ACTIVITY RELATIONSHIP OF NEW NICOTINAMIDE PHOSPHORIBOSYLTRANSFERASE (NAMPT) INHIBITORS WITH ANTITUMOR ACTIVITY ON SOLID AND HAEMATOLOGICAL CANCER.....	26
1.1. INTRODUCTION.....	28
1.1.1. The Role of Nicotinamide Phosphoribosyl Transferase in cancer cell growth and proliferation	28
1.1.2. NAMPT: Enzymatic reaction and crystal structure	30
1.1.3. NAMPT inhibitors in clinical trials	33
1.1.4. Medicinal chemistry of NAMPT inhibitors	35
1.1.4.1. Previous results of our research group.....	36
1.1.4.2. Chemical modification of the Cap group.....	37
1.1.4.3. Chemical modification of the connecting unit	38
1.1.4.4. Miscellaneous modifications of the spacer and the tail group	39
1.1.4.5. Nonsubstrate NAMPT inhibitors	40
1.2. OBJECTIVES.....	42
1.3. RESULTS AND DISCUSSION	43
1.3.1. CHEMISTRY	43

1.3.1.1.	Preparation of (pyridin-3-yl)triazole-based inhibitors.....	43
1.3.1.2.	Preparation of (pyridin-3-yl)thiourea-based inhibitors.....	44
1.3.1.3.	Preparation of (pyridin-3/4-yl)cyanoguanidine-based inhibitors.....	47
1.3.1.4.	Synthesis of nonsubstrate compounds.....	50
1.3.2.	BIOLOGICAL EVALUATION.....	53
1.3.2.1.	Cytotoxicity on MIA PaCa-2 cells, effect on intracellular NAD ⁺ concentration and NAMPT inhibition.....	53
1.3.2.2.	Cytotoxicity on haematological cancer cells.....	62
1.3.2.3.	<i>In vivo</i> antitumor activity.....	67
1.3.3.	MOLECULAR MODELLING.....	69
1.4.	EXPERIMENTAL PART.....	71
2.	SYNTHESIS OF NEW INNOVATIVE PAYLOADS AND GLUTATHIONE-SENSITIVE LINKERS FOR ANTIBODY-DRUG CONJUGATES (ADCs).....	121
2.1.	INTRODUCTION.....	122
2.1.1.	Antibody-Drug Conjugates in the market.....	122
2.1.2.	Internalizing and non-internalizing ADCs.....	123
2.1.3.	Target antigen selection and mechanism of action of ADCs.....	124
2.1.4.	Antibodies.....	125
2.1.5.	Chemical Linkers in Antibody-Drug Conjugates.....	125

2.1.5.1. Non-Cleavable Linkers	126
2.1.5.2. Cleavable Linkers	127
2.1.5.2.1. Chemically cleavable linkers.....	127
2.1.5.2.1.1. Acid-sensitive linkers.....	127
2.1.5.2.1.2. Glutathione-sensitive disulfide linkers.....	128
2.1.5.2.2. Enzymatically cleavable linkers.....	129
2.1.5.2.2.1. Cathepsin B-sensitive linker.....	129
2.1.5.2.2.2. β -Glucuronidase-sensitive linker.....	130
2.1.6. Cytotoxic Payloads	131
2.1.6.1. Microtubule-disrupting drugs	131
2.1.6.1.1. Auristatins.....	131
2.1.6.1.2. Maytansinoid derivatives.....	134
2.1.6.2. DNA damaging agents	135
2.1.6.2.1. Calicheamicin.....	135
2.1.6.2.2. Camptothecins.....	136
2.1.6.2.3. Pyrrolobenzodiazepines.....	138
2.1.6.2.4. Duocarmycins.....	139
2.1.6.3. Innovative drugs – New payloads for Antibody-Drug Conjugates..	140
2.1.6.3.1. Amatoxins.....	140

2.1.6.3.2.	NAMPT inhibitors.....	141
2.1.7.	Bioconjugation strategies	142
2.1.7.1.	Drug-to-antibody ratio (DAR).....	142
2.1.7.2.	Classical chemical bioconjugation	143
2.1.7.3.	New linker technologies	144
2.1.7.3.1.	Next-Generation Maleimides (NGM).....	145
2.1.7.3.1.1.	<i>N</i> -Aryl maleimides.....	145
2.1.7.3.1.2.	β -amino maleimides.....	145
2.1.7.3.2.	Non-classic bioconjugation systems.....	146
2.1.7.3.2.1.	Oxanorbornadienes (ONDs).....	146
2.1.7.3.2.2.	Azanorbornadienic vinyl sulfones.....	148
2.1.7.3.2.3.	Azanorbornadienic bromovinyl sulfones.....	149
2.2.	OBJECTIVES	151
2.3.	RESULTS AND DISCUSSION.....	153
2.3.1.	CHEMISTRY.....	153
2.3.1.1.	Preparation of new bioconjugable NAMPT inhibitors	153
2.3.1.1.1.	Preparation of new furfurylamine derivatives.....	155
2.3.1.1.2.	Preparation of new pyrrolidine and piperidine derivatives.....	159
2.3.2.	BIOLOGICAL EVALUATION.....	161

2.3.2.1. Viability assays on ML2 and RPMI8226 cells.....	161
2.3.3. PREPARATION OF NAMPT INHIBITOR-BASED ADCs.....	164
2.3.4. OXANORBORNADIENES AS PUTATIVE NOVEL LINKERS FOR ADCs	168
2.3.4.1. Synthesis of oxanorbornadienes	169
2.3.4.2. Kinetic studies of the OND fragmentation	170
2.3.4.3. Reactivity of electrophilic ONDs and activated alkynes towards pyridine derivatives	173
2.3.5. SYNTHESIS OF PUTATIVE NAMPT INHIBITORS CONTAINING A FLUOROPYRIDINE MOIETY.....	175
2.3.5.1. Acrylamide-containing family.....	175
2.3.5.2. Cyanoguanidine-containing family.....	177
2.3.6. BIOLOGICAL EVALUATION.....	179
2.3.6.1. <i>In vitro</i> viability assays of the newly prepared compounds on MIA PaCa-2 cell line.....	179
2.3.7. PRELIMINARY DA REACTIONS WITH FURAN-BASED NAMPT INHIBITORS.....	182
2.4. EXPERIMENTAL PART.....	183
CONCLUSIONS	246
MATERIALS AND METHODS	249
REFERENCES	256

ABBREVIATIONS

Ac	Acetyl group
MeCN	Acetonitrile
AcOH	Acetic acid
ADC	Antibody Drug Conjugate
Boc	<i>tert</i> -Butyloxycarbonyl
bs	broad signal
Bu	Butyl
calcd.	Calculated
CDI	1,1-Carbonyldiimidazol
CuAAC	Copper(I)-catalyzed azide alkyne cycloaddition
Cy	Cyclohexane
Cys	Cysteine
d	Doublet
dd	Doublet of doublet
Da	Dalton
DAD	Diode array detector
DAR	Drug-to-antibody ratio
DCM	Dichloromethane
DEPT	Distortionless Enhancement by Polarization Transfer
DHE	Dihydroethidium
DIPEA	<i>N,N</i> -Diisopropylethylamine
DMF	<i>N,N</i> -Dimethylformamide

DMSO	Dimethyl sulfoxide
DNA	Deoxyribonucleic acid
EC ₅₀	Half maximal effective concentration
EtOAc	Ethyl acetate
ESI-LRMS	ElectroSpray Ionization Low Resolution Mass Spectrometry
ESI-HRMS	ElectroSpray Ionization High Resolution Mass Spectrometry
Et ₂ O	Diethyl ether
EtOH	Ethanol
Fab	Antigen binding fragment
FDA	Food and Drug Administration
Fmoc	Fluorenylmethyloxycarbonyl
GSH	Glutathione
h	Hour
His	Histidine
HOBt	<i>N</i> -Hydroxybenzotriazole
HOMO	Highest energy Occupied Molecular Orbital
HPLC	High Performance Liquid Chromatography
HSQC	Heteronuclear Single Quantum Correlation
iEDDA	inverse Electron Demand Diels-Alder
i.p.	Intraperitoneal
IUPAC	International Union of Pure and Applied Chemistry
i.v.	Intravenous
<i>J</i>	Coupling constant

k_d	Dissociation constant
LC-MS	Liquid Chromatography-Mass Spectrometry
LUMO	Lowest energy Unoccupied Molecular Orbital
Lys	Lysine
m	Multiplet
mAb	Monoclonal antibody
Me	Methyl
MeOH	Methanol
min	Minute
MMAE	Monomethyl Auristatin E
NBS	<i>N</i> -Bromosuccinimide
NCS	<i>N</i> -Chlorosuccinimide
NMR	Nuclear Magnetic Resonance
NOE	Nuclear Overhauser Effect
OND	Oxanorbornadiene
PABA	<i>p</i> -Aminobenzyl alcohol
PBS	Phosphate-buffered solution
PDB	Pyrrrolobenzodiazepine
Ph	Phenyl
PK	Pharmacokinetics
ppm	parts-per-million
PTSA	<i>p</i> -toluenesulfonic acid
q	quartet

quant	quantitative
rDA	<i>retro</i> Diels-Alder
RP-HPLC	Reversed Phase-High Performance Liquid Chromatography
r.t.	Room temperature
s	singlet
SAR	Structure-Activity Relationship
SDS-PAGE	Sodium Dodecyl Sulphate - PolyAcrylamide Gel Electrophoresis
SEC-HPLC	Size Exclusion-High Performance Liquid Chromatography
S _N V _σ	Nucleophilic vinylic substitution
t	triplet
t _{1/2}	half-life
TBAF	Tetrabutylammonium fluoride
TBDMSCl	<i>tert</i> -Butyldimethylsilyl chloride
^t Bu	<i>tert</i> -Butyl
TCEP	Tris(2-carboxyethyl)phosphine
TFA	Trifluoroacetic acid
THF	Tetrahydrofuran
TME	tumor microenvironment
TMRM	Tetramethylrhodamine methyl ester perchlorate
TMS	Trimethylsilyl
Ts	Tosyl
Tz	Tetrazine

SUMMARY

Nicotinamide phosphoribosyltransferase (NAMPT) catalyzes the rate-limiting step in the biosynthesis of Nicotinamide Adenine Dinucleotide (NAD⁺), a cofactor essential for several cellular processes. NAD⁺ is involved in important biological processes such as energy metabolism, sirtuin function, DNA repair machinery and intracellular oxidative stress. Cancer cells are highly dependent on NAMPT activity for proliferation due to an increased metabolism and a high activity of NAD⁺-consuming enzymes. NAMPT represents an interesting target for the development of anticancer drugs given that this enzyme is overexpressed in different types of tumours and that NAMPT expression appears to be related with tumour progression. The reference compound in the field of NAMPT inhibition is **FK866**. Despite its potent antiproliferative activity both *in vitro* and *in vivo*, it failed in human cancer trials (phase II clinical trial) because of the lack of antitumor benefit and the presence of side effects. In the last two decades several analogues have been described and, recently, some of them have also reached clinical phase trials.

In the first chapter of this thesis, we present the synthesis and biological evaluation of a library of new NAMPT inhibitors (Figure 1). A structure-guided design was used for the preparation of the new inhibitors. For this goal, we made use of significant data from reported structure activity relationships of known NAMPT inhibitors and of crystallographic data of known complexes enzyme-inhibitors. Chemical structural variations were made at the cap group, connecting unit, linker, and tail group of **FK866** (Figure 1). A furan moiety that could mimic the benzamide of **FK866** while increase the polarity of the molecule and thus the water solubility, was incorporated in most of the new compounds. Additionally, furan could act as a handle for bioconjugation strategies that may be used for the generation of antibody-drug-conjugates (ADCs, Chapter 2). The new inhibitors prepared in this chapter showed excellent *in vitro* anticancer activity in MIA PaCa-2 pancreatic cancer cells and in several haematological cancer cell lines. Some candidates exhibited a much higher

cytotoxicity than that showed by reference compound **FK866**. However, when the lead compounds were assayed in *in vivo* xenograft mouse models, unfortunately, there was not a good correlation between the *in vitro* results and the *in vivo* activity.

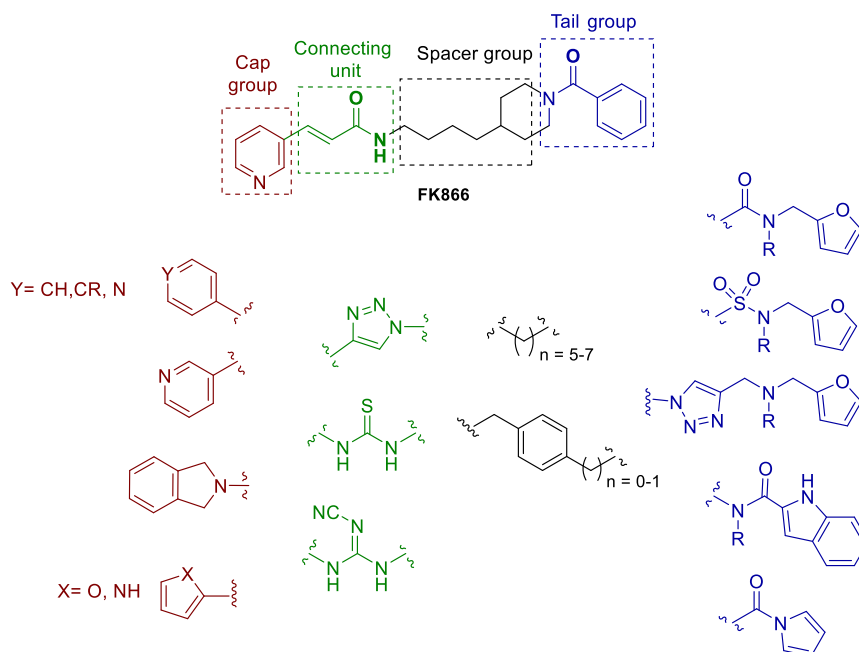


Figure 1. Structural motifs for the new inhibitors prepared in this Thesis.

The second chapter of the Thesis deals with the preparation of antibody-drug-conjugates (ADCs). An ADC consists of a potent cytotoxic compound (payload) that is bioconjugated to a tumour-targeted antibody by a chemical linker. This type of conjugates can deliver the cytotoxic payload directly to tumour cells while sparing healthy cells. Several drugs of this type have been developed for the treatment of several cancers that do not respond to other therapies. Due to the lack of activity of the most cytotoxic compounds prepared in chapter 1 in the *in vivo* biological evaluation, we accomplished structural modifications of the most promising candidates to provide these molecules with a chemical function that could act as a handle for bioconjugation purposes. With these molecules in hand, we focused on the preparation of NAMPT inhibitor-based ADCs which have been scarcely explored in the field of selective drug delivery up to now.

Two different approaches have been followed: (1) preparation of ADCs using classical peptide linkers; (2) development of a new strategy of drug-release based on the chemistry of oxanorbordienes (ONDs) that could be used for the preparation of novel ADCs. The first approach allowed the preparation of six new ADCs, by combination of the new modified NAMPT inhibitors with several classical enzymatically cleavable linkers (peptide linkers). The bioconjugation of the resulting inhibitor-linker ensembles with the monoclonal antibody CD138 afforded the final ADCs (Figure 2). Biological evaluation of the new ADCs is underway and is not included in this Thesis.

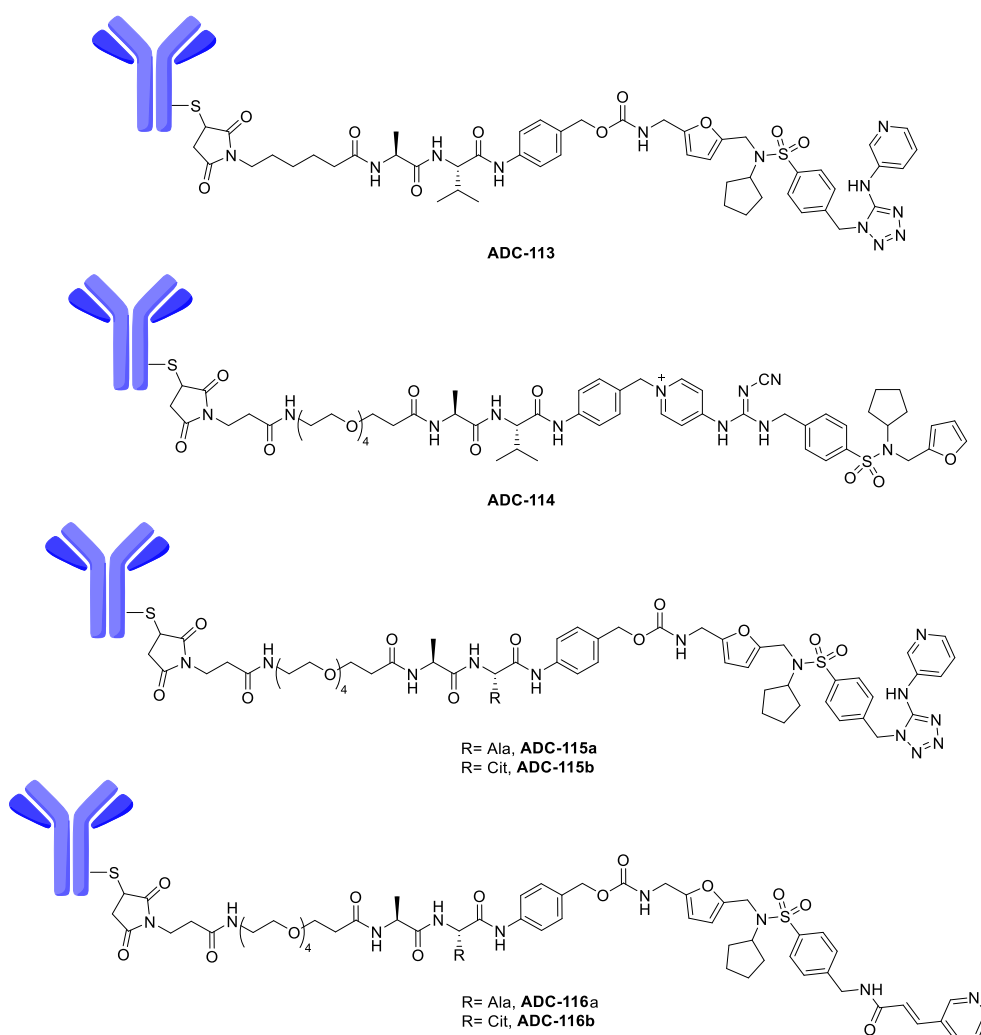
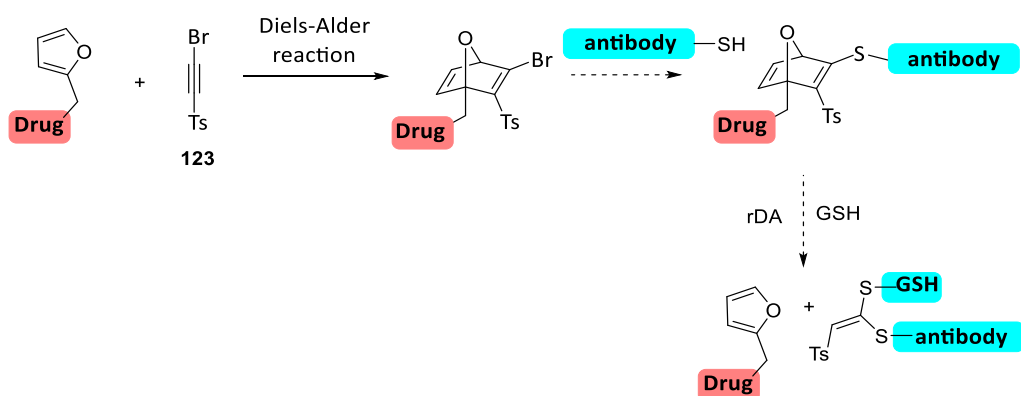


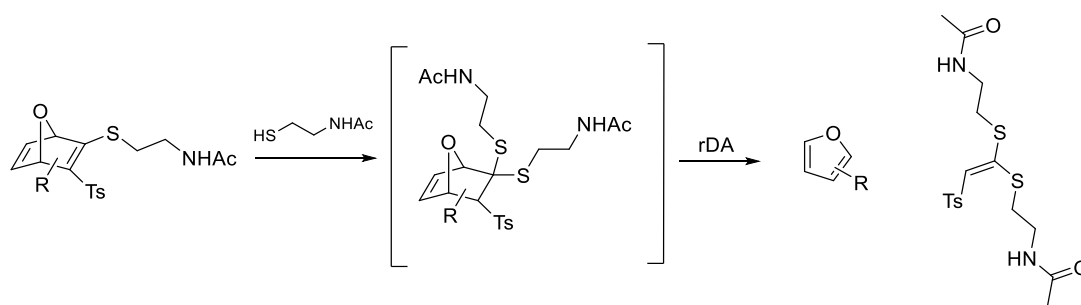
Figure 2. New NAMPT inhibitor-based ADCs.

The second strategy is based on the reactivity of heteronorbomadiene systems. The high reactivity of these compounds makes them useful as linkers for bioconjugation reactions, where fast reactions with nucleophilic amino acids of the proteins are needed. As most of the inhibitors prepared in chapter 1 contains a furan tail, the Diels Alder (DA) reaction between the furan moiety of the inhibitor and an activated alkyne would afford bioconjugable oxanorbomadienic NAMPT inhibitors. Our hypothesis is based on the ability of these OND-based bioconjugable inhibitors to be attached to an antibody by cysteine-selective bioconjugation (Scheme 1), through a process that was previously studied in our group with azanorbomadiene analogues. A cleavable mechanism should liberate the drug from the antibody inside the cells following a strategy of glutathione (GSH)-triggered release.



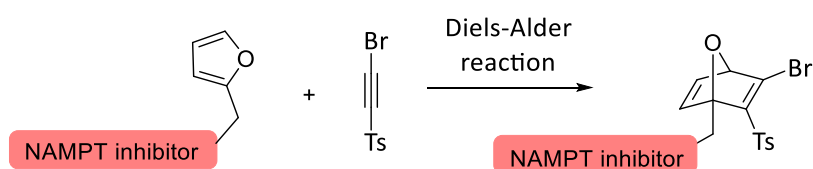
Scheme 1. ONDs as linkers in drug delivery systems.

In order to validate the strategy of glutathione-triggered release of cytotoxic drugs in our OND systems, we first explored the reactivity of simple models of oxanorbomadienic thiovinyl sulfones in the presence of an excess of a thiol derivative (Scheme 2). We have demonstrated that these OND systems can suffer a fragmentation reaction *via* a two-reaction sequence: a conjugate addition followed by a spontaneous retro-Diels-Alder (rDA) reaction. Therefore, these ONDs could be used as thiol-sensitive linkers for drug delivery strategies.



Scheme 2. Fragmentation of ONDs in the presence of thiols.

We then assayed the DA reaction of some of the furan-tailed NAMPT inhibitors with the adequate activated alkyne for the preparation of bioconjugable oxanorbornadienic inhibitors. The first reaction attempts revealed that the nucleophilic pyridine moiety of the inhibitor gave side reactions with the alkyne/oxanorbornadiene system, hence not allowing the formation of the desired OND system. To overcome this problem, we accomplished the preparation and biological evaluation of a small library of 2-fluoropyridine analogues, where the nucleophilicity of the pyridinic N is clearly decreased. Although the biological evaluation of these new analogues showed lower cytotoxicity than the non-fluorinated ones, the level of cytotoxicity is still enough for ADC applications. Attempts to transform these new 2-fluoropyridine-based NAMPT inhibitors into oxanorbornadienic bioconjugable inhibitors worked as it was expected (Scheme 3). This strategy represents a preliminary approach for the use of oxanorbornadienes as innovative linkers in the field of selective drug delivery.



Scheme 3. Incorporation of furan-containing NAMPT inhibitors into bioconjugable electrophilic oxanorbornadienes.

**1. SYNTHESIS AND STRUCTURE-ACTIVITY RELATIONSHIP OF NEW
NICOTINAMIDE PHOSPHORIBOSYLTRANSFERASE (NAMPT) INHIBITORS WITH
ANTITUMOR ACTIVITY ON SOLID AND HAEMATOLOGICAL CANCER.**

1.1 INTRODUCTION

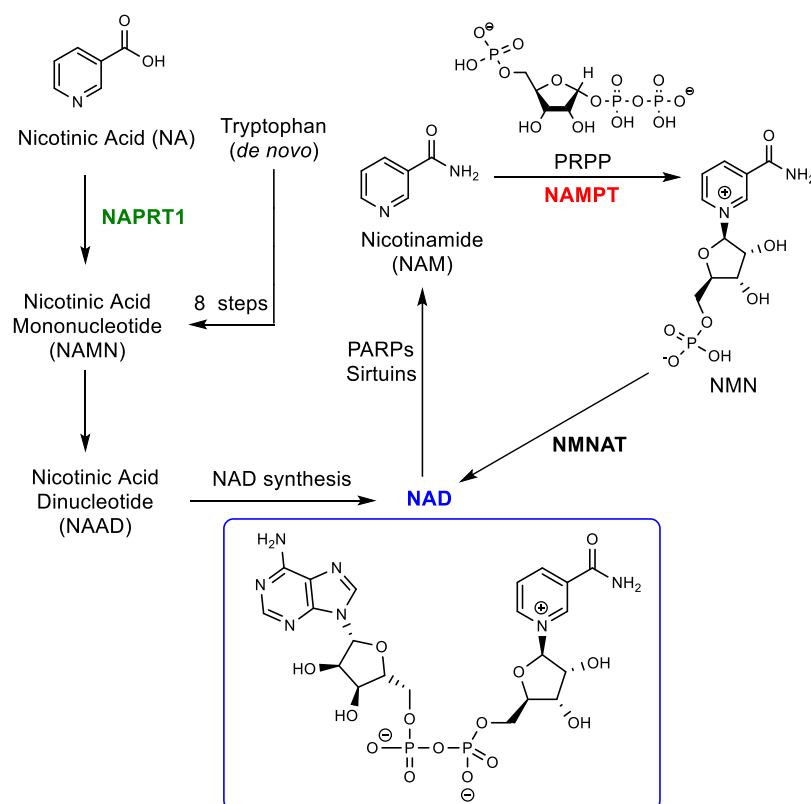
1.1.1 The Role of Nicotinamide Phosphoribosyl Transferase in cancer cell growth and proliferation

Otto Warburg, who received the Nobel prize in Medicine in 1931, hypothesised more than 80 years ago that in cancer cells, energy conversion is reprogrammed, switching from oxidative phosphorylation to glycolysis, which are the two main metabolic pathways for cell energy production. Although it is still under investigation, Warburg's effect is supported by the fact that although aerobic glycolysis produces less ATP (per mole of glucose) than oxidative phosphorylation, production is faster.⁶ The higher energy that cancer cells need is strongly dependent on Nicotinamide Adenine Dinucleotide (NAD⁺) production, a key molecule involved in glycolysis and other important cellular functions. NAD can be biosynthesized from several precursors through three main pathways (Scheme 4).¹ Moreover, the importance of NAMPT in tumor cells is sustained by the increased levels of this enzyme found in different types of cancers (Table 1).¹ NAD⁺ can be synthesized from precursors containing a pyridine moiety such as nicotinic acid (NA), nicotinamide (NAM) and nicotinamide riboside (NR) and from tryptophan. Regarding the de novo synthesis of NAD⁺ from tryptophan, this route requires a series of steps and occurs notably in the liver⁷ but, unlike NAM or NA, tryptophan alone is insufficient to maintain normal levels of NAD⁺ in cells. Instead, the primary salvage pathway in which NAD⁺ is synthesized from NAM in a two-reaction sequence mediated by Nicotinamide Phosphoribosyltransferase (NAMPT, rate-limiting enzyme) and Nicotinamide mononucleotide adenylyltransferase (NMNAT) is predominant in mammalian cells. NAMPT catalyzes the synthesis of Nicotinamide mononucleotide (NMN) from NAM and 5-phosphoribosyl pyrophosphate (PRPP) (Scheme 4). NMN is then converted to NAD by NMNAT. Due to the high activity of NAD⁺-consuming enzymes and the overexpression of NAMPT in cancer cells, great efforts have been performed to

develop potent NAMPT inhibitors. Recently, NAMPT has been also identified as possible target for the synthesis of anti-cancer agents.⁸

Table 1. Main correlation in tumors associated with high expression of NAMPT.⁹

Condition	Level of investigation	Main finding associated with overexpression of NAMPT
Breast cancer	Tissual protein	Associated with poor disease-free and overall survival
Postmenopausal breast cancer (PBC)	Serum level	Elevated (associated with risk of PBC)
	Tissual protein and mRNA	Increased
Gastric cancer	Serum level	Increased (positive correlation with stage progression)
	Tissual protein	Increased (correlation with VEGF-A expression, negatively correlated with survival)
Lymphomas	Tissual protein	Increased (highly expressed in Hodgkin's lymphoma)
Prostate cancer	Tissual protein	Increased
Ovarian cancer	Tissual protein	Increased
Colorectal cancer	Blood level	Increased (correlated with stage progression)
Malignant astrocytomas: anaplastic astrocytoma (AA, grade III) and glioblastoma (GBM, grade IV)	Serum level tissual protein and mRNA	Increased (correlated with tumor grade, coexpression with p53 in GBM tissue was associated with poor survival)
Esophageal cancer	Serum levels, tissual mRNA	Increased (independent factor of mortality)
Melanoma	Tissual protein and mRNA	Increased (independent of BRAF mutations and Clark's levels)



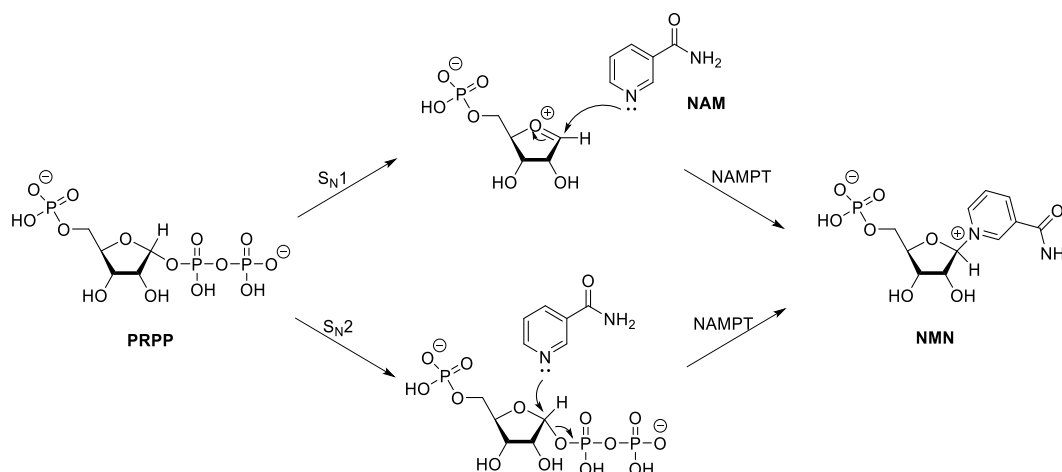
Scheme 4. NAD⁺ biochemical pathways.¹⁰

Intracellular NAMPT (iNAMPT) can be found in the cytoplasm, mitochondria, and nucleus. It has been discovered to be further involved in sirtuin function, DNA repair machinery and intracellular oxidative stress, among others.¹¹ Extracellular NAMPT (eNAMPT) has been reported to function as a cytokine, a growth factor, and has been shown to display pro-tumoral and pro-inflammatory activities.¹²

1.1.2 NAMPT: Enzymatic reaction and crystal structure

Human NAMPT is a glycosyltransferase that contains a total of 491 amino acids and belongs to a dimeric class of type II phosphoribosyltransferases. Two possible reaction mechanisms of NAMPT catalysis can be advanced (Scheme 5).¹³ In general, for most glycosidases including enzymes that catalyse the substitution at the glycoside linkages, the plausible mechanism assumed is a S_N1-type reaction. This usually results in a highly distorted conformation of the sugar ring and the presence

of a negative charge in the active site of the enzyme that could stabilize the cationic intermediate through an ion pair interaction. These requirements have not been found in the active site of NAMPT, thus suggesting that the S_N2 -type mechanism is the most likely one.



Scheme 5. Possible reaction mechanisms of NAMPT catalysis.¹³

The crystal structure of human NAMPT was first published in 2006¹⁴ when NMN and **FK866**, one of the first described NAMPT inhibitors, were co-crystallized to study their binding mode. The active site of NAMPT is located in the two subunits interface and NMN is bound near the top of the central β -sheet in domain B. The co-crystal revealed the importance of both domains B and A, with the latter having several residues playing a crucial role in recognizing NMN, thus suggesting that NAMPT is only active in its dimeric form (Figure 3).¹⁵

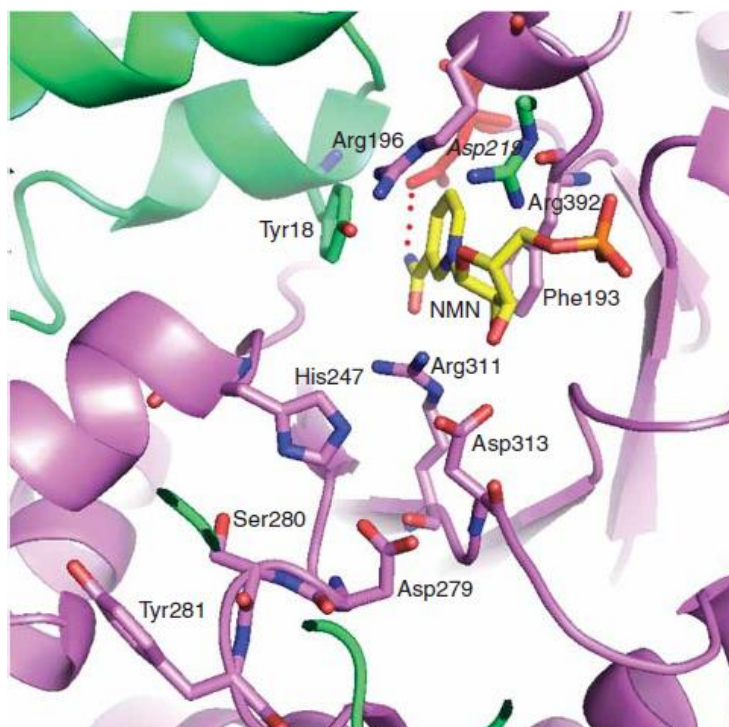


Figure 3. Nicotinamide mononucleotide (NMN, in yellow) complexed in the active site of NAMPT.¹⁶

The crystal structure of **FK866** (compound **1**) in complex with NAMPT is shown in Figure 4. The pyridine moiety of FK866 is sandwiched between the side chain of Phe193 and Tyr18, similarly to nicotinamide (NAM) in complex with NAMPT, making a π - π stacking interaction. The oxygen atom of acrylamide makes a hydrogen bond with Ser275 while nitrogen uses a molecule of water to bridge and stabilize the interactions with Ser245, Asp219, and Val242. The alkyl chain does not add any affinity in the hydrophobic tunnel (Val242, Ile309, Ile351, and His191), but it is mandatory since it serves as a linker between the acrylamide and the benzoyl group. The solvent-exposed part of the molecule, the benzoyl-piperidine group, can be considered as a tail group that anchors the molecule and increases the affinity toward the enzyme.

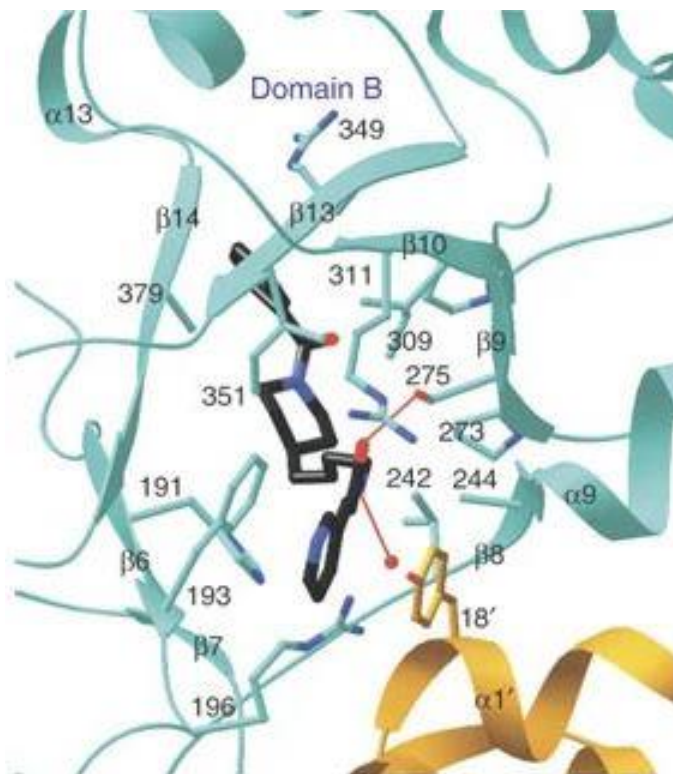


Figure 4. Binding pose of compound **1** complexed in the active site of NAMPT.

Furthermore, it has been found that an autophosphorylation at His247 residue stabilizes the interactions of the two monomers increasing the affinity for its substrate PRPP by 10-fold.¹⁷ Even if it is transient and represents only an intermediate of the reaction, this post-translational modification on NAMPT enhances the affinity for NAM by 160,000-fold and increases its enzymatic activity by 1125-fold.¹⁸

1.1.3 NAMPT inhibitors in clinical trials

NAMPT enzyme plays an important role in the proliferation and growth of cancer cells, therefore represents an important therapeutic target for the development of anti-cancer drugs. The disclosure of the crystal structure of **1** (**FK866**) in complex with the enzyme,¹⁵ encouraged and boosted the synthesis of new NAMPT inhibitors in the last two decades (Figure 5).

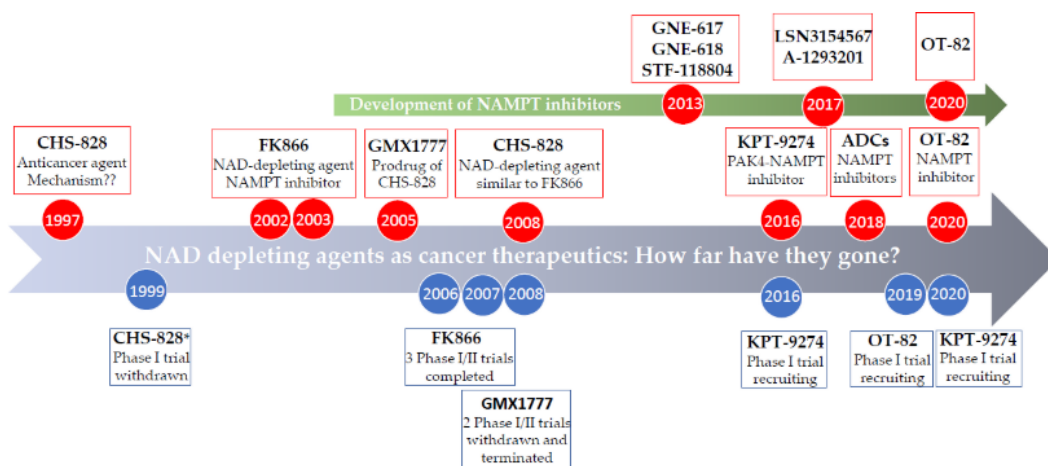


Figure 5. Timeline of NAMPT inhibitors.³

Over the past years, several compounds have been identified as potent NAMPT inhibitors with strong anti-cancer activity. Compound **FK866**¹⁹ (compound **1**, Figure 6) was the first identified selective NAMPT inhibitor, with cytotoxicity at nM concentrations in different types of cancers. Although this molecule entered clinical trials in patients with advanced solid tumors, the results were disappointing due to the lack of antitumor efficacy and secondary side effects (e.g., thrombocytopenia). Similar results were obtained in patients treated with Teglalinad, a prodrug of the known NAMPT inhibitor **CHS828**²⁰ (compound **2**, Figure 6), which was found to induce thrombocytopenia and gastrointestinal symptoms, without beneficial clinical effects. However, inhibition of NAMPT still remains a promising strategy for cancer therapy, as it has been demonstrated with the entry of new compounds in human clinical phase. For instance, **KPT-9274**²¹ (compound **3**, Figure 6) a dual inhibitor of NAMPT and of the serine/threonine protein kinase PAK4, was successfully transited in phase I from solid tumors to acute myeloid leukemia. Compound **OT-82**²² (compound **4**, Figure 6) was also recently identified as a new NAMPT inhibitor with marked efficacy against hematopoietic malignancies such as leukemia, lymphoma, and myeloma and is also being currently evaluated in clinical studies.

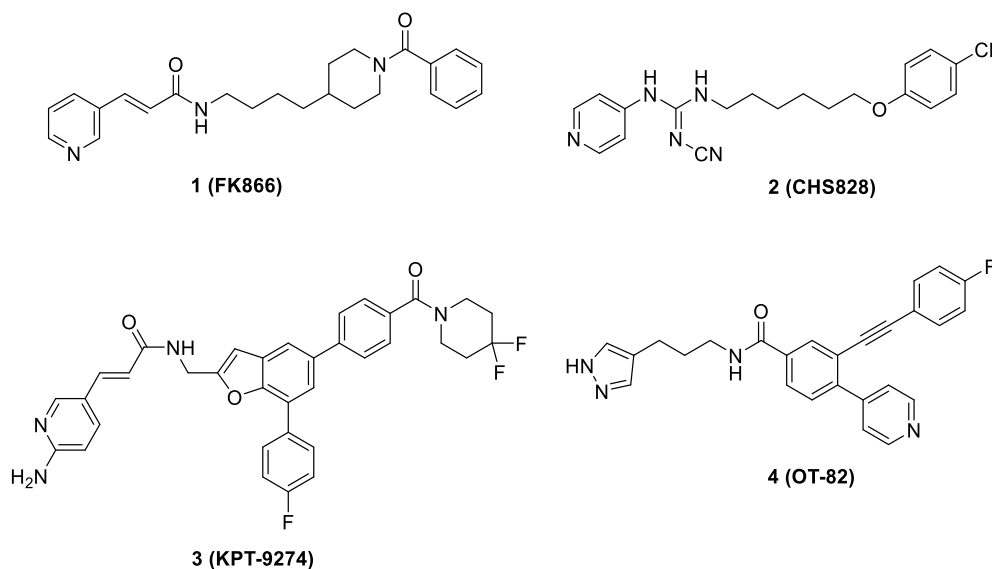


Figure 6. Representative examples of known NAMPT inhibitors with relevant anti-cancer activity.

The limitations of **FK866**, **CH828**, and **KPT9274** in the clinical phase for solid tumors and the off-target toxicities such as thrombocytopenia may endorse the development of NAMPT inhibitors towards haematological cancers.²²

1.1.4 Medicinal chemistry of NAMPT inhibitors

The crystal structures of NAMPT in complex with different inhibitors revealed a common pharmacophore based on the nature of the pocket of the active site (Figure 7). This model contains a NAM mimic group that is constituted of a pyridine or any other nitrogen-containing heterocycle and a connecting unit able to form hydrogen bonds with Ser275 and Asp219. Besides, a hydrophobic tunnel binder serves as spacer group between the connecting unit and the tail group that is important to make interactions in the solvent-exposed region of the enzyme.

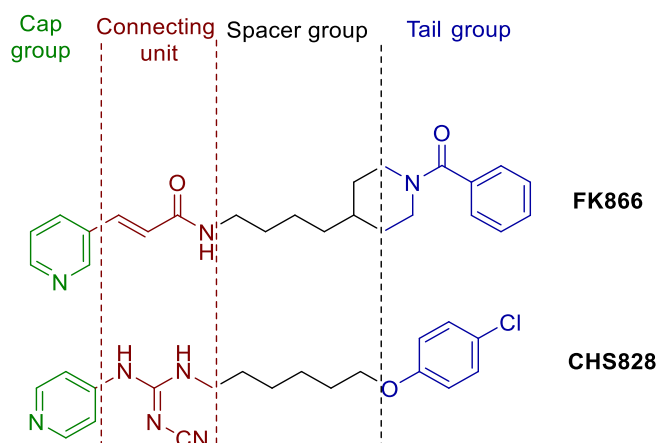


Figure 7. NAMPT inhibitors pharmacophoric model.

Structure-Activity Relationship (SAR) studies performed in the last 20 years by academic or industrial research groups are remarkable. As a result, triazole-, urea-, thiourea-, amide-, and cyanoguanidine derivatives were identified as potent NAMPT inhibitors showing similar or improved NAMPT inhibition and/or cytotoxicity with respect to **FK866** and **CHS828**.^{1,9,23}

1.1.4.1 Previous results of our research group

Very recently, our group published a research work about the synthesis and biological evaluation of more than fifty **FK866** analogues.²⁴ The modifications were focused on the phenyl ring of the piperidine benzamide group of **FK866**, and on the central alkyl chain. Several compounds showed low nanomolar or sub-nanomolar cell growth inhibitory activity towards pancreatic cell lines (Figure 8). It is worth to highlight that this work also demonstrated that the *N*-oxidation of the pyridine cap group led to a completely non-active compound. Although compound **7** showed a similar cytotoxicity than **FK866** in MIA PaCa-2 cell line, it may be less prone to *N*-oxidation, and therefore, could be more stable and less toxic upon blood circulation.

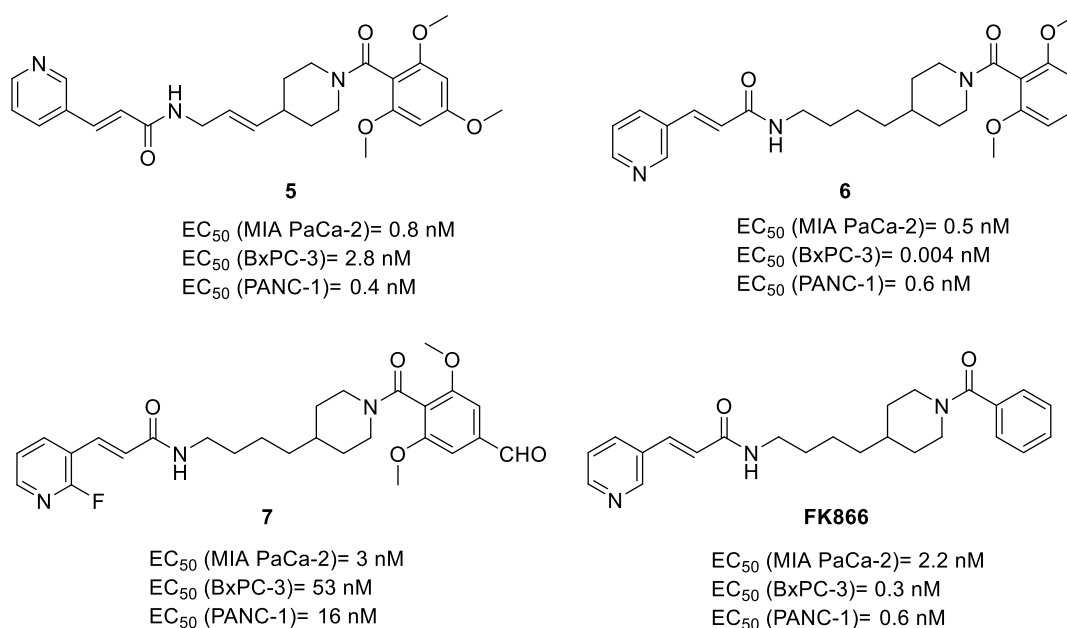


Figure 8. *In vitro* anti-proliferative activity of **FK866** and its analogues **5**, **6** and **7** toward three pancreatic cancer cell lines (IC_{50} s calculated after 72 h).²⁴

1.1.4.2 Chemical modification of the Cap group

The short half-life of **FK866** during phase 1 of clinical trial was found to be approximately 8 h and the *N*-oxidation of the pyridine was detected as the main chemical modification during metabolism.¹⁹ This suggested that the rapid clearance was in part due to the formation of *N*-oxide metabolites, which are non-active compounds towards NAMPT.²⁵ Moreover, replacement of the pyridine moiety by the phenyl group led to an inactive compound²⁶ and therefore chemical efforts were focused to find new heterocyclic moieties as pyridine mimetic moieties (Figure 9). Compound **8**²⁷ depicted in Figure 9 is one of the rare examples in literature where the IC_{50} was comparable to **FK866**, even though the cap group was replaced with a heterocycle different from pyridine. In most of the cases, the presence of a nitrogenated heterocycle in the compound is mandatory to have NAMPT inhibitors with potent cytotoxic activity (compound **9**, Figure 9).

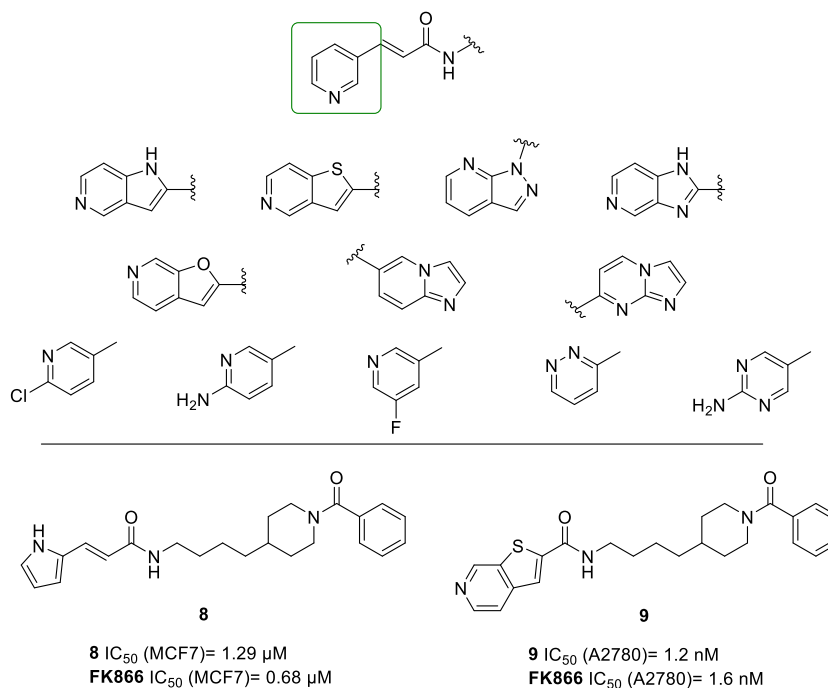


Figure 9. Replacement of the pyridine with heterocycles as cap group. MCF7= Breast cancer; A2780= Ovarian cancer.

1.1.4.3 Chemical modification of the connecting unit

Replacement of the acrylamide of **FK866** was investigated by different research groups both in academia and pharmaceutical companies with the aim to find a moiety that could bind the active site of NAMPT as the vinylogous amide group does.^{28,29} It is worth to point out that the substitution of acrylamide by a sulphonamide moiety resulted in a completely inactive compound, while replacement with a 1,2,3-triazole led to a cytotoxic compound (compounds **10** and **11**, Figure 10).^{30,31} Several SAR studies indicated that a hydrogen bond acceptor should be at a 3-carbon distance from the cap group in order to maintain strong binding interactions within the active site.¹

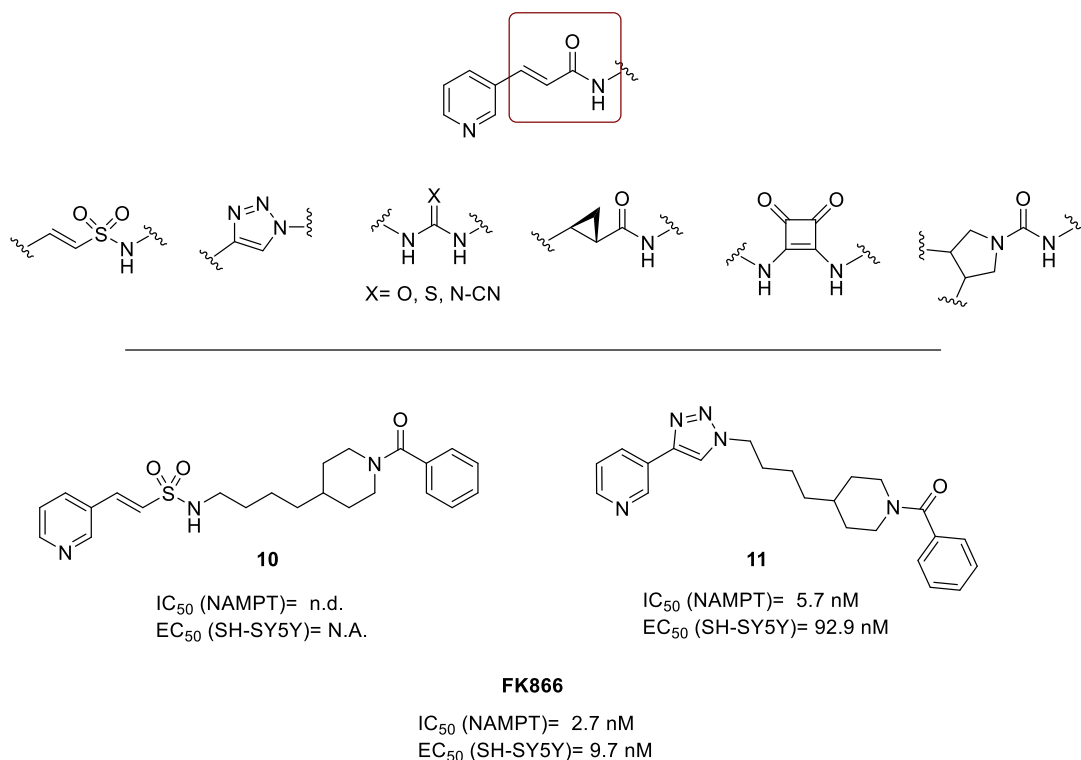


Figure 10. Modifications of the acrylamide connecting unit of **FK866**. SH-SY5Y= Neuroblastoma; n.d.= not determined, N.A.= not active.

1.1.4.4 Miscellaneous modifications of the spacer and the tail group

The *N*-benzoyl 4-butylpiperidine moiety of **FK866** was also modified with the aim of increasing the affinity towards the hydrophobic tunnel that connects the cap group with the solvent-exposed area of the active site of NAMPT. The result is an extensive variety of spacer groups such as hexyl, heptyl, and octyl chains or benzene rings (Figure 11). Modification of the tail group was important to anchor the molecule to the external part of the enzyme, increasing the possibility for the molecule to be retained in the pocket.^{23,28}

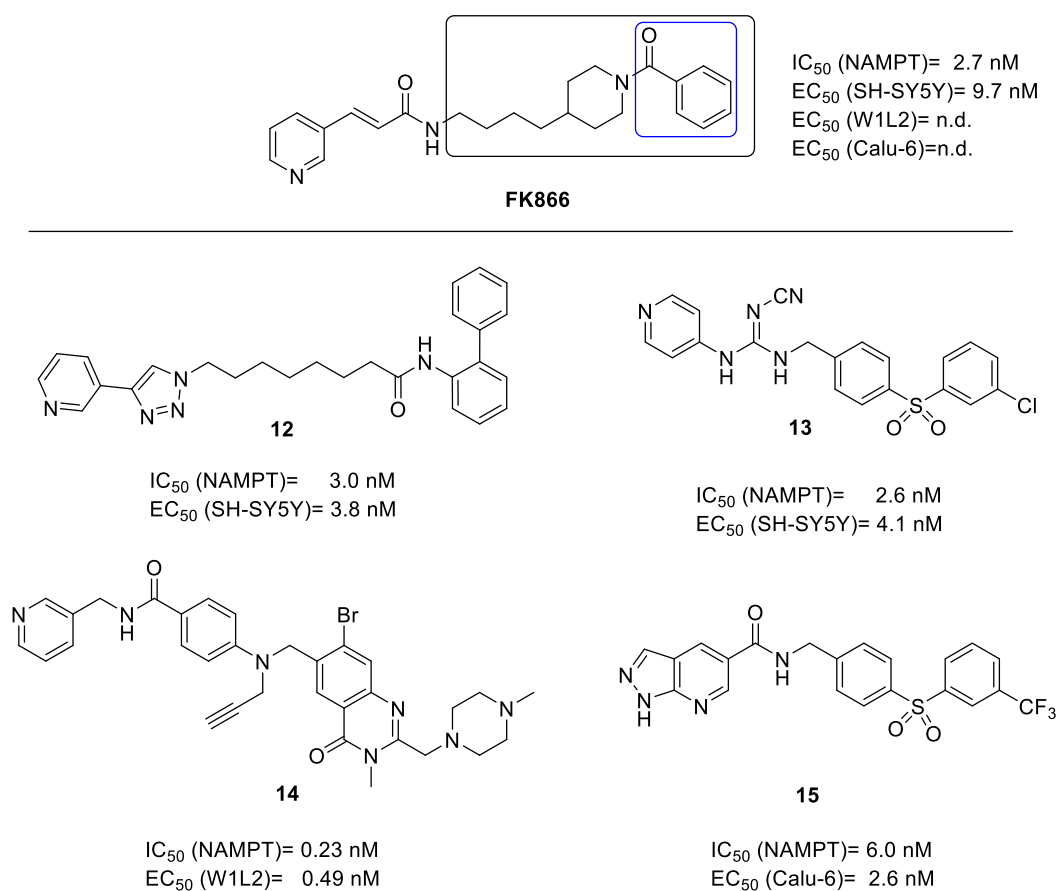
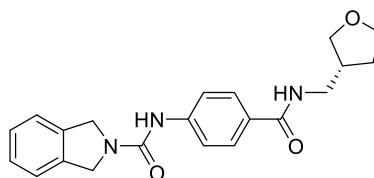


Figure 11. NAMPT inhibitors with modifications of the spacer and tail groups. W1L2= Lymphoblastoid; Calu-8= Lung cancer; n.d.= not determined.

1.1.4.5 Nonsubstrate NAMPT inhibitors

The pyridine moiety is present in the most potent NAMPT inhibitors reported so far, which could be explained considering that NAM, a pyridine-containing molecule, is the substrate of NAMPT. As previously commented, crystallographic data showed that pyridine ring of **FK866** is sandwiched between Tyr18 and Phe193 of the active site, by a π - π stacking interaction mimicking the position of NAM and establishing a hydrogen bond with the OH group of Ser275 and the N of the pyridine ring.¹⁴ *In vitro* metabolic stability studies on previously reported pyridine-based NAMPT inhibitors have shown that pyridine nitrogen is prone to microsomal oxidation, giving the corresponding *N*-oxide metabolite whose cytotoxicity is reduced with respect to the

non-oxidized precursor.²⁵ This fact could be one of the reasons for the lack of efficacy of inhibitors in *in vivo* xenograft models. Moreover, a recent published paper about nonsubstrate NAMPT inhibitor **A1293201** (Figure 12), demonstrated that phosphoribosylation of the pyridine nitrogen of NAMPT inhibitors is not required for *in vivo* antitumor efficacy³² as it was previously postulated.³³ In this work, Wilsbacher *et al.* identified a series of substrate and nonsubstrate NAMPT inhibitors and proved that both types of compounds effectively deplete intracellular level of NAD⁺ and ATP leading cancer cells to death by NAMPT inhibition. This evidence led to explore nonsubstrate compounds as possible NAMPT inhibitors.⁹



A1293201

Figure 12. Nonsubstrate NAMPT inhibitor **A1293201**.

1.2 OBJECTIVES

The design of a “next-generation” NAMPT inhibitors is a subject of current and growing interest in medicinal chemistry both for academic and industrial groups. As part of a Marie-Curie ITN program for the development of new NAMPT inhibitors with improved anti-cancer activity (<https://www.integrata-h2020.eu/>), in this Thesis we are presenting the preparation and biological evaluation of **FK866** analogues where the cap group (red), the connecting unit (green), the tunnel binder (black), and the tail group (blue) have been modified (Figure 13). The most promising compounds were tested *in vitro* towards solid and haematological cancer cell lines, as well as in *in vivo* xenograft model to evaluate the antitumor potency of this class of molecules in comparison with **FK866**. Recent publications have demonstrated that biologically relevant furan containing cargos can be easily and selectively released in *in vivo* models in a novel strategy for targeted drug delivery.^{4,5} Consequently, furan has been chosen as a tail group for most of the newly prepared compounds.

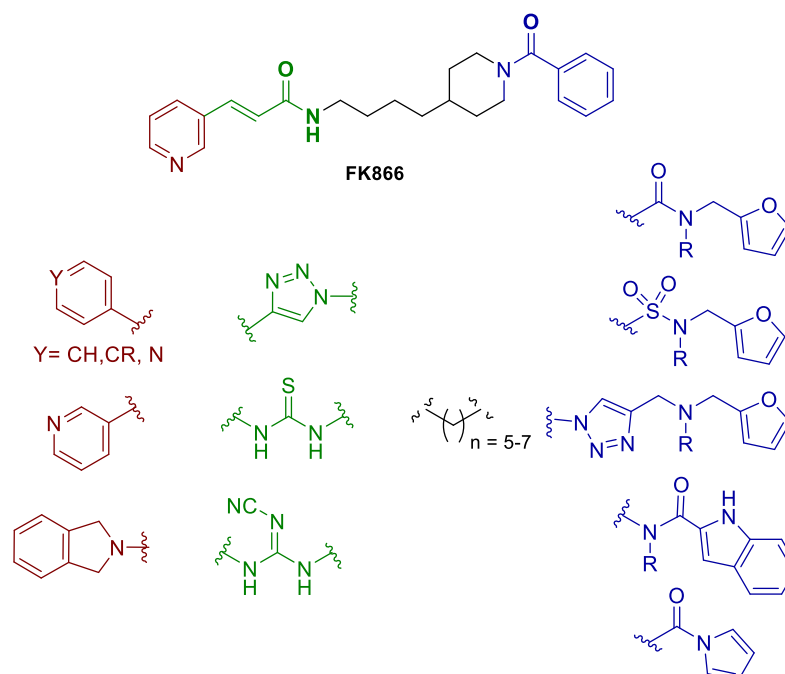


Figure 13. Structural motifs for the new inhibitors prepared in this Thesis.

1.3 RESULTS AND DISCUSSION

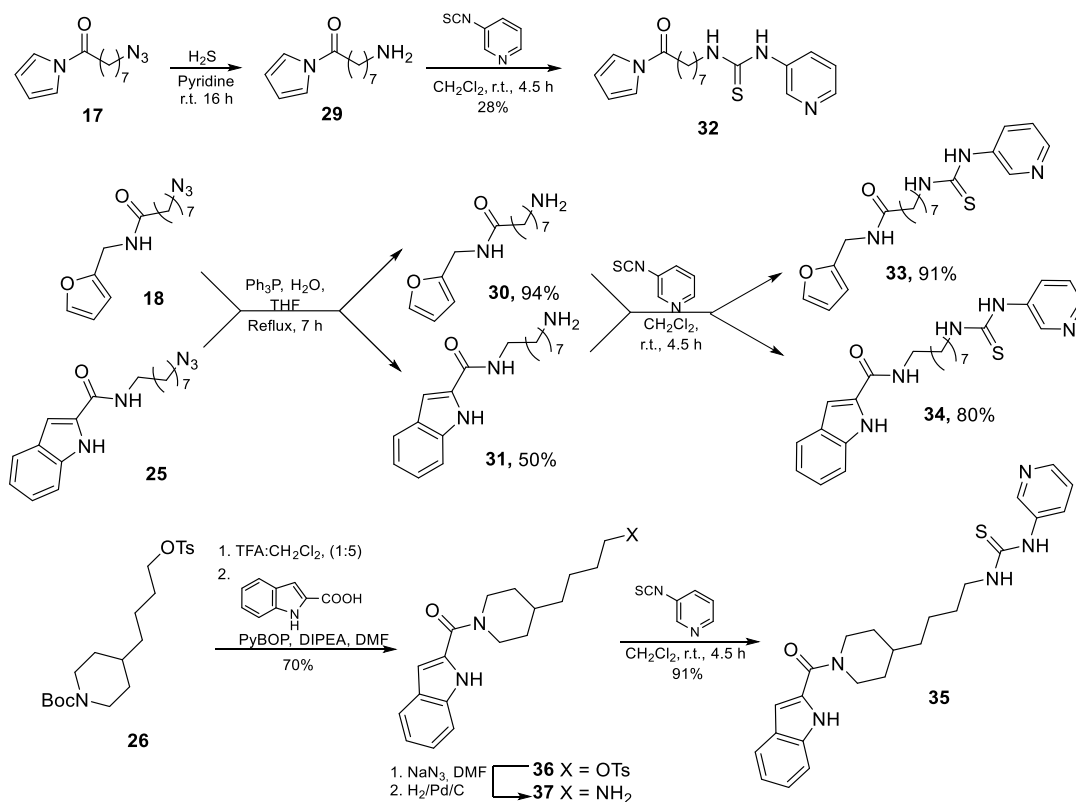
1.3.1 CHEMISTRY

The chemistry part of this first chapter is divided into 4 sections, each one refers to a family of compounds. The first three families contain triazole, thiourea or cyanoguanidine moieties as connecting units. The last group instead, represents the nonsubstrate NAMPT inhibitors where the pyridine (cap group) has been substituted by other heterocyclic moieties.

1.3.1.1 Preparation of (pyridin-3-yl)triazole-based inhibitors

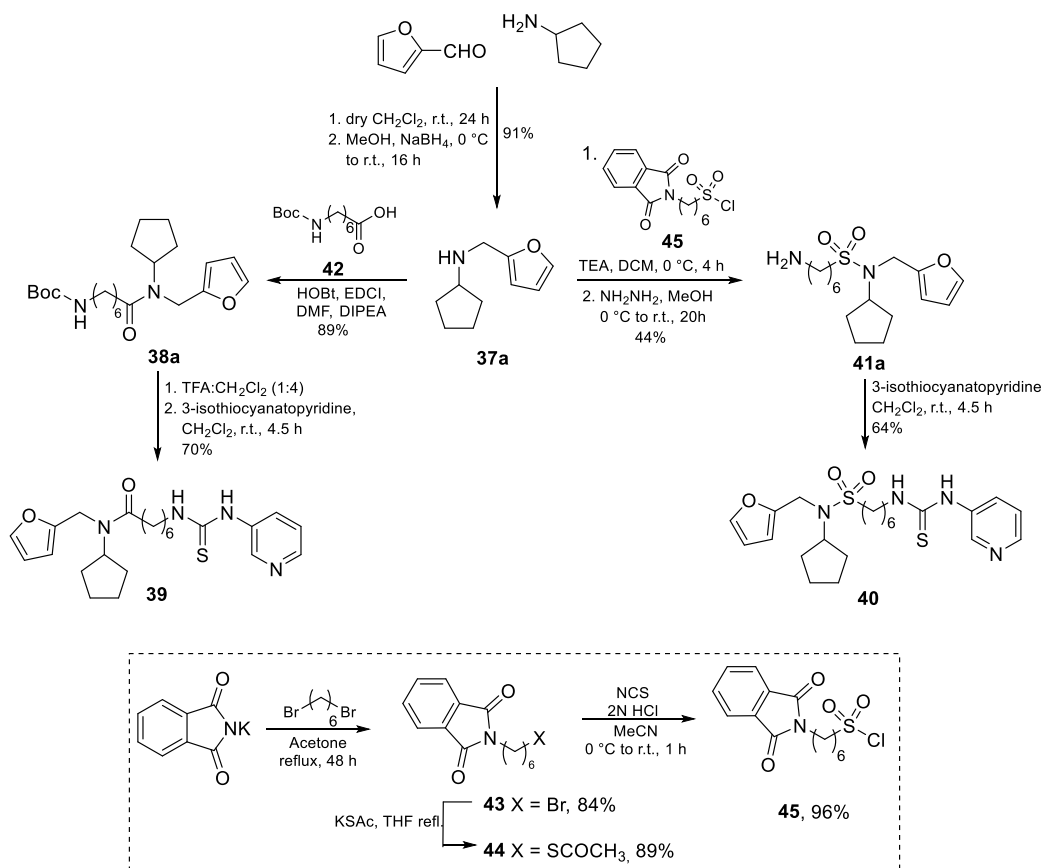
This family of compounds (**19-23**, Scheme 6) is characterized by a 3-triazolylpyridine unit connected to the piperidine alkyl chain of **FK866** or to a flexible carbon chain. The phenyl group of **FK866** was substituted by different more hydrophilic heteroaromatic moieties (furan, pyrrole, indole), which could improve the water solubility of the resulting inhibitor. In this set of compounds, incorporation of the pyridine moiety into the inhibitor was carried out by copper-catalysed alkyne azide cycloaddition (CuAAC) of commercial 3-ethynylpyridine with azide-functionalized derivatives **17**, **18**, **25** and **27**. The preparation of the target compounds is depicted in Scheme 5. The reaction of sodium azide with commercial 8-bromooctanoic acid, followed by coupling of the resulting intermediate with lithium pyrrolate in the presence of 1,1-carbonyldiimidazol (CDI), gave the azido-acylated pyrrole **17** in 38% yield. On its side, standard amide coupling of 8-azidooctanoic acid with furfurylamine provided **18** in 78% overall yield. CuAAC reaction of azides **17** and **18** with 3-ethynylpyridine in the presence of catalytic amount of CuI and DIPEA in toluene led to triazoles **19** and **20** in moderate-to-good yield. On the other hand, starting from commercial 1,8-dibromooctane, S_N2 displacement with NaN_3 gave the corresponding diazido derivative. Monoreduction of one of the azido groups was feasible by the Staudinger reaction in biphasic media (toluene- HCl aq.). Standard coupling reaction of the resulting amine **24** with 1*H*-indole-2-carboxylic acid gave derivative **25** in 62%

enzyme. For instance, Zheng *et al.* studied crystal structures of a thiourea-derived compound in complex with NAMPT and observed that Asp219 and Ser245 interact with the NH of the thiourea moiety through a water-mediated hydrogen bond.³⁶ We envisioned that substitution of the acrylamide group by a more powerful hydrogen-bond-donating group could enhance the interaction with the enzyme and therefore, increase the inhibitory activity towards NAMPT. The preparation of these compounds is described in Scheme 7. The azido derivatives **17**, **18**, and **25** were reduced to the corresponding amino derivatives **29-31**. Subsequent coupling with commercial 3-isothiocyanatopyridine gave thiourea analogues **32-34** in moderate-to-good yield. The preparation of **35** requires Boc-deprotection of *tert*-butyl-4-(4-tosyloxybutyl)piperidine-1-carboxylate **26**³⁴ followed by coupling with 1*H*-indole-2-carboxylic acid, displacement of the tosylate group with NaN₃ and subsequent azido reduction, affording amine **37** in 70% overall yield (4 steps). Reaction of **37** with 3-isothiocyanatopyridine gave compound **35** in excellent yield.



Scheme 7. Synthesis of (pyridin-3-yl)thiourea-based inhibitors **33-35**.

The preparation of **39** and **40** followed a similar strategy using *N*-cyclopentylfurfurylamine **37a** as starting furan precursor (Scheme 8). Compound **37a** was obtained through reductive amination from furfural and cyclopentylamine. Conventional amide coupling of **37a** with carboxylic acid **42**³⁷ afforded compound **38**. Subsequent Boc deprotection followed by reaction with 3-isothiocyanatopyridine furnished **39** in a good overall yield. The preparation of thiourea **40** was carried out starting from **37a** after reaction with (1,3-dioxoisindolin-2-yl)hexanesulfonyl chloride **45** followed by hydrazinolysis and coupling with 3-isothiocyanatopyridine. The synthesis of sulfonyl chloride **45** started with *N*-alkylation of potassium phthalimide with 1,6-dibromohexane to give compound **43**. Reaction of **43** with potassium thioacetate in THF afforded *S*-alkyl thioacetate **44** that was finally converted into the sulfonyl chloride **45** by reaction with NCS and 2M HCl in MeCN.

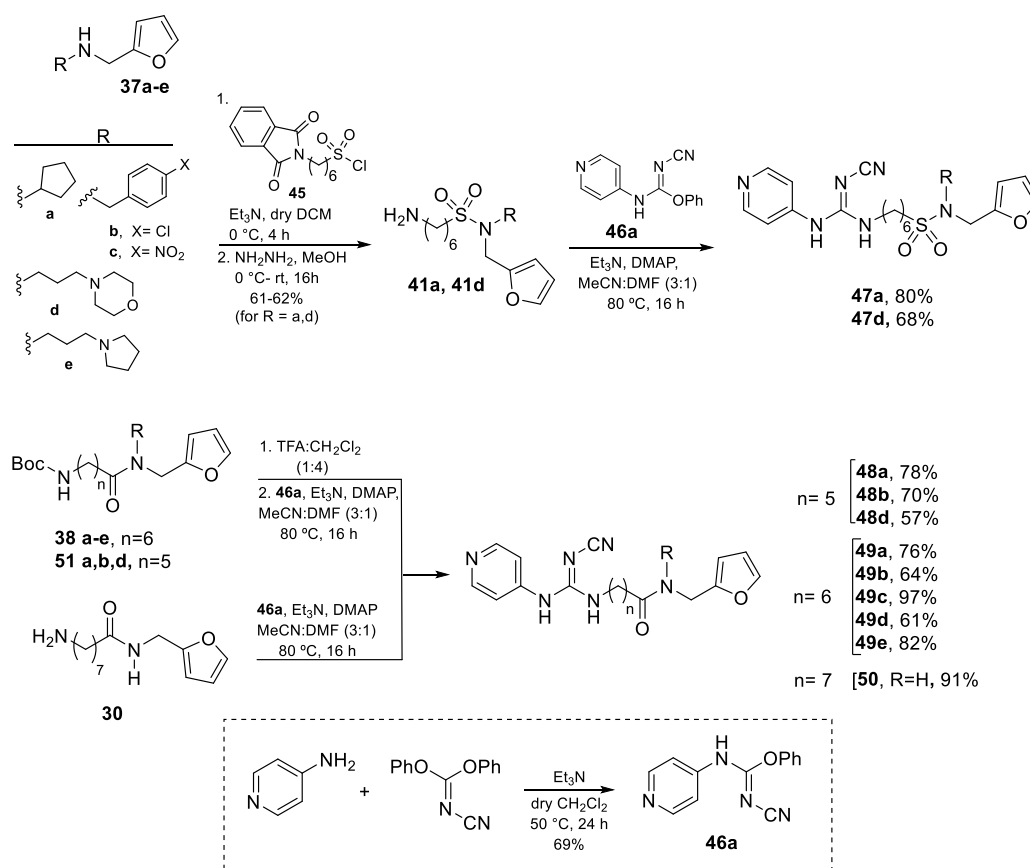


Scheme 8. Synthesis of (pyridin-3-yl)thiourea-based compounds **39** and **40**.

1.3.1.3 Preparation of (pyridin-3/4-yl)cyanoguanidine-based inhibitors

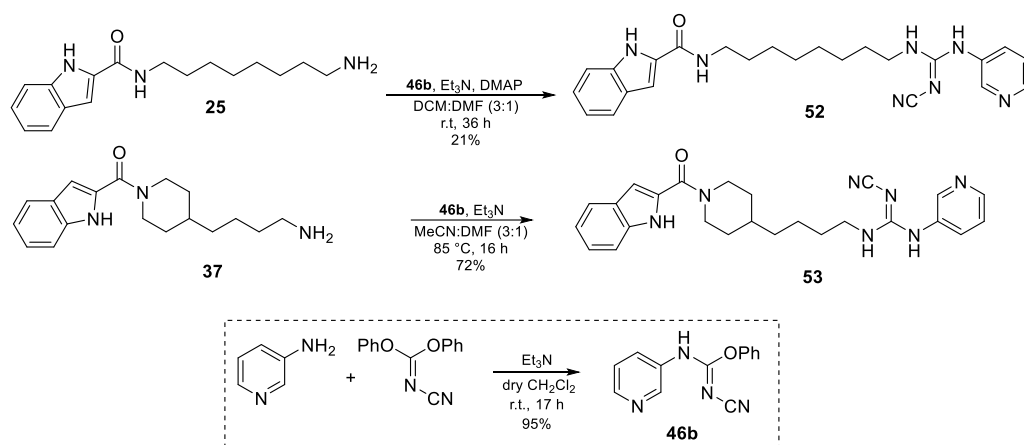
The preparation of this family of compounds (Scheme 9) was carried out starting from *N*-alkyl furfurylamine precursors **37a-e**, obtained through reductive amination of furfural with several commercial amines (see Experimental Section for synthetic details). Reaction of **37a** and **37d** with sulfonyl chloride **45** followed by hydrazinolysis gave sulfonamides **41a** and **41d**. Subsequent coupling with phenyl *N*-cyano-*N'*-(pyridin-4-yl)carbamimidate **46a**, easily prepared from commercial diphenyl cyanocarbonimidate, gave compounds **47a** and **47d**, respectively in moderate-to-good yields. On the other hand, deprotection of Boc derivatives **38a-e**, **51a**, **51b**, **51d** (see Experimental Section for their synthesis) and subsequent coupling with carbamimidate **46a** furnished derivatives **48a**, **48b**, **48d** and **49a-e** in moderate-to-

good yields. Compound **50** was obtained by reaction of **30** with **46a** under the same standard coupling conditions.



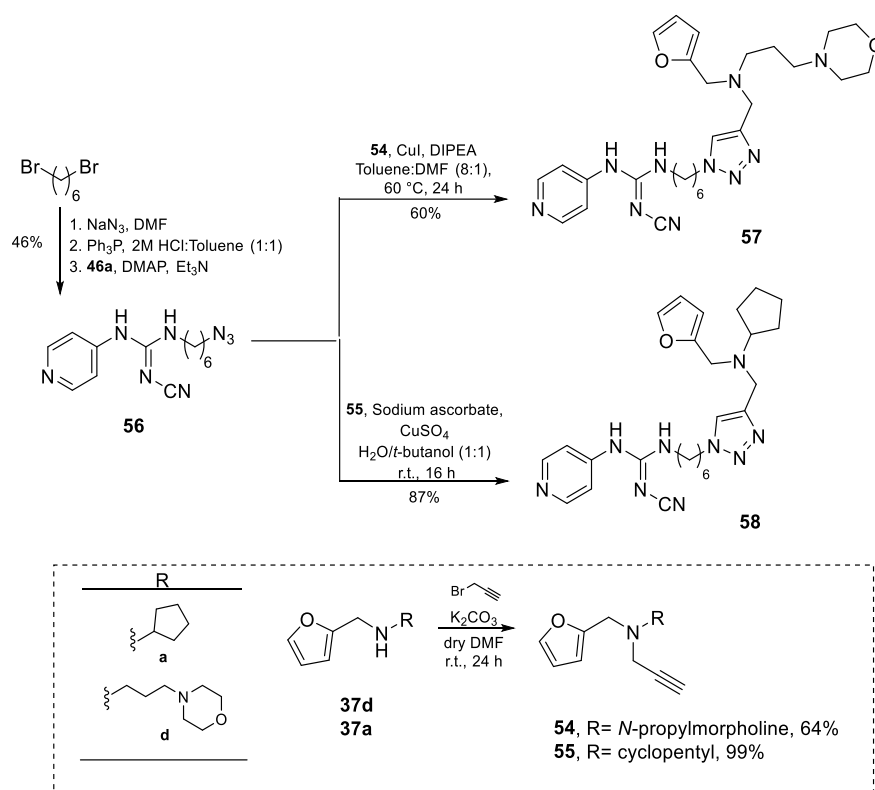
Scheme 9. Synthesis of (pyridin-4-yl)cyanoguanidine-based inhibitors **47a**, **47d**, **48a-b**, **48d**, **49a-e** and **50**.

Reaction of indole derivatives **25** and **37** with phenyl *N*-cyano-*N'*-(pyridin-3-yl)carbamimidate **46b**, easily prepared from commercial diphenyl cyanocarbonimidate and 3-aminopyridine, afforded indole (pyridin-3-yl) cyanoguanidine derivatives **52** and **53** in moderate-to-good yields (Scheme 10).



Scheme 10. Synthesis of (pyridin-3-yl)cyanoguanidine-based inhibitors **52** and **53**.

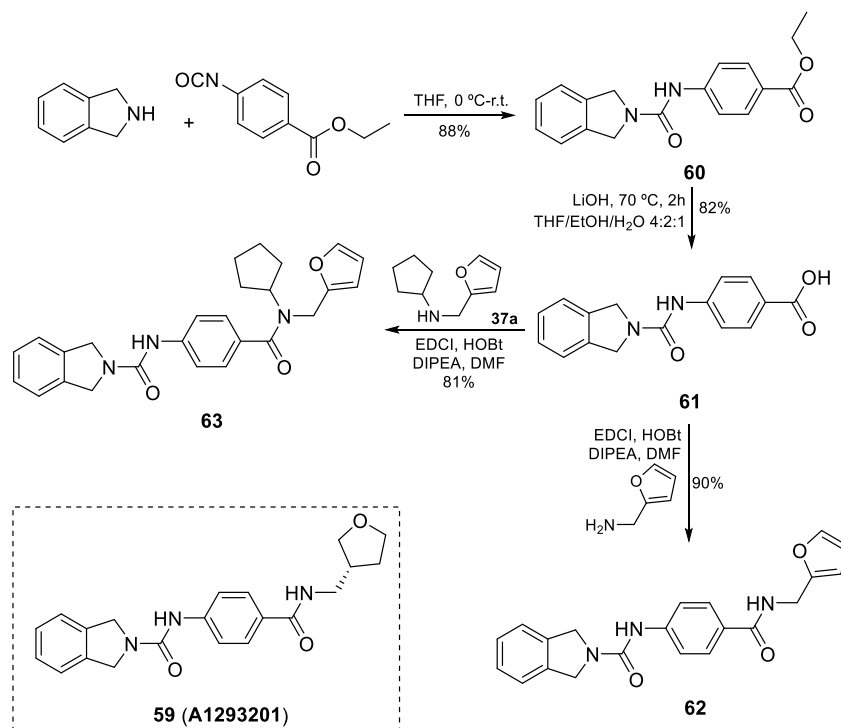
As most compounds of these two subfamilies showed excellent results in cytotoxicity assays (see Table 2, pag. 57), two new analogues (compounds **57** and **58**) that present a triazole moiety linking the tunnel binder and the furan tail were prepared (Scheme 11). Thus, reaction of 1,6-dibromohexane with an excess of sodium azide gave the corresponding diazido derivative, which was further subjected to a controlled Staudinger reduction in biphasic media affording the corresponding monoamino derivative. Subsequent coupling with **46a** gave azido derivative **56** with a moderate overall yield (46%, 3 steps). CuAAC reactions of **56** and terminal alkynes **54** and **55**, previously synthesized by *N*-alkylation of **37d** and **37a** with propargyl bromide, gave final compounds **57** and **58** in good-to-excellent yields, respectively.



Scheme 11. Synthesis of (pyridin-4-yl)cyanoguanidine-based inhibitors **57** and **58**.

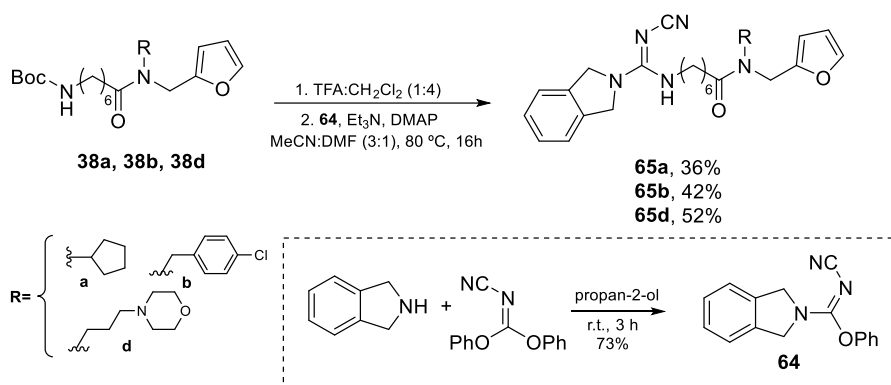
1.3.1.4 Synthesis of nonsubstrate compounds

It has been recently demonstrated that phosphorylation of the pyridine nitrogen of NAMPT inhibitors is not required for *in vivo* antitumor efficacy³² as it has been previously postulated.³³ Therefore, we decided to synthesize non pyridine-based structures as possible NAMPT inhibitors. First, we focused on the preparation of isoindoline-based derivatives inspired by the interesting results previously obtained with NAMPT inhibitor **A1293201** (Figure 12, pag. 41).³² Thus, the reaction between commercial isoindoline and ethyl 4-isocyanobenzoate gave urea **60** (Scheme 12). Basic hydrolysis of **60** followed by standard amide coupling between the resulting acid **61** and furfurylamine provided final compound **62** (the furyl analogue of **59**). A similar strategy was followed for the preparation of **63**, except that *N*-cyclopentylfurfurylamine **37a** was used in the final coupling.



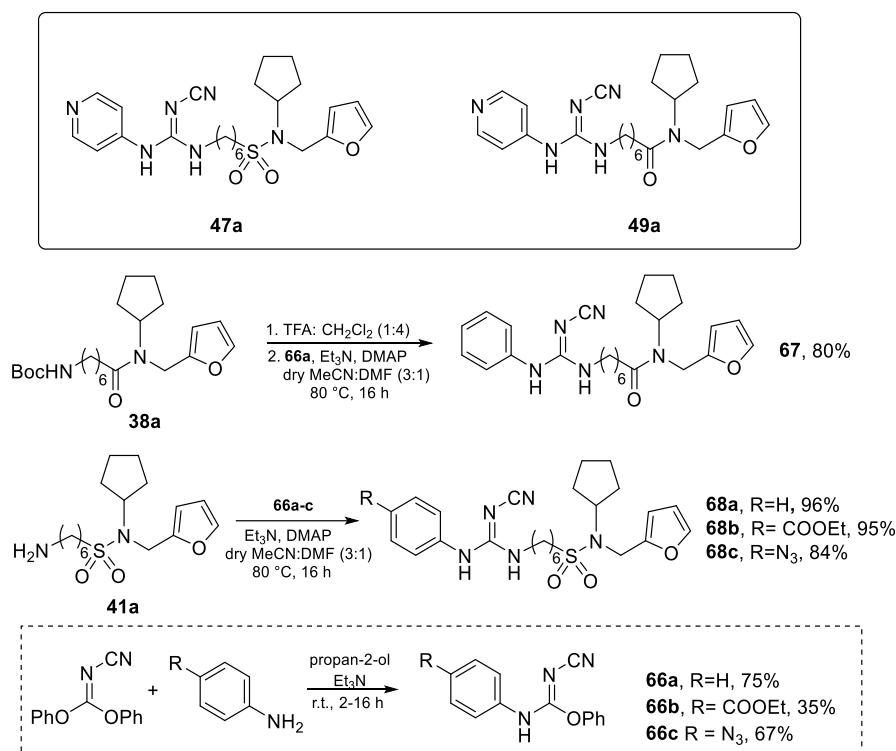
Scheme 12. Synthesis of isoindoline-based NAMPT inhibitors **62** and **63**.

Then, we decided to synthesize the isoindoline analogues (compounds **65a**, **65b** and **65d**, Scheme 13) of three of the most cytotoxic cyanoguanidine derivatives (**49a**, **49b**, **49d**, (Scheme 9, pag. 48; Table 2, pag. 57)). Thus, acidic deprotection of **38a**, **38b** and **38d** followed by reaction with phenyl *N*-cyanoisoindoline-2-carbimide **64**, previously synthesized by coupling of isoindoline with diphenyl cyanocarbonimide, afforded **65a**, **65b** and **65d** respectively, in moderate yield.



Scheme 13. Synthesis of isoindoline-based inhibitors **65a**, **65b** and **65d**.

Finally, we decided to replace the pyridin-4-yl moiety by a phenyl group in two highly cytotoxic cyanoguanidines, sulfonamide **47a** and its amide analogue **49a**. The synthesis of these new non-pyridine analogues (compounds **67** and **68a-c**) is depicted in Scheme 14. Acidic deprotection of compound **38a** followed by coupling reaction with phenyl *N*-cyano-*N'*-phenylcarbamimidate **66a** afforded derivative **67** in good yield. Similarly, reaction of amine **41a** with carbamimidates **66a-c** yielded final compounds **68a-c**. (*p*-Substituted) phenyl *N*-cyano-*N'*-phenylcarbamimidates **66a-c** were prepared by reaction of diphenyl cyanocarbonimidate with *p*-substituted anilines under the same conditions previously used for the preparation of analogue **64**.



Scheme 14. Synthesis of phenyl-based inhibitors **67**, and **68a-c**.

1.3.2 BIOLOGICAL EVALUATION

1.3.2.1 Cytotoxicity on MIA PaCa-2 cells, effect on intracellular NAD⁺ concentration and NAMPT inhibition.

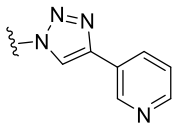
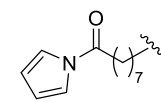
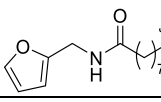
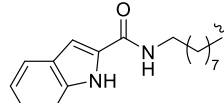
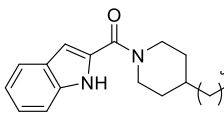
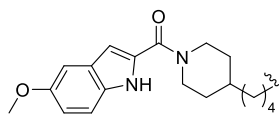
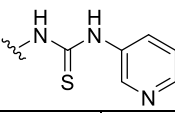
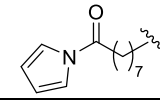
The new compounds were tested *in vitro* for their anti-proliferative effects towards MIA PaCa-2 cells in Dr. Alessio Nencioni's group at the University of Genova (Table 2). The human pancreatic cancer cell line MIA PaCa-2 was used as a model in the cytotoxicity assays as it is known that this cell line is sensitive to NAMPT inhibitors.³⁸ Triazoles **19-23** were much less active than **FK866** (Table 2, entries 2-6) towards MIA PaCa-2, with IC₅₀ values in the micromolar range. Compounds **22** and **23** were approximately 300-fold less cytotoxic than **FK866**, what indicates that the substitution of the acrylamide group by a triazole and the benzamido group by a more hydrophilic indole substituent was detrimental for the biological activity. A similar modification was introduced in compounds **35** (Table 2, entry 10), and **53** (Table 2,

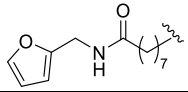
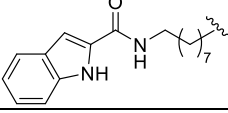
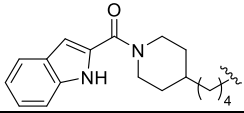
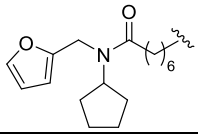
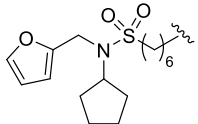

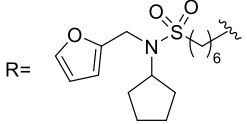
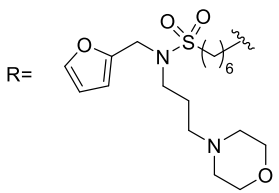
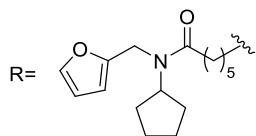
entry 25), with the exception that a thiourea and a cyanoguanidine groups were incorporated, respectively, instead of the triazole moiety of **22**. Cyanoguanidine **53** (Table 2, entry 25) showed a cytotoxic effect 6.4-fold greater than triazole **22** while the cytotoxicity of thiourea **35** (Table 2, entry 10) was even lower than that presented by compound **22**. Other pyridine-3-yl thioureas were also prepared using a more flexible tunnel binder (C6 or C7 alkyl chain) to connect the thiourea and tail groups. One of the members of this family, sulfonamide **40**, showed a high cytotoxicity ($IC_{50} = 16.4$ nM, Table 2, entry 12). The comparison of the cytotoxicity of **40** and its amide analogue **39** ($IC_{50} = 153$ nM, Table 2, entry 11) clearly showed the benefit of having a sulfonamide group to connect the tail group (a furan moiety in both cases). Additionally, the sulfonamide can behave as a very good hydrogen bond acceptor for the interaction within the binding site of NAMPT. The analysis of the cytotoxicity of (pyridin-3/4-yl)cyanoguanidine derivatives **47a**, **47d**, **48a**, **48b**, **48d**, **49a-49e**, **52** and **53** afforded several conclusions. Most cyanoguanidines (Table 2, entries 13-22) belong to a general structure which contains: 1) a flexible alkyl C5 or C6 carbon chain as a tunnel binder connecting cyanoguanidine and tail groups through a tertiary amide/sulfonamide function and 2) a furan as a tail group. The cytotoxicity of these compounds was excellent with $IC_{50} < 16$ nM. In fact, in many cases, the IC_{50} values were lower than those obtained for **FK866** in this cell line (2.4 nM). The C5 alkyl chain was always found to lead to slightly higher IC_{50} values (less cytotoxicity) than the C6 alkyl chain in different analogues (entry 15 vs 18, entry 16 vs 19, entry 17 vs 21). In the series of tertiary amides, different *N*-substituents together with the 2-furfuryl group were used, but no high differences in cytotoxicity were observed, being the compounds with *N*-cyclopentyl group slightly better cytotoxic agents than the rest of molecules (entry 15 vs entries 16,17; entry 18 vs entries 19-22). As was already observed for the family of pyridine-3-yl thioureas, the substitution of the amide function in *N*-cyclopentylamide **49a** with a *N*-cyclopentylsulfonamide led to a great improvement of the cytotoxic activity (entry 18 vs 13), yielding the most potent compound of this study (compound **47a**, $IC_{50} = 5$ μ M). Another example where the

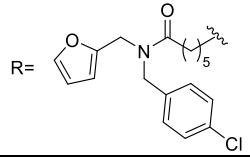
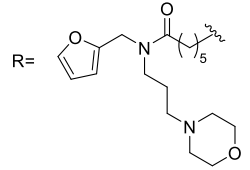
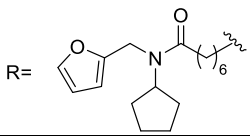
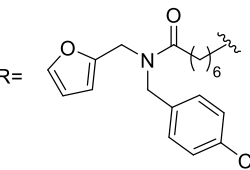
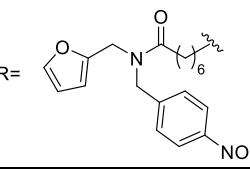
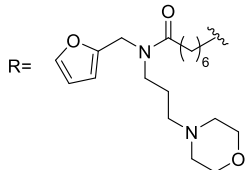
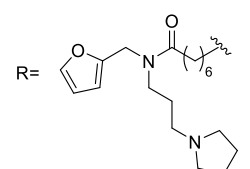
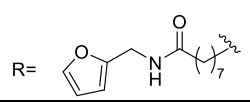
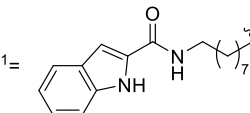
bioisosterism led to a compound with improved potency is represented by the non-substrate inhibitor **68a** (Table 2, entry 34). Compared to the amide analogue **67** (entry 34 vs 33), the sulfonamide **68a** showed an increase in potency of 40-fold. However, amide **49d** and sulfonamide **47d** (Table 2, entries 21 and 14), presented similar cytotoxicity. The NMR spectra of **47d** showed signals corresponding to a mixture of rotamers, in contrast with the other sulfonamide derivatives where only one set of signals was observed in the ^1H and ^{13}C NMR spectra. Our hypothesis to explain the lower cytotoxicity of **47d** compared to other sulfonamide derivatives is that one of the rotamers could fit better than the other at the active site of NAMPT due to a more favorable binding pose, leading to a decrease in the global binding efficacy of the compound. In addition to amide and sulfonamide connecting groups, the triazole moiety was also explored in some of the cyanoguanidine family of compounds. The biological evaluation of **57** and **58** showed a decrease in their cytotoxicity compared to amides **49d** and **49a** or sulfonamides **47d** and **47a**, respectively (entry 26 vs entries 21,14; entry 27 vs entries 18 and 13). Finally, the activity of the series of non-pyridine-based compounds was also analysed. Replacement of pyridine with an isoindoline group was detrimental to the antitumor activity of the compounds in all cases (entries 28-32 vs. entries 19-21). Compounds **62** and **63** (Table 2, entries 28, 29), which have a 2-furyl moiety instead of the 3-tetrahydrofuryl group of **A1293201** (compound **59**, Scheme 12, pag. 51), showed cytotoxicity in the μM range (entries 28 and 29) as in the case of the other isoindoline analogues **65a**, **65b** and **65d** (entries 30-32). Replacement of the pyridine-4-yl moiety in the highly cytotoxic sulfonamide **47a** with a phenyl or 4-substituted phenyl moieties (compounds **67** and **68a-c**) was detrimental in terms of cytotoxicity (entry 13 vs. entries 33-36). Compound **68a** was the most cytotoxic compound in this family of non-pyridine-based inhibitors with an IC_{50} = 176 nM.

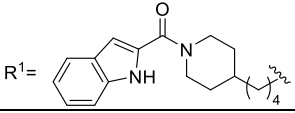
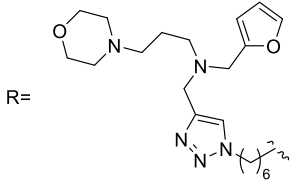
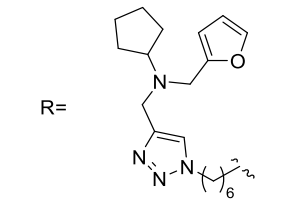
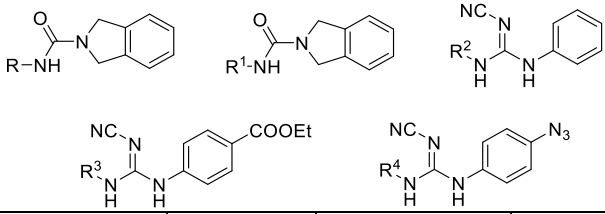
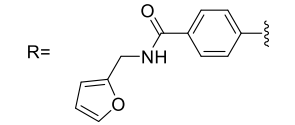
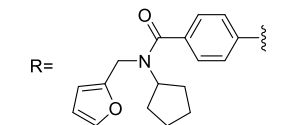
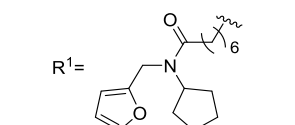
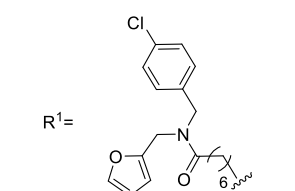
Next, we evaluated intracellular NAD⁺ concentration (iNAD⁺) in MIA PaCa-2 cells in response to the most cytotoxic compounds, to confirm that the observed antitumor effect was associated with NAD⁺ depletion, which would be in line with these compounds being NAMPT inhibitors. Consistent with this hypothesis, all the compounds tested reduced the concentration of NAD⁺ in cells (Table 2). Some of the compounds (**40**, **47a**, **47d**, **48a**, **48b**, **49a-c**) reduced iNAD⁺ to similar, or even greater extent, compared to **FK866**. Compound **68a**, a non-pyridine-based compound, reduced iNAD⁺ when added in the nM range. Compounds **40**, **47a**, **49a** and **58**, which all effectively lowered iNAD⁺ levels, were also assayed as NAMPT inhibitors on the recombinant enzyme. All these compounds exerted a strong inhibition of NAMPT activity (IC₅₀ < 70 nM). Again, compound **47a** showed the highest potency (ie, IC₅₀ = 3.5 nM), which was similar to the potency of the reference compound, **FK866** (IC₅₀ = 3.3 nM). Interestingly, the potency of **47a** in terms of inhibition of recombinant NAMPT did not exactly match its cytotoxic activity in MIA PaCa-2 cells, the latter being already clearly detectable in the low μ M range. For the other compounds, **40**, **49a** and **58**, inhibiting NAMPT activity in the sub-nanomolar range, no such discrepancy was observed. Therefore, these results suggest that the exceptional cytotoxic activity of **47a** may also reflect other mechanisms in addition to NAMPT inhibition in MIA PaCa-2 cells. Indeed, in MDA-MB-231 (triple-negative breast cancer cell line), the IC₅₀s obtained with **47a** for iNAD⁺ reduction and for cell toxicity were similar (0.56 \pm 0.15 and 0.47 \pm 0.64 nM, respectively). By comparison, in these cells, the **FK866** IC₅₀s for iNAD⁺ depletion and cell toxicity were 0.54 \pm 0.12 and 3.47 \pm 0.41 nM, respectively, being similar values to those obtained in MIA PaCa-2 cells. The time-dependent decrease in NAD⁺ and ATP levels in MIA PaCa-2 cells demonstrated that the high cytotoxic activity observed in the presence of **47a** is not due to a NAD⁺-unrelated intracellular ATP depletion, since NAD⁺ decrease preceded the fall in ATP levels (Figure 14A). Cell death induced by **FK866** analogues could be due to the triggering of apoptotic processes, as confirmed by the detection of PARP cleavage after 48 hours of treatment with compound **47a** and **58** (Figure 14B).

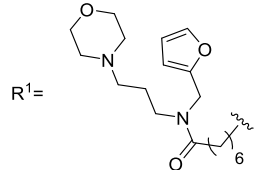
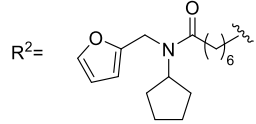
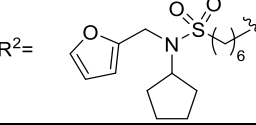
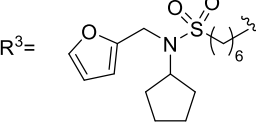
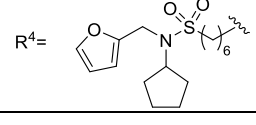
Table 2. Evaluation of the cytotoxicity and iNAD⁺ depletion on MIA PaCa-2 cells for the new compounds. NAMPT inhibition assays. NA = not available. a) Data are mean ± SD, n ≥ 3.

Entry	R	Compound	Viability MIA PaCa-2 cells (IC ₅₀ in nM, except when indicated)	iNAD ⁺ depletion 24h on MIA PaCa-2 cells (IC ₅₀ in nM)	NAMPT inhibition assay (IC ₅₀ in nM)
1		1 (FK866)	2.4±0.5	0.34±0.08	3.27±0.38
(Pyridin-3-yl)triazoles					
					
2		19	494±143	NA	NA
3		20	> 1000	NA	NA
4		21	549±101	NA	NA
5		22	727±187	NA	NA
6		23	860±191	NA	NA
(Pyridin-3-yl)thioureas					
					
7		32	854±188.5	NA	NA

8		33	> 1000	NA	NA
9		34	605±140.5	NA	NA
10		35	> 1000	NA	NA
11		39	153±17.4	NA	NA
12		40	16.4±2.4	0.43±0.11	69.1±4.43
<i>(Pyridin-3/4-yl)cyanoguanidines</i>					
					
13	R= 	47a	0.005±0.001	0.25±0.08	3.50±0.77
14	R= 	47d	2.26±0.37	1.50±0.62	NA
15	R= 	48a	3.0±0.9	0.20±0.05	NA

16		48b	6.3±1.7	0.50±0.12	NA
17		48d	16.3±2.6	11.25±0.65	NA
18		49a	0.45±0.09	0.88±0.32	12.45±0.50
19		49b	1.7±0.4	0.17±0.05	NA
20		49c	2.1±0.6	0.14±0.04	NA
21		49d	3.0±0.8	1.43±0.49	NA
22		49e	4.5±0.1	2.00±0.78	NA
23		50	> 1000	NA	NA
24		52	81±15	NA	NA

25		53	113±14	NA	NA
26		57	25.8±6.7	2.36±0.75	NA
27		58	2.81±0.76	1.48±0.33	4.98±0.46
<i>Non pyridine-based inhibitors</i>					
					
28		62	> 1000	NA	NA
29		63	> 1000	NA	NA
30		65a	> 1000	NA	NA
31		65b	> 1000	NA	NA

32	R ¹ = 	65d	> 1000	NA	NA
33	R ² = 	67	> 1000	NA	NA
34	R ² = 	68a	176 ± 12	4.70 ± 0.27	NA
35	R ³ = 	68b	738 ± 148	NA	NA
36	R ⁴ = 	68c	> 1000	NA	NA

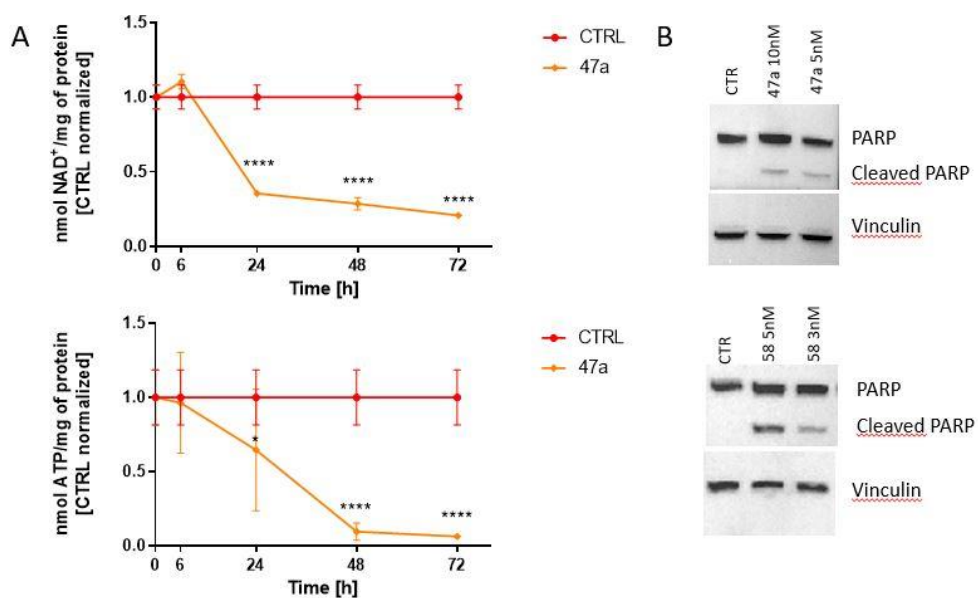


Figure 14. A) Time-dependent intracellular NAD⁺ and ATP depletion of **47a** on MIA PaCa-2 cells. **B)** Cleaved PARP detection after 48h treatment with **47a** and **58** on MIA PaCa-2 cells.

1.3.2.2 Cytotoxicity on haematological cancer cells

To demonstrate the broad antitumor activity of the new compounds, a selection of the most promising ones was evaluated *in vitro* by the research group of Prof. Michel Duchosal at the Centre Hospitalier Universitaire Vaudois (CHUV, Lausanne). The compounds have been evaluated in cells from various haematological malignancies, including acute myeloid leukemia (AML; ML2 and NB4); acute lymphoblastic leukemia (ALL; Jurkat); Burkitt's lymphoma (BL; Namalwa) and multiple myeloma (MM; RPMI8226). As summarized in Table 3, **47a** showed the highest antitumor activity against acute myeloid leukemia (ML2), with IC_{50} in the picomolar range (IC_{50} = 18 pM). Two other compounds **49a** and **58** also presented cytotoxicity in the picomolar range with IC_{50} of 46 and 49 pM, respectively. Overall, these three molecules were the most potent cytotoxic compounds, and AML cells were the most sensitive cells to all inhibitors tested.

Table 3. Evaluation of the cytotoxicity on different haematological cancer cell lines for compounds **40**, **47a**, **48a**, **49a**, **49c**, **58** and **68a** depicted as IC_{50} [nM]. NA = not available. nd: not detected; ML2: acute myeloid leukemia (M4); JRKT: acute lymphoblastic leukemia; NMLW: Burkitt lymphoma; RPMI8226: multiple myeloma; NB4: acute myeloid leukemia (M3). Data are mean \pm SD, $n \geq 3$.

Compound	MIA PaCa-2	ML2	JRKT	NMLW	RPMI8226	NB4
1 (FK866)	2.4 \pm 0.5	0.24 \pm 0.08	0.73 \pm 0.04	0.37 \pm 0.09	0.76 \pm 0.08	2.0 \pm 0.2
40	16.4 \pm 2.4	3.1 \pm 0.1	NA	4.23 \pm 1	20.15 \pm 2	NA
47a	0.005 \pm 0.001	0.018 \pm 0.001	0.15 \pm 0.001	0.23 \pm 0.08	0.16 \pm 0.04	0.4 \pm 0.1
48a	3.0 \pm 0.9	0.36 \pm 0.01	NA	1.77 \pm 0.1	1.9 \pm 0.1	NA
49a	0.45 \pm 0.09	0.046 \pm 0.01	0.2 \pm 0.01	0.33 \pm 0.01	0.27 \pm 0.01	0.6 \pm 0.03
49c	2.1 \pm 0.6	0.32 \pm 0.01	NA	1.39 \pm 0.5	2.1 \pm 0.2	NA
58	2.81 \pm 0.76	0.049 \pm 0.01	0.5 \pm 0.01	0.3 \pm 0.04	0.47 \pm 0.09	0.7 \pm 0.01
68a	176 \pm 12	nd	NA	nd	nd	NA

Therefore, **47a**, **49a** and **58** together with **FK866** as a positive control were further used to decipher their molecular mechanism of action in blood cancers. To this end, the effect of the new NAMPT inhibitors on the intracellular NAD⁺ contents was assessed in several hematopoietic malignant cells.^{2,26,39} In agreement with data obtained on MIA PaCa-2 cells, all tested compounds led to a profound NAD⁺ depletion in a time dependent manner (Figure 15A, B, C). NAD⁺ concentrations decreased by half already after 6 hours and were completely depleted after 24 hours. Moreover, compound **47a** was the most efficient to deplete iNAD⁺ in haematological cancer cells, with the lowest iNAD⁺ IC₅₀ compared to **FK866** (Table 4). As NAD⁺ cell content plays an important role in ATP synthesis, the impact of these NAMPT inhibitors on intracellular ATP content was next evaluated. As expected, the drop in NAD⁺ cell content was followed by that of ATP (Figure 15D, E, F).

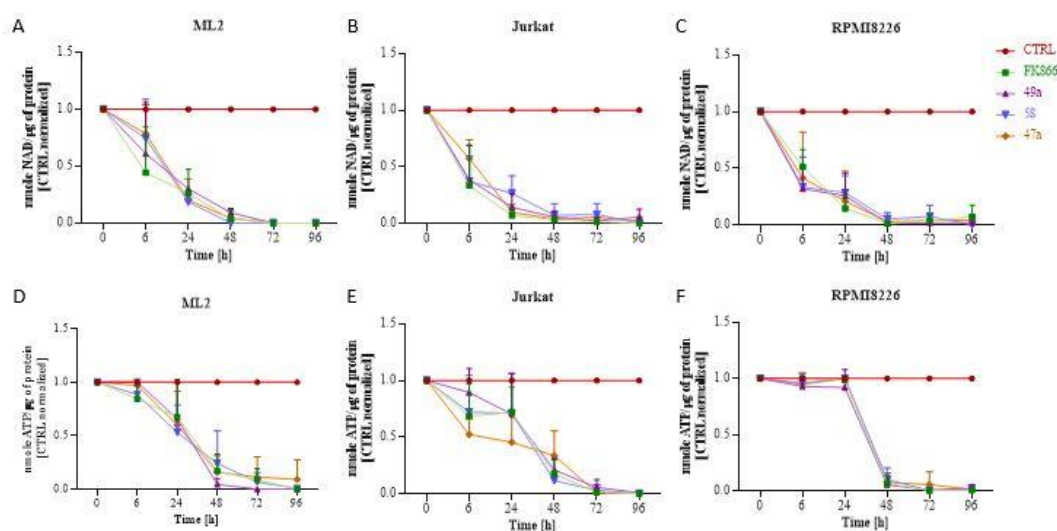


Figure 15. NAMPT inhibitors induce depletion of intracellular NAD⁺ and ATP. ML2 (A, D), Jurkat (B, E) and RPMI8226 (C, F) cells were incubated with **FK866**, **47a**, **49a** and **58** for 96 hours. Intracellular NAD⁺ (A, B, C) and ATP (D, E, F) contents were measured every day. Both, NAD⁺ and ATP concentrations were first normalized to the total protein and then to control at each time point. Data are \pm SD, n=4.

Table 4. Evaluation of iNAD⁺ depletion after 24h of drug treatment on different haematological cancer cell lines for compounds **FK866**, **47a**, and **58** depicted as IC₅₀ [nM]. Data are mean ± SD, n ≥ 3.

Compound	ML2	JRKT	RPMI8226
1 (FK866)	0.11±0.03	0.37±0.003	0.1±0.005
47a	0.05±0.03	0.09±0.009	0.05±0.01
58	0.09±0.01	0.21±0.2	0.06±0.04

The intracellular content of NAD(P)H/NAD(P)⁺ plays a crucial role in oxidative stress and thus, the depletion of NAD⁺ upon exposure to NAMPT inhibitors is expected to result in an increased ROS production.⁴⁰ To test this issue, mitochondrial (mO₂⁻) and cytosolic (cO₂⁻) superoxide anions, as well as intracellular hydrogen peroxide (H₂O₂) were monitored in leukemic cells treated with **FK866**, **47a**, **49a** and **58** using MitoSOX, DHE, and carboxy-H2DCFDA probes, respectively. The novel compounds caused a tremendous increase in ROS levels production in all treated cell types (Figure 16A-F).

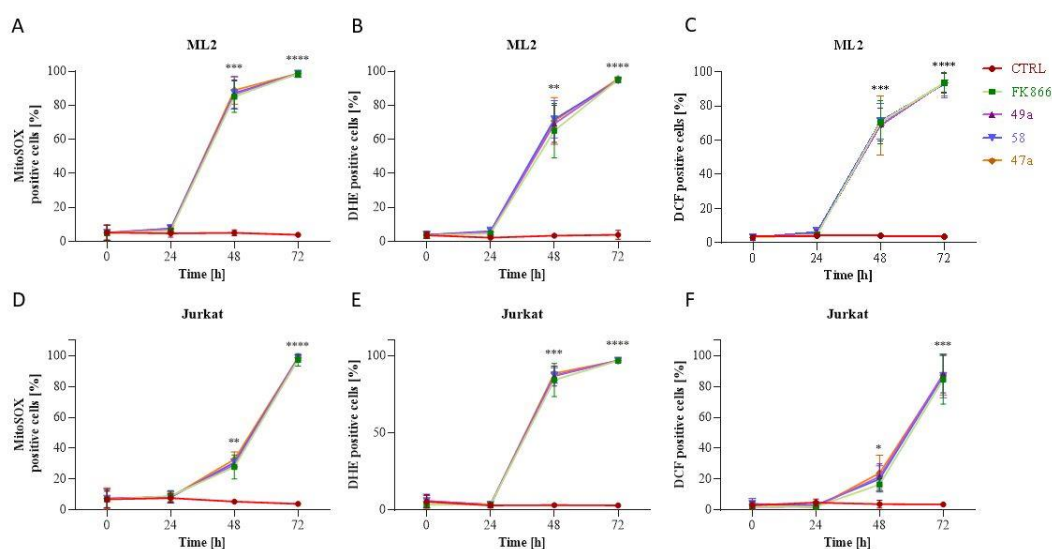


Figure 16. NAMPT inhibitors induce ROS production upon cell death in malignant cells. ML2 (A, B, C) and Jurkat (D, E, F) cells were treated with **FK866**, **47a**, **49a** and **58** for 72 h. Mitochondrial (A, D), cytosolic (B, E) superoxide anions, and hydrogen peroxide (C, F) were detected with MitoSOX, DHE and H2DCFDA probes, respectively, using flow cytometry. The percentage of positive cells is proportional to the amount of superoxide anions and hydrogen peroxide produced. Data are ± SD, n=3, **P<0.005, ***P<0.001, ****P<0.0001.

Excess ROS generation is known to lead to mitochondrial damage. Therefore, we evaluated whether these compounds could affect the mitochondrial membrane potential (MMP). Different hematopoietic malignant cells were exposed to NAMPT inhibitors and a time-dependent analysis of the MMP loss was measured using a fluorescent dye (TMRM) and flow cytometry analysis. As shown in Figure 17A – C, treatment with the new NAMPT inhibitors (**47a**, **49a** and **58**) induced a potent, time-dependent mitochondrial membrane depolarization at 72 hours, but not at earlier time point (24 hours; Figure 17A – C). The timing of MMP loss correlates with that of cell death (Figure 17D – F).

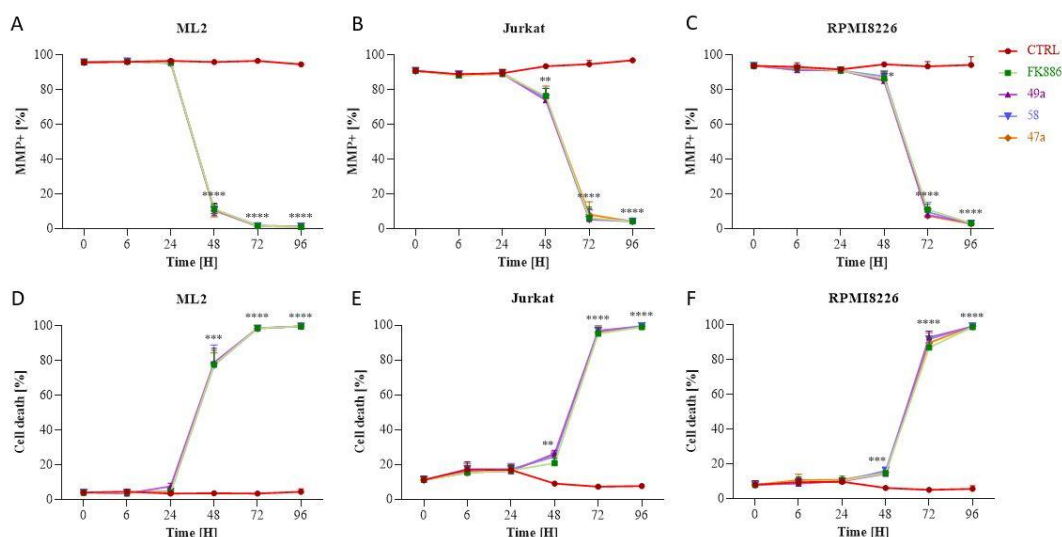


Figure 17. NAMPT inhibitors induce the loss of MMP and cell death over time. ML2 (A, D), Jurkat (B, E) and RPMI8226 (C, F) cells were incubated with **FK866**, **47a**, **49a** and **58** for 96 hours. MMP (A, B, C) and cell death (D, E, F) were measured every day over a period of 96 hours. MMP was measured using TMRM staining, and cell death is depicted here as a total cell death consisting of annexin V (ANXN) and 7AAD stainings. Both were assessed with flow cytometry. Data are \pm SD, $n=3$. * $P<0.05$, ** $P<0.005$, *** $P<0.001$, **** $P<0.0001$.

To provide evidence that NAD^+ depletion is the primary cause of cell death in malignant cells treated with the new NAMPT inhibitors **47a**, **49a** and **58**, various hematopoietic malignant cells were incubated with the inhibitors and with an excess of NAD^+ precursors (NAM, nicotinic acid [NA]) or NAD^+ itself. Cell death was monitored as described above. Indeed, supplementation with NAM, NA, or NAD^+ fully

blunted the killing effect of all tested NAMPT inhibitors (Figure 18A – C), supporting that NAD⁺ depletion was responsible for cell death.

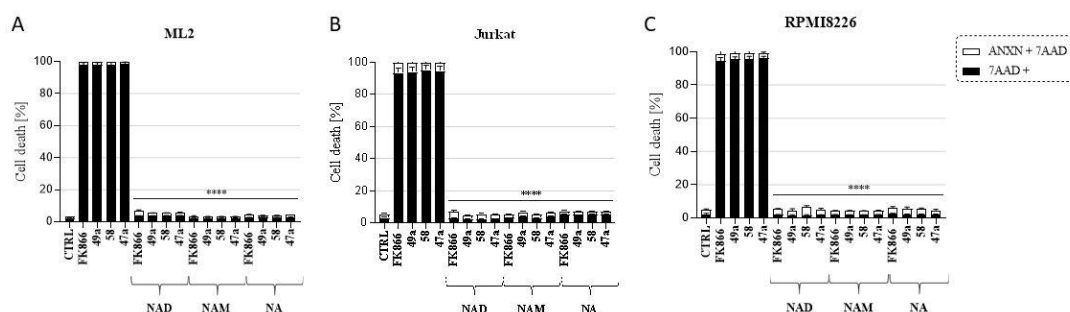


Figure 18. The addition of NAD, NAM, and NA can reverse the cytotoxic effect of NAMPT inhibitors. ML2 (A), Jurkat (B) and RPMI8226 (C) cells were incubated for 96 hours with **FK866**, **47a**, **49a** and **58** without or with NAD (0.5 mM), NAM (1 mM) or NA (10 μ M). Cell death was assessed with flow cytometry by double staining with annexin V (ANXN) and 7AAD after 96 hours of treatment. The percentages of early apoptotic cells (ANXN+ 7AAD-) are shown in white and the percentage of late apoptotic and dead cells (7AAD+) are shown in black. Data are \pm SD, n=3. ****P<0.0001 (inhibitors treated vs. NAD, NAM, and NA groups).

Duchosal *et al*/ previously reported that treatment with **FK866** leads to the decrease in catalase (CAT), a powerful ROS scavenger enzyme, resulting in ROS accumulation, what ultimately leads to cell death. Therefore, we tested the ability of CAT to prevent the cell death mediated by the new NAMPT inhibitors. As shown in Figure 19 the extracellular addition of CAT before **47a**, **49a** and **58** fully abrogated their cytotoxic effects, which is in line with previous studies.^{41,42}

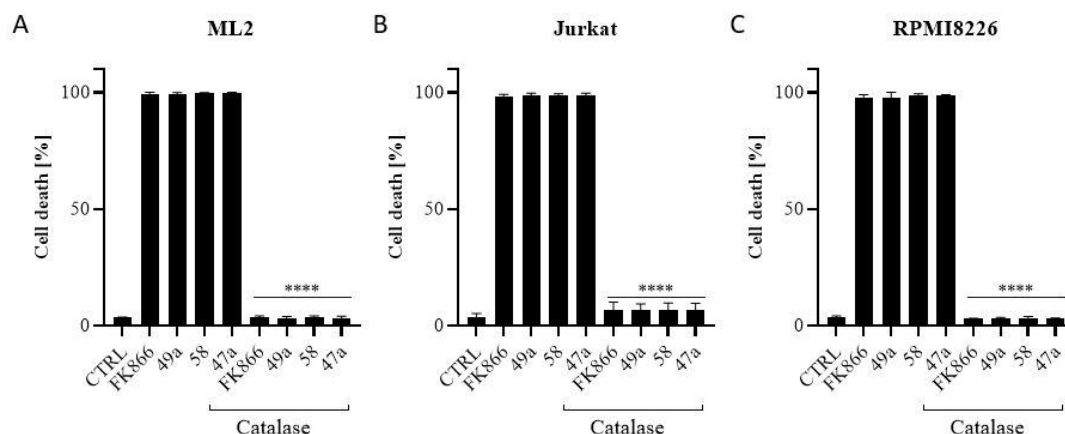


Figure 19. Supplementation of catalase abrogates the killing effect of **FK866**, **49a**, **58** and **47a** in tested cell lines. Catalase was added 1 hour before the inhibitors. The cell death at 96 hours was assessed on ML2 (A), Jurkat (B) and RPMI8226 (C). Cell death was determined as in Figure 18 and is depicted here as total cell death. Data are \pm SD, n=3. ****P<0.0001 (inhibitors treated vs. catalase treated groups).

Altogether, these results indicate that the new NAMPT inhibitors (**47a**, **49a** and **58**) could be promising antitumor agents. Mechanistically, these data demonstrate that, similarly to **FK866**, they deplete NAD^+ cell content, which induces ROS accumulation that damage mitochondria, leading to ATP loss, and ultimately to cell death. NAD^+ depletion was indeed responsible for cell death.

1.3.2.3 *In vivo* antitumor activity

Compounds **47a** and **58** were selected to further evaluate their *in vivo* efficacy using a xenograft mouse model of human acute myeloid leukemia. Both compounds had shown similar or increased potency in cytotoxicity, iNAD^+ depletion and NAMPT inhibition compared to reference compound **1** (**FK866**). The compounds (10 mg/Kg) were administered intraperitoneally twice a day for 4 days in a row for 3 weeks. In terms of safety, this dose was well tolerated, without signs of toxicity including no premature deaths, loss of body weight (Figure 20), lethargy or rough coat.

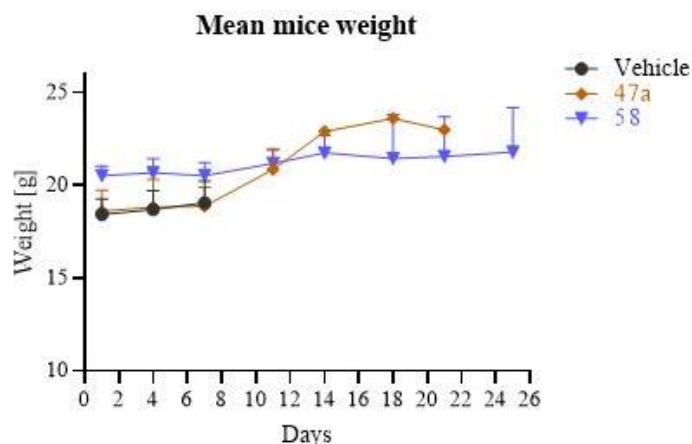


Figure 20. Mean mice weight after treatment with **47a** and **58**; $n_{\text{vehicle}}=3$, $n_{47a,58}=4$.

Regarding the *in vivo* efficacy, mice treated with compound **58** compared to vehicle (untreated), significantly delayed the tumor growth and prolonged mouse survival. On the other hand, only one tumor treated with **47a** decreased in volume up to two weeks and then increased again after the second cycle; the other tumors essentially grew similarly as in untreated group (Figure 21).

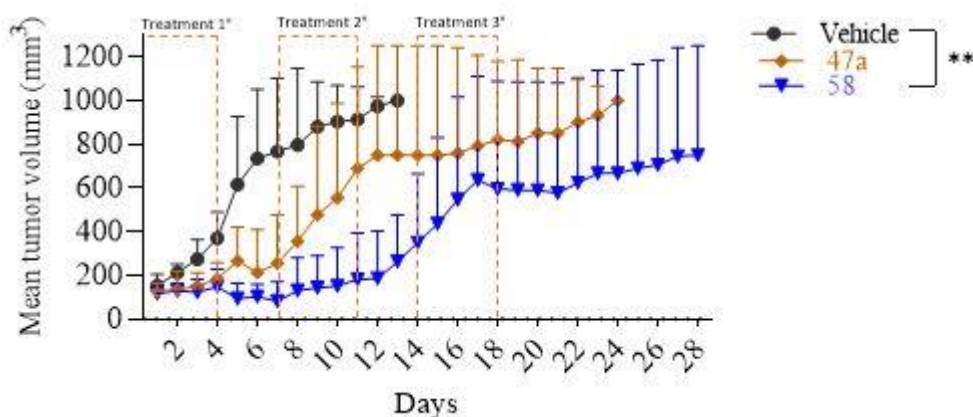


Figure 21. Mean tumor volume after treatment with **47a** and **58**. Treatment days are indicated in grey; $n_{\text{vehicle}}=3$, $n_{47a,58}=4$ with SD ** $P < 0.05$.

Although **FK866** significantly prolonged the life of the treated mice compared to **47a** and **58** (Figure 22), it is interesting to note that, especially in the latter group, the tumors relapsed at different time points.

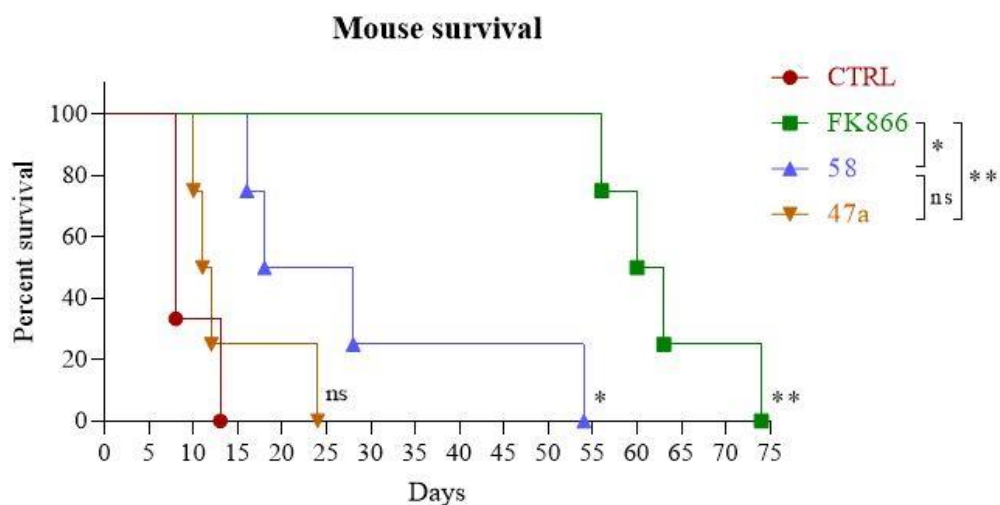


Figure 22. Mouse survival graph.

1.3.3 MOLECULAR MODELLING

Docking analysis (Glide) was performed to investigate the potential role of the furan of **47a** in the binding site of NAMPT (Crystal structure, PDB: 2GVJ). The binding pose of **1** (**FK866**) was mainly stabilized in the active site by a π - π stacking interaction of the pyridine ring with Phe193 and Tyr18' and H-bonding of the carbonyl group with Ser275 (Figure 23A). On the other hand, the docked structure of compound **47a** (Figure 23B) showed the π - π stacking interaction of the pyridine ring with Phe193, two hydrogen bonds between the cyanoguanidine moiety and Asp219 and a π - π stacking interaction of the furan tail group with Tyr188. As showed in recent publications, interactions of the tail group of NAMPT inhibitors with the enzyme have been reported to strongly enhance the inhibitory potency.⁹

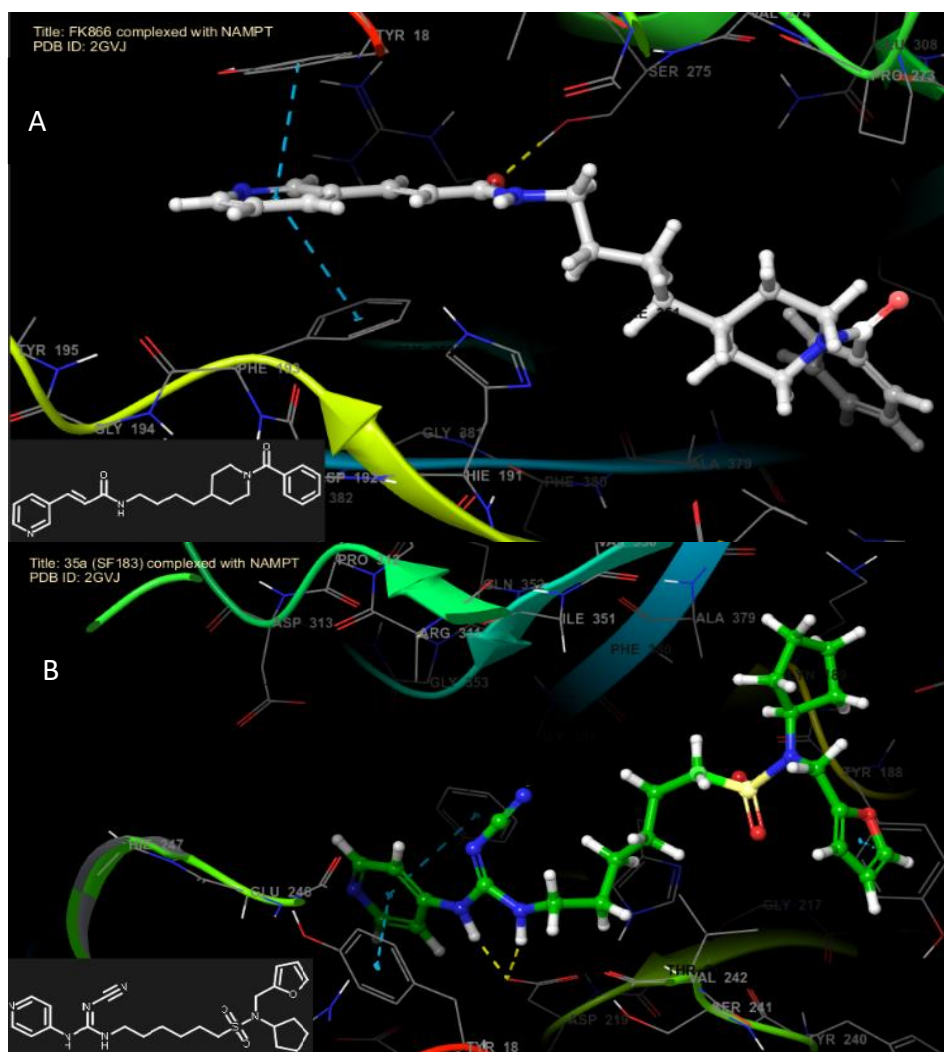
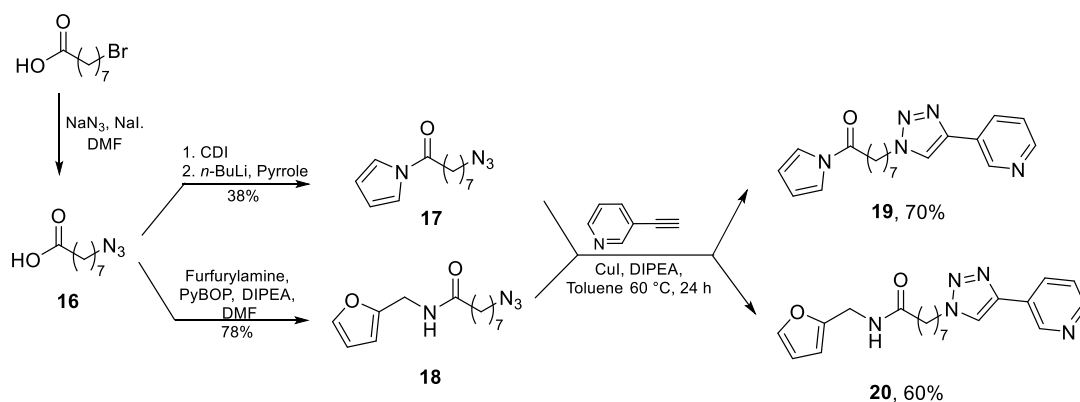


Figure 23. Compounds **1** (FK866) (A) and **47a** (B) docked in the active site of NAMPT (Crystal structure, PDB: 2GVJ). The cyanoguanidine moiety of compound **47a** clearly forms two hydrogen bonds with Asp219 while the furan group is stabilized by a π - π stacking interaction with Tyr188.

1.4 EXPERIMENTAL PART

Scheme 15. Synthesis of (pyridin-3-yl)triazole-based inhibitors **19** and **20**.**8-Azido-octanoic acid (16)**⁴³

Sodium azide (1.0 g, 16 mmol) and NaI (100 mg, 900 μ mol) in DMF (50 mL) were mixed. The mixture was stirred to form a heterogeneous suspension and 8-bromooctanoic acid (2.0 g, 9 mmol) was added. The reaction mixture was stirred at r.t. for 16 h, EtOAc was added, and the solution was cooled to 0 °C. To the resulting solution, 1 M HCl was added dropwise until the suspension became clear. The reaction mixture was extracted with EtOAc (3x). The organic layer was washed with brine (3x), dried over anhydrous Na₂SO₄, filtered, and concentrated *in vacuo* resulting in **16** as a yellow oil. The crude product was used in the next step without further purification. ¹H NMR (300 MHz, CDCl₃, δ ppm) 10.40 (s, 1H), 3.23 (t, *J* = 6.9 Hz, 2H), 2.32 (t, *J* = 7.4 Hz, 2H), 1.69 – 1.52 (m, 4H), 1.43 – 1.23 (m, 6H). NMR data match with those previously reported for this compound.

8-Azido-1-(1H-pyrrol-1-yl)octan-1-one (17)

A mixture of **16** (1.6 g, 8.4 mmol) and 1,1'-carbonyldiimidazole (1.4 g, 8.6 mmol) was dissolved in dry THF (20 mL) and the reaction was stirred under argon at r.t. for 16 h. Pyrrole (0.7 mL, 9.5 mmol) was taken up in dry THF (5 mL) and the solution was cooled to -78 °C. *n*-Butyl lithium (2.5 M in hexanes; 5 mL, 13 mmol) was added and the

mixture was stirred at -78 °C for 3 h under argon. Then, the activated compound was added quickly *via* syringe and the reaction was slowly warmed to r.t. and stirred overnight. A sat. aq. soln. of NH₄Cl was added and the mixture extracted with EtOAc (3x). The organic phases were dried over anh. NaSO₄, filtered, and concentrated in *vacuo*. Purification was performed by chromatography column on silica gel (EtOAc:Cy, 1:15) to yield **17** (800 mg, 38%) as a white solid. ¹H NMR (300 MHz, CDCl₃, δ ppm) 7.37 – 7.25 (m, 2H, pyrrole), 6.33 – 6.24 (m, 2H, pyrrole), 3.26 (t, *J* = 6.9 Hz, 2H, CH₂-N₃), 2.82 (t, *J* = 7.4 Hz, 2H, CH₂-CO), 1.84 – 1.73 (m, 2H, CH₂), 1.67 – 1.54 (m, 2H, CH₂), 1.43 – 1.35 (m, 6H, 3 CH₂). ¹³C NMR (75.4 MHz, CDCl₃, δ ppm) 170.6 (C=O), 119.1 (2 CH, pyrrole), 113.1 (2 CH, pyrrole), 51.5 (CH₂-N₃), 34.6 (CH₂-CO), 29.1 (CH₂), 29.0 (CH₂), 28.9 (CH₂), 26.6 (CH₂), 24.5 (CH₂). ESI-HRMS *m/z* calcd for C₁₂H₁₈N₄ONa [M+Na]⁺, 257.1373; found, 257.1373.

8-(4-(Pyridin-3-yl)-1H-1,2,3-triazol-1-yl)-1-(1H-pyrrol-1-yl)octan-1-one (19)

To a solution of **17** (50 mg, 210 μmol) in toluene (3 mL), 3-ethynylpyridine (45 mg, 430 μmol), DIPEA (140 μL, 810 μmol) and CuI (8 mg, 40 μmol) were added, and the solution was stirred at 60°C for 24 h. Quadrasil® resin (150 mg) was added and the mixture stirred for 1 h at r.t. Then, it was filtrated through a celite pad, and the solvent evaporated. The resulting residue was dissolved in EtOAc and a sat. aq. soln. of NaHCO₃ was added. The aq. phase was extracted with EtOAc (x3) and the organic layers were dried over anh. Na₂SO₄, filtered and evaporated. The resulting residue was purified by chromatography column on silica gel (EtOAc:Cy, 7:1) to obtain **19** (50 mg, 70%) as a white solid. ¹H NMR (300 MHz, CDCl₃, δ ppm) 9.00 (br s, 1H, Py), 8.56 (br s, 1H, Py), 8.25 – 8.14 (m, 1H, Py), 7.84 (s, 1H, triazole), 7.41 – 7.32 (m, 1H, Py), 7.31 – 7.25 (m, 2H, pyrrole), 6.32 – 6.22 (m, 2H, pyrrole), 4.41 (t, *J* = 7.2 Hz, 2H, CH₂-triazole), 2.80 (t, *J* = 7.3 Hz, 2H, CH₂-CO), 2.03 – 1.90 (m, 2H, CH₂), 1.83 – 1.69 (m, 2H, CH₂), 1.44 – 1.34 (m, 6H, 3 CH₂). ¹³C NMR (75.4 MHz, CDCl₃, δ ppm) 170.5 (C=O), 149.2 (qC, Py), 147.1 (CH, Py), 144.8 (qC, triazole), 133.1 (CH, Py), 127.0 (CH, Py), 123.9 (2 CH, pyrrole), 119.9 (CH, Py), 119.1 (CH, triazole), 113.2 (2 CH, pyrrole), 50.6 (CH₂-

triazole), 34.5 ($\underline{\text{C}}\text{H}_2\text{-CO}$), 30.3 (CH_2), 28.9 (CH_2), 28.8 (CH_2), 26.4 (CH_2), 24.4 (CH_2). ESI-HRMS m/z calcd for $\text{C}_{19}\text{H}_{24}\text{N}_5\text{O}$ $[\text{M}+\text{H}]^+$, 338.1975; found, 338.1975.

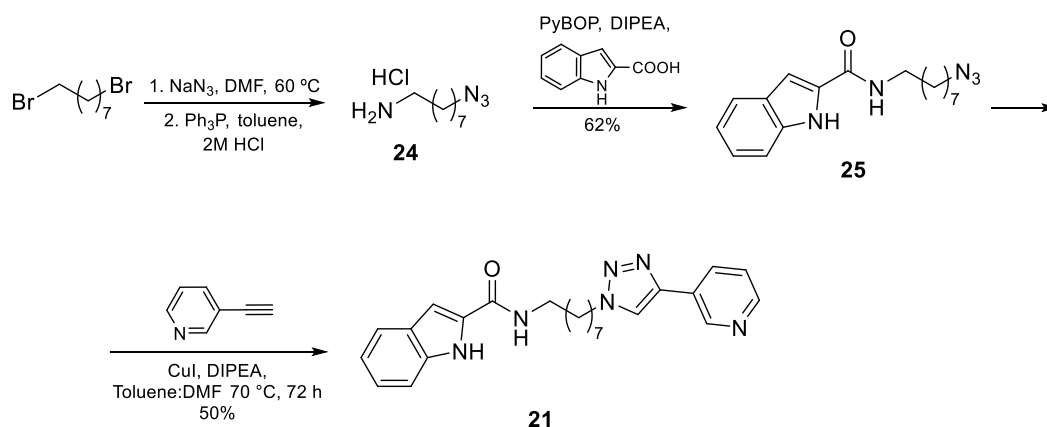
8-Azido-*N*-(furan-2-ylmethyl)octanamide (**18**)

A solution of **16** (1.7 g, 9.0 mmol), furfurylamine (1.2 mL, 13.0 mmol) and PyBOP (7.9 g, 15.0 mmol) in DMF (36 mL) was cooled to 0 °C. DIPEA (7.5 mL, 43.0 mmol) was slowly added at 0 °C, and the reaction mixture was stirred at r.t. for 16 h. Then, the solvent was evaporated and the resulting crude diluted with EtOAc (50 mL), washed with 1 M HCl (x3) and brine (x3), dried over anh. Na_2SO_4 , filtered, and concentrated *in vacuo*. The crude was purified by chromatography column on silica gel (EtOAc:Cy 1:2) to yield **18** (1.9 g, 78%) as a white solid. ^1H NMR (300 MHz, CDCl_3 , δ ppm) 7.37 – 7.29 (m, 1H, furan), 6.30 (dd, $J = 3.1, 1.9$ Hz, 1H, furan), 6.20 (d, $J = 3.2$ Hz, 1H, furan), 5.92 (br s, 1H, NH-CO), 4.41 (d, $J = 5.3$ Hz, 2H, $\underline{\text{C}}\text{H}_2\text{-NH}$), 3.23 (t, $J = 6.9$ Hz, 2H, $\text{CH}_2\text{-N}_3$), 2.17 (t, $J = 7.2$ Hz, 2H, $\text{CH}_2\text{-CO}$), 1.69 – 1.50 (m, 4H, 2 CH_2), 1.39 – 1.26 (m, 6H, 3 CH_2). ^{13}C NMR (75.4 MHz, CDCl_3 , δ ppm) 172.9 (C=O), 151.5 (qC, furan), 142.3 (CH, furan), 110.6 (CH, furan), 107.5 (CH, furan), 51.5 ($\text{CH}_2\text{-N}_3$), 36.6 (2 C, $\text{CH}_2\text{-NH}$, $\underline{\text{C}}\text{H}_2\text{-CO}$), 29.1 (CH_2), 28.9 (CH_2), 28.8 (CH_2), 26.6 (CH_2), 25.6 (CH_2). ESI-HRMS m/z calcd. for $\text{C}_{13}\text{H}_{20}\text{N}_4\text{O}_2\text{Na}$ $[\text{M}+\text{Na}]^+$, 287.1479; found, 287.1478.

N-(Furan-2-ylmethyl)-8-(4-(pyridin-3-yl)-1H-1,2,3-triazol-1-yl)octanamide (**20**)

To a solution of **18** (50 mg, 210 μmol) in toluene (3 mL), 3-ethynylpyridine (40 mg, 400 μmol), DIPEA (130 μL , 720 μmol) and CuI (7 mg, 40 μmol) were added, and the solution was stirred at 60 °C for 24 h. Quadrasil[®] resin (150 mg) was added and the mixture was stirred at r.t. for 1 h. Then, it was filtrated through a celite pad, and the solvent evaporated. The resulting residue was dissolved in CH_2Cl_2 and a sat. aq. soln. of NaHCO_3 was added. The aq. phase was extracted with CH_2Cl_2 (x2), and the organic layers were dried over anh. Na_2SO_4 , filtered, and evaporated. The resulting residue was purified by chromatography column on silica gel (MeOH:EtOAc: CH_2Cl_2 , 0.4:5:1)

to yield **20** (42 mg, 60%) as a white solid. ^1H NMR (500 MHz, CDCl_3 , δ ppm) 8.99 (s, 1H, Py), 8.57 (d, $J = 3.6$ Hz, 1H, Py), 8.21 (dd, $J = 6.1, 1.8$ Hz, 1H, Py), 7.84 (s, 1H, triazole), 7.41 – 7.29 (m, 2H, 1H Py, 1H furan), 6.35 – 6.26 (m, 1H, furan), 6.21 (d, $J = 2.9$ Hz, 1H, furan), 5.79 (s, 1H, NH), 4.47 – 4.36 (m, 4H, $\text{CH}_2\text{-NH}$, $\text{CH}_2\text{-triazole}$), 2.24 – 2.11 (m, 2H, $\text{CH}_2\text{-C=O}$), 2.01 – 1.89 (m, 2H, CH_2), 1.68 – 1.57 (m, 2H, CH_2), 1.43 – 1.28 (m, 6H, 3 CH_2). ^{13}C NMR (125.7 MHz, CDCl_3 , δ ppm) 172.7 (C=O), 151.6 (qC, furan), 149.3 (CH, Py), 147.2 (CH, Py), 144.9 (qC, triazole), 142.3 (CH, furan), 133.2 (CH, Py), 127.0 (qC, Py), 123.9 (CH, Py), 119.9 (CH, triazole), 110.6 (CH, furan), 107.5 (CH, furan), 50.6 ($\text{CH}_2\text{-NH}$), 36.6 ($\text{CH}_2\text{-triazole}$), 36.5 ($\text{CH}_2\text{-C=O}$), 30.3 (CH_2), 28.9 (CH_2), 28.6 (CH_2), 26.3 (CH_2), 25.4 (CH_2). ESI-HRMS m/z calcd for $\text{C}_{20}\text{H}_{26}\text{N}_5\text{O}_2$ $[\text{M}+\text{H}]^+$, 368.2076; found, 368.2081.



Scheme 16. Synthesis of (pyridin-3-yl)triazole-based inhibitor **21**.

8-Azido-octan-1-amine hydrochloride (**24**)⁴⁴

Sodium azide (977 mg, 15 mmol) was added to a solution of 1,8-dibromooctane (1.0 mL, 5.4 mmol) in DMF (25 mL) and the mixture was stirred at 60°C for 10 h. Then, water was added (125 mL) and the product was extracted with Et_2O (3x). The organic phase was washed with water (3x), dried over anhydrous Na_2SO_4 , filtered and the solvent was evaporated to afford 1,8-diazido-octane⁴⁵ as a colourless oil that was used in the next step without further purification. ^1H NMR (300 MHz, CDCl_3 , δ ppm) 3.25 (t, $J =$

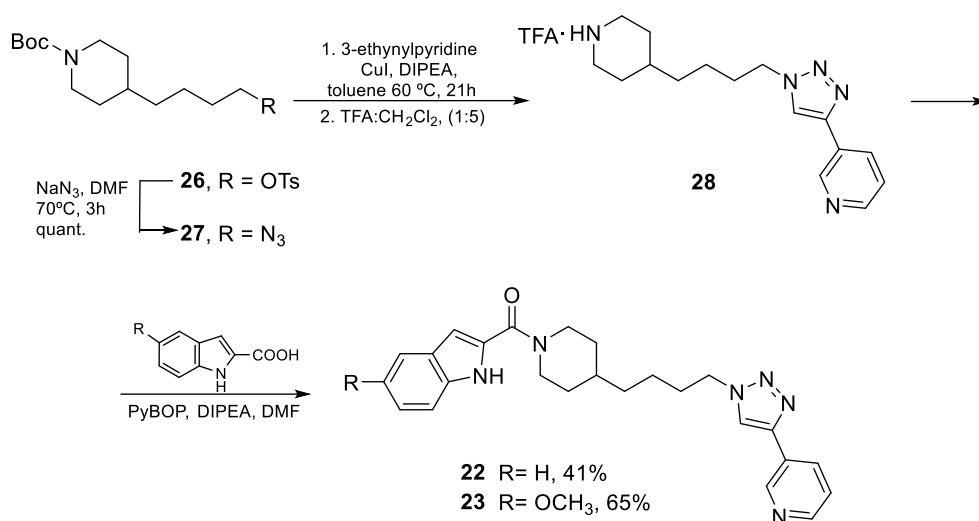
6.9 Hz, 4H), 1.67 – 1.51 (m, 4H), 1.47 – 1.27 (m, 8H). To a solution of 1,8-diazidooctane (930 mg, 4.7 mmol) in toluene:HCl 2M (1:1, 80 mL) Ph₃P (1.24 g, 4.74 mmol) was slowly added, and the mixture was vigorously stirred at r.t. for 16 h. The aqueous phase was separated and washed with Et₂O (x3) and dried under vacuum to obtain **24** as a colourless oil that was used in the next step without further purification. ¹H NMR (300 MHz, CDCl₃, δ ppm) 3.25 (t, *J* = 6.9, 2H), 2.68 (t, *J* = 6.9, 2H), 1.68 – 1.51 (m, 2H), 1.50 – 1.40 (m, 4H), 1.39 – 1.27 (m, 8H). ESI-HRMS *m/z* calcd for C₈H₁₉N₄ [M+H]⁺, 171.1601; found, 171.1604. NMR data match with those previously reported for this compound.

***N*-(8-Azidooctyl)-1H-indole-2-carboxamide (25)**

A solution of **24** (720 mg, 3.5 mmol), 1H-indole-2-carboxylic acid (842 mg, 5.2 mmol) and PyBOP (3.1 g, 5.9 mmol) in DMF (16 mL) was cooled to 0 °C. DIPEA (2.9 mL, 17.0 mmol) was slowly added at 0 °C, and the reaction mixture was stirred at r.t. overnight. Then, it was diluted with EtOAc (160 mL) and washed with 1 M HCl (x3) and brine (x3), dried over anh. Na₂SO₄, filtered, and concentrated *in vacuo*. The crude was purified by chromatography column on silica gel (EtOAc:Toluene 1:9) to yield **25** (860 mg, 62%) as a white solid. ¹H NMR (300 MHz, CDCl₃, δ ppm) 10.00 (s, 1H, NH indole), 7.64 (d, *J* = 8.0 Hz, 1H, indole), 7.45 (t, *J* = 7.0 Hz, 1H, indole), 7.32 – 7.23 (m, 1H, indole), 7.13 (t, *J* = 7.2 Hz, 1H, indole), 6.85 (d, *J* = 1.4 Hz, 1H, indole), 6.36 (s, 1H, NH-CO), 3.57 – 3.45 (m, 2H, CH₂-N₃), 3.24 (t, *J* = 6.9 Hz, 2H, CH₂-NH), 1.77 – 1.49 (m, 4H, 2 CH₂), 1.46 – 1.25 (m, 8H, 4 CH₂). ¹³C NMR (75.4 MHz, CDCl₃, δ ppm) 162.0 (C=O), 136.6 (qC, indole), 130.9 (qC, indole), 127.7 (qC, indole), 124.5 (CH, indole), 121.9 (CH, indole), 120.7 (CH, indole), 112.2 (CH, indole), 101.9 (CH, indole), 51.5 (CH₂-N₃), 39.9 (CH₂-NH), 29.9 (CH₂), 29.3 (CH₂), 29.1 (CH₂), 28.9 (CH₂), 27.0 (CH₂), 27.7 (CH₂). ESI-HRMS *m/z* calcd for C₁₇H₂₃N₅ONa [M+Na]⁺, 336.1793; found, 336.1795.

***N*-(8-(4-(Pyridin-3-yl)-1H-1,2,3-triazol-1-yl)octyl)-1H-indole-2-carboxamide (**21**)**

To a solution of **25** (50 mg, 160 μ mol) in Toluene:DMF (3:1, 3 mL), 3-ethynylpyridine (50 mg, 480 μ mol), DIPEA (110 μ L, 610 μ mol) and CuI (12 mg, 60 μ mol) were added, and the solution was stirred at 70 °C for 72 h. Quadrasil[®] resin (150 mg) was added and the mixture stirred for 1h at r.t. Then, it was filtered through a celite pad, and the solvent evaporated. The resulting residue was dissolved in CH₂Cl₂ and a sat. aq. soln. of NaHCO₃ was added. The aq. phase was extracted with CH₂Cl₂ (x2), and the organic layers were dried over anh. Na₂SO₄, filtered, and evaporated. The resulting residue was purified by chromatography column on silica gel (MeOH:EtOAc:CH₂Cl₂, 1:5:1) to obtain **21** (35 mg, 50%) as a white solid. ¹H NMR (300 MHz, DMSO-*d*₆, δ ppm) 11.51 (s, 1H, NH indole), 9.05 (d, *J* = 1.5 Hz, 1H, Py), 8.70 (s, 1H, triazole), 8.53 (dd, *J* = 4.8, 1.5 Hz, 1H, Py), 8.45 – 8.38 (m, 1H, NH-CO), 8.24 – 8.16 (m, 1H, Py), 7.62 – 7.56 (m, 1H, Py), 7.48 (dd, *J* = 8.0, 4.8 Hz, 1H, indole), 7.42 (d, *J* = 8.2 Hz, 1H, indole), 7.20 – 7.12 (m, 1H, indole), 7.09 (d, *J* = 1.4 Hz, 1H, indole), 7.06 – 6.98 (m, 1H, indole), 4.40 (t, *J* = 7.1 Hz, 2H, CH₂-triazole), 3.26 (q, *J* = 6.7 Hz, 2H, CH₂-NH), 1.94 – 1.80 (m, 2H, CH₂), 1.60 – 1.46 (m, 2H, CH₂), 1.34 – 1.26 (m, 8H, 4 CH₂). ¹³C NMR (75.4 MHz, DMSO-*d*₆, δ ppm) 160.9 (C=O), 148.7 (CH, Py), 146.3 (CH, Py), 143.4 (qC, triazole), 136.3 (qC, indole), 132.4 (qC, Py), 131.9 (qC, indole), 127.1 (CH, Py), 126.8 (qC, indole), 124.0 (CH, indole), 123.1 (CH, Py), 121.9 (CH, triazole), 121.4 (CH, indole), 119.6 (CH, indole), 112.2 (CH, indole), 102.1 (CH, indole), 49.6 (CH₂-triazole), 39.0 (CH₂-NH), 29.6 (CH₂), 29.2 (CH₂), 28.6 (CH₂), 28.4 (CH₂), 26.4 (CH₂), 25.8 (CH₂). ESI-HRMS *m/z* calcd for C₂₄H₂₉N₆O [M+H]⁺, 417.2392; found, 417.2397.



Scheme 17. Synthesis of (pyridin-3-yl)triazole-based inhibitors **22** and **23**.

3-(1-(4-(Piperidin-4-yl)butyl)-1H-1,2,3-triazol-4-yl)pyridine-2,2,2-trifluoroacetate (28)

Compound **26**³⁴ (636 mg, 1.6 mmol) was dissolved in DMF (10 mL), NaN₃ (302 mg, 4.6 mmol) was added and the mixture was stirred at 70 °C for 3 h. After this time, the solvent was evaporated under vacuum and the residue dissolved in CH₂Cl₂. The organic layer was washed with water and brine, dried over anhydrous Na₂SO₄, filtered, and concentrated *in vacuo* to give **27** as a colourless oil. To a solution of **27** (192 mg, 680 μmol) in toluene (7 mL), 3-ethynylpyridine (175 mg, 1.7 mmol), DIPEA (0.57 mL, 3.30 mmol) and CuI (26 mg, 140 μmol) were added, and the solution was stirred at 60 °C for 21 h. Quadrasil® resin (480 mg) was added and the mixture stirred for 1 h at r.t. Then, it was filtrated through a celite pad, and the solvent evaporated. The resulting residue was dissolved in EtOAc and a sat. aq. soln. of NaHCO₃ was added. The aq. phase was extracted with EtOAc (x2) and the organic layers were dried over Na₂SO₄, filtered and evaporated. The crude was purified by chromatography column on silica gel (gradient from CH₂Cl₂ to Acetone:CH₂Cl₂, 1:5) to yield the corresponding protected triazole derivative (230 mg, 88%) as a white solid. ¹H NMR (300 MHz, CDCl₃, δ ppm) 8.98 (dd, *J* = 2.2, 0.8 Hz, 1H, Py), 8.56 (dd, *J* = 4.8, 2.2 Hz, 1H, Py), 8.25 – 8.16

(m, 1H, Py), 7.83 (s, 1H, triazole), 7.36 (ddd, $J = 8.0, 4.8, 0.8$ Hz, 1H, Py), 4.42 (t, $J = 7.2$ Hz, 2H, $\underline{\text{CH}}_2$ -triazole), 4.22 – 3.90 (m, 2H, piperidine), 2.73 – 2.54 (m, 2H, piperidine), 2.02 – 1.88 (m, 2H, piperidine), 1.67 – 1.53 (m, 2H, piperidine), 1.48 – 1.19 (m, 14H, C(CH₃), 2 CH₂, CH piperidine), 1.14 – 0.96 (m, 2H, CH₂). ¹³C NMR (75.4 MHz, CDCl₃, δ ppm) 155.0 (C=O), 149.4 (CH, Py), 147.1 (CH, Py), 144.8 (qC, triazole), 133.1 (CH, Py), 126.9 (qC, Py), 123.9 (CH, Py), 119.8 (CH, triazole), 79.4 (C-(CH₃)₃), 50.6 ($\underline{\text{C}}\text{H}_2$ -triazole), 44.0 (2 C, piperidine), 36.0 (CH₂), 32.3 (2 C, piperidine, CH₂), 30.6 (piperidine), 28.6 (3C, C-(CH₃)₃), 23.7 (CH₂).

This compound was dissolved in 20 % TFA/CH₂Cl₂ (5 mL) at 0 °C and the mixture was stirred at r.t. for 3.5 h. The solvent was evaporated *in vacuo* and the solvent was co-evaporated with toluene to yield **28** as a white solid that was used in the next step without further purification.

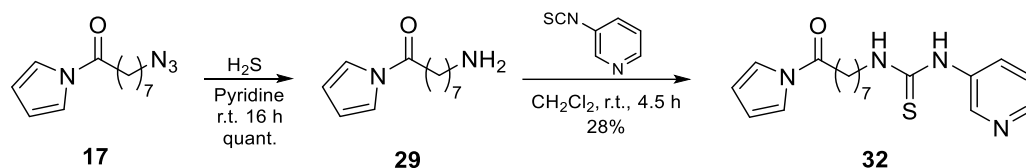
(1H-Indol-2-yl)(4-(4-(4-(pyridin-3-yl)-1H-1,2,3-triazol-1-yl)butyl)piperidin-1-yl)methanone (22)

A solution of **28** (112 mg, 280 μmol), 1H-Indole-2-carboxylic acid (68 mg, 420 μmol) and PyBOP (248 mg, 480 μmol) in dry DMF (2.5 mL) was cooled to 0 °C. DIPEA (0.24 mL, 1.35 mmol) was slowly added at 0 °C, and the reaction mixture was stirred at r.t. for 16 h. The solvent was evaporated under reduced pressure and the crude was diluted with EtOAc (20 mL) and washed with sat. aq. soln. of NH₄Cl (x3), dried over anh. Na₂SO₄, filtered and concentrated. The residue was purified by chromatography column on silica gel (MeOH:EtOAc, 1:20→1:10) to yield **22** (56 mg, 41%) as a white solid. ¹H NMR (300 MHz, DMSO-*d*₆, δ ppm) 11.51 (s, 1H, NH indole), 9.11 – 8.99 (m, 1H, Py), 8.72 (s, 1H, triazole), 8.54 (dd, $J = 4.8, 1.5$ Hz, 1H, Py), 8.21 (dt, $J = 7.9, 1.9$ Hz, 1H, Py), 7.59 (d, $J = 7.9$ Hz, 1H, indole), 7.52 – 7.44 (m, 1H, Py), 7.40 (d, $J = 7.9$ Hz, 1H, indole), 7.23 – 7.10 (m, 1H, indole), 7.09 – 6.98 (m, 1H, indole), 6.75 – 6.67 (m, 1H, indole), 4.53 – 4.31 (m, 4H, $\underline{\text{C}}\text{H}_2$ -triazole, 2H piperidine), 2.96 (br s, 2H, piperidine), 1.96 – 1.81 (m, 2H, piperidine), 1.78 – 1.66 (m, 2H, piperidine), 1.62 – 1.44 (m, 1H,

piperidine), 1.39 – 1.19 (m, 4H, 2 CH₂), 1.18 – 1.00 (m, 2H, CH₂). ¹³C NMR (75.4 MHz, DMSO-*d*₆, δ ppm) 161.8, 148.8, 146.3, 143.5, 135.8, 132.3, 130.3, 126.8, 124.0, 123.0, 122.0, 121.2, 119.6, 112.0, 103.4, 49.6, 35.4, 35.3, 32.2, 32.1, 27.7, 22.1. ESI-HRMS *m/z* calcd for C₂₅H₂₉N₆O [M+H]⁺, 429.2391; found, 429.2397.

(5-Methoxy-1H-indol-2-yl)(4-(4-(4-(pyridin-3-yl)-1H-1,2,3-triazol-1-yl)butyl)piperidin-1-yl)methanone (23)

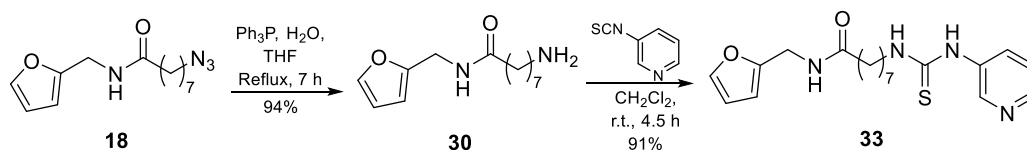
Reaction of **28** (112 mg, 280 μmol) and 5-methoxy-1H-indole-2-carboxylic acid (80 mg, 420 μmol) was performed according to the procedure that was previously employed for the preparation of **22**. Chromatography column (MeOH:EtOAc, 1:20→1:10). Yield: 65%, white solid. ¹H NMR (300 MHz, DMSO-*d*₆, δ ppm) 11.37 (s, 1H, NH, indole), 9.06 (d, *J* = 1.7 Hz, 1H, Py), 8.72 (s, 1H, triazole), 8.58 – 8.50 (m, 1H, Py), 8.28 – 8.15 (m, 1H, Py), 7.55 – 7.41 (m, 1H, Py), 7.29 (d, *J* = 8.9 Hz, 1H, indole), 7.06 (d, *J* = 2.3 Hz, 1H, indole), 6.82 (dd, *J* = 8.9, 2.4 Hz, 1H, indole), 6.63 (d, *J* = 1.6 Hz, 1H, indole), 4.54 – 4.29 (m, 4H, CH₂-triazole, 2H piperidine), 3.74 (s, 3H, OCH₃), 2.96 (br s, 2H, piperidine), 1.96 – 1.81 (m, 2H, piperidine), 1.79 – 1.64 (m, 2H, piperidine), 1.63 – 1.44 (m, 1H, piperidine), 1.40 – 1.20 (m, 4H, CH₂), 1.19 – 0.98 (m, 2H, CH₂). ¹³C NMR (75.4 MHz, DMSO-*d*₆, δ ppm) 161.8, 153.7, 148.8, 146.3, 143.5, 132.3, 131.1, 130.7, 127.1, 126.8, 124.0, 122.0, 114.0, 112.8, 103.2, 101.9, 55.2, 49.6, 35.2, 35.1, 32.1, 29.7, 22.1. ESI-HRMS *m/z* calcd for C₂₆H₃₁N₆O₂ [M+H]⁺, 459.2495; found, 459.2503.



Scheme 18. Synthesis of (pyridin-3-yl)thiourea based inhibitor **32**.

1-(8-Oxo-8-(1H-pyrrol-1-yl)octyl)-3-(pyridin-3-yl)thiourea (**32**)

To a solution of **17** (0.5 g, 2.1 mmol) in pyridine (15 mL), H₂S was bubbled. After stirring at r.t. overnight the mixture was evaporated under vacuum. The crude product **29** was used directly in the next step without any further purification. ESI-HRMS *m/z* calcd for C₁₂H₂₁N₂O [M+H]⁺, 209.1647; found, 209.1648. To a solution of **29** (60 mg, 300 μmol) in dry CH₂Cl₂ (5 mL), 3-pyridyl isothiocyanate (40 μL, 400 μmol) was added. After stirring at r.t. for 6 h, the solvent was removed under *vacuum* and the resulting residue was purified by chromatography column on silica gel (EtOAc: Cy 4:1) to give **32** (25 mg, 28%) as a white solid. ¹H NMR (300 MHz, CDCl₃, δ ppm) 8.58 – 8.49 (m, 1H, Py), 8.48 – 8.40 (m, 1H, Py), 8.32 (br s, 1H, NH-Py), 7.89 – 7.80 (m, 1H, Py), 7.42 – 7.34 (m, 1H, Py), 7.29 (br s, 2H, pyrrole), 6.44 – 6.31 (m, 1H, NH-CH₂), 6.31 – 6.24 (m, 2H, pyrrole), 3.60 (q, *J* = 6.4 Hz, 2H, CH₂-NH), 2.81 (t, *J* = 7.3 Hz, 2H, CH₂-CO), 1.82 – 1.68 (m, 2H, CH₂), 1.68 – 1.52 (m, 2H, CH₂), 1.44 – 1.30 (m, 6H, 3 CH₂). ¹³C NMR (75.4 MHz, CDCl₃, δ ppm) 181.3 (C=S), 170.8 (C=O), 147.4 (qC, Py), 146.1 (CH, Py), 134.2 (CH, Py) 132.6 (CH, Py), 124.3 (CH, Py), 119.1 (2CH, pyrrole), 113.2 (2CH, pyrrole), 45.5 (CH₂-NH), 35.5 (CH₂-CO), 29.8 (CH₂), 29.0 (CH₂), 28.8 (CH₂), 26.6 (CH₂), 24.4 (CH₂). ESI-HRMS *m/z* calcd for C₁₈H₂₅N₄OS [M+H]⁺, 345.1737; found, 345.1744.



Scheme 19. Synthesis of (pyridin-3-yl)thiourea based inhibitor **33**.

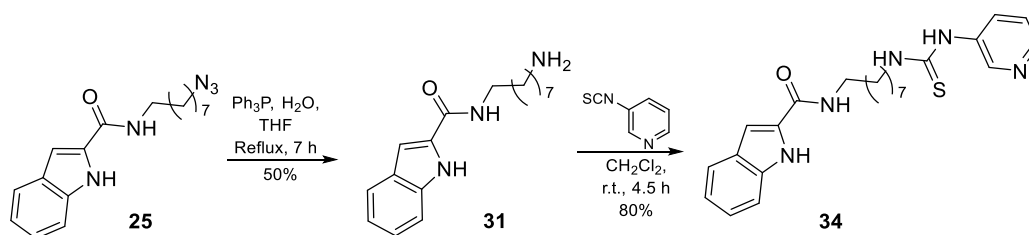
8-Amino-*N*-(furan-2-ylmethyl)octanamide (**30**)

To a solution of **18** (100 mg, 380 μmol) in THF (1 mL), H₂O (40 μL) and Ph₃P (150 mg, 600 μmol) were added. The reaction mixture was stirred at reflux for 7 h, evaporated under vacuum and the residue purified by chromatography column on silica gel (NH₄OH:MeOH:CH₂Cl₂, 0.1:1:10) to yield **30** (85 mg, 94%) as a white solid. ¹H NMR (500 MHz, CDCl₃, δ ppm) 7.33 (dd, $J = 1.8, 0.7$ Hz, 1H, furan), 6.30 (dd, $J = 3.2, 1.9$ Hz, 1H, furan), 6.20 (dd, $J = 3.2, 0.6$ Hz, 1H, furan), 5.87 (br s, 1H, NH-C=O), 4.42 (d, $J = 5.5$ Hz, 2H, CH₂-NH), 2.67 (br s, 2H, NH₂), 2.17 (t, $J = 7.5$ Hz, 2H, CH₂-C=O), 1.68 – 1.57 (m, 2H, CH₂-(CH₂-CO)), 1.49 – 1.36 (m, 4H, CH₂-NH₂, CH₂), 1.35 – 1.24 (m, 6H, 3 CH₂). ¹³C NMR (125.7 MHz, CDCl₃, δ ppm) 172.9 (C=O), 151.6 (qC, furan), 142.3 (CH, furan), 110.6 (CH, furan), 107.5 (CH, furan), 42.0 (CH₂-NH₂), 36.7 (CH₂-NH), 36.6 (CH₂-CO), 33.7 (CH₂), 29.3 (CH₂), 28.8 (CH₂), 26.8 (CH₂), 25.7 (CH₂). ESI-HRMS m/z calcd for C₁₃H₂₃N₂O₂ [M+H]⁺, 239.1753; found, 239.1754.

N-(Furan-2-ylmethyl)-8-(3-(pyridin-3-yl)thioureido)octanamide (**33**)

Reaction of **30** (70 mg, 300 μmol) and 3-pyridyl isothiocyanate (80 μL , 800 μmol) was performed according to the same procedure as that used to prepare **32**. Chromatography column (MeOH:EtOAc:CH₂Cl₂, 0.4:5:1). Yield: 91%, white solid. ¹H NMR (300 MHz, CD₃OD, δ ppm) 8.57 (dd, $J = 2.5, 0.6$ Hz, 1H, Py), 8.28 (dd, $J = 4.8, 1.3$ Hz, 1H, Py), 8.10 – 7.89 (m, 1H, Py), 7.44 – 7.36 (m, 2H, 1H Py, 1H furan), 6.33 (dd, $J = 3.2, 1.9$ Hz, 1H, furan), 6.22 (dd, $J = 3.2, 0.7$ Hz, 1H, furan), 4.34 (s, 2H, CH₂-NH), 3.68 – 3.44 (m, 2H, CH₂-thiourea), 2.21 (t, $J = 7.4$ Hz, 2H, CH₂-CO), 1.71 – 1.54 (m, 4H, 2 CH₂), 1.44 – 1.29 (m, 6H, 3 CH₂). ¹³C NMR (75.4 MHz, CD₃OD, δ ppm) 183.1 (C=S),

176.1 (C=O), 153.2 (qC, furan), 145.8 (2CH, Py), 143.3 (CH, furan), 138.3 (qC, Py), 133.3 (CH, Py), 124.9 (CH, Py), 111.3 (CH, furan), 108.0 (CH, furan), 45.6 (CH₂-thiourea), 37.1 (CH₂-NH), 36.9 (CH₂-CO), 30.04 (CH₂), 30.02 (CH₂), 27.8 (CH₂), 26.8 (CH₂), 25.7 (CH₂). ESI-HRMS *m/z* calcd for C₁₉H₂₇N₄O₂S [M+H]⁺, 375.1845; found, 375.1849.



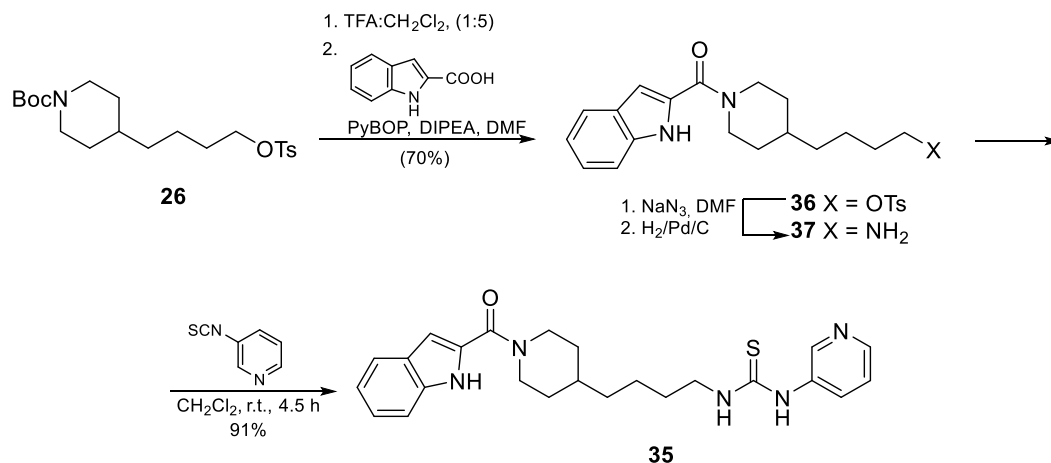
Scheme 20. Synthesis of (pyridin-3-yl)thiourea based inhibitor **34**.

***N*-(8-Amino-octyl)-1H-indole-2-carboxamide (31)**

To a solution of **25** (100 mg, 32 mmol) in THF (1 mL), H₂O (30 μL) and Ph₃P (126 mg, 500 μmol) were added. The reaction mixture was stirred at reflux for 30 h, evaporated under vacuum and the residue purified by chromatography column on silica gel (NH₄OH:MeOH:CH₂Cl₂, 0.1:1:10) to yield **31** (45 mg, 50%) as a white solid. ¹H NMR (300 MHz, DMSO-*d*₆, δ ppm) 11.42 (br s, 1H, NH indole), 8.48 – 8.33 (m, 1H, NH-C=O), 7.59 (d, *J* = 7.8 Hz, 1H, indole), 7.42 (d, *J* = 8.3 Hz, 1H, indole), 7.16 (t, *J* = 7.4 Hz, 1H, indole), 7.09 (s, 1H, indole), 7.02 (t, *J* = 7.4 Hz, 1H, indole), 3.27 (q, *J* = 6.7 Hz, 2H, CH₂-NH), 2.62 – 2.37 (m, 2H, CH₂-NH₂), 1.61 – 1.45 (m, 2H, CH₂-(CH₂-NH)), 1.41 – 1.17 (m, 10H, 5 CH₂). ¹³C NMR (75.4 MHz, DMSO-*d*₆, δ ppm) 160.9 (C=O), 136.3 (qC, indole), 131.9 (qC, indole), 127.1 (qC, indole), 123.1 (CH, indole), 121.4 (CH, indole), 119.6 (CH, indole), 112.2 (CH, indole), 102.1 (CH, indole), 41.5 (CH₂-NH₂), 39.1 (CH₂-(NH-CO)), 33.1 (CH₂), 29.3 (CH₂), 29.0 (CH₂), 28.8 (CH₂), 26.5 (CH₂), 26.4 (CH₂). ESI-HRMS *m/z* calcd for C₁₇H₂₆N₃O [M+H]⁺, 288.2070; found, 288.2070.

***N*-(8-(3-(Pyridin-3-yl)thioureido)octyl)-1H-indole-2-carboxamide (34)**

Reaction of **21** (37 mg, 0.1 mmol) and 3-pyridyl isothiocyanate (36 μL , 300 μmol) was performed according to the procedure used to prepare **32**. Chromatography column (MeOH:EtOAc:CH₂Cl₂, 0.4:5:1). Yield: 80%, white solid. ¹H NMR (300 MHz, DMSO-*d*₆, δ ppm) 11.52 (s, 1H, NH indole), 9.53 (s, 1H, NH-Py), 8.55 (t, *J* = 2.2 Hz, 1H, Py), 8.43 (t, *J* = 5.7 Hz, 1H, NH-C=O), 8.28 (dd, *J* = 4.7, 1.4 Hz, 1H, Py), 8.03 – 7.86 (m, 1H, Py), 7.60 (d, *J* = 7.9 Hz, 1H, indole), 7.42 (dd, *J* = 8.2, 0.7 Hz, 1H, indole), 7.33 (dd, *J* = 8.2, 4.7 Hz, 1H, Py), 7.20 – 7.12 (m, 1H, indole), 7.09 (s, 1H, indole), 7.07 – 6.98 (m, 1H, indole), 3.51 – 3.39 (m, 2H, CH₂-thiourea), 3.28 (q, *J* = 6.4 Hz, 2H, CH₂-amide), 1.60 – 1.49 (m, 4H, 2 CH₂), 1.40 – 1.26 (m, 8H, 4 CH₂). ¹³C NMR (75.4 MHz, DMSO-*d*₆, δ ppm) 180.9 (C=S), 161.0 (C=O), 144.6 (CH, Py), 144.4 (CH, Py), 136.3 (qC, indole), 131.9 (qC, indole), 131.8 (qC, Py), 130.2 (CH, Py), 127.1 (qC, indole), 123.1 (2CH, Py, indole), 121.4 (CH, indole), 119.6 (CH, indole), 112.2 (CH, indole), 102.1 (CH, indole), 43.9 (CH₂-thiourea), 38.7 (CH₂-amide), 29.3 (CH₂), 28.8 (2(CH₂)), 28.4 (CH₂), 26.5 (CH₂), 26.4 (CH₂). ESI-HRMS *m/z* calcd for C₂₃H₃₀N₅OS [M+H]⁺, 424.2162; found, 424.2166.



Scheme 21. Synthesis of (pyridin-3-yl)thiourea based inhibitor **35**.

4-(1-(1H-Indole-2-carbonyl)piperidin-4-yl)butyl 4-methylbenzenesulfonate (**36**)

Compound **26** (483 mg, 1.2 mmol) was dissolved in 20 % TFA/CH₂Cl₂ (9 mL) and the mixture was stirred at r.t. for 4.5 h. The mixture was evaporated under vacuum and the crude used directly in the next step. This compound (257 mg, 600 μmol), 1H-

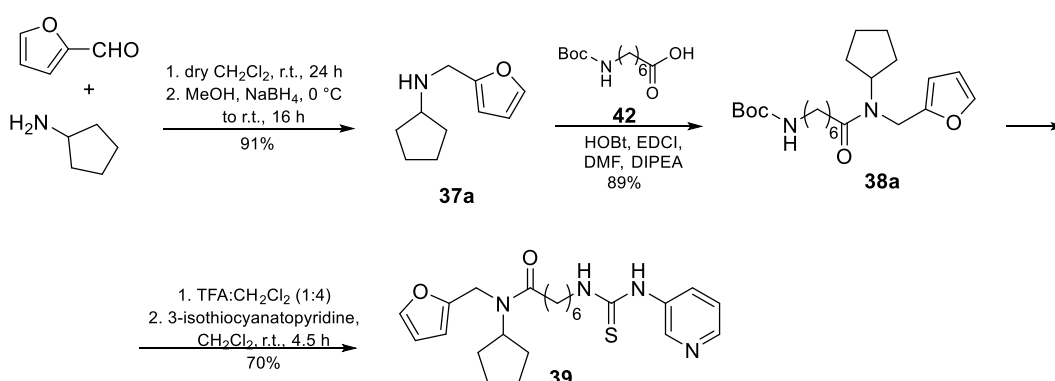
indole-2-carboxylic acid (146 mg, 910 μmol) and PyBOP (534 mg, 1 mmol) in DMF (3.5 mL) were mixed and cooled to 0 °C. DIPEA (0.51 mL, 2.90 mmol) was slowly added at 0 °C, and the reaction mixture was stirred at r.t. for 16 h. The reaction mixture was diluted with EtOAc (35 mL) and washed with 1 M HCl (x3) and brine (x3), dried over Na_2SO_4 , filtered, and concentrated in *vacuo*. The crude was purified by chromatography column on silica gel (EtOAc:Toluene, 1:2) to yield **36** (193 mg, 70%) as a white solid. ^1H NMR (300 MHz, $\text{DMSO-}d_6$, δ ppm) 11.53 (s, 1H, NH indole), 8.07 (d, $J = 8.4$ Hz, 1H, indole), 7.82 (d, $J = 8.3$ Hz, 1H, indole), 7.68 – 7.55 (m, 2H, Ts), 7.51 – 7.37 (m, 2H, Ts), 7.20 – 7.11 (m, 1H, indole), 7.10 – 6.98 (m, 1H, indole), 6.73 (d, $J = 1.4$ Hz, 1H, indole), 4.56 (t, $J = 6.4$ Hz, 2H, $\text{CH}_2\text{-OTs}$), 4.50 – 4.37 (br d, 2H, piperidine), 3.00 (br s, 2H, piperidine), 2.50 (s, 3H, CH_3 Ts), 1.84 – 1.70 (m, 4H, piperidine), 1.65 – 1.47 (m, 1H, CH piperidine), 1.38 – 1.24 (m, 2H, CH_2), 1.24 – 1.01 (m, 2H, CH_2). ^{13}C NMR (75.4 MHz, $\text{DMSO-}d_6$, δ ppm) 161.8, 142.8, 135.8, 130.3, 128.4, 127.0, 126.8, 125.0, 123.0, 121.2, 119.7, 119.6, 112.0, 109.2, 103.4, 80.8, 40.0, 35.4, 35.3, 32.5, 32.1, 27.7, 22.1.

(4-(4-Aminobutyl)piperidin-1-yl)(1H-indol-2-yl)methanone (37)

Compound **36** (170 mg, 370 μmol) was dissolved in DMF (2.5 mL), NaN_3 (73 mg, 1.1 mmol) was added, and the mixture was stirred at 120 °C for 32 h. The mixture was evaporated under vacuum and the residue dissolved in CH_2Cl_2 . The organic layer was washed with water and brine, dried over anh. Na_2SO_4 , filtered, and concentrated in *vacuo*. The residue obtained (113 mg, 350 μmol) was dissolved in MeOH (10 mL), Pd/C 10% (50 mg) was added, and the reaction mixture was stirred under H_2 (1 atm) at r.t. overnight. The mixture was filtered through a celite pad and concentrated in *vacuo*. The crude product was used in the next step without further purification.

1-(4-(1-(1H-Indole-2-carbonyl)piperidin-4-yl)butyl)-3-(pyridin-3-yl)thiourea (35)

Reaction of **37** (22 mg, 100 μ mol) and 3-pyridyl isothiocyanate (18 μ L, 200 μ mol) was performed according to the same procedure as that used to prepare **32**. Chromatography column (MeOH:EtOAc:CH₂Cl₂, 0:5:1 to 1:5:1). Yield: 91%, white solid. ¹H NMR (300 MHz, Acetone-*d*₆, δ ppm) 10.63 (s, 1H, NH indole), 8.91 (s, 1H, NH-Py), 8.65 – 8.53 (m, 1H, Py), 8.31 (dd, *J* = 4.7, 1.3 Hz, 1H, Py), 8.07 – 7.94 (m, 1H, Py), 7.68 – 7.58 (m, 1H, indole), 7.57 – 7.39 (m, 2H, 1H indole, NH-CH₂), 7.31 (dd, *J* = 8.1, 4.6 Hz, 1H, Py), 7.27 – 7.15 (m, 1H, indole), 7.15 – 7.00 (m, 1H, indole), 6.80 (d, *J* = 1.3 Hz, 1H, indole), 4.71 – 4.51 (m, 2H, piperidine), 3.72 – 3.54 (m, 2H, CH₂-NH), 3.00 (br s, 2H, piperidine), 1.90 – 1.75 (m, 2H, piperidine), 1.75 – 1.55 (m, 3H, 1H piperidine, CH₂), 1.52 – 1.10 (m, 2H piperidine, 2 CH₂). ¹³C NMR (75.4 MHz, Acetone-*d*₆, δ ppm) 181.8, 161.8, 145.3, 136.1, 136.0, 130.4, 127.5, 123.3, 122.9, 121.3, 119.8, 111.8, 111.7, 103.8, 103.7, 44.9, 44.2, 35.9, 32.4, 28.8, 23.6. ESI-HRMS *m/z* calcd for C₂₄H₃₀N₅OS [M+H]⁺, 436.2158; found, 436.2166.



Scheme 22. Synthesis of (pyridin-3-yl)thiourea-based inhibitor **39**.

***N*-(Furan-2-ylmethyl)cyclopentanamine (**37a**)⁴⁶**

A solution of furfural (6.9 mL, 83.0 mmol) and cyclopentanamine (8.2 mL, 83.0 mmol) was stirred in dry CH₂Cl₂ (200 mL) over 3 Å MS at r.t. for 24 h. Then the reaction mixture was concentrated *in vacuo* and the residue was dissolved in MeOH (200 mL). NaBH₄ (6.3 g, 0.2 mol) was added in small portions to the mixture at 0 °C. The reaction was warmed to r.t. and stirred for 16 h. The solvent was removed under reduce

pressure and the residue was dissolved in water and extracted with EtOAc (3x). The organic phases were extracted with 3% HCl (3x), and the pH of the obtained acidic aqueous solution was raised to pH 10 with sat. aq. soln. of NaOH. The aqueous phase was extracted with EtOAc (3x), and the organic phases were washed with water, brine, and dried over anh. Na₂SO₄. The solvent was evaporated in *vacuo* to give **37a** (13 g, 91%) as a yellow oil. ¹H NMR (300 MHz, CDCl₃, δ ppm) 7.34 (dd, *J* = 1.8, 0.8 Hz, 1H), 6.29 (dd, *J* = 3.1, 1.9 Hz, 1H), 6.16 (dd, *J* = 3.2, 0.7 Hz, 1H), 3.76 (s, 2H), 3.08 (quint, *J* = 6.6 Hz, 1H), 1.91 – 1.76 (m, 2H), 1.76 – 1.60 (m, 3H), 1.60 – 1.44 (m, 2H), 1.44 – 1.26 (m, 2H). NMR data match with those previously reported for this compound.⁴⁶

7-((*tert*-Butoxycarbonyl)amino)heptanoic acid (42**)³⁷**

7-Aminoheptanoic acid (2 g, 14 mmol) and NaOH (550 mg, 14 mmol) were dissolved in dioxane-H₂O (2:1, 60 mL). This mixture was cooled to 0 °C and Boc₂O (3.3 g, 15.2 mmol) was added in small portions. The reaction mixture was stirred at r.t. for 16 h, and then was concentrated under reduced pressure. The basic residue was redissolved in H₂O and washed with EtOAc (2x). The aqueous phase was acidified to pH 1-2 with aqueous 1M HCl and extracted with EtOAc (3x). The combined organic extracts were dried over anh. Na₂SO₄, filtered, and concentrated under reduced pressure to afford **42** as colourless oil, which slowly became a white solid. The crude product was used in the next step without further purification. ESI-HRMS *m/z* calcd for C₁₂H₂₃NO₄Na [M+Na]⁺, 268.1523; found, 268.1519.

***tert*-Butyl (7-(cyclopentyl(furan-2-ylmethyl)amino)-7-oxoheptyl)carbamate (**38a**)**

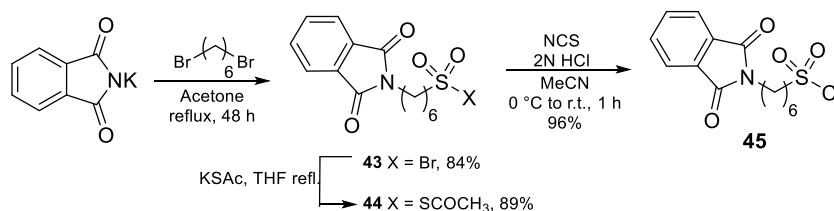
A solution of **37a** (80 mg, 480 μmol), **42** (178 mg, 730 μmol) and PyBOP (428 mg, 820 μmol) in DMF (2.5 mL) was cooled to 0 °C. DIPEA (0.21 mL, 1.21 mmol) was slowly added at 0 °C, and the reaction mixture was stirred at r.t. for 16 h. Then, it was concentrated in *vacuo*, diluted with EtOAc and washed with 1 M HCl (x3) and brine (x3), dried over anh. Na₂SO₄ and concentrated *in vacuo*. The crude was purified by

chromatography column on silica gel (EtOAc:Cy, 1:4→1:1) to yield **38a** (170 mg, 89%) as a colourless oil. ¹H NMR (300 MHz, CDCl₃, δ ppm, mixture of rotamers) 7.46 – 7.10 (m, 2H, furan), 6.39 – 6.23 (m, 2H, furan), 6.23 – 6.07 (m, 2H, furan), 4.86 – 4.63 (m, 1H, CH cyclopentyl rotamer A), 4.58 – 4.28 (m, 6H, 2 CH₂-furan, 2 NH), 4.28 – 4.10 (m, 1H, CH cyclopentyl rotamer B), 3.08 (br s, 4H, 2 CH₂-NH), 2.50 – 2.26 (m, 4H, 2 CH₂-C=O), 1.91 – 1.21 (m, 50H, 8 CH₂, 8 CH₂ cyclopentyl, 2 C(CH₃)₃). ¹³C NMR (75.4 MHz, CDCl₃, δ ppm, mixture of rotamers) 173.9, 173.2, 156.2, 152.3, 152.3, 142.1, 141.0, 110.6, 107.6, 107.0, 79.2, 77.6, 77.2, 76.7, 60.5, 58.8, 56.2, 41.9, 38.4, 30.1, 29.8, 29.2, 28.6, 26.7, 25.4, 23.9, 14.3. ESI-HRMS *m/z* calcd for C₂₂H₃₆N₂O₄Na[M+Na]⁺, 415.2564; found, 493.2567.

***N*-Cyclopentyl-*N*-(furan-2-ylmethyl)-7-(3-(pyridin-3-yl)thioureido)heptanamide (39)**

Compound **38a** (156 mg, 400 μmol) was dissolved in 20 % TFA/CH₂Cl₂ (2.5 mL) at 0 °C and the mixture was stirred at r.t. for 3 h. The solvent was evaporated under *vacuum* and the residue was azeotropically dried with toluene (2x). Finally, the residue was dried under high *vacuum* to yield a colourless oil that was used in the next step without further purification. To a solution of this compound (110 mg, 270 μmol) in dry CH₂Cl₂ (6 mL), 3-pyridyl isothiocyanate (75 μL, 700 μmol) was added. After stirring at r.t. for 3 h, the solvent was removed under *vacuum* and the resulting residue was purified by chromatography column on silica gel (MeOH:EtOAc, 1:9) to give **39** (80 mg, 70%) as a white solid. ¹H NMR (300 MHz, CDCl₃, δ ppm, mixture of rotamers) 8.92 – 8.72 (m, 2H, Py), 8.55 – 8.41 (m, 2H, Py), 8.41 – 8.26 (m, 2H, Py), 8.18 – 8.00 (m, 2H, Py), 7.41 – 7.07 (m, 6h, 2H furan, 2 NH-Py, 2 NH-CH₂), 6.40 – 6.16 (m, 2H, furan), 6.18 – 6.02 (m, 2H, furan), 4.69 (quint, *J* = 8.3 Hz, 1H, CH cyclopentyl rotamer A), 4.40 (br d, 4H, 2 CH₂-furan), 4.29 – 4.09 (m, 1H, CH cyclopentyl rotamer B), 3.72 – 3.51 (m, 4H, 2 CH₂-NH), 2.67 – 2.31 (m, 4H, 2 CH₂-C=O), 1.94 – 1.23 (m, 32H, 8 CH₂ cyclopentyl, 8 CH₂). ¹³C NMR (75.4 MHz, CDCl₃, δ ppm, mixture of rotamers) 181.8, 174.5, 173.9, 152.0, 151.6, 145.8, 145.6, 145.0, 142.3, 141.4, 136.0, 132.2, 123.6, 123.6, 110.6,

107.3, 77.6, 77.2, 76.7, 59.0, 56.5, 45.2, 44.9, 41.8, 38.8, 33.6, 33.3, 30.0, 29.1, 28.3, 27.6, 27.1, 26.8, 24.6, 24.4, 23.9, 23.8. ESI-HRMS m/z calcd for $C_{23}H_{33}N_4O_2S$ $[M+H]^+$, 429.2316; found, 429.2319.



Scheme 23. Synthesis of intermediate **45**.

2-(6-Bromohexyl)isoindoline-1,3-dione (**43**)⁴⁷

Potassium phthalimide (12.0 g, 65 mmol) was suspended in acetone (200 mL) and 1,6-dibromohexane (25 mL, 200 mmol) was added. The suspension was refluxed for 48 h and the solvent was evaporated under vacuum. The residue was dissolved in water and extracted with EtOAc (x2). The combined organic layers were dried over anh. Na_2SO_4 , filtered, and concentrated *in vacuo*. The crude product was purified by column chromatography on silica gel (EtOAc: Cy, 1:5) to provide **43** (17.0 g, 84%) as white crystals. ^1H NMR (300 MHz, CDCl_3 , δ ppm) 7.84 (dd, $J = 5.5, 3.1$ Hz, 2H), 7.70 (dd, $J = 5.5, 3.1$ Hz, 2H), 3.68 (t, $J = 7.2$ Hz, 2H), 3.39 (t, $J = 6.8$ Hz, 2H), 1.93 – 1.78 (m, 2H), 1.70 (quint, $J = 7.5$ Hz, 2H), 1.56 – 1.31 (m, 4H). NMR data match with those previously reported for this compound.

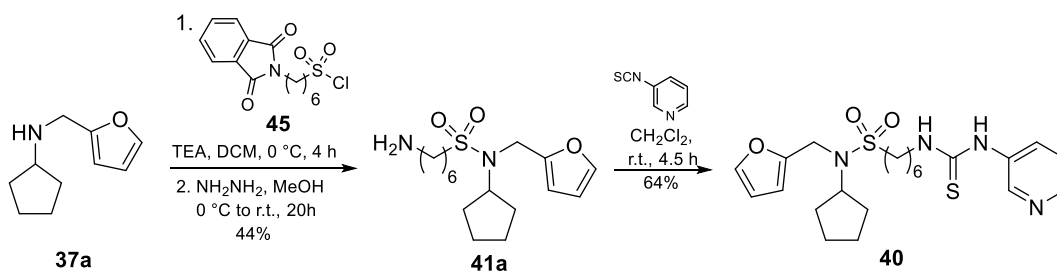
S-(6-(1,3-Dioxoisoindolin-2-yl)hexyl) ethanethioate (**44**)⁴⁸

To a stirred solution of **43** (3.9 g, 12.5 mmol) in THF (150 mL) was added KSAc (4.3 g, 37.5 mmol) in small portions during 20 min and the mixture was refluxed for 3 h. The solvent was evaporated *in vacuo*, water was added to the residue and extracted with EtOAc (3x). The combined organic phases were washed with water and brine, dried over anh. Na_2SO_4 and concentrated *in vacuo*. The crude product was purified by flash chromatography on silica gel (EtOAc: Cy, 1:2) to give **44** (3.4 g, 89%) as light brown

crystals. ^1H NMR (300 MHz, CDCl_3 , δ ppm) 7.91 – 7.77 (m, 2H), 7.76 – 7.64 (m, 2H), 3.74 – 3.59 (m, 2H), 2.85 (t, $J = 7.2$ Hz, 2H), 2.30 (s, 3H), 1.74 – 1.50 (m, 4H), 1.50 – 1.27 (m, 4H). NMR data match with those previously reported for this compound.

6-(1,3-Dioxoisindolin-2-yl)hexane-1-sulfonyl chloride (**45**)²⁸

2N HCl (2.4 mL) was added to a stirred solution of **44** (1.3 g, 4.3 mmol) in MeCN (24 mL) at 0 °C. NCS (2.4 g, 18.3 mmol) was added in small portions over 30 min and the reaction mixture was warmed to r.t. and stirred for 1 h. Then, it was quenched with ice-cold water and extracted with Et_2O (x3). The combined organic layers were washed with sat. aq. soln. of NaHCO_3 , water and brine, dried over anh. Na_2SO_4 and concentrated to afford **45** (1.35 g, 96%) as a white solid that was used in the next step without further purification. ^1H NMR (300 MHz, CDCl_3 , δ ppm) 7.84 (dd, $J = 5.4, 3.1$ Hz, 2H), 7.71 (dd, $J = 5.4, 3.1$ Hz, 2H), 3.77 – 3.59 (m, 4H), 2.14 – 1.96 (m, 2H), 1.72 (quint, $J = 7.2$ Hz, 2H), 1.66 – 1.49 (m, 2H), 1.49 – 1.33 (m, 2H). ESI-HRMS m/z calcd for $\text{C}_{14}\text{H}_{16}\text{ClNO}_4\text{SNa}$ $[\text{M}+\text{Na}]^+$, 352.0378; found, 352.0381. NMR data match with those previously reported for this compound.



Scheme 24. Synthesis of (pyridin-3-yl)thiourea-based inhibitor **40**.

6-Amino-N-cyclopentyl-N-(furan-2-ylmethyl)hexane-1-sulfonamide (**41a**)

To a suspension of **37a** (1.1 g, 6.7 mmol) in dry CH_2Cl_2 (38 mL), Et_3N (2.6 mL, 19.0 mmol) was added under argon at 0 °C and stirred over 3 Å MS. Compound **45** (5.3 g, 16.0 mmol) in dry CH_2Cl_2 (40 mL) was added over 1 h and the resulting mixture was stirred for 3 h at 0 °C. Then, it was quenched with water and extracted with CH_2Cl_2

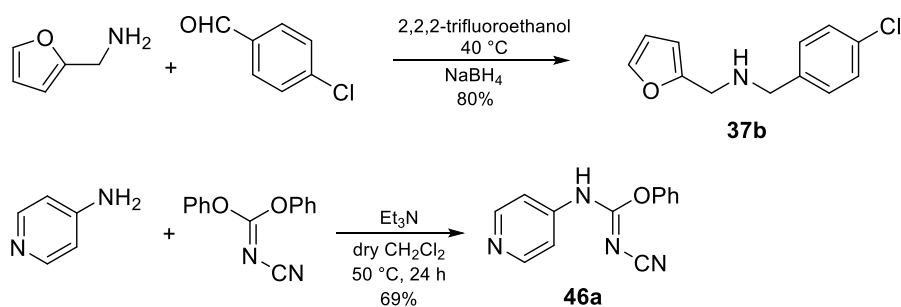
(x3). The combined organic layers were washed with water, brine, dried over anhydrous Na_2SO_4 and concentrated *in vacuo*. The crude product was purified by flash chromatography on silica gel (toluene:EtOAc, 20:1→12:1) to give the protected sulfonamide (1.8 g, 62%) as a white solid. ^1H NMR (300 MHz, CDCl_3 , δ ppm) 7.84 (dd, $J = 5.5, 3.1$ Hz, 2H, Ph), 7.71 (dd, $J = 5.5, 3.1$ Hz, 2H, Ph), 7.36 (dd, $J = 1.7, 0.9$ Hz, 1H, furan), 6.36 – 6.26 (m, 2H, furan), 4.36 (s, 2H, CH_2 -furan), 4.15 (quint, $J = 8.3$ Hz, 1H, CH cyclopentyl), 3.67 (t, $J = 7.2$ Hz, 2H, CH_2 -Pth), 2.80 – 2.69 (m, 2H, CH_2SO_2), 1.93 – 1.20 (m, 16 H, 8 CH_2). ^{13}C NMR (75.4 MHz, CDCl_3 , δ ppm) 168.6 (2 C=O), 151.5 (qC, furan), 142.2 (CH, furan), 134.1 (2 CH, Ph), 132.3 (2 qC, Ph), 123.32 (2 CH, Ph), 110.8 (CH, furan), 109.2 (CH, furan), 59.3 (CH, cyclopentyl), 53.4 (CH_2SO_2), 40.0 (CH_2 -furan), 37.9 (CH_2 -Pth), 30.0 (2 CH_2 , cyclopentyl), 28.4 (CH_2), 28.0 (CH_2), 26.4 (CH_2), 23.6 (2 CH_2 , cyclopentyl), 23.4 (CH_2). ESI-HRMS m/z calcd for $\text{C}_{24}\text{H}_{30}\text{N}_2\text{O}_5\text{SNa}$ $[\text{M}+\text{Na}]^+$, 481.1764; found, 481.1768.

To a stirred solution of protected sulfonamide (1.8 g, 4.2 mmol) in dry MeOH (20 mL), NH_2NH_2 (1.2 mL, 25 mmol) was added, and the reaction was stirred at 0 °C for 3 h and at r.t. overnight. Then, the white precipitate was filtered off and washed with MeOH (20 mL). The solvent was evaporated *in vacuo* and the crude product was dissolved in 2N HCl and washed with Et_2O (x3). The aqueous layer was basified with sat. aq. soln. of NaOH to pH=8 and extracted with EtOAc (x3). The organic layers were collected and dried over anhydrous Na_2SO_4 and concentrated *in vacuo* to yield **41a** as a sticky solid that was carried forward to the next step without purification.

***N*-Cyclopentyl-*N*-(furan-2-ylmethyl)-6-(3-(pyridin-3-yl)thioureido)hexane-1-sulfonamide (40)**

Reaction of **41a** (115 mg, 350 μmol) and 3-pyridyl isothiocyanate (100 μL , 900 μmol) was performed according to the same procedure used to prepare **32**. Chromatography column (EtOAc:Cy, 9:1). Yield: 64%, white solid. ^1H NMR (300 MHz, CDCl_3 , δ ppm) 8.62 – 8.51 (m, 1H, Py), 8.50 – 8.37 (m, 1H, Py), 8.17 (br s, 1H, NH -Py),

7.96 – 7.76 (m, 1H, Py), 7.42 – 7.30 (m, 2H, Py, furan), 6.45 – 6.22 (m, 3H, 2H furan, NH-CH₂), 4.36 (s, 2H, CH₂-furan), 4.24 – 4.04 (m, 1H, CH cyclopentyl), 3.60 (q, *J* = 6.6 Hz, 2H, CH₂-NH), 2.88 – 2.67 (m, 2H, CH₂SO₂), 1.98 – 1.47 (m, 12H, 8H cyclopentyl, 2 CH₂), 1.47 – 1.21 (m, 4H, 2 CH₂). ¹³C NMR (75.4 MHz, CDCl₃, δ ppm) 181.5 (C=S), 151.4 (qC, furan), 147.0 (CH, Py), 145.7 (CH, Py), 142.3 (CH, furan), 134.6 (qC, Py), 132.7 (CH, Py), 124.3 (CH, Py), 110.8 (CH, furan), 109.2 (CH, furan), 59.3 (CH, cyclopentyl), 53.2 (CH₂SO₂), 45.2 (CH₂-NH), 40.1 (CH₂-furan), 30.0 (2CH₂, cyclopentyl), 28.5 (CH₂), 27.9 (CH₂), 26.3 (CH₂), 23.6 (2CH₂, cyclopentyl), 23.3 (CH₂). ESI-HRMS *m/z* calcd for C₂₂H₃₃N₄O₃S₂ [M+H]⁺, 465.1982; found, 465.1989.



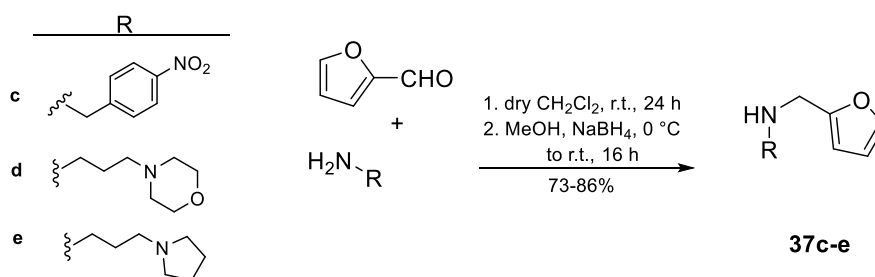
Scheme 25. Synthesis of starting materials **37b** and **46a**.

***N*-(4-Chlorobenzyl)-1-(furan-2-yl)methanamine (**37b**)⁴⁹**

A solution of 4-chlorobenzaldehyde (868 mg, 6.2 mmol) and 2,2,2-trifluoroethanol (2 mL) was magnetically stirred at 40 °C for 5 min. Furfuryl amine (0.55 mL, 6.20 mmol) was added, and the mixture was vigorously stirred for 10 min at 40 °C. NaBH₄ (280 mg, 7.40 mmol) was added, and the mixture was stirred at r.t. for 10 min. The reaction mixture was filtered, and the residue was washed with 2,2,2-trifluoroethanol (2 mL) and dried under high vacuum. The crude product was purified by column chromatography on silica gel (EtOAc:Cy, 1:4→1:2) to yield **37b** (1.10 g, 80%) as a colourless oil. ¹H NMR (300 MHz, CDCl₃, δ ppm) 7.38 – 7.30 (m, 1H), 7.29 – 7.19 (m, 4H), 6.35 – 6.27 (m, 1H), 6.20 – 6.10 (m, 1H), 3.78 – 3.68 (m, 4H), 1.84 (s, 1H). NMR data match with those previously reported for this compound.

Phenyl (Z)-N'-cyano-N-(pyridin-4-yl)carbamimidate (46a)⁵⁰

To a solution of 4-aminopyridine (2.0 g, 21 mmol) in CH₂Cl₂ (25 mL) were added diphenylcyanocarbonimidate (5.6 g, 23.0 mmol) and Et₃N (3.3 mL, 23.0 mmol). The reaction mixture was stirred under nitrogen for 24 h at 50 °C. The mixture was concentrated *in vacuo* and the residue was purified by column chromatography on silica gel (MeOH:EtOAc, 1:20) to give **46a** (3.5 g, 69%) as a white solid. ¹H NMR (300 MHz, DMSO-*d*₆, δ ppm) 12.64 (br s, 1H), 8.33 (d, *J* = 6.5 Hz, 2H), 7.47 – 7.30 (m, 4H), 7.29 – 7.17 (m, 3H). ESI-HRMS *m/z* calcd for C₁₃H₁₁N₄O [M+H]⁺, 239.0926; found, 239.0927. NMR data match with those previously reported for this compound.



Scheme 26. Synthesis of amines **37c-e**.

1-(Furan-2-yl)-N-(4-nitrobenzyl)methanamine (37c)

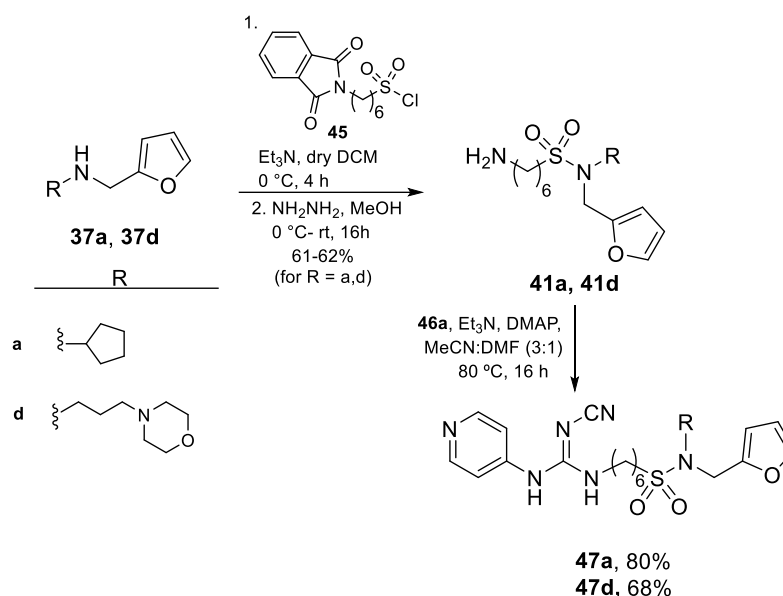
Reaction of furfuryl amine (0.73 mL, 8.20 mmol) and 4-nitrobenzaldehyde (1.24 g, 8.20 mmol) was performed according to the same procedure used to prepare **37a** (pag. 85). Yield: 75%, red oil. ¹H NMR (300 MHz, CDCl₃, δ ppm) 8.17 (d, *J* = 8.7 Hz, 2H, Ph), 7.51 (d, *J* = 8.8 Hz, 2H, Ph), 7.42 – 7.32 (m, 1H, furan), 6.37 – 6.25 (m, 1H, furan), 6.24 – 6.12 (m, 1H, furan), 3.89 (s, 2H, CH₂-Ph), 3.80 (s, 2H, CH₂-furan), 1.85 (s, 1H, NH). ¹³C NMR (75.4 MHz, CDCl₃, δ ppm) 153.3 (qC, Furan), 147.7 (qC, Ph), 147.3 (qC, Ph), 142.2 (CH, furan), 128.9 (2 CH, Ph), 123.8 (2 CH, Ph), 110.4 (CH, furan), 107.6 (CH, furan), 52.0 (CH₂-furan), 45.5 (CH₂-Ph). ESI-HRMS *m/z* calcd for C₁₂H₁₃N₂O₃ [M+H]⁺, 233.0922; found, 233.0921.

N-(Furan-2-ylmethyl)-3-morpholinopropan-1-amine (37d)

Reaction of furfural (3.5 mL, 42.0 mmol) and 3-morpholinopropan-1-amine (6.1 mL, 42.0 mmol) was performed according to the same procedure used to prepare **37a** (pag. 85). Yield: 86%, yellow oil. ^1H NMR (300 MHz, CDCl_3 , δ ppm) 7.34 (dd, $J = 1.8$, 0.8 Hz, 1H, furan), 6.30 (dd, $J = 3.2$, 1.8 Hz, 1H, furan), 6.17 (dd, $J = 3.2$, 0.8 Hz, 1H, furan), 3.77 (s, 2H, CH_2 -furan), 3.73 – 3.63 (m, 4H, morpholine), 2.67 (t, $J = 6.8$ Hz, 2H, CH_2), 2.48 – 2.34 (m, 6H, morpholine, CH_2), 2.16 (s, 1H, NH), 1.76 – 1.62 (m, 2H, CH_2). ^{13}C NMR (75.4 MHz, CDCl_3 , δ ppm) 153.9 (qC, furan), 141.9 (CH, furan), 110.2 (CH, furan), 107.0 (CH, furan), 67.1 (2 C, morpholine), 57.5 (CH_2), 53.9 (2 C, morpholine), 47.9 (CH_2), 46.3 (CH_2 -furan), 26.6 (CH_2). ESI-HRMS m/z calcd for $\text{C}_{12}\text{H}_{21}\text{N}_2\text{O}_2$ $[\text{M}+\text{H}]^+$, 225.1596; found, 225.1598.

***N*-(Furan-2-ylmethyl)-3-(pyrrolidin-1-yl)propan-1-amine (37e)**

Reaction of furfural (0.34 mL, 4.20 mmol) and 3-(pyrrolidin-1-yl)propan-1-amine (0.53 mL, 4.20 mmol) was performed according to the same procedure used to prepare **37a** (pag. 85). Yield: 73%, colourless oil. ^1H NMR (300 MHz, CDCl_3 , δ ppm) 7.34 (dd, $J = 1.9$, 0.9 Hz, 1H, furan), 6.29 (dd, $J = 3.2$, 1.9 Hz, 1H, furan), 6.18 – 6.12 (m, 1H, furan), 3.81 – 3.72 (m, 2H, CH_2 -furan), 2.66 (t, $J = 7.0$ Hz, 2H, CH_2), 2.55 – 2.43 (m, 6H, CH_2 , 2 CH_2 pyrrolidine), 2.05 (s, 1H, NH), 1.83 – 1.65 (m, 6H, CH_2 , 2 CH_2 pyrrolidine). ^{13}C NMR (75.4 MHz, CDCl_3 , δ ppm) 154.1 (qC, furan), 141.8 (CH, furan), 110.1 (CH, furan), 106.8 (CH, furan), 54.8 (CH_2), 54.3 (2 C, pyrrolidine), 47.9 (CH_2), 46.3 (CH_2 -furan), 29.3 (CH_2), 23.5 (2 C, pyrrolidine). ESI-HRMS m/z calcd for $\text{C}_{12}\text{H}_{21}\text{N}_2\text{O}$ $[\text{M}+\text{H}]^+$, 209.1649; found, 209.1648.



Scheme 27. Synthesis of (pyridin-3/4-yl)cyanoguanidine-based inhibitors **47a** and **47d**.

6-Amino-N-(furan-2-ylmethyl)-N-(3-morpholinopropyl)hexane-1-sulfonamide (41d)

Reaction of **37d** (643 mg, 2 mmol) and **45** (643 mg, 2 mmol) followed the procedure described for **41a** (pag. 89). Chromatography column (MeOH:CH₂Cl₂, 1:20). Yield: 62%, white solid. ¹H NMR (300 MHz, CDCl₃, δ ppm) 7.84 (dd, *J* = 5.4, 3.1 Hz, 2H, Ph), 7.71 (dd, *J* = 5.5, 3.1 Hz, 2H, Ph), 7.45 – 7.34 (m, 1H, furan), 6.38 – 6.26 (m, 2H, furan), 4.41 (s, 2H, CH₂-furan), 3.78 – 3.62 (m, 6H, 2 CH₂-O morpholine, CH₂-Pth), 3.33 – 3.18 (m, 2H, CH₂-NSO₂), 2.95 – 2.80 (m, 2H, CH₂SO₂), 2.52 – 2.29 (m, 6H, 2 CH₂ morpholine, CH₂), 1.84 – 1.58 (m, 6H, 3 CH₂), 1.47 – 1.23 (m, 4H, 2 CH₂). ¹³C NMR (75.4 MHz, CDCl₃, δ ppm) 168.5 (2 C=O), 150.2 (qC, furan), 142.9 (CH, furan), 134.1 (2 CH, Ph), 132.3 (2 qC, Ph), 123.3 (2 CH, Ph), 110.7 (CH, furan), 109.9 (CH, furan), 67.0 (2 CH₂-O morpholine), 55.8 (CH₂), 53.8 (2 CH₂ morpholine), 52.4 (CH₂SO₂), 45.4 (CH₂-NSO₂), 43.1 (CH₂-furan), 37.9 (CH₂-Pth), 28.4 (CH₂), 28.1 (CH₂), 26.4 (CH₂), 25.5 (CH₂), 23.3 (CH₂). ESI-HRMS *m/z* calcd for C₂₆H₃₆N₃O₆S [M+H]⁺, 518.2317; found, 518.2319.

(E)-6-(2-Cyano-3-(pyridin-4-yl)guanidino)-N-cyclopentyl-N-(furan-2-ylmethyl)hexane-1-sulfonamide (47a)

Compound **46a** (920 mg, 3.9 mmol) was dissolved in dry MeCN:DMF (48 mL, 3:1), **41a** (1.65 g, 5.02 mmol), Et₃N (1.51 mL, 10.8 mmol) and DMAP (100 mg, 810 μmol) were added, and the mixture was heated and stirred at 80 °C under argon for 16 h. The reaction mixture was concentrated *in vacuo* and the residue was purified by flash chromatography on silica gel (MeOH:EtOAc, 1:12) to yield **47a** (1.48 g, 81%) as a white solid. ¹H NMR (300 MHz, CDCl₃, δ ppm) 8.50 – 8.33 (m, 2H, Py), 7.41 – 7.30 (m, 1H, furan), 7.30 – 7.16 (m, 2H, Py), 6.37 – 6.22 (m, 2H, furan), 6.10 (t, *J* = 5.6 Hz, 1H, NH-CH₂), 4.34 (s, 2H, CH₂-furan), 4.11 (quint, *J* = 8.5 Hz, 1H, CH cyclopentyl), 3.36 (q, *J* = 6.7 Hz, 2H, CH₂-NH), 2.82 – 2.67 (m, 2H, CH₂SO₂), 1.94 – 1.45 (m, 12H, 8H cyclopentyl, 2 CH₂), 1.45 – 1.23 (m, 4H, 2 CH₂). ¹³C NMR (75.4 MHz, CDCl₃, δ ppm) 157.7 (C=N), 151.3 (qC, furan), 150.5 (2CH, Py), 145.4 (qC, Py), 142.3 (CH, furan), 117.1 (CN), 115.8 (CH, Py), 110.8 (CH, furan), 109.2 (CH, furan), 59.3 (CH, cyclopentyl), 53.1 (CH₂SO₂), 42.5 (CH₂-NH), 40.1 (CH₂-furan), 30.0 (2CH₂, cyclopentyl), 28.9 (CH₂), 27.8 (CH₂), 26.1 (CH₂), 23.6 (2CH₂, cyclopentyl), 23.2 (CH₂). ESI-HRMS *m/z* calcd for C₂₃H₃₃N₆O₃S [M+H]⁺, 473.2328; found, 473.2329.

(E)-6-(2-Cyano-3-(pyridin-4-yl)guanidino)-N-(furan-2-ylmethyl)-N-(3-morpholinopropyl)hexane-1-sulfonamide (47d)

Reaction of **46a** (73 mg, 310 μmol) and **41d** (130 mg, 340 μmol) followed the procedure described for **47a**. Chromatography column (MeOH:EtOAc, 1:6). Yield: 68%, white solid. ¹H NMR (300 MHz, CDCl₃, δ ppm, mixture of rotamers) 8.56 – 8.33 (m, 2H, Py), 7.62 – 7.34 (m, 4H, 2H furan, 2 NH-Py), 7.31 – 7.16 (m, 2H, Py), 6.88 (t, *J* = 5.7 Hz, 1H, NH-CH₂ rotamer A), 6.41 – 6.23 (m, 4H, furan), 5.94 (t, *J* = 5.5 Hz, 1H, NH-CH₂ rotamer B), 4.40 (s, 4H, 2 CH₂-furan), 3.77 – 3.60 (m, 8H, 4 CH₂ morpholine), 3.43 – 3.31 (m, 4H, 2 CH₂-NH), 3.24 (t, *J* = 7.3 Hz, 4H, 2 CH₂-NSO₂), 2.95 – 2.81 (m, 4H, 2 CH₂SO₂), 2.51 – 2.28 (m, 12H, 4 CH₂ morpholine, 2 CH₂), 1.82 – 1.67 (m, 8H, 4 CH₂),

(75.4 MHz, CDCl₃, δ ppm, mixture of rotamers) 173.7, 173.3, 156.1, 154.2, 151.0, 150.1, 142.8, 142.3, 136.1, 135.4, 133.4, 133.2, 129.7, 129.1, 128.8, 127.8, 110.5, 108.9, 108.3, 79.1, 77.6, 77.2, 76.7, 56.0, 50.0, 49.8, 47.5, 43.7, 41.5, 35.7, 33.2, 33.1, 32.8, 31.0, 30.0, 30.0, 29.1, 29.0, 28.9, 28.5, 26.7, 26.6, 26.4, 25.6, 25.4, 25.2, 25.1, 24.8. ESI-HRMS *m/z* calcd for C₂₄H₃₃ClN₂O₄Na [M+Na]⁺, 471.2016; found, 471.2021.

***tert*-Butyl-(7-((furan-2-ylmethyl)(4-nitrobenzyl)amino)-7-oxoheptyl)carbamate (38c)**

Compound **38c** was prepared according to the same procedure that was employed for **38b**, except that **37c** was used as starting material. Chromatography column (EtOAc:Cy, 1:2→1:1). Yield: 76%, yellow oil. ¹H NMR (300 MHz, CDCl₃, δ ppm, mixture of rotamers) 8.23 – 7.94 (m, 4H, Ph), 7.35 – 7.14 (m, 6H, 2H furan, 4H Ph), 6.29 – 6.18 (m, 2H, furan), 6.18 – 6.06 (m, 2H, furan), 4.69 – 4.22 (m, 10H, 2 NH, 2 CH₂-furan, 2 CH₂-Ph), 3.13 – 2.88 (m, 4H, 2 CH₂-NH), 2.60 – 2.15 (m, 4H, 2 CH₂-C=O), 1.93 – 1.49 (m, 6H, 3 CH₂), 1.49 – 0.96 (m, 28H, 2 C(CH₃)₃, 5 CH₂). ¹³C NMR (75.4 MHz, CDCl₃, δ ppm, mixture of rotamers) 173.4, 173.1, 156.0, 154.1, 150.5, 149.6, 147.5, 147.2, 145.3, 144.5, 142.9, 142.3, 128.6, 127.0, 124.1, 123.7, 110.5, 110.4, 109.2, 108.6, 79.0, 77.5, 77.1, 76.7, 50.3, 49.3, 48.2, 44.4, 41.8, 35.6, 33.7, 33.1, 33.0, 32.7, 30.9, 29.9, 29.0, 28.9, 28.8, 28.4, 26.6, 26.5, 26.3, 25.6, 25.5, 25.3, 25.0, 25.0, 24.9, 24.7. ESI-HRMS *m/z* calcd for C₂₄H₃₃N₃O₆Na [M+Na]⁺, 482.2259; found, 482.2262.

***tert*-Butyl-(7-((furan-2-ylmethyl)(3-morpholinopropyl)amino)-7-oxoheptyl)carbamate (38d)**

Compound **38d** was prepared according to the same procedure that was employed for **38b**, except that **37d** was used as starting material. Chromatography column (MeOH:EtOAc, 1:10→1:6). Yield: 67%, colourless oil. ¹H NMR (300 MHz, CDCl₃, δ ppm, mixture of rotamers) 7.36 – 7.31 (m, 1H, furan rotamer A), 7.31 – 7.27 (m, 1H, furan rotamer B), 6.36 – 6.23 (m, 2H, furan), 6.23 – 6.10 (m, 2H, furan), 4.68 – 4.45 (m, 4H,

CH₂-furan rotamer A, 2 NH), 4.40 (s, 2H, CH₂-furan rotamer B), 3.76 – 3.54 (m, 8H, 4 CH₂), 3.46 – 3.22 (m, 4H, 2 CH₂), 3.13 – 2.92 (m, 4H, 2 CH₂), 2.53 – 2.12 (m, 16H, morpholine), 1.77 – 1.54 (m, 8H, 4 CH₂), 1.54 – 1.21 (m, 30H, 2 C(CH₃)₃, 2 NH, 5 CH₂). ¹³C NMR (75.4 MHz, CDCl₃, δ ppm, mixture of rotamers) 173.0, 172.9, 156.1, 151.6, 150.7, 142.6, 141.9, 110.5, 110.4, 108.4, 107.8, 79.0, 77.6, 77.2, 76.7, 67.0, 67.0, 56.2, 55.5, 53.7, 53.6, 45.2, 45.1, 44.4, 41.4, 33.2, 33.0, 30.0, 29.7, 29.2, 29.1, 28.5, 26.7, 26.6, 25.5, 25.3, 25.1, 24.5.

***tert*-Butyl-(7-((furan-2-ylmethyl)(3-(pyrrolidin-1-yl)propyl)amino)-7-oxoheptyl)carbamate (38e)**

Compound **38e** was prepared according to the same procedure that was employed for **38b**, except that **37e** was used as starting material. Chromatography column (MeOH:DCM:NH₄OH, 1:20:0.1→1:10:0.1). Yield: 44%, colourless oil. ¹H NMR (300 MHz, CDCl₃, δ ppm, mixture of rotamers) 7.36 – 7.21 (m, 2H, furan), 6.31 – 6.20 (m, 2H, furan), 6.20 – 6.11 (m, 2H, furan), 4.59 (s, 2H, 2 NH), 4.49 (s, 2H, CH₂-furan rotamer A), 4.39 (s, 2H, CH₂-furan rotamer B), 3.44 – 3.22 (m, 4H, 2 CH₂-NH), 3.09 – 2.97 (m, 4H, CH₂-N-C=O), 2.84 – 2.70 (m, 4H, 2 CH₂-N), 2.69 – 2.22 (m, 12H, 4 CH₂ pyrrolidine, 2 CH₂-C=O), 1.92 – 1.77 (m, 6H, 2 CH₂ pyrrolidine, CH₂), 1.77 – 1.65 (m, 4H, 2 CH₂ pyrrolidine), 1.65 – 1.49 (m, 4H, 2 CH₂), 1.49 – 1.11 (m, 30H, 2 C(CH₃)₃, 6 CH₂). ¹³C NMR (75.4 MHz, CDCl₃, δ ppm, mixture of rotamers) 173.4, 172.9, 156.0, 151.5, 150.3, 142.6, 141.8, 110.4, 110.4, 108.3, 108.2, 78.9, 77.6, 77.2, 76.7, 54.0, 53.8, 53.5, 53.0, 45.4, 44.8, 43.6, 41.4, 33.0, 32.8, 30.1, 29.9, 29.6, 29.3, 29.0, 28.9, 28.4, 27.6, 26.6, 26.5, 25.7, 25.2, 25.0, 23.3. ESI-HRMS *m/z* calcd for C₂₄H₄₂N₃O₄ [M+H]⁺, 436.3165; found, 436.3170.

***tert*-Butyl (6-(cyclopentyl(furan-2-ylmethyl)amino)-6-oxohexyl)carbamate (51a)**

A solution of **37a** (80 mg, 500 μmol), 6-((*tert*-butoxycarbonyl)amino)hexanoic acid⁵¹ (168 mg, 730 μmol) and PyBOP (428 mg, 820 μmol) in DMF (2.5 mL) was cooled to 0

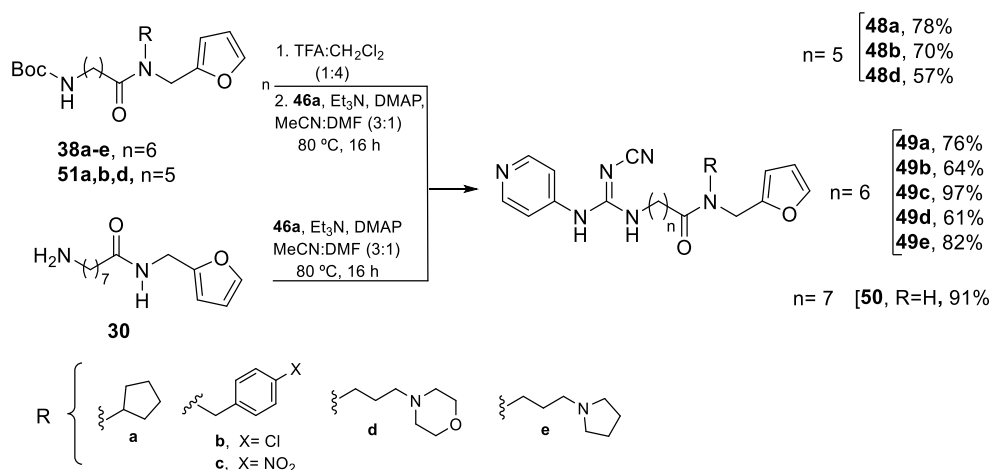
°C. DIPEA (0.41 mL, 2.32 mmol) was slowly added at 0 °C, and the reaction mixture was stirred at r.t. for 16 h. The reaction mixture was concentrated in *vacuo* and diluted with EtOAc and washed with 1 M HCl (x3) and brine (x3), dried over Na₂SO₄ and concentrated in *vacuo*. The crude was purified by chromatography column on silica gel (EtOAc:Cy, 1:1) to yield **51a** (166 mg, 90%) as a yellow oil. ¹H NMR (300 MHz, CDCl₃, δ ppm, mixture of rotamers) 7.40 – 7.19 (m, 2H, furan), 6.38 – 6.23 (m, 2H, furan), 6.23 – 6.05 (m, 2H, furan), 4.88 – 4.30 (m, 7H, 2 CH₂-furan, CH ciclopentyl rotamer A, 2 NH), 4.29 – 4.03 (m, 1H, CH ciclopentyl rotamer B), 3.22 – 2.94 (m, 4H, 2 CH₂-NH), 2.49 – 2.26 (m, 4H, 2 CH₂-C=O), 1.88 – 1.17 (m, 46H, 6 CH₂, 8 CH₂ ciclopentyl, 2 C(CH₃)₃). ¹³C NMR (75.4 MHz, CDCl₃, δ ppm, mixture of rotamers) 173.1, 156.1, 152.7, 152.3, 142.1, 141.0, 110.6, 107.6, 107.0, 79.2, 58.7, 56.2, 41.9, 40.7, 38.4, 33.8, 33.6, 30.0, 29.2, 28.6, 26.7, 25.1, 23.9. ESI-HRMS *m/z* calcd for C₂₁H₃₄N₂O₄Na [M+Na]⁺, 401.2407; found, 401.2411.

***tert*-Butyl(6-((4-chlorobenzyl)(furan-2-ylmethyl)amino)-6-oxohexyl)carbamate (51b)**

Reaction of **37b** (80 mg, 360 μmol), 6-((*tert*-butoxycarbonyl)amino)hexanoic acid⁵¹ (125 mg, 540 μmol) was performed according to the same procedure used to prepare **51a**. Chromatography column (EtOAc:Cy, 1:2→1:1). Yield: 83%, colourless oil. ¹H NMR (300 MHz, CDCl₃, δ ppm, mixture of rotamers) 7.45 – 7.20 (m, 6H, 2H furan, 4H Ph), 7.20 – 7.00 (m, 4H, Ph), 6.38 – 6.23 (m, 2H, furan), 6.23 – 6.09 (m, 2H, furan), 4.60 – 4.29 (m, 10H, 2 NH, 2 CH₂-furan, 2 CH₂-Ph), 3.21 – 2.99 (m, 4H, 2 CH₂-NH), 2.53 (t, *J* = 7.6 Hz, 2H, CH₂-C=O rotamer A), 2.32 (t, *J* = 7.3 Hz, 2H, CH₂-C=O rotamer B) 1.80 – 1.60 (m, 4H, 2 CH₂), 1.57 – 1.20 (m, 26H, 2 C(CH₃)₃, 4 CH₂). ¹³C NMR (75.4 MHz, CDCl₃, δ ppm, mixture of rotamers) 173.2, 156.2, 151.0, 150.1, 142.9, 142.4, 136.1, 135.4, 133.5, 133.3, 129.8, 129.2, 128.8, 127.8, 110.5, 109.0, 108.4, 79.1, 50.1, 47.6, 43.7, 41.6, 40.7, 33.2, 30.0, 28.6, 26.7, 25.0. ESI-HRMS *m/z* calcd for C₂₃H₃₁ClN₂O₄Na [M+Na]⁺, 457.1860; found, 457.1865.

***tert*-Butyl(6-((furan-2-ylmethyl)(3-morpholinopropyl)amino)-6-oxohexyl)carbamate (51d)**

A solution of **37d** (80 mg, 480 μ mol), 6-((*tert*-butoxycarbonyl)amino)hexanoic acid⁵¹ (124 mg, 540 μ mol) was performed according to the same procedure used to prepare **51a**. Chromatography column (MeOH:EtOAc, 1:12 \rightarrow 1:6). Yield: 80%, yellow oil. ¹H NMR (300 MHz, CDCl₃, δ ppm, mixture of rotamers) 7.40 – 7.33 (m, 1H, furan rotamer A), 7.34 – 7.28 (m, 1H, furan rotamer B), 6.35 – 6.25 (m, 2H, furan), 6.25 – 6.15 (m, 2H, furan), 4.65 – 4.47 (m, 4H, CH₂-furan rotamer A, 2 NH), 4.43 (s, 2H, CH₂-furan rotamer B), 3.82 – 3.62 (m, 8H, morpholine), 3.49 – 3.24 (m, 4H, 2 CH₂), 3.13 – 3.05 (m, 4H, 2 CH₂), 2.61 – 2.21 (m, 16H, 8H morpholine, 4 CH₂), 1.76 – 1.56 (m, 12H, 6 CH₂), 1.56 – 1.26 (m, 24H, 2 C(CH₃)₃, 2 NH, 2 CH₂). ¹³C NMR (75.4 MHz, CDCl₃, δ ppm, mixture of rotamers) 173.2, 172.9, 156.1, 151.6, 150.6, 142.7, 142.0, 110.6, 110.5, 108.5, 108.1, 79.1, 77.6, 77.2, 76.7, 66.9, 66.4, 56.2, 55.6, 53.7, 53.4, 45.3, 45.1, 44.2, 41.5, 34.4, 33.2, 33.0, 30.0, 29.8, 28.5, 26.7, 25.5, 25.0, 24.9, 24.1. ESI-HRMS *m/z* calcd for C₂₃H₄₀N₃O₅ [M+H]⁺, 438.2959; found, 438.2962.



Scheme 29. Synthesis of (pyridin-3/4-yl)cyanoguanidine-based inhibitors **48a,b,d**, **49a-e** and **50**.

(E)-6-(2-Cyano-3-(pyridin-4-yl)guanidino)-N-cyclopentyl-N-(furan-2-ylmethyl)hexanamide (48a)

Compound **51a** (144 mg, 380 μmol) was dissolved in 20% TFA/ CH_2Cl_2 (500 μL TFA, 2 mL CH_2Cl_2) at 0 °C and the mixture was stirred at r.t. for 2.5 h. The solvent was evaporated *in vacuo* and the residue was azeotropically dried with toluene (2 \times 5 mL). Finally, the residue was dried under high vacuum to yield a colourless oil that was used in the next step without further purification. This compound (149 mg, 380 μmol) was dissolved in dry MeCN:DMF (4 mL, 3:1) and **46a** (82 mg, 350 μmol), Et_3N (0.23 mL, 1.70 mmol) and DMAP (9 mg, 70 μmol) were added, and the mixture was heated and stirred at 80 °C under argon for 16 h. The reaction mixture was concentrated under vacuum and the residue was purified by chromatography column on silica gel (MeOH:EtOAc: CH_2Cl_2 , 0.8:5:1) to give **48a** (113 mg, 78%) as a white sticky solid. ^1H NMR (300 MHz, CDCl_3 , δ ppm, mixture of rotamers) 8.50 – 8.30 (m, 4H, Py), 7.40 – 7.20 (m, 4H, 2H Py, 2H furan), 6.49 (br s, 2H, 2 NH -Py), 6.39 – 6.21 (m, 2H, furan), 6.15 – 6.03 (m, 2H, furan), 4.72 – 4.53 (m, 1H, CH cyclopentyl rotamer A), 4.38 (s, 4H, 2 CH_2 -furan), 4.28 – 4.09 (m, 1H, CH cyclopentyl rotamer B), 3.52 – 3.40 (m, 4H, 2 CH_2 -NH), 2.52 – 2.31 (m, 4H, 2 CH_2 -C=O), 1.91 – 1.21 (m, 30H, 6 CH_2 , 8 CH_2 cyclopentyl, 2 NH - CH_2). ^{13}C NMR (75.4 MHz, CDCl_3 , δ ppm, mixture of rotamers) 173.6, 157.7, 152.1, 151.6, 150.4, 150.2, 145.7, 142.3, 141.4, 117.0, 115.5, 115.3, 110.7, 107.2, 58.9, 56.3, 42.2, 41.6, 38.8, 33.4, 33.1, 30.0, 29.8, 29.1, 28.3, 28.1, 26.0, 25.8, 23.8. ESI-HRMS m/z calcd for $\text{C}_{23}\text{H}_{31}\text{N}_6\text{O}_2$ $[\text{M}+\text{H}]^+$, 423.2497; found, 423.2503.

(E)-N-(4-Chlorobenzyl)-6-(2-cyano-3-(pyridin-4-yl)guanidino)-N-(furan-2-ylmethyl)hexanamide (48b)

Compound **48b** was prepared according to the same procedure that was employed for **48a**, except that **51b** was used as starting material. Chromatography column (NH_4OH :MeOH:EtOAc, 0.1:0.5:10). Yield: 70%, colourless sticky solid. ^1H NMR (300 MHz, CDCl_3 , δ ppm, mixture of rotamers) 8.51 – 8.25 (m, 4H, Py), 7.43 – 7.18 (m, 10H,

2H furan, 4H Ph, 4H Py), 7.16 – 6.94 (m, 4H, Ph), 6.51 – 6.36 (m, 2H, 2 NH-Py), 6.36 – 6.24 (m, 2H, furan), 6.19 – 6.10 (m, 2H, furan), 4.55 – 4.28 (m, 8H, 2 CH₂-Ph, 2 CH₂-furan), 3.51 – 3.41 (m, 4H, 2 CH₂-NH), 2.58 (t, *J* = 6.7 Hz, 2H, CH₂-C=O rotamer A), 2.35 (t, *J* = 6.7 Hz, 2H, CH₂-C=O rotamer B), 1.80 – 1.30 (m, 14H, 6 CH₂, 2 NH-CH₂). ¹³C NMR (75.4 MHz, CDCl₃, δ ppm, mixture of rotamers) 173.6, 157.7, 150.4, 150.2, 149.6, 145.7, 145.7, 143.0, 142.6, 135.6, 134.9, 133.7, 133.4, 129.3, 128.9, 127.8, 117.1, 115.6, 110.6, 109.1, 108.8, 50.8, 50.1, 47.9, 43.9, 42.2, 41.8, 32.8, 32.7, 28.5, 28.4, 26.2, 26.0, 23.5, 23.4. ESI-HRMS *m/z* calcd for C₂₅H₂₈ClN₆O₂ [M+H]⁺, 479.1949; found, 479.1957.

(*E*)-6-(2-Cyano-3-(pyridin-4-yl)guanidino)-*N*-(furan-2-ylmethyl)-*N*-(3-morpholinopropyl)hexanamide (48d)

Compound **48d** was prepared according to the same procedure that was employed for **48a**, except that **51d** was used as starting material. Chromatography column (MeOH:Acetone:CH₂Cl₂, 0.4:1:1). Yield: 57%, white sticky solid. ¹H NMR (300 MHz, CDCl₃, δ ppm, mixture of rotamers) 8.43 – 8.31 (m, 4H, Py), 7.40 – 7.18 (m, 6H, 4H Py, 2H furan), 6.62 – 6.42 (m, 2H, 2 NH-Py), 6.36 – 6.22 (m, 2H, furan), 6.22 – 6.10 (m, 2H, furan), 4.49 – 4.37 (m, 4H, 2 CH₂-furan), 3.70 – 3.57 (m, 8H, 4 CH₂ morpholine), 3.48 – 3.26 (m, 8H, 4 CH₂), 2.61 – 2.12 (m, 18H, 2 NH, 4 CH₂ morpholine, 4 CH₂), 1.72 – 1.50 (m, 12H, 6 CH₂), 1.45 – 1.28 (m, 4H, 2 CH₂). ¹³C NMR (75.4 MHz, CDCl₃, δ ppm, mixture of rotamers) 173.1, 157.7, 150.3, 150.3, 145.5, 142.7, 142.1, 117.1, 115.4, 110.5, 108.4, 108.1, 66.9, 66.8, 55.0, 55.3, 53.6, 53.5, 45.3, 45.1, 44.5, 42.2, 42.0, 41.7, 32.7, 32.4, 28.5, 28.4, 26.1, 26.0, 25.3, 24.4, 23.6, 23.5. ESI-HRMS *m/z* calcd for C₂₅H₃₆N₇O₃[M+H]⁺, 482.2868; found, 482.2874.

(*E*)-7-(2-Cyano-3-(pyridin-4-yl)guanidino)-*N*-cyclopentyl-*N*-(furan-2-ylmethyl)heptanamide (49a)

Compound **49a** was prepared according to the same procedure that was employed for **48a**, except that **38a** was used as starting material. Chromatography column (MeOH:EtOAc:DCM, 0.8:5:1). Yield: 76%, white sticky solid. ^1H NMR (300 MHz, CDCl_3 , δ ppm, mixture of rotamers) 8.50 – 8.30 (m, 4H, Py), 7.40 – 7.20 (m, 6H, 4H Py, 2H furan), 6.49 (br s, 2H, NH -Py), 6.39 – 6.21 (m, 2H, furan), 6.15 – 6.03 (m, 2H, furan), 4.82 – 4.64 (m, 1H, CH cyclopentyl rotamer A), 4.53 – 4.30 (m, 4H, 2 CH_2 -furan), 4.26 – 4.08 (m, 1H, CH cyclopentyl rotamer B), 3.52 – 3.40 (m, 4H, 2 CH_2 -NH), 2.52 – 2.31 (m, 4H, 2 CH_2 -C=O), 1.91 – 1.21 (m, 32H, 8 CH_2 , 8 CH_2 cyclopentyl, 2 NH - CH_2). ^{13}C NMR (75.4 MHz, CDCl_3 , δ ppm, mixture of rotamers) 174.3, 173.6, 157.7, 152.1, 151.6, 150.4, 150.2, 145.7, 142.3, 141.4, 117.0, 115.5, 115.3, 110.7, 110.7, 107.2, 77.6, 77.2, 76.7, 58.9, 56.3, 42.2, 41.6, 38.8, 33.4, 33.0, 30.0, 29.8, 29.1, 28.3, 26.1, 26.0, 23.8, 23.3. ESI-HRMS m/z calcd for $\text{C}_{24}\text{H}_{33}\text{N}_6\text{O}_2$ $[\text{M}+\text{H}]^+$, 437.2656; found, 437.2660.

(E)-N-(4-Chlorobenzyl)-7-(2-cyano-3-(pyridin-4-yl)guanidino)-N-(furan-2-ylmethyl)heptanamide (49b)

Compound **49b** was prepared according to the same procedure that was employed for **48a**, except that **38b** was used as starting material. Chromatography column (MeOH:EtOAc:DCM, 0.8:5:1). Yield: 64%, white sticky solid. ^1H NMR (300 MHz, CDCl_3 , δ ppm, mixture of rotamers) 8.46 – 8.30 (m, 4H, Py), 7.42 – 7.20 (m, 10H, 2H furan, 4H Ph, 4H Py), 7.16 – 6.99 (m, 4H, Ph), 6.37 – 6.23 (m, 4H, 2H furan, 2 NH -Py), 6.21 – 6.09 (m, 2H, furan), 4.58 – 4.30 (m, 8H, 2 CH_2 -Ph, 2 CH_2 -furan), 3.49 – 3.35 (m, 4H, 2 CH_2 -NH), 2.57 (t, $J = 6.9$ Hz, 2H, CH_2 -C=O rotamer A), 2.35 (t, $J = 6.9$ Hz, 2H, CH_2 -C=O rotamer B), 1.77 – 1.23 (m, 18H, 8 CH_2 , 2 NH - CH_2). ^{13}C NMR (75.4 MHz, CDCl_3 , δ ppm, mixture of rotamers) 173.6, 157.5, 150.5, 149.9, 149.7, 145.9, 143.0, 142.5, 135.7, 135.0, 133.4, 129.4, 129.3, 128.9, 127.8, 116.9, 115.6, 110.6, 109.1, 108.7, 77.6, 77.2, 76.7, 50.1, 47.9, 43.9, 42.4, 41.8, 32.9, 28.6, 28.5, 28.3, 28.1, 26.1, 24.3. ESI-HRMS m/z calcd for $\text{C}_{26}\text{H}_{30}\text{ClN}_6\text{O}_2$ $[\text{M}+\text{H}]^+$, 493.2107; found, 493.2113.

(E)-7-(2-Cyano-3-(pyridin-4-yl)guanidino)-N-(furan-2-ylmethyl)-N-(4-nitrobenzyl)heptanamide (49c)

Compound **49c** was prepared according to the same procedure that was employed for **48a**, except that **38c** was used as starting material. Chromatography column (MeOH:EtOAc:DCM, 0.8:5:1). Yield: 96%, yellow sticky solid. ^1H NMR (300 MHz, CDCl_3 , δ ppm, mixture of rotamers) 8.44 – 8.33 (m, 4H, Py), 8.24 – 8.04 (m, 4H, Py), 7.40 – 7.18 (m, 8H, 2H furan, 4H Ph), 6.41 – 6.23 (m, 4H, 2H furan, 2 NH -Py), 6.23 – 6.11 (m, 2H, furan), 4.75 – 4.35 (m, 8H, 2 CH_2 -Ph, 2 CH_2 -furan), 3.45 – 3.31 (m, 4H, 2 CH_2 -NH), 2.69 – 2.25 (m, 4H, 2 CH_2 -C=O), 1.82 – 1.29 (m, 18H, 8 CH_2 , 2 NH - CH_2). ^{13}C NMR (75.4 MHz, CDCl_3 , δ ppm, mixture of rotamers) 173.9, 173.7, 157.5, 150.1, 149.9, 149.3, 147.7, 147.4, 146.0, 145.0, 143.1, 142.7, 128.5, 127.1, 124.3, 123.9, 116.9, 116.8, 115.7, 110.7, 109.5, 109.1, 77.6, 77.4, 77.2, 76.7, 50.9, 48.5, 44.7, 42.5, 42.2, 33.0, 28.7, 28.5, 28.2, 26.2, 24.5. ESI-HRMS m/z calcd for $\text{C}_{26}\text{H}_{30}\text{N}_7\text{O}_4$ $[\text{M}+\text{H}]^+$, 504.2346; found, 504.2354.

(E)-7-(2-Cyano-3-(pyridin-4-yl)guanidino)-N-(furan-2-ylmethyl)-N-(3-morpholinopropyl)heptanamide (49d)

Compound **49d** was prepared according to the same procedure that was employed for **48a**, except that **38d** was used as starting material. Chromatography column (MeOH:EtOAc: NH_4OH , 1:10:0.1 \rightarrow 1:6:0.1). Yield: 61%, white sticky solid. ^1H NMR (300 MHz, CDCl_3 , δ ppm, mixture of rotamers) 8.49 – 8.34 (m, 4H, Py), 7.42 – 7.22 (m, 6H, 4H Py, 2H furan), 6.36 – 6.26 (m, 2H, furan), 6.26 – 6.12 (m, 4H, furan, 2 NH -Py), 4.53 (s, 2H, CH_2 -furan rotamer A), 4.45 (s, 2H, CH_2 -furan rotamer B), 3.75 – 3.58 (m, 8H, 4 CH_2 morpholine), 3.52 – 3.28 (m, 8H, 4 CH_2), 2.53 – 2.22 (m, 16H, 4 CH_2 morpholine, 4 CH_2), 1.77 – 1.52 (m, 12H, 6 CH_2), 1.52 – 1.22 (m, 10H, 2 NH , 4 CH_2). ^{13}C NMR (75.4 MHz, CDCl_3 , δ ppm, mixture of rotamers) 173.4, 173.4, 157.6, 151.0, 150.6, 150.5, 150.3, 145.4, 142.8, 142.3, 117.0, 115.6, 115.6, 110.6, 110.6, 108.5, 108.2, 77.6, 77.2, 76.7, 67.0, 66.8, 56.1, 55.5, 53.8, 53.6, 50.8, 45.5, 45.2, 44.5, 42.4, 42.3, 41.9, 32.9,

32.6, 28.5, 28.2, 28.0, 26.0, 25.9, 25.5, 24.4, 24.2, 24.0. ESI-HRMS m/z calcd for $C_{26}H_{38}N_7O_3$ $[M+H]^+$, 496.3021; found, 496.3031.

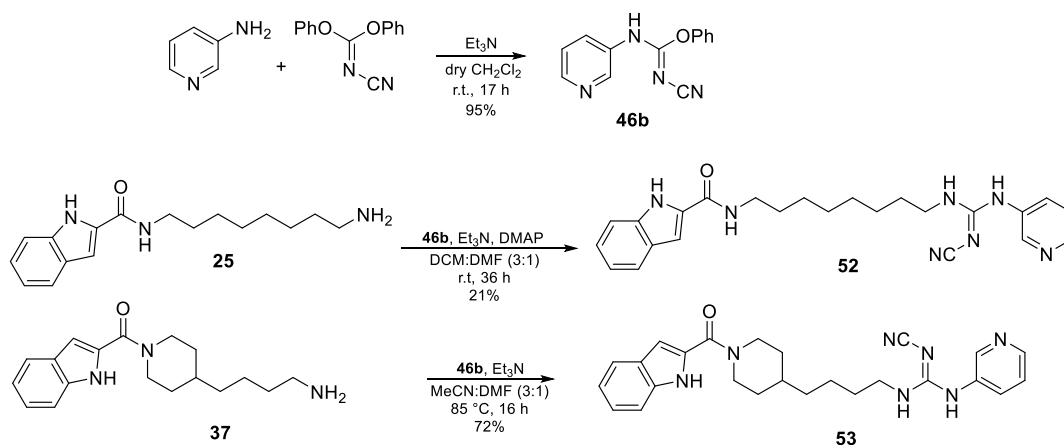
(E)-7-(2-Cyano-3-(pyridin-4-yl)guanidino)-N-(furan-2-ylmethyl)-N-(3-(pyrrolidin-1-yl)propyl)heptanamide (49e)

Compound **49e** was prepared according to the same procedure that was employed for **48a**, except that **38e** was used as starting material. Chromatography column (MeOH:DCM:NH₄OH, 1:10:0.1→1:6:0.1). Yield: 82%, white sticky solid. ¹H NMR (300 MHz, CDCl₃, δ ppm, mixture of rotamers) 8.36 – 8.23 (m, 4H, Py), 7.36 – 7.24 (m, 6H, 4H Py, 2H furan), 6.50 (br s, 2H, 2 NH-Py), 6.32 – 6.28 (m, 2H, furan), 6.24 – 6.20 (m, 2H, furan), 4.54 – 4.33 (m, 4H, 2 CH₂-furan), 3.51 – 3.28 (m, 8H, 2 CH₂-NH, 2 CH₂-N-C=O), 3.12 – 2.59 (m, 12H, 2 CH₂-N, 4 CH₂ pyrrolidine), 2.52 – 2.24 (m, 4H, 2 CH₂-C=O), 2.04 – 1.89 (m, 6H, 3 CH₂), 1.89 – 1.70 (m, 6H, 3 CH₂), 1.69 – 1.47 (m, 8H, 4 CH₂), 1.42 – 1.20 (m, 8H, 4 CH₂). ¹³C NMR (75.4 MHz, CDCl₃, δ ppm, mixture of rotamers) 174.3, 173.2, 162.7, 157.2, 150.2, 149.7, 145.8, 142.9, 142.1, 116.9, 114.9, 110.6, 108.7, 77.5, 77.0, 76.6, 54.0, 53.8, 53.1, 52.8, 45.1, 43.2, 42.3, 41.8, 32.7, 31.5, 30.1, 29.7, 29.2, 28.8, 28.2, 26.0, 24.9, 24.4, 23.4, 23.2, 22.7, 14.1. ESI-HRMS m/z calcd for $C_{26}H_{38}N_7O_2$ $[M+H]^+$, 480.3075; found, 480.3081.

(E)-8-(2-Cyano-3-(pyridin-4-yl)guanidino)-N-(furan-2-ylmethyl)octanamide (50)

The preparation of **50** from **46a** (64 mg, 270 μmol) and **30** (70 mg, 300 μmol) followed the same procedure described previously for **47a** (pag. 95). Chromatography column (MeOH:EtOAc, 1:10→1:5). Yield: 91%, white solid. ¹H NMR (300 MHz, CD₃OD, δ ppm) 8.43 – 8.35 (m, 2H, Py), 7.46 – 7.39 (m, 1H, furan), 7.39 – 7.31 (m, 2H, Py), 6.33 (dd, J = 3.1, 1.9 Hz, 1H, furan), 6.28 – 6.21 (m, 1H, furan), 4.34 (s, 2H, CH₂-furan), 3.38 (t, J = 7.2 Hz, 2H, CH₂-NH-C=N), 2.21 (t, J = 7.4 Hz, 2H, CH₂-C=O), 1.70 – 1.53 (m, 4H, 2 CH₂), 1.43 – 1.30 (m, 6H, 3 CH₂). ¹³C NMR (75.4 MHz, CD₃OD, δ ppm) 176.0 (C=O), 159.2 (C=N), 153.2 (qC, Py), 150.6 (2CH, Py), 148.4 (qC-furan), 143.3 (CH, furan), 117.8

(C≡N), 116.4 (2CH, Py), 111.3 (CH, furan), 108.0 (CH, furan), 43.4 (CH₂-NH-C=N), 37.1 (CH₂-furan), 36.8 (CH₂), 30.2 (CH₂), 30.0 (CH₂), 29.9 (CH₂), 27.6 (CH₂), 26.8 (CH₂). ESI-HRMS *m/z* calcd for C₂₀H₂₇N₆O₂ [M+H]⁺, 383.2186; found, 383.2190.



Scheme 30. Synthesis of (pyridin-3-yl)cyanoguanidine-based inhibitors **52** and **53**.

***N*-Cyano-*O*-phenyl-*N*-(3-pyridyl)isourea (**46b**)⁵²**

To a solution of 3-aminopyridine (175 mg, 1.9 mmol) in CH₂Cl₂ (6 mL) were added diphenylcyanocarbonyl imidate (490 mg, 2.1 mmol) and Et₃N (0.3 mL, 2.1 mmol). The reaction mixture was stirred under nitrogen for 17 h at r.t. The mixture was concentrated *in vacuo* and the residue was purified by column chromatography on silica gel (MeOH:EtOAc, 1:20) to give **46b** (420 mg, 95%) as a white solid. ¹H NMR (300 MHz, CDCl₃, δ ppm) 9.54 (br s, 1H), 8.79 – 8.60 (m, 1H), 8.59 – 8.40 (m, 1H), 7.83 – 7.68 (m, 1H), 7.49 – 7.37 (m, 2H), 7.37 – 7.24 (m, 2H), 7.19 – 7.06 (m, 2H). ESI-HRMS *m/z* calcd for C₁₃H₁₁N₄O [M+H]⁺, 239.0926; found, 239.0927. NMR data match with those previously reported for this compound.

(*E*)-*N*-(8-(2-Cyano-3-(pyridin-3-yl)guanidino)octyl)-1H-indole-2-carboxamide (52**)**

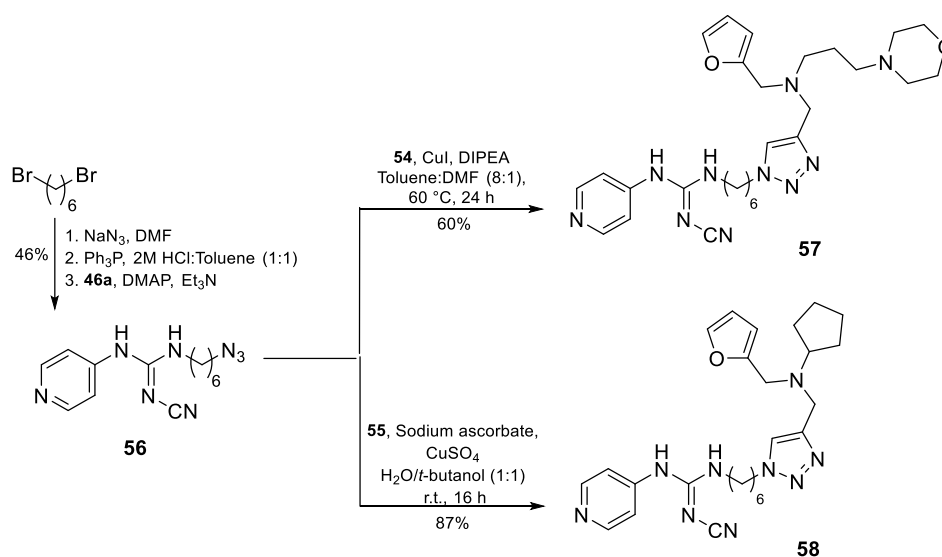
A solution of **25** (48 mg, 170 μmol), **46b** (44 mg, 180 μmol) and Et₃N (26 μL, 180 μmol) in dry CH₂Cl₂:DMF (3:1, 6.6 mL) was stirred at r.t. for 36 h. Then, the solvent was evaporated under reduced pressure and the residue was purified by chromatography

column on silica gel (MeOH:EtOAc, 1:40) to yield **52** (15 mg, 21%) as a white solid. ^1H NMR (300 MHz, CD_3OD , δ ppm) 8.51 – 8.42 (m, 1H, Py), 8.37 – 8.29 (m, 1H, Py), 7.83 – 7.71 (m, 1H, Py), 7.63 – 7.53 (m, 1H, indole), 7.45 – 7.38 (m, 2H, 1H Py, 1H indole), 7.24 – 7.16 (m, 1H, indole), 7.09 – 7.00 (m, 2H, indole), 3.39 (t, $J = 7.1$ Hz, 2H, $\text{CH}_2\text{-NH-C=N}$), 1.68 – 1.55 (m, 4H, $\text{CH}_2\text{-NH}$, CH_2), 1.44 – 1.35 (m, 10H, 5 CH_2). ^{13}C NMR (75.4 MHz, CD_3OD , δ ppm) 164.2 (C=O), 160.1 (C=N), 146.8 (CH, Py), 146.1 (CH, Py), 138.3 (qC, Py), 136.3 (qC, indole), 133.7 (CH, Py), 132.4 (qC, indole), 129.1 (qC, indole), 125.5 (CH, indole), 125.0 (CH, indole), 122.7 (CH, indole), 121.1 (CH, indole), 118.7 (CN), 113.0 (CH, Py), 104.2 (CH, indole), 43.2 ($\text{CH}_2\text{-NH-C=N}$), 40.6 ($\text{CH}_2\text{-C=O}$), 30.6 (CH_2), 30.4 (CH_2), 30.3 (CH_2), 30.2 (CH_2), 28.0 (CH_2), 27.7 (CH_2). ESI-HRMS m/z calcd for $\text{C}_{24}\text{H}_{30}\text{N}_7\text{O}$ $[\text{M}+\text{H}]^+$, 432.2507; found, 432.2506.

(E)-1-(4-(1-(1H-Indole-2-carbonyl)piperidin-4-yl)butyl)-2-cyano-3-(pyridin-3-yl)guanidine (53)

A solution of compound **37** (35 mg, 100 μmol), **46b** (26 mg, 100 μmol) and Et_3N (16 μL , 100 μmol) in dry MeCN:DMF, (3:1, 4 mL), was stirred at 85 $^\circ\text{C}$ for 16 h. The solvent was evaporated under reduced pressure and the residue was purified by chromatography column on silica gel (MeOH:EtOAc: CH_2Cl_2 , 1:5:1) to give **53** (34 mg, 72%) as a white solid. ^1H NMR (300 MHz, Acetone- d_6 , δ ppm) 10.62 (s, 1H, NH, indole), 8.68 – 8.52 (m, 1H, Py), 8.47 – 8.27 (m, 2H, NH-Py , 1H Py), 7.90 – 7.73 (m, 1H, Py), 7.69 – 7.57 (m, 1H, indole), 7.57 – 7.45 (m, 1H, indole), 7.45 – 7.31 (m, 1H, Py), 7.31 – 7.13 (m, 1H, indole), 7.13 – 6.98 (m, 1H, indole), 6.84 – 6.76 (m, 1H, indole), 6.77 – 6.63 (m, 1H, NH-CH_2), 4.70 – 4.52 (m, 2H, piperidine), 3.49 – 3.32 (m, 2H, $\text{CH}_2\text{-NH}$), 3.01 (br s, 2H, piperidine), 1.93 – 1.75 (m, 2H, piperidine), 1.72 – 1.54 (m, 3H, 1H piperidine, CH_2), 1.51 – 1.08 (m, 6H, 2H piperidine, 2 CH_2). ^{13}C NMR (75.4 MHz, Acetone- d_6 , δ ppm) 161.8, 160.1, 146.8, 146.1, 138.3, 136.0, 132.4, 127.5, 123.2, 121.4, 119.8, 118.7, 111.8, 111.7, 103.8, 103.7, 43.3, 41.7, 35.9, 32.4, 29.7, 23.4. ESI-HRMS m/z calcd for $\text{C}_{25}\text{H}_{30}\text{N}_7\text{O}$ $[\text{M}+\text{H}]^+$, 444.2501; found, 444.2506.

(s, 2H, CH_2 -furan), 3.37 (d, $J = 2.4$ Hz, 2H, $\text{CH}_2\text{-C}\equiv\text{CH}$), 3.01 – 2.87 (m, 1H, CH), 2.24 – 2.17 (m, 1H, $\text{CH}\equiv\text{C}$), 2.04 – 1.87 (m, 2H, CH_2), 1.82 – 1.67 (m, 2H, CH_2), 1.67 – 1.39 (m, 4H, 2 CH_2). ^{13}C NMR (75.4 MHz, CDCl_3 , δ ppm) 152.1 (qC, furan), 142.3 (CH, Furan), 110.2 (CH, Furan), 109.0 (CH, Furan), 78.7 ($\text{C}\equiv\text{CH}$), 73.2 ($\text{CH}\equiv\text{C}$), 63.3 (CH, cyclopentyl), 48.5 (CH_2 -furan), 40.7 ($\text{CH}_2\text{-C}\equiv\text{CH}$), 31.5 (2 CH_2), 24.1 (2 CH_2). ESI-HRMS m/z calcd for $\text{C}_{13}\text{H}_{18}\text{NO}$ $[\text{M}+\text{H}]^+$, 204.1380; found, 204.1383.



Scheme 32. Synthesis of (pyridin-4-yl)cyanoguanidine-based inhibitors **57** and **58**.

(E)-1-(6-Azidohexyl)-2-cyano-3-(pyridin-4-yl)guanidine (56**)**

Sodium azide (6.5 g, 100.0 mmol) was added to a solution of 1,6-dibromohexane (5.5 mL, 36.0 mmol) in DMF (100 mL). The mixture was stirred at 60 °C for 10 h and the solvent evaporated *in vacuo*. To the residue water was added and the product was extracted with Et_2O (3x). The organic phase was washed with water, dried over Na_2SO_4 , filtered and the solvent was evaporated to yield 1,6-diaza-1,6-hexanedithione (5.7 g, 94%) as a colourless oil. To a solution of this compound (5.7 g, 29 mmol) in toluene:HCl 2M (1:1, 150 mL), Ph_3P (7.6 g, 29 mmol) was slowly added, and the mixture was vigorously stirred for 16 h at r.t. The aqueous phase was separated and washed three times with Et_2O and dried under vacuum to obtain a colourless oil that

was used in the next step without further purification. ^1H NMR (300 MHz, CDCl_3 , δ ppm) 3.26 (t, $J = 6.9$ Hz, 2H), 2.72 (t, $J = 6.9$ Hz, 2H), 2.07 (s, 2H), 1.68 – 1.56 (m, 2H), 1.56 – 1.30 (m, 6H). ESI-HRMS m/z calcd for $\text{C}_{16}\text{H}_{15}\text{N}_4$ $[\text{M}+\text{H}]^+$, 143.1289; found, 143.1291. NMR data match with those previously reported for this compound.⁵³ To this compound (500 mg, 3.52 mmol) dissolved in dry MeCN:DMF (54 mL, 3:1), compound **46a** (762 mg, 3.2 mmol), Et_3N (1.25 mL, 8.95 mmol) and DMAP (82 mg, 0.7 mmol) were added, and the mixture was heated and stirred at 80 °C under argon overnight. The reaction mixture was concentrated under vacuum and the residue was purified by chromatography column on silica gel (MeOH: CH_2Cl_2 , 1:8) to yield **56** (722 mg, 46%) as a white solid. ^1H NMR (300 MHz, CDCl_3 , δ ppm) 8.48 – 8.29 (m, 2H, Py), 7.25 – 7.15 (m, 2H, Py), 6.24 – 6.04 (m, 1H, NH -Py), 3.37 (q, $J = 6.8$ Hz, 2H, CH_2 -NH), 3.25 (t, $J = 6.7$ Hz, 2H, CH_2 -N₃), 1.69 – 1.49 (m, 4H, 2 CH_2), 1.49 – 1.29 (m, 4H, 2 CH_2). ^{13}C NMR (75.4 MHz, CDCl_3 , δ ppm) 157.7 (C=N), 150.3 (2 CH, Py), 145.6 (Cq, Py), 117.1 (CN), 115.9 (2 CH, Py), 51.4 (CH_2 -N₃), 42.6 (CH_2 -NH), 29.2 (CH_2), 28.8 (CH_2), 26.4 (CH_2), 26.4 (CH_2). ESI-HRMS m/z calcd for $\text{C}_{13}\text{H}_{19}\text{N}_8$ $[\text{M}+\text{H}]^+$, 287.1729; found, 287.1727.

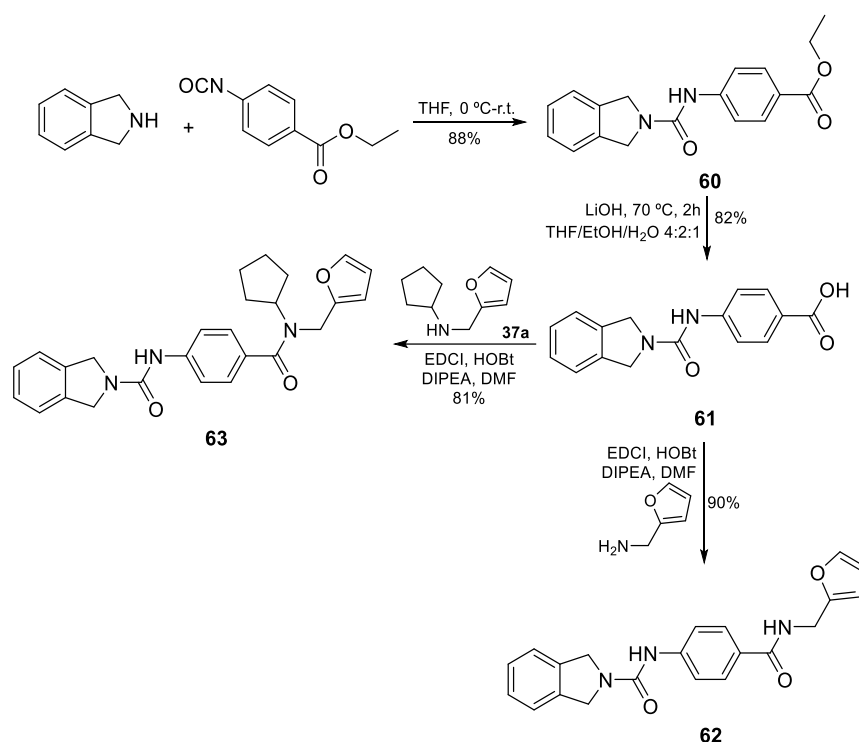
(E)-2-Cyano-1-(6-(4-(((furan-2-ylmethyl)(3-morpholinopropyl)amino)methyl)-1H-1,2,3-triazol-1-yl)hexyl)-3-(pyridin-4-yl)guanidine (57)

To a solution of **56** (48 mg, 170 μmol) in toluene:DMF (8:1, 4.5 mL), **54** (97 mg, 370 μmol), DIPEA (140 μL , 810 μmol) and CuI (6 mg, 34 μmol) were added, and the solution was stirred at 60 °C for 24 h. After evaporation, the resulting residue was dissolved in EtOAc and washed with a sat. aq. soln. of NaHCO_3 . The aq. phase was extracted with EtOAc (x2), and the organic phases were collected, dried over anh. Na_2SO_4 , filtered, and evaporated. The resulting residue was purified by chromatography column on silica gel (NH_4OH :MeOH:EtOAc, 0.1:1:9) to yield **57** (54 mg, 60%) as a white solid. ^1H NMR (300 MHz, CDCl_3 , δ ppm) 8.49 – 8.30 (m, 2H, Py), 7.48 (s, 1H, triazole), 7.34 (d, $J = 1.9$ Hz, 1H, furan), 7.30 – 7.20 (m, 2H, Py), 6.37 – 6.23 (m, 2H, furan, NH - CH_2), 6.19 (d, $J = 3.2$ Hz, 1H, furan), 4.32 (t, $J = 6.9$ Hz, 2H, CH_2 -triazole), 3.81 – 3.54 (m, 8H, CH_2 -furan, N- CH_2 -triazole, 2 CH_2 -O morpholine), 3.38 (q,

$J = 6.5$ Hz, 2H, $\text{CH}_2\text{-NH}$), 2.56 – 2.24 (m, 8H, 2 CH_2 morpholine, 2 CH_2), 1.95 – 1.81 (m, 2H, CH_2), 1.80 – 1.64 (m, 2H, CH_2), 1.64 – 1.50 (m, 2H, CH_2), 1.46 – 1.20 (m, 4H, 2 CH_2). ^{13}C NMR (75.4 MHz, CDCl_3 , δ ppm) 157.5 (C=N), 152.1 (qC, furan), 150.6 (2 CH, Py), 145.5 (qC, Py), 142.1 (CH, furan), 122.9 (CH, triazole), 116.9 (qC, triazole), 115.6 (2 CH, Py), 110.3 (CH, furan), 109.0 (CH, furan), 66.9 (2 $\text{CH}_2\text{-O}$ morpholine), 56.9 (CH_2), 53.8 (2 CH_2 morpholine), 51.5 (CH_2), 50.1 ($\text{CH}_2\text{-triazole}$), 49.9 (N- $\text{CH}_2\text{-triazole}$), 48.8 ($\text{CH}_2\text{-furan}$), 42.2 ($\text{CH}_2\text{-NH}$), 29.9 (CH_2), 29.0 (CH_2), 25.8 (CH_2), 25.7 (CH_2), 24.2 (CH_2). ESI-HRMS m/z calcd for $\text{C}_{28}\text{H}_{41}\text{N}_{10}\text{O}_2$ $[\text{M}+\text{H}]^+$, 549.3405; found, 549.3408.

(E)-2-Cyano-1-(6-(4-((cyclopentyl(furan-2-ylmethyl)amino)methyl)-1H-1,2,3-triazol-1-yl)hexyl)-3-(pyridin-4-yl)guanidine (58)

Compounds **56** (118 mg, 410 μmol) and **55** (134 mg, 660 μmol) were suspended in a mixture of $\text{H}_2\text{O}/t\text{-butanol}$ (1:1, 4 mL). Sodium ascorbate (16.3 mg, 82.4 μmol) and $\text{CuSO}_4 \cdot 5\text{H}_2\text{O}$ (2.1 mg, 8.2 μmol) were dissolved in H_2O (1 mL) and added to the mixture. The resulting solution was stirred at r.t. for 16 h. The solvent was evaporated, and the residue was purified by flash chromatography on silica gel ($\text{NH}_4\text{OH}:\text{MeOH}:\text{EtOAc}$, 0.1:1:9 \rightarrow 0.1:1:5) to yield **58** (175 mg, 87%) as a white solid. ^1H NMR (300 MHz, CDCl_3 , δ ppm) 8.46 – 8.34 (m, 2H, Py), 7.49 (s, 1H, triazole), 7.39 – 7.33 (m, 1H, furan), 7.31 – 7.23 (m, 2H, Py), 6.37 – 6.26 (m, 2H, furan, NH-CH_2), 6.22 (d, $J = 3.2$ Hz, 1H, furan), 4.32 (t, $J = 6.9$ Hz, 2H, $\text{CH}_2\text{-triazole}$), 3.79 (s, 2H, $\text{CH}_2\text{-furan}$), 3.66 (s, 2H, N- $\text{CH}_2\text{-triazole}$), 3.39 (q, $J = 6.7$ Hz, 2H, $\text{CH}_2\text{-NH}$), 3.02 – 2.84 (m, 1H, CH cyclopentyl), 1.99 – 1.79 (m, 4H, 2 CH_2), 1.76 – 1.39 (m, 8H, 4 CH_2), 1.39 – 1.22 (m, 4H, 2 CH_2). ^{13}C NMR (75.4 MHz, CDCl_3 , δ ppm) 157.5 (C=N), 152.2 (qC, furan), 150.6 (2 CH, Py), 145.8 (qC, Py), 142.1 (CH, furan), 123.2 (CH, triazole), 117.0 (qC, triazole), 115.5 (2 CH, Py), 110.3 (CH, furan), 109.2 (CH, furan), 63.6 (CH, cyclopentyl), 50.0 ($\text{CH}_2\text{-triazole}$), 47.8 (N- $\text{CH}_2\text{-triazole}$), 46.4 ($\text{CH}_2\text{-furan}$), 42.2 ($\text{CH}_2\text{-NH}$), 30.6 (2 CH_2), 29.9 (CH_2), 28.9 (CH_2), 25.7 (CH_2), 25.6 (CH_2), 24.3 (2 CH_2). ESI-HRMS m/z calcd for $\text{C}_{26}\text{H}_{36}\text{N}_9\text{O}$ $[\text{M}+\text{H}]^+$, 490.3036; found, 490.3037.



Scheme 33. Synthesis of isoindoline-based inhibitors **62** and **63**.

Ethyl 4-(isoindoline-2-carboxamide)benzoate (**60**)⁵⁴

Isoindoline (60 μL , 530 μmol) was dissolved in THF (5 mL) and cooled to 0 °C. Then, methyl 4-isocyanatobenzoate (84 mg, 440 μmol) was added and the resulting mixture was warmed to r.t. and stirred for 16h. The solution was concentrated, Et₂O was added, and the resulting precipitate was filtered to provide **60** (119 mg, 88%) as a white solid. ¹H NMR (300 MHz, CDCl₃, δ ppm) 7.98 (d, J = 8.3 Hz, 2H, Ph), 7.57 (d, J = 8.4 Hz, 2H, Ph), 7.35 – 7.23 (m, 4H, CH isoindoline), 6.65 (s, 1H, NH), 4.84 (s, 4H, 2 CH₂, isoindoline), 4.34 (q, J = 7.1 Hz, 2H, OCH₂CH₃) 1.38 (t, J = 7.1 Hz, 3H, OCH₂CH₃). ¹³C NMR (75 MHz, CDCl₃, δ ppm) 166.5 (C=O), 153.4 (C=O, urea), 143.5 (2 qC, isoindoline), 136.3 (qC, Ph), 130.9 (2 CH, Ph), 127.9 (2 CH, isoindoline), 124.8 (qC, Ph), 122.9 (2 CH, isoindoline), 118.4 (2 CH, Ph), 60.8 (OCH₂CH₃), 52.3 (2 CH₂, isoindoline), 14.5 (OCH₂CH₃). NMR data match with those previously reported for this compound.

4-(Isoindoline-2-carboxamido)benzoic acid (**61**)³²

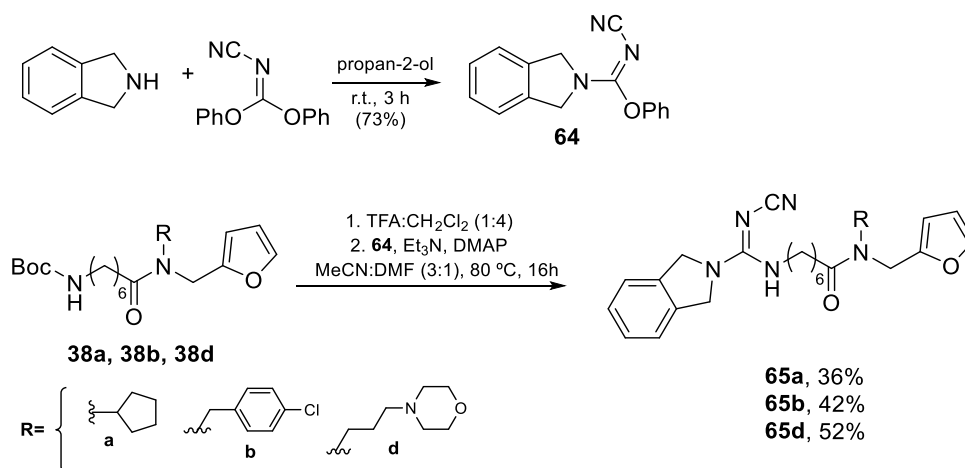
Compound **60** (90 mg, 320 μmol) was dissolved in THF (2 mL), EtOH (1 mL) and H₂O (0.5 mL), and LiOH (30 mg, 1.3 mmol) were added. The mixture was stirred at 70 °C for 2h and then the solvent was removed *in vacuo*. The obtained residue was dissolved in water, the pH was adjusted to 3 with HCl 2M and the resulting precipitate was filtered and washed with water to provide **61** (73 mg, 82%) as a white solid. ¹H NMR (300 MHz, DMSO-*d*₆, δ ppm) 12.53 (br s, OH), 8.68 (s, 1H, NH), 7.86 (d, *J* = 9.0 Hz, 2H, Ph), 7.73 (d, *J* = 9.0 Hz, 2H, Ph), 7.43 – 7.26 (m, 4H, CH isoindoline), 4.80 (s, 4H, CH₂, isoindoline). ¹³C NMR (75.4 MHz, DMSO-*d*₆, δ ppm) 167.6 (C=O), 154.0 (C=O, urea), 145.3 (2 qC, isoindoline), 137.1 (qC, Ph), 130.6 (2 CH, Ph), 127.8 (2 CH, isoindoline), 124.0 (qC, Ph), 123.3 (2 CH, isoindoline), 118.7 (2 CH, Ph), 52.4 (2 CH₂, isoindoline). NMR data match with those previously reported for this compound.

***N*-(4-((Furan-2-ylmethyl)carbamoyl)phenyl)isoindoline-2-carboxamide (62)**

Compound **61** (45 mg, 160 μmol), HOBt (32 mg, 240 μmol), furfurylamine (19 mg, 190 μmol) and DIPEA (110 μL , 640 μmol) were suspended in DMF (0.5 mL) and treated with EDCI (46 mg, 240 μmol). The mixture was stirred at r.t. overnight to give a solution that was diluted with 5 mL of ice water. The resulting turbid mixture was stirred at 0 °C for 1 h, then filtered and concentrated to yield **62** (52 mg, 90%) as an off-white solid. ¹H NMR (300 MHz, DMSO-*d*₆, δ ppm) δ 8.76 (t, *J* = 5.8 Hz, 1H, NH amide), 8.58 (s, 1H, NH urea), 7.81 (d, *J* = 8.4 Hz, 2H, Ph), 7.67 (d, *J* = 8.4 Hz, 2H, Ph), 7.56 (d, *J* = 1.8 Hz, 1H, furan), 7.44 – 7.23 (m, 4H, isoindoline), 6.39 (br t, 1H, furan), 6.26 (br d, 1H, furan), 4.79 (s, 4H, CH₂, isoindoline), 4.45 (d, *J* = 5.6 Hz, CH₂-furan). ¹³C NMR (75.4 MHz, DMSO-*d*₆, δ ppm) δ 165.7 (C=O, amide), 153.6 (C=O, urea), 152.7 (qC, furan), 143.3 (qC, isoindoline), 141.9 (CH, furan), 136.7 (qC, Ph), 127.8 (2 CH, Ph), 127.3 (CH, isoindoline), 127.0 (qC, Ph), 122.7 (2 CH, isoindoline), 118.2 (2 CH, Ph), 110.4 (CH, furan) 106.7 (CH, furan), 51.9 (CH₂, isoindoline), 35.9 (N-CH₂). ESI-HRMS *m/z* calcd for C₂₁H₁₉N₃O₃Na [M+Na]⁺: 384.1324; found, 384.1313.

***N*-[4-(Cyclopentyl(furan-2-ylmethyl)carbamoyl)phenyl]isoindoline-2-carboxamide (63)**

Compound **63** was prepared according to the same procedure that was employed for **62**, except that **37a** was used as starting material. Yield: 81%, off-white solid. ^1H NMR (300 MHz, DMSO- d_6 , δ ppm) δ 8.52 (s, 1H, NH, urea), 7.65 (d, J = 8.2 Hz, 2H, Ph), 7.57 (d, J = 1.9 Hz, 1H, furan), 7.42 – 7.26 (m, 6H, Ph, isoindoline), 6.40 (t, J = 2.7 Hz, 1H, furan), 6.26 (d, J = 3.2 Hz, 1H, furan), 4.79 (s, 4H, CH₂ Isoindoline), 4.52 (s, 2H, CH₂-furan), 4.21 (br s, 1H, CH Cyclopentyl), 1.80 - 1.32 (m, 8H, 4 CH₂ Cyclopentyl). ^{13}C NMR (75.4 MHz, DMSO- d_6 , δ ppm) δ 171.4 (C=O, amide), 154.3 (C=O, urea), 152.9 (CH, furan), 142.2 (qC, Ph), 142.0 (CH, furan), 137.2 (qC, isoindoline), 130.6 (qC, Ph), 127.8 (CH, isoindoline), 127.4 (2 CH, Ph), 123.3 (CH, isoindoline), 119.2 (2 CH, Ph), 111.1 (CH, furan), 107.4 (CH, furan), 59.6 (CH, Cyclopentyl), 52.4 (CH₂, Isoindoline), 40.4 (N-CH₂), 29.5 (2 CH₂, Cyclopentyl), 24.0 (2 CH₂, Cyclopentyl). ESI-HRMS m/z calcd for C₂₆H₂₇N₃O₃Na [M+Na]⁺: 452.1950; found, 452.1940.



Scheme 34. Synthesis of isoindoline-based inhibitors **65a**, **65b** and **65d**.

Phenyl (*E*)-*N*-cyanoisoindoline-2-carbimide (64)

Isoindoline (60 μL , 530 μmol) was added to a solution of diphenylcyanocarbonimidate (130 mg, 530 μmol) in propan-2-ol (1.2 mL). The reaction mixture was stirred under

nitrogen for 3 h at r.t. The precipitate was filtered, washed with propan-2-ol and dried to yield **64** (102 mg, 73%) as a white solid. ^1H NMR (300 MHz, CDCl_3 , δ ppm) 7.48 – 7.12 (m, 9H, 5H Ph, 4H isoindoline), 5.20 (s, 2H, isoindoline), 5.01 (s, 2H, isoindoline). ^{13}C NMR (75.4 MHz, CDCl_3 , δ ppm) 157.0 (qC, Ph), 151.8 (C=N), 134.9 (2 qC, isoindoline), 130.0 (2 CH, Ph), 128.4 (2 CH, isoindoline), 126.5 (CH, Ph), 122.8 (2 CH, isoindoline), 120.4 (2 CH, Ph), 113.7 (C=N), 54.3 (2 CH_2 isoindoline). ESI-HRMS m/z calcd for $\text{C}_{16}\text{H}_{13}\text{N}_3\text{ONa}$ $[\text{M}+\text{Na}]^+$, 286.0951; found, 286.0951.

(E)-7-(N'-Cyanoisoindoline-2-carboximidamido)-N-cyclopentyl-N-(furan-2-ylmethyl)heptanamide (65a)

Compound **65a** was prepared according to the same procedure that was employed for **48a** (pag. 101), except that **38a** and **64** were used as starting materials. Chromatography column (EtOAc:Cy, 2:1). Yield: 36%, white solid. ^1H NMR (300 MHz, CDCl_3 , δ ppm, mixture of rotamers) 7.42 – 7.17 (m, 10H, 8H isoindoline, 2H furan), 6.29 (br d, 2H, furan), 6.14 (br s, 2H, furan), 5.36 (br s, 1H, NH-CH_2 rotamer A), 5.25 (br s, 1H, NH-CH_2 rotamer B), 4.90 (s, 8H, 4 CH_2 isoindoline), 4.81 – 4.61 (m, 1H, CH cyclopentyl rotamer A), 4.48 – 4.33 (m, 4H, 2 CH_2 -furan), 4.27 – 4.11 (m, 1H, CH cyclopentyl rotamer B), 3.62 – 3.44 (m, 4H, 2 CH_2 -NH), 2.49 – 2.28 (m, 4H, 2 CH_2 -C=O), 1.91 – 1.28 (m, 32H, 8 CH_2 cyclopentyl, 8 CH_2). ^{13}C NMR (75.4 MHz, CDCl_3 , δ ppm, mixture of rotamers) 173.8, 173.2, 156.0, 152.7, 152.1, 142.1, 141.1, 135.5, 128.0, 122.7, 118.0, 110.6, 107.3, 107.1, 103.3, 77.6, 77.2, 76.7, 58.8, 56.3, 53.7, 43.0, 42.7, 41.9, 38.5, 33.7, 33.5, 30.1, 29.9, 29.1, 28.7, 28.4, 26.4, 26.0, 25.1, 23.9. ESI-HRMS m/z calcd for $\text{C}_{27}\text{H}_{36}\text{N}_5\text{O}_2$ $[\text{M}+\text{H}]^+$, 462.2860; found, 462.2864.

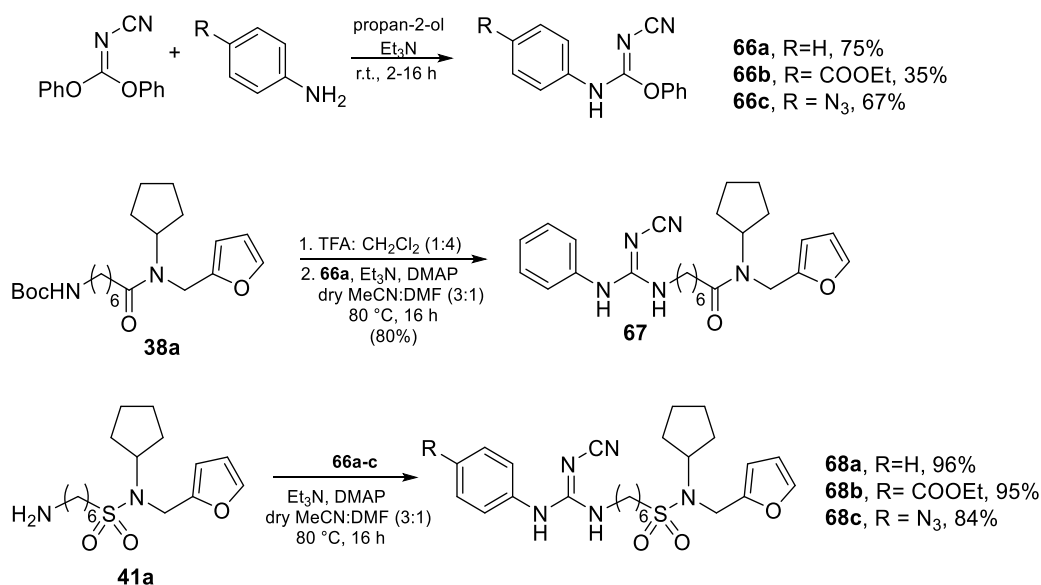
(E)-N-(4-Chlorobenzyl)-7-(N'-cyanoisoindoline-2-carboximidamido)-N-(furan-2-ylmethyl)heptanamide (65b)

Compound **65b** was prepared according to the same procedure that was employed for **48a** (pag. 101), except that **38b** and **64** were used as starting materials.

Chromatography column (EtOAc:Cy, 2:1). Yield: 42%, white solid. ^1H NMR (300 MHz, CDCl_3 , δ ppm, mixture of rotamers) 7.40 – 7.02 (m, 18H, 8H Ph, 8H isoindoline, 2H furan), 6.41 – 6.25 (m, 2H, furan), 6.25 – 6.11 (m, 2H, furan), 5.17 – 5.01 (m, 2H, NH-CH_2), 4.89 (s, 8H, 4 CH_2 isoindoline), 4.58 – 4.29 (m, 8H, 2 CH_2 -Ph, 2 CH_2 -furan), 3.66 – 3.44 (m, 4H, CH_2 -NH), 2.55 (t, $J = 7.3$ Hz, 2H, CH_2 -C=O rotamer A), 2.35 (t, $J = 7.3$ Hz, 2H, CH_2 -C=O rotamer B), 1.83 – 1.27 (m, 16H, 8 CH_2). ^{13}C NMR (75.4 MHz, CDCl_3 , δ ppm, mixture of rotamers) 173.4, 156.0, 150.9, 150.0, 142.9, 142.4, 136.1, 135.4, 135.3, 133.6, 133.3, 129.6, 129.2, 128.9, 128.1, 127.9, 122.7, 117.9, 110.5, 108.9, 108.5, 77.6, 77.2, 76.7, 53.7, 50.1, 47.7, 43.8, 43.1, 41.6, 33.0, 30.0, 28.8, 28.6, 26.4, 26.3, 25.0. ESI-HRMS m/z calcd for $\text{C}_{29}\text{H}_{33}\text{ClN}_5\text{O}_2$ $[\text{M}+\text{H}]^+$, 518.2314; found, 518.2317.

(*E*)-7-(*N'*-Cyanoisoindoline-2-carboximidamido)-*N*-(furan-2-ylmethyl)-*N*-(3)-morpholinopropyl)heptanamide (65d)

Compound **65d** was prepared according to the same procedure that was employed for **48a** (pag. 101), except that **38d** and **64** were used as starting materials. Chromatography column ($\text{NH}_4\text{OH}:\text{MeOH}:\text{EtOAc}$, 0.1:1:10). Yield: 52%, colourless oil. ^1H NMR (300 MHz, CDCl_3 , δ ppm, mixture of rotamers) 7.42 – 7.22 (m, 10H, 8H isoindoline, 2H furan), 6.36 – 6.26 (m, 2H, furan), 6.26 – 6.15 (m, 2H, furan), 5.15 – 4.99 (m, 2H, 2 NH-CH_2), 4.90 (s, 8H, isoindoline), 4.56 (s, 2H, CH_2 -furan rotamer A), 4.45 (s, 2H, CH_2 -furan rotamer B), 3.77 – 3.64 (m, 8H, 4 CH_2 morpholine), 3.62 – 3.49 (m, 4H, 2 CH_2 -NH), 3.44 – 3.29 (m, 4H, 2 CH_2), 2.54 – 2.23 (m, 16H, 4 CH_2 morpholine, 4 CH_2), 1.78 – 1.53 (m, 8H, 4 CH_2), 1.52 – 1.30 (m, 8H, 4 CH_2). ^{13}C NMR (75.4 MHz, CDCl_3 , δ ppm, mixture of rotamers) 173.2, 173.0, 156.0, 151.5, 150.7, 142.7, 142.1, 135.4, 128.1, 122.8, 117.8, 110.6, 108.4, 108.1, 77.6, 77.2, 76.7, 67.1, 67.0, 56.3, 55.6, 53.8, 53.7, 50.9, 45.4, 45.2, 44.5, 43.1, 43.0, 41.6, 33.1, 32.9, 30.0, 29.9, 28.7, 26.3, 26.3, 25.6, 25.1, 25.0, 24.5. ESI-HRMS m/z calcd for $\text{C}_{29}\text{H}_{41}\text{N}_6\text{O}_3$ $[\text{M}+\text{H}]^+$, 521.3239; found, 521.3235.

Scheme 35. Phenyl-based inhibitors **67**, **68a-c**.**Phenyl (Z)-N'-cyano-N-phenylcarbamide (66a)**⁵⁵

Aniline (0.2 mL, 2.2 mmol) was added to a solution of diphenyl *N*-cyanocarbonimidate (524 mg, 2.20 mmol) in propan-2-ol (5 mL). The reaction mixture was stirred under nitrogen for 2 h at r.t. The precipitate was filtered, washed with propan-2-ol and dried to yield **66a** (450 mg, 75%) as a white solid. ¹H NMR (300 MHz, DMSO-*d*₆, δ ppm) 10.84 (s, 1H), 7.55-7.36 (m, 6H), 7.35 – 7.21 (m, 4H). NMR data match with those previously reported for this compound.

Ethyl (Z)-4-(((cyanoimino)(phenoxy)methyl)amino)benzoate (66b)

Compound **66b** was prepared according to the same procedure that was employed for **66a**, except that ethyl 4-aminobenzoate was used as starting material. Yield: 35%, white solid. ¹H NMR (300 MHz, CDCl₃, δ ppm) 9.11 (s, 1H, NH), 8.05 (d, *J* = 8.6 Hz, 2H, Ph), 7.53 – 7.28 (m, 5H, OPh), 7.15 (d, *J* = 8.6 Hz, 2H, Ph), 4.37 (q, *J* = 7.1 Hz, 2H, CH₂CH₃), 1.39 (t, *J* = 7.1 Hz, 3H, CH₃CH₂). ¹³C NMR (75.4 MHz, CDCl₃, δ ppm) 165.9 (C=O), 151.0 (C=N), 139.6 (CN), 130.9 (2CH, Ph), 130.0 (2CH, OPh), 128.18 (qC, Ph), 127.22 (2CH, OPh), 122.01 (2C, qC, CH OPh), 121.45 (2CH, Ph), 61.26 (CH₂CH₃), 14.45

(CH₂CH₃). ESI-HRMS m/z calcd for C₁₇H₁₅N₃O₃Na [M+Na]⁺, 332.1004; found, 332.1006.

Phenyl (*Z*)-*N*-(4-azidophenyl)-*N'*-cyanocarbamimidate (66c)

Compound **66c** was prepared according to the same procedure that was employed for **66a**, except that ethyl 4-azidoaniline hydrochloride was used as starting material. Yield: 67%, light-brown solid. ¹H NMR (300 MHz, CDCl₃, δ ppm) 8.59 (s, 1H, NH), 7.50 – 7.28 (m, 5H, OPh), 7.13 (d, $J = 7.8$ Hz, 2H, Ph), 7.04 (d, $J = 8.8$ Hz, 2H, Ph). ¹³C NMR (75.4 MHz, CDCl₃, δ ppm) 151.0 (2C, C=N, qC OPh), 138.6 (C≡N), 132.1 (2qC, Ph), 129.9 (2CH, OPh), 127.2 (CH, OPh), 124.9 (2CH, OPh), 121.5 (2CH, Ph), 119.9 (CH, Ph). ESI-HRMS m/z calcd for C₁₄H₁₀N₆O₃Na [M+Na]⁺, 301.0809; found, 301.0808.

(*E*)-7-(2-Cyano-3-phenylguanidino)-*N*-cyclopentyl-*N'*-(furan-2-ylmethyl)heptanamide (67)

Compound **67** was prepared according to the same procedure that was employed for **48a** (pag. 101), except that **66a** was used as starting material. Chromatography column (EtOAc:Cy, 1:1→2:1). Yield: 80%, white solid. ¹H NMR (300 MHz, CDCl₃, δ ppm, mixture of rotamers) 7.60 – 7.16 (m, 14H, 10H Ph, 2H furan, 2 NH-Ph), 6.29 (br d, 2H, furan), 6.13 (br s, 2H, furan), 5.02 (s, 2H, 2 NH-CH₂), 4.80 – 4.60 (m, 1H, CH cyclopentyl rotamer A), 4.38 (br d, 4H, 2 CH₂-furan), 4.28 – 4.06 (m, 1H, CH cyclopentyl rotamer B), 3.33 – 3.17 (m, 4H, 2 CH₂-NH), 2.47 – 2.23 (m, 4H, 2 CH₂-C=O), 1.89 – 1.15 (m, 32H, 8 CH₂ cyclopentyl, 8 CH₂). ¹³C NMR (75.4 MHz, CDCl₃, δ ppm, mixture of rotamers) 173.7, 173.0, 158.8, 152.7, 152.2, 142.1, 141.0, 135.6, 130.2, 127.4, 125.5, 118.0, 110.6, 107.5, 107.0, 77.6, 77.2, 76.7, 58.7, 56.2, 41.9, 41.8, 38.4, 33.7, 33.5, 30.0, 29.1, 29.0, 28.7, 26.4, 25.0, 23.9. ESI-HRMS m/z calcd for C₂₅H₃₄N₅O₂ [M+H]⁺, 436.2707; found, 436.2707.

(*E*)-6-(2-Cyano-3-phenylguanidino)-*N*-cyclopentyl-*N'*-(furan-2-ylmethyl)hexane-1-sulfonamide (68a)

Compound **68a** was prepared according to the same procedure that was employed for **47a** (pag. 95), except that **66a** was used as starting material. Chromatography column (EtOAc:Cy, 1:1→2:1). Yield: 96%, white solid. ^1H NMR (300 MHz, CDCl_3 , δ ppm) 7.52 – 7.16 (m, 7H, 5H Ph, 1H furan, NH-Py), 6.41 – 6.21 (m, 2H, furan), 4.89 (t, $J = 5.8$ Hz, 1H, NH-CH_2), 4.35 (s, 2H, CH_2 -furan), 4.13 (quint, $J = 8.3$ Hz, 1H, CH cyclopentyl), 3.31 – 3.18 (m, 2H, CH_2 -NH), 2.80 – 2.67 (m, 2H, CH_2SO_2), 1.95 – 1.41 (m, 12H, 8H cyclopentyl, 2 CH_2), 1.41 – 1.17 (m, 4H, 2 CH_2). ^{13}C NMR (75.4 MHz, CDCl_3 , δ ppm) 158.9 (C=N), 151.5 (qC, furan), 142.2 (CH, furan), 135.4 (qC, Ph), 130.3 (2CH, Ph), 127.8 (CH, Ph), 125.8 (2CH, Ph), 118.0 (CN), 110.8 (CH, furan), 109.2 (CH, furan), 59.3 (CH, cyclopentyl), 53.3 (CH_2SO_2), 41.8 (CH_2 -NH), 40.0 (CH_2 -furan), 30.0 (2 CH_2 , cyclopentyl), 29.1 (CH_2), 27.9 (CH_2), 26.2 (CH_2), 23.6 (2 CH_2 , cyclopentyl), 23.3 (CH_2). ESI-HRMS m/z calcd for $\text{C}_{24}\text{H}_{33}\text{N}_5\text{O}_3\text{SNa}$ [$\text{M}+\text{Na}$] $^+$, 494.2196; found, 494.2196.

Ethyl(*E*)-4-(2-cyano-3-(6-(*N*-cyclopentyl-*N*-(furan-2-ylmethyl)sulfamoyl)hexyl)guanidino)benzoate (68b)

Compound **68b** was prepared according to the same procedure that was employed for **47a** (pag. 95), except that **66b** was used as starting material. Chromatography column (EtOAc:Cy, 1:2→1:1). Yield: 95%, pale-yellow solid. ^1H NMR (300 MHz, CDCl_3 , δ ppm) 8.06 (d, $J = 8.6$ Hz, 2H, Ph), 7.88 (s, 1H, NH-Ph), 7.38 – 7.34 (m, 1H, furan), 7.30 (d, $J = 8.6$ Hz, 2H, Ph), 6.36 – 6.25 (m, 2H, furan), 5.24 (br s, 1H, NH-CH_2), 4.43 – 4.30 (m, 4H, CH_2CH_3 , CH_2 -furan), 4.13 (quint, $J = 8.4$ Hz, 1H, CH cyclopentyl), 3.30 (q, $J = 6.8$ Hz, 2H, CH_2 -NH), 2.79 – 2.70 (m, 2H, CH_2SO_2), 1.92 – 1.45 (m, 12H, 8H cyclopentyl, 2 CH_2), 1.45 – 1.20 (m, 7H, CH_3CH_2 , 2 CH_2). ^{13}C NMR (75.4 MHz, CDCl_3 , δ ppm) 165.7 (C=O), 158.2 (C=N), 151.4 (qC, furan), 142.2 (CH, furan), 140.2 (qC, Ph) 131.5 (2CH, Ph), 128.5 (qC, Ph), 123.5 (2CH, Ph), 110.8 (CH, furan), 109.2 (CH, furan), 61.4 (CH_2CH_3), 59.3 (CH, cyclopentyl), 53.2 (CH_2SO_2), 42.1 (CH_2 -NH), 40.0 (CH_2 -furan), 30.0 (2 CH_2 , cyclopentyl), 29.0 (CH_2), 27.8 (CH_2), 26.2 (CH_2), 23.6 (2 CH_2 , cyclopentyl), 23.3(CH_2), 14.4 (CH_3CH_2). ESI-HRMS m/z calcd for $\text{C}_{27}\text{H}_{37}\text{N}_5\text{O}_3\text{SNa}$ [$\text{M}+\text{Na}$] $^+$, 566.2400; found, 566.2408.

(E)-6-(3-(4-Azidophenyl)-2-cyanoguanidino)-N-cyclopentyl-N-(furan-2-ylmethyl)hexane-1-sulfonamide (68c)

Compound **68c** was prepared according to the same procedure that was employed for **47a** (pag. 95), except that **66c** was used as starting material. Chromatography column (EtOAc:Cy, 1:2→1:1). Yield: 84%, light-red solid. ^1H NMR (300 MHz, CDCl_3 , δ ppm) 7.64 (s, 1H, NH-Ph), 7.35 (dd, $J = 1.9, 0.9$ Hz, 1H, furan), 7.23 (d, $J = 8.7$ Hz, 2H, Ph), 7.06 (d, $J = 8.7$ Hz, 2H, Ph) 6.40 – 6.16 (m, 2H, furan), 4.89 (br s, 1H, NH-CH_2), 4.35 (s, 2H, CH_2 -furan), 4.13 (quint, $J = 8.5$ Hz, 1H, CH, cyclopentyl), 3.24 (q, $J = 6.8$ Hz, 2H, CH_2 -NH), 2.80 – 2.69 (m, 2H, CH_2SO_2), 1.95 – 1.41 (m, 12H, 8H cyclopentyl, CH_2), 1.41 – 1.08 (m, 6H, 3 CH_2). ^{13}C NMR (75.4 MHz, CDCl_3 , δ ppm) 159.0 (C=N), 151.5 (qC, furan), 142.2 (CH, furan), 139.6 (C \equiv N), 132.1 (qC, Ph), 127.4 (2CH, Ph), 120.7 (2CH, Ph), 118.0 (qC, Ph), 110.8 (CH, furan), 109.2 (CH, furan), 59.3 (CH, cyclopentyl), 53.2 (CH_2SO_2), 41.9 (CH_2 -NH), 40.0 (CH_2 -furan), 30.0 (2 CH_2 , cyclopentyl), 29.8 (CH_2), 29.1 (CH_2), 27.9 (CH_2), 26.2 (CH_2 , cyclopentyl), 23.6 (CH_2 , cyclopentyl), 23.3 (CH_2). ESI-HRMS m/z calcd for $\text{C}_{24}\text{H}_{32}\text{N}_8\text{O}_3\text{SNa}$ [$\text{M}+\text{Na}$] $^+$, 535.2209; found, 535.2210.

2. SYNTHESIS OF NEW INNOVATIVE PAYLOADS AND GLUTATHIONE-SENSITIVE LINKERS FOR ANTIBODY-DRUG CONJUGATES (ADCs)

2.1 INTRODUCTION

2.1.1 Antibody-Drug Conjugates in the market

Antibody-drug conjugates (ADCs) are among the most complex, rising, and promising cancer therapeutics. Considerable progress has been made in this field during the last years since the approval of Gemtuzumab Ozogamicin (Mylotarg®) in 2000. The primary function of an ADC is to selectively deliver a very potent cytotoxic drug to tumor cells, thus reducing side effects by leaving healthy cells unharmed. ADCs are made up of a monoclonal antibody (mAb), responsible for antigen binding, which is connected to a cytotoxic molecule (payload) through a linker that plays a fundamental role for plasma stability and drug release (Figure 24).⁵⁶

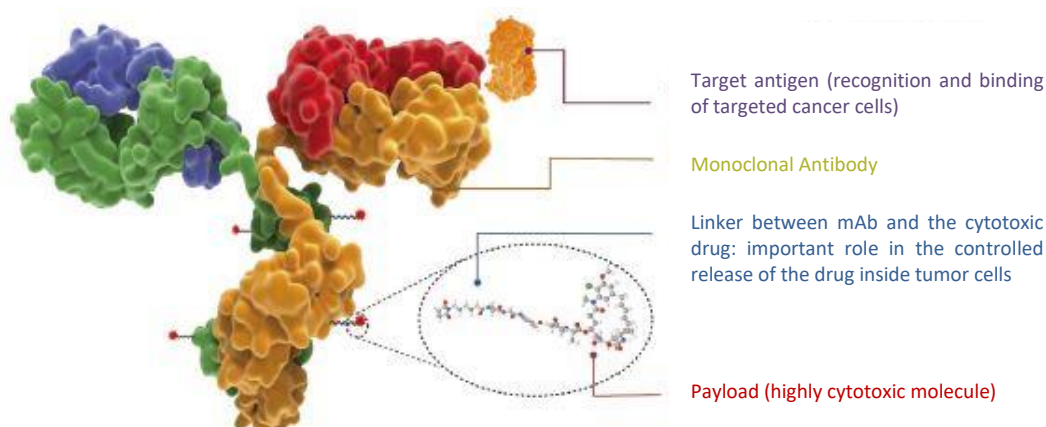


Figure 24. Composition of an Antibody-Drug Conjugate and role descriptions of its key parts.⁵⁷

By December 2021, 14 ADCs have been approved (Table 5) for both hematological and solid tumors, and more than 100 candidates are in clinical trials at present.⁵⁸ Antibody-drug conjugates are leading a new era of targeted cancer therapy and are expected to be an alternative for conventional chemotherapies in the near future, contributing to widening therapeutic windows for highly cytotoxic drugs. Although many ADCs have shown impressive activity against refractory cancers, their use is still limited due to toxicity problems, poor understanding of resistance mechanistic pathways, limited solid tumor penetration and sophisticated design.

Table 5. Approved Antibody-Drug Conjugates (ADCs) up to date.

API	Linker	Payload	Indication	Approval status
Gemtuzumab ozogamicin	Hydrazone	Calicheamicin	Acute myeloid leukemia	Approved 2000 Withdrawn 2010 Reapproved 2017
Brentuximab vedotin	Dipeptide (VC)	MMAE	Hodgkin lymphoma	Accelerated approval 2011
Trastuzumab emtansine	Non-cleavable (SMCC)	DM1	HER2-positive breast cancer	Approved 2013
Inotuzumab ozogamicin	Hydrazone	Calicheamicin	Acute lymphoblastic leukemia	Approved 2017
Moxetumomab pasudotox	Hydrazone	Pasudotox-tdfk	Relapsed hairy cell leukemia	Approved 2018
Polatuzumab vedotin	Dipeptide (VC)	MMAE	Relapsed or refractory diffuse large B-cell lymphoma	Approved 2019
Enfortumab vedotin	Dipeptide (VC)	MMAE	Solid and urothelial tumors	Approved 2019
Trastuzumab deruxtecan	Non-cleavable (mc)	Deruxtecan	HER2-positive breast cancer	Approved 2019
Sacituzumab govitecan	Acid-labile ester	SN-38	Triple-negative breast cancer, urothelial and other cancers	Approved 2020
Belantamab mafodotin-blmf	Non-cleavable (mc)	MMAE	Multiple myeloma	Approved 2020
Cetuximab sarotalocan	No linker	Irdye 700DX	Head and neck cancer	Approved 2020
Loncastuximab tesirine-lpyl	Dipeptide (VA)	PDB	large B-cell lymphoma	Approved 2021
Tisotumab vedotin tftv	Dipeptide (VC)	MMAE	Metastatic cervical cancer	Approved 2021
Disitamab vedotin	Dipeptide (VC)	MMAE	Solid tumors	Approved 2021

API= Active Pharmaceutical Ingredient; VC= valine-citrulline; VA= valine-alanine; SMCC= N-succinimidyl-4-(N-maleimidomethyl)Cy-1-carboxylate, mc= maleimidocaproyl; No linker= payload directly linked to mAb *via* Lysine residues; MMAE= Monomethyl auristatin E; DM1= Mertansine; SN-38= 7-Ethyl-10-hydroxycamptothecin; PDB= pyrrolbenzodiazepines.

2.1.2 Internalizing and non-internalizing ADCs

Conventionally, ADCs have been developed by using mAbs with high internalizing capacity, to achieve efficient delivery of the payload within the cancer cells. However, tumor cell antigens often exhibit limited diffusion into solid tumor mass due to different reasons, including slow extravasation caused by mAb accumulation and antibody trapping by abundant stroma possessed by most human solid tumors.⁵⁹ Therefore, during the last years a new technology based on non-internalizing ADCs has been developed by different research groups.^{60,61} The principle underlying this new approach is based on the reducing conditions in the tumor microenvironment

(TME), that promote the release of the payload extracellularly, and its subsequent diffusion inside the tumor cells provoking their death. Even though in this thesis work the focus will be only on internalizing ADCs, a review that covers the differences between these two ADC technologies, is worth reading.⁶²

2.1.3 Target antigen selection and mechanism of action of ADCs

As previously discussed, one of the three most important aspects of ADC design is identifying a highly expressed target antigen that is mainly present in tumor cell but not in healthy tissue. Internalizing ADCs are designed to deliver a highly cytotoxic drug to any cell expressing its unique antigenic target, that should be a cell surface protein to be recognized by the circulating mAb. Furthermore, the overall positive result relies also on the internalization process and the release of the drug from the lysosome to the cytosol.⁶³ In more details, the pathway of an ADC (Figure 25) begins upon administration in the blood stream. Once the ADC reaches the tumor site (Step 1, Figure 25), it diffuses slowly and passively from the capillaries to target cells in the tumor microenvironment (TME). Then, the mAb binds the target antigen (Step 2, Figure 25) and the internalization process (Step 3, Figure 25) starts. While some ADCs are recycled and transported outside the cell (Step 4, Figure 25), in the endosome or lysosome, acidic or proteolytic cleavage of the linkers occurs with the release of the drug (Step 5, Figure 25). The payload is now free for target engagement ultimately leading to cell death (Step 6, Figure 25). It is worth to highlight that depending on the lipophilic nature of the payloads, some cytotoxic drugs are able to pass the cell membrane and to enter other neighbouring cells regardless of the target expression, a process known as “bystander effect”.^{57,64}

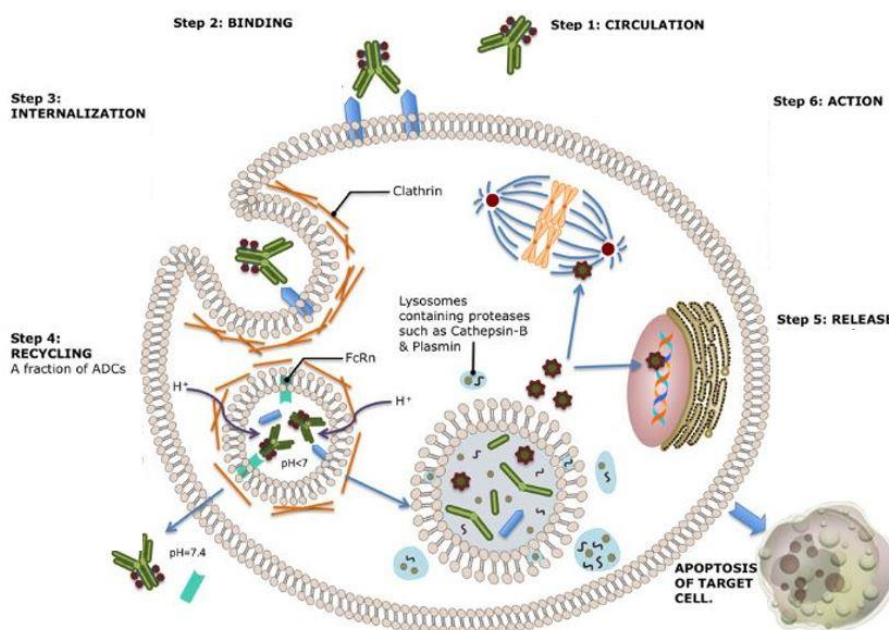


Figure 25. Mechanism of action of Antibody-Drug Conjugates.

2.1.4 Antibodies

Antibodies are immune system-related proteins called immunoglobulins. Each antibody consists of four polypeptides, that is, two heavy chains and two light chains joined to form a "Y" shaped macromolecule. The heavy and light chains include constant and variable regions. The variable regions (FaB) determine the antigen binding site. The constant regions (Fc) of the heavy chains determine the immunoglobulin class to which the antibody belongs.⁶⁵ Nowadays, ADCs are made of engineered humanized antibody skeleton by combining the variable domains of non-human antibodies with human constant domains to avoid hypersensitive reaction such as immune response.⁶⁴

2.1.5 Chemical Linkers in Antibody-Drug Conjugates

The linker in an ADC system has two purposes; the first one is to firmly keep the cytotoxic drug anchored to the ADC before reaching the target, while the second one is to release the payload efficiently within the tumor cells. There are two general

families of chemical linkers based on their release mechanism, cleavable and non-cleavable linkers (Figure 26)

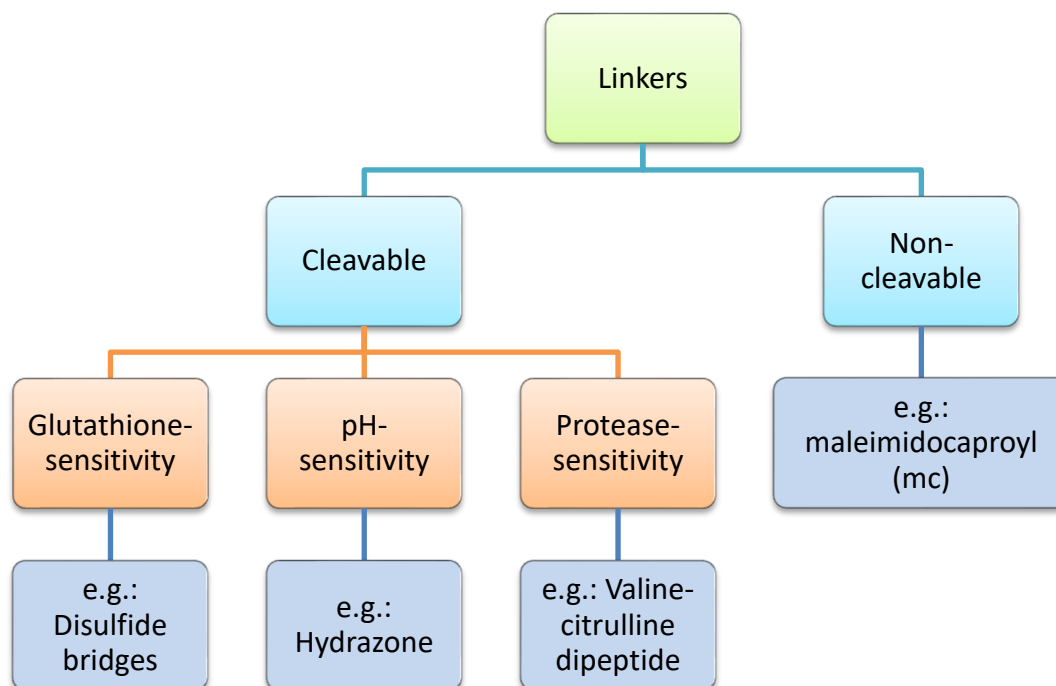


Figure 26. Types of ADC linkers.

2.1.5.1 Non-Cleavable Linkers

Non-cleavable linkers are much more stable in plasma and thus they have lower toxicity outside the target cell than cleavable linkers. Even though, non-degradable spacers do not have as well defined a cleavage mechanism as degradable ones, they indeed degrade. The release of the cytotoxic agent is based on the degradation of the monoclonal antibody by the action of lysosomal enzymes once the ADC has entered the cell. The most representative non-cleavable linkers are based on the reagents *N*-succinimidyl-4-(*N*-maleimidomethyl)cyclohexane-1-carboxylate (SMCC, Figure 27A) and maleimidocaproyl (mc, Figure 27B), among others. One successful example of ADC with this class of linkers is trastuzumab-DM1, that has proved to be efficient for the treatment of HER2 positive breast cancer.⁶⁶

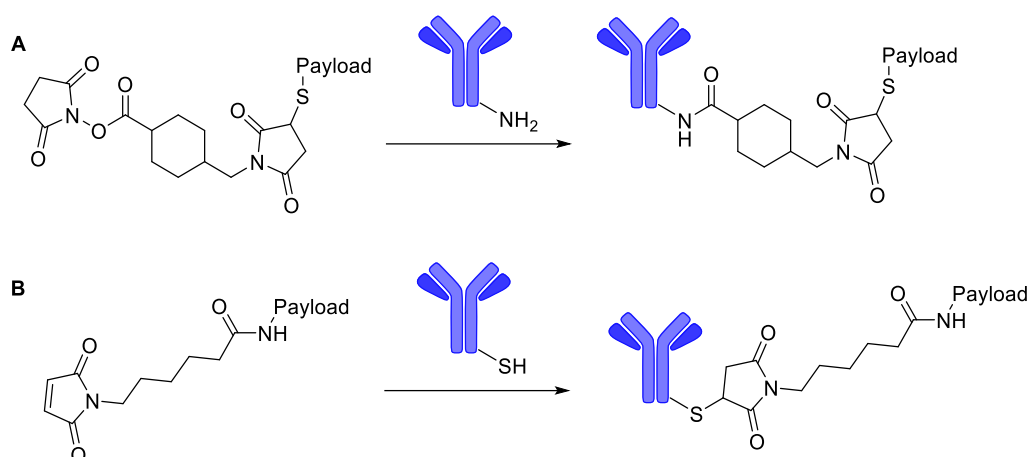


Figure 27. A) SMCC linker, B) mc linker.

2.1.5.2 Cleavable Linkers

Cleavable linkers are the most used linkers in ADCs at present and they fall into two subcategories: 1) chemically cleavable linkers, 2) enzymatically cleavable linkers. Both types of cleavable linkers allow the payload to be released intracellularly in the lysosome or in the TME.

2.1.5.2.1 Chemically cleavable linkers

This type of linkers makes use of intracellular chemical stimulus such as difference in pH or concentration of reducing agents (i.e. glutathione) for selective release of the drug.

2.1.5.2.1.1 Acid-sensitive linkers

This group of linkers include hydrazone, phosphoramidate, acetal and orthoester-based linkers, among others. These linkers remain stable in systemic circulation (pH 7-8), but hydrolyse upon cellular internalization in the lysosome (pH 4.8) and endosome (pH 5-6).⁶⁷ The hydrazone linker has been widely used and can be applied when the drug incorporates a ketone or aldehyde function that can be coupled to a hydrazine-derived linker. Two Pfizer-developed ADCs with hydrazone linkers,

Mylotarg[®] and Besponsa[®], reached the market in 2000 and 2017 respectively, with the first one being withdrawn (2010) because of an increase in treatment-related deaths compared to the control group receiving normal chemotherapy.

2.1.5.2.1.2 Glutathione-sensitive disulfide linkers

ADCs that present disulfide-linkers undergo nucleophilic attack by thiol-containing molecules such as glutathione (GSH) (Figure 28A), which concentration is much higher in the cytosol (ca. 10 mmol/L) than in the extracellular environment (ca. 10 μ mol/L).⁶⁸ This difference between the intracellular and blood (extracellular) concentration of GSH, as well as the oxidative stress, contributes to the preferential release of the drug inside cancer cells. The most representative payload associated with disulfide linkers is Maytansine, a tubulin disruptor (Figure 28B). The steric hindrance on carbon atoms adjacent to the disulfide bond has been reported to impact the overall resistance to the reduction and thus the plasma stability.⁶⁹ Compound SAR-3419 (Figure 28B), an ADC containing maytansine as payload and a disulfide linker with *gem*-dimethyl groups, presented the perfect balance of plasma stability, high rate of *in situ* drug release, and cytotoxic activity.^{70,71}

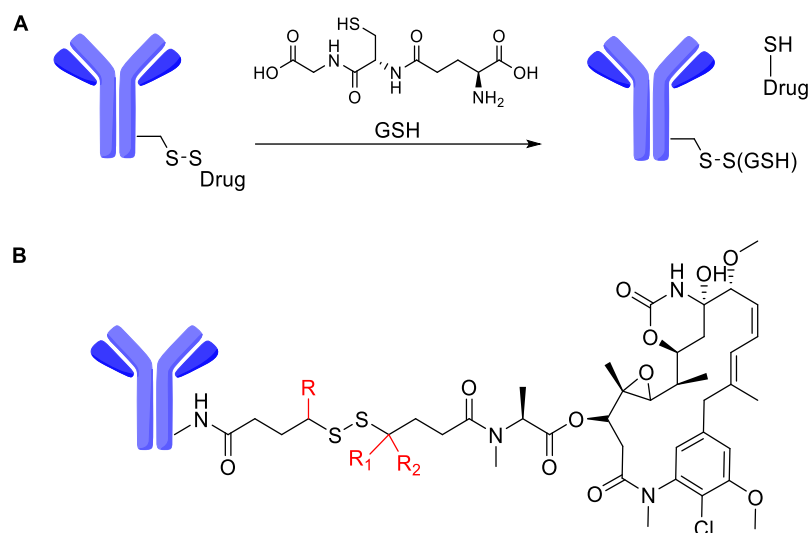


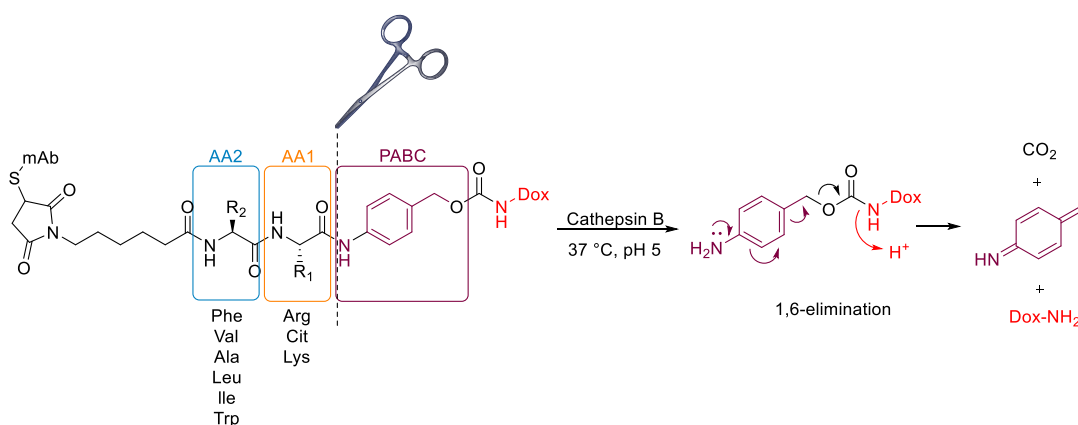
Figure 28. A) Schematic structure reactivity of glutathione-sensitive linkers. B) Chemical structure of SAR-3419 (R= H, R₁=R₂= CH₃), an ADC containing maytansine as payload and a disulfide linker.

2.1.5.2.2 Enzymatically cleavable linkers

To effectively release the drug in the cancer cell, the proteome of the lysosome has been targeted to exploit the high concentration of the enzymes able to cleave the linkers and release the drug. These peptide-based linkers can be divided into Cathepsin B-, β -Glucuronidase-, Phosphatase-, Pyrophosphatase-, β -Galactosidase- and Sulfatase-sensitive linkers.

2.1.5.2.2.1 Cathepsin B-sensitive linker

Cathepsin-B is a lysosomal cysteine protease that has been found to be overexpressed in several human cancers. The very first use of this strategy was the incorporation of highly cytotoxic anti-cancer agents such as Doxorubicin (DOX), Paclitaxel and Mitomycin C (MCC) conjugated to PABC (*p*-aminobenzyl carbamate) and a dipeptide linker (Scheme 36).⁷² The PABC self-immolative group serves as linker between the drug and the cleavable amide group. The faster drug release combination was given when there was a protonable/hydrophilic residue in AA1 and a hydrophobic residue in AA2 position.



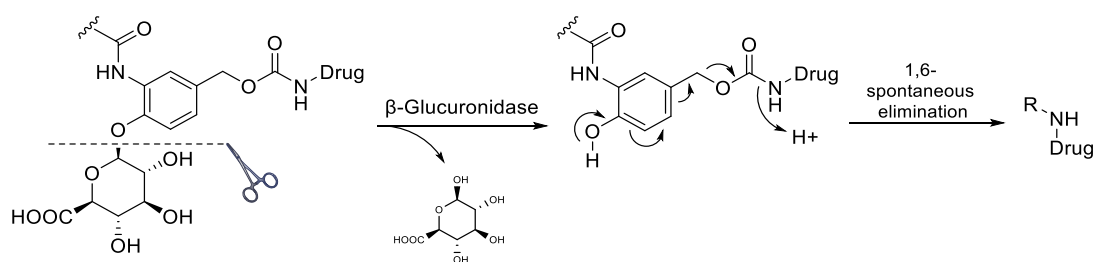
Scheme 36. Doxorubicin-released mechanism via Cathepsin B-sensitive dipeptide linker.

The most widely used dipeptide linker is Val-Cit with five FDA-approved ADCs on the market and 25 in clinical trials in 2021.⁶³ With nine ADCs in clinical trials, Val-Ala has

also drawn attention recently due to the first FDA approval of Val-Ala-based ADC Zynlonta® in 2021. Numerous comparisons have been described in the literature between Val-Cit and Val-Ala based ADCs.^{60,73,74} Most reports highlight the benefits of using Val-Ala over Val-Cit, mainly due to the lower ADC aggregation (non-specific interactions arising from attached drug and linker moieties on the mAb).^{75,76}

2.1.5.2.2.2 β -Glucuronidase-sensitive linker

β -glucuronidases are hydrolytic enzymes that have been found mainly in the lysosome, with an increased activity in tumour tissues respect to healthy ones.⁷⁷ Remarkably, these enzymes are inactive (10% of activity) at physiological pH and present their optimal activity at pH 4, which is the pH of the lysosome.⁷⁸ The main driving forces that have led chemists to design efficient β -glucuronidase cleavable linkers for prodrugs and ADCs are their abundance in the lysosome and in the tumor microenvironment as well as their strong plasma stability.^{79,80} The hydrophilic nature of the β -glucuronide linker is ideal for highly hydrophobic payloads, which suffer from ADC aggregation. Due to the hydrophilicity, the lower aggregation phenomena, better clearance and solubility than dipeptide-based linkers, the use of β -glucuronidase-sensitive linkers is considered an excellent strategy for target drug delivery (Scheme 37).^{81,82}



Scheme 37. Enzymatic hydrolysis of the glycosidic bond of β -glucuronidase-sensitive linker is followed by the spontaneous decomposition of the spacer group, leading to the release of the active payload.

2.1.6 Cytotoxic Payloads

Two types of cytotoxic molecules have been used for the synthesis of clinically approved ADCs, microtubule-disrupting drugs and DNA damaging agents. Recently, another class of cytotoxic agents are emerging as new payloads for ADCs, such as apoptosis inducer molecules like amatoxins and NAMPT inhibitors.⁸³ As several studies pointed out that only 1-2% of injected ADCs reached the tumor site,^{84,85} more potent payloads (IC_{50} of 10^{-10} - 10^{-12} M) are needed when designing an ADC. Payloads should also have low molecular weight to reduce immunogenicity and should be synthetically accessible to allow derivatization with the linker while retaining their potency. Furthermore, an adequate balance between aqueous solubility and stability as conjugate in aqueous formulations are important physico-chemical requirements for a payload in order to avoid antibody aggregation.⁵⁶

2.1.6.1 Microtubule-disrupting drugs

Tubulin inhibitors constitute more than 70% of the payloads in clinical ADCs, being auristatins and maytansinoids the two main families of compounds.

2.1.6.1.1 Auristatins

Auristatins are synthetic analogues of linear pentapeptide Dolastatin 10 (Figure 29), isolated from marine mollusc *Dolabella auricularia*.⁸⁶ Dolastatin 10 strongly inhibits the microtubule polymerization and tubulin-dependent GTP hydrolysis, which causes cell cycle arrest in the G2/M phase and apoptosis.^{87,88}

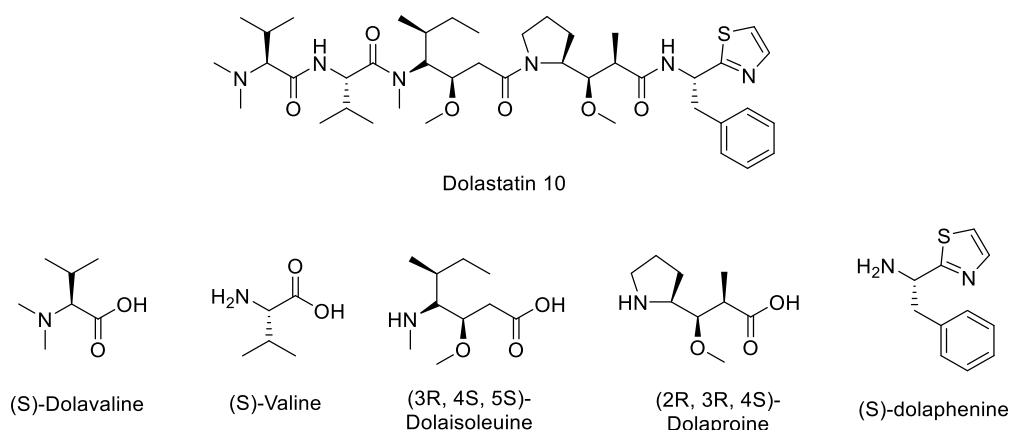


Figure 29. Structure of Dolastatin 10 and its key building blocks.

Although Dolastatin 10 was advanced into human clinical trials due to its high cytotoxicity in several human cancer cell lines, no significant therapeutic effect was achieved mainly due to its toxicity at maximum tolerated dose (MTD). Several research groups, both in academia and industry performed Structure-Activity Relationship (SAR) studies for the use of these compounds as potent anti-cancer agents.⁸⁹ Miyazaky *et al.* determined some of the structural requirements that have been used as key points for synthetic modifications of Dolastatin 10 (Figure 30).⁹⁰ Noteworthy are the two analogues of auristatins (MMAE and MMAF)^{91,92} developed by Seattle Genetics (Doronina *et al.*), which are currently being employed as payloads in six commercially-available ADCs in the market and more than twenty in clinical studies.^{57,58,93}

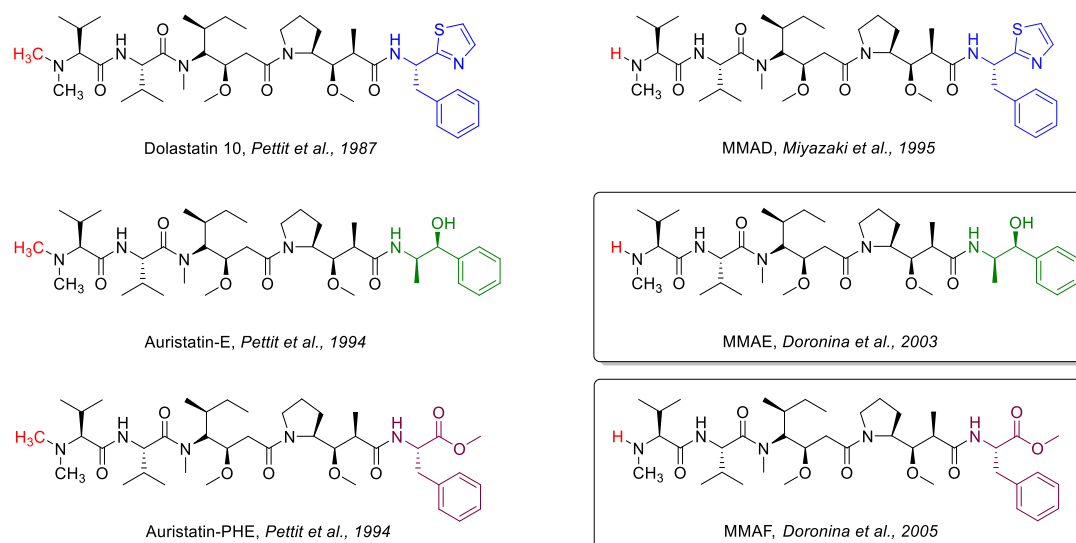


Figure 30. Chemical structures of key auristatin analogues.⁹⁴

Adcetris® (SGN-35 or Brentuximab vedotin, Figure 31), the first auristatin-based FDA-approved ADC in 2011, incorporates MMAE to a maleimidocaproyl-Val-Cit-PABC linker that is bioconjugated to a chimeric IgG1 anti-CD-30 mAb through a cysteine residue.⁹⁵ After ADC internalization, cathepsin B triggers the release of the PABC-MMAE intermediate that immediately release the drug by a spontaneous 1,6-elimination. The released MMAE kills the targeted cells and diffuses across the cell membrane to reach and destroy other CD30-positive as well as CD30-negative cancer cells, a phenomenon called the bystander killing effect. As a result, cancer cells that do not express the targeted antigen will also be killed.^{96–98}

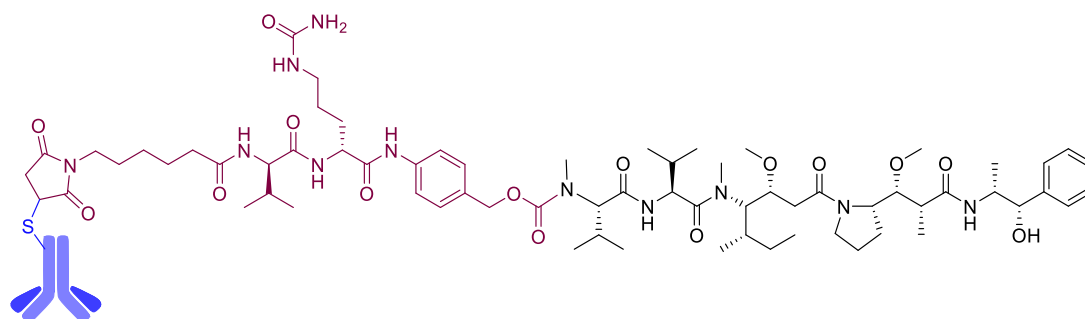


Figure 31. Chemical structure of commercially approved anti-CD30 Brentuximab vedotin (Adcetris®).

2.1.6.1.2 Maytansinoid derivatives

Maytansine and its derivatives (Maytansinoids, Figure 32A) are benzoansamacrolide antibiotics that were originally isolated from the bark of the Ethiopian shrubs *Maytenus ovatus* and *Maytenus serrata*.⁹⁹ Like auristatins, they share the same tubulin binding site and mechanism of action as vinca alkaloids by depolymerizing microtubules and arresting cells in the mitosis stage (G2/M phase). As maytansine does not present any suitable chemical handle for linker conjugation, several sulfhydryl-containing analogues were prepared.¹⁰⁰ DM1 (Mertansine or Emtansine) and DM4 (Ravtansine or Soravtansine) are examples of new synthetic maytansinoids that have been employed as payloads in numerous ADCs (i.e. Kadcyla[®], Figure 32B). At present, there are ca. ten maytansinoid-containing ADCs in clinical trials, with seven of them in phase II/III.^{101–106}

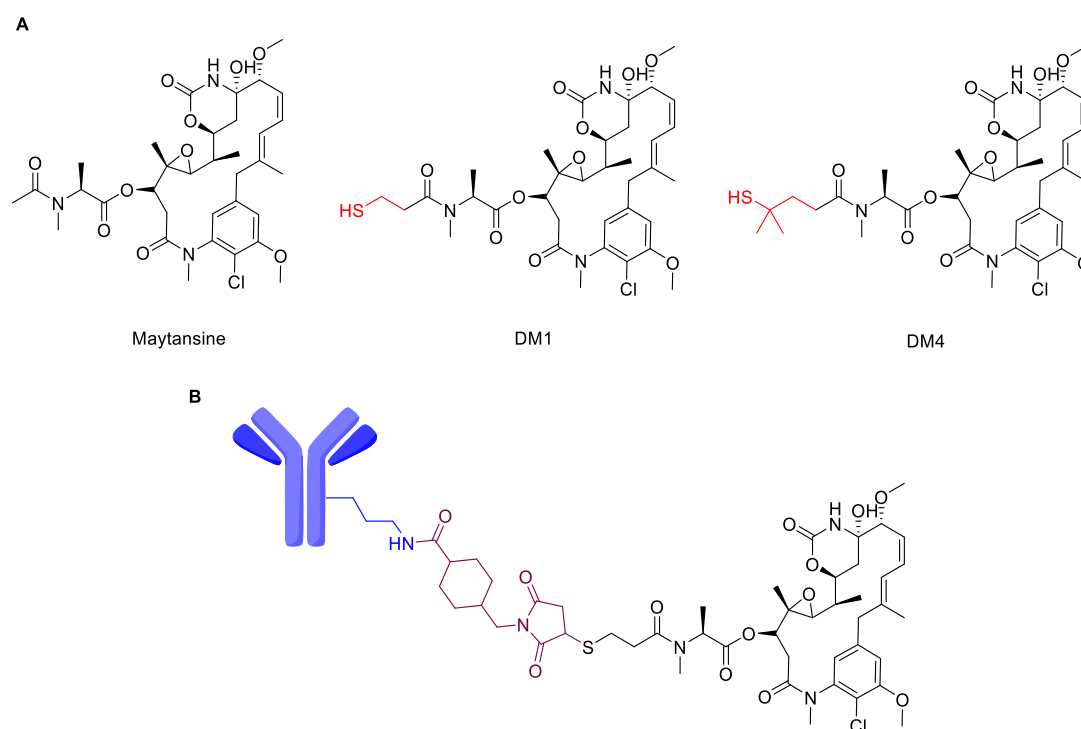


Figure 32. A) Chemical structures of Maytansinoids; B) Chemical structure of commercially approved Kadcyla[®].

2.1.6.2 DNA damaging agents

2.1.6.2.1 Calicheamicin

Calicheamicins are natural compounds originally isolated from the fermentation broth of a soil microorganism called *Micromonospora echinospora*.¹⁰⁷ The first generation of ADCs represented by Mylotarg® and Besponsa® (Figure 33A) are the only examples using Calicheamicin as payload. After ADC internalization, the payload release proceeds in two steps: 1) the hydrazone bond is cleaved at endosomal acidic pH, 2) intracellular glutathione-promoted disulfide reduction releases the drug. The thiolate Calicheamicin analogue that is released undergoes a Bergman cyclization,^{108,109} generates a highly reactive diradical compound that induces double-strand DNA cleavage, leading cancer cells to death (Figure 33B).¹¹⁰

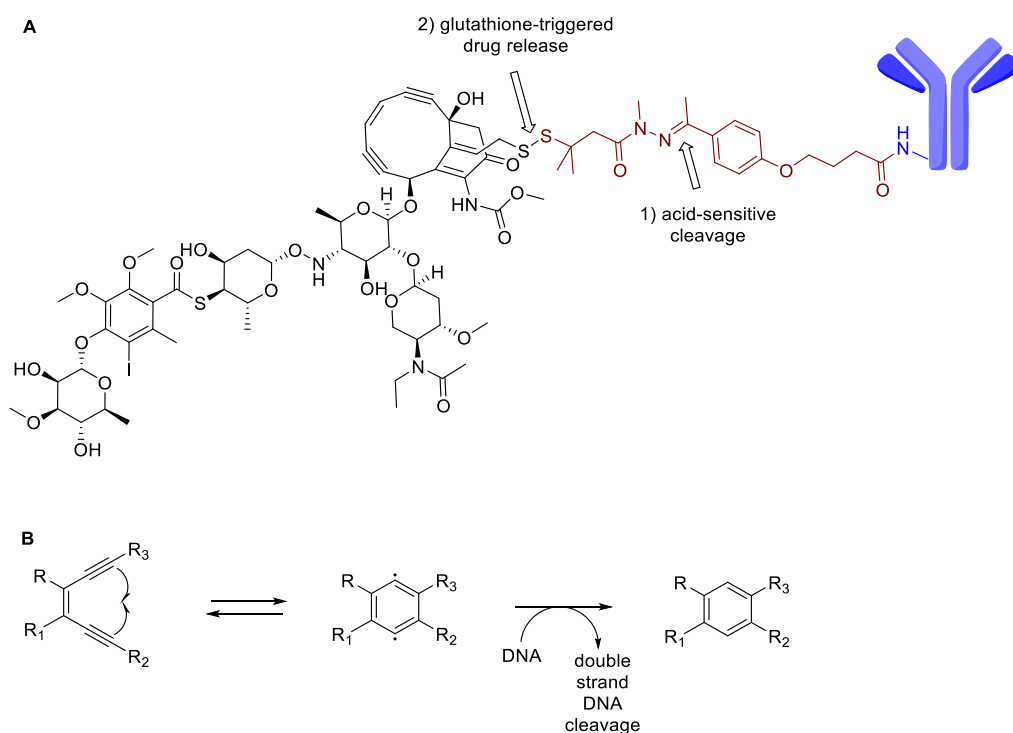


Figure 33. A) Schematic representation of the 1st generation FDA-approved ADCs, anti-CD33 Mylotarg®, and anti-CD22 Besponsa®; B) Bergman cyclization followed by DNA damage mechanism.

2.1.6.2.2 Camptothecins

Camptothecin (CPT) is a Topoisomerase I inhibitor that functions as a roadblock for the replication fork resulting in DNA double-strand cleavage, which leads to cell death.^{111,112} Structure-Activity Relationship studies indicated that the carboxylic acid of the CPT presented less antitumor activity than its lactone form (Figure 34A). The inability to resolve the water-insolubility of CPT lactone limited its use as anti-cancer agent and clinical studies were discontinued. However, the water-soluble form of CPT, Irinotecan (Figure 34B) was approved for metastatic colorectal cancer. Its active metabolite, SN38 is generated *in vivo* through the cleavage of the carbamate bond by human liver carboxylesterase.

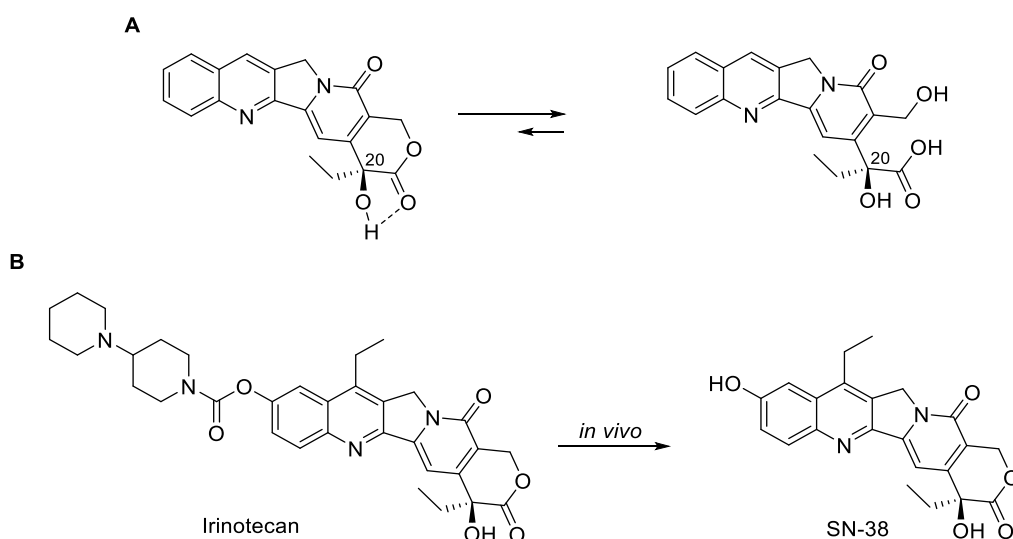


Figure 34. A) Chemical structure of Camptothecin in its lactone active form in equilibrium with CPT in its carboxylate inactive form; B) *in vivo* transformation of Irinotecan into SN-38.

Two different ADC strategies were adopted towards the stabilization of the lactone form of CTP analogues. The first one led to the approval of Enhertu[®] in 2019 that incorporated Exathecans (10-fold more potent against ovarian cancer than SN-38) as payload.^{113,114} The cyclohexane ring that bridges the 7 and 9 position confers the necessary rigidity to favour the equilibrium towards the lactone form, while the amino group contributes to increase the overall water solubility. The payload is

connected to a tetrapeptide enzyme-sensitive linker through an amino methylene self-immolative spacer. Once the ADC is internalized, the cleavage of the linker releases a hemiaminal intermediate that rapidly gives the toxin and methylene imine as product (Figure 35).¹¹⁵

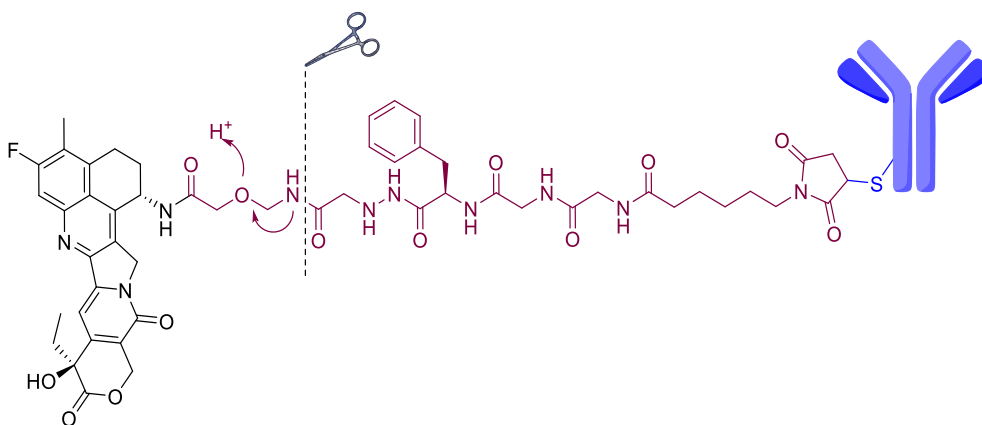


Figure 35. Enhertu[®] is composed of an anti-HER2 Trastuzumab conjugated to Exatecan *via* a tetrapeptide protease-sensitive linker (Gly-Gly-Phe-Gly).

The second strategy implied the attachment of metabolite SN-38 to the linker through a cleavable carbonate bond. Conjugation of anti-TROP-2 antibody afforded ADC IMMU-132, approved by the FDA in 2020 and commercialized as Trodelvy[®].¹¹⁶ Scientists at Immunomedics envisioned two different linker attachments on the active metabolite of Irinotecan, SN-38 and came out with an idea based on a previous study.¹¹⁷ IMMU132 is a result of the attempt of stabilising the lactone form of SN-38 by connecting the C-20 hydroxyl group through a carbonate bond, thus leaving the lactone ring intact while coupled to the linker (Figure 36).^{118,119}

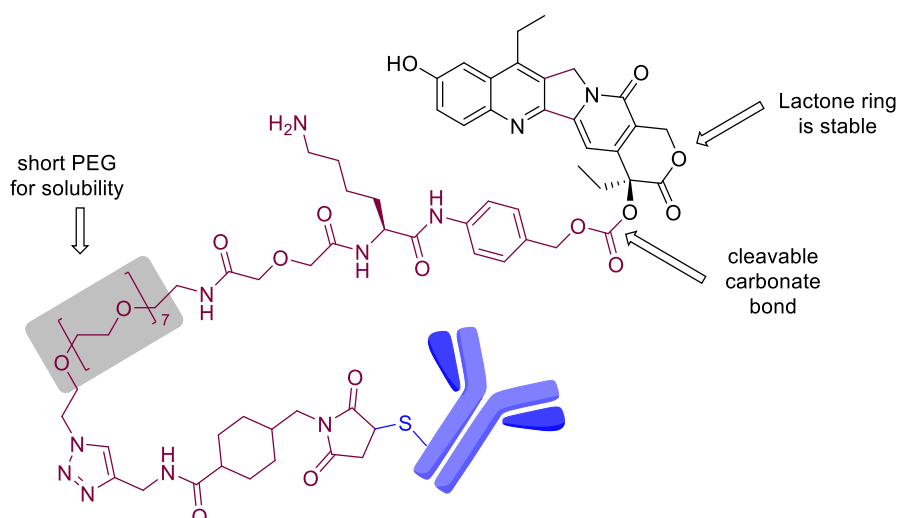


Figure 36. Trodelvy® or IMMU-132 is comprised of an anti-TROP-2 antibody conjugated to SN-38 through an acid-sensitive cleavable linker.

2.1.6.2.3 Pyrrolobenzodiazepines

Anthramycin is a tricyclic ring natural product that belongs to the pyrrolo[2,1-c][1,4]benzodiazepine (PBD) family of antitumor antibiotics.¹²⁰ PBD and its analogues are sequence-selective DNA minor-groove binding agents and their mode of action involves the amino group in position 2 of a DNA guanine base that makes a covalent bond with the electrophilic imine on the C11 of PBD (Figure 37).¹²¹

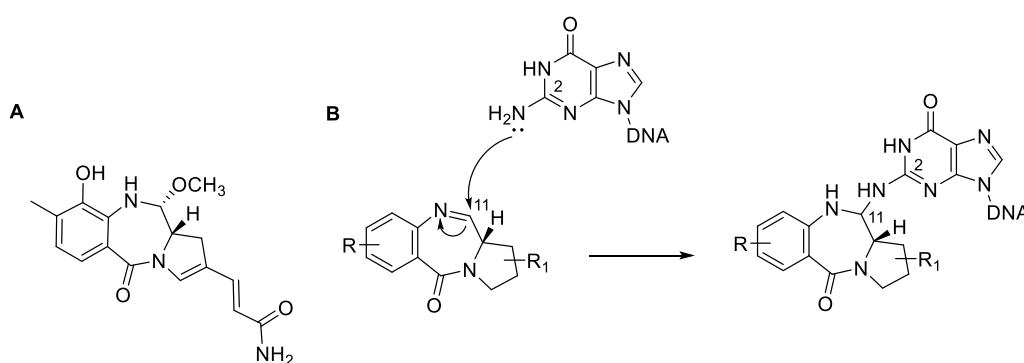


Figure 37. A) Chemical structure of Anthramycin; B) Mode of action of benzodiazepines through selective alkylation of DNA.

Since the discovery of Anthramycin, several PBDs have been developed by various academic and industrial groups. PBD dimers containing two alkylating imine functions

have greater stability and higher antitumor cytotoxicity in comparison to PDB monomers. PDB dimers exhibit picomolar activity toward many tumor cell lines, meaning 50-100 times more potent than MMAE or DM1 that are classic payloads for ADCs.¹²² Due to their significant cytotoxicity, Spirogen and Seattle Genetics first introduced PDB dimers as payloads for antibody–drug conjugates (ADC) in the late 2000s.^{123,124} The latest PDB-based ADC in the late stages of clinical trials and the very recent FDA-approved Zynlonta[®] suggest that monofunctional DNA alkylators are better tolerated while maintaining robust antitumor activity (Figure 38).^{125–127}

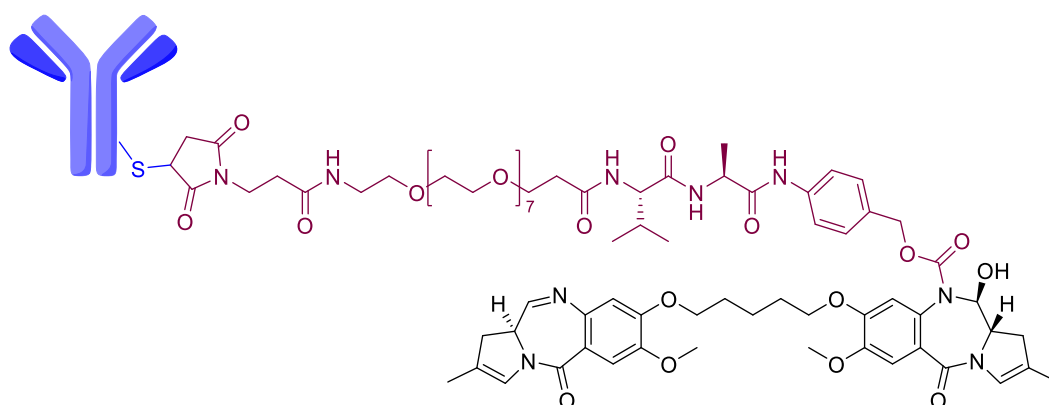


Figure 38. Chemical structure of Zynlonta[®] approved in 2021.

2.1.6.2.4 Duocarmycins

Duocarmycins are antibiotics isolated from the culture broth of *Streptomyces sp.* that can bind to the minor groove of DNA by alkylating the adenine at the N3 position through their reactive cyclopropane ring (Figure 39A).¹²⁸ The non-cyclized form of duocarmycins shows reduced cytotoxic activity, thus the linker strategies have been focused on the attachment of the phenol group, whose release would generate the active form by mesomeric effect. SYD985 (Figure 39B) was developed at Synton company, and presents the payload connected to a Val-Cit-PABC linker through a dimethylethylenediamine-like spacer group that releases the drug *via* a spontaneous cyclization after Cathepsin B cleavage.^{129–131}

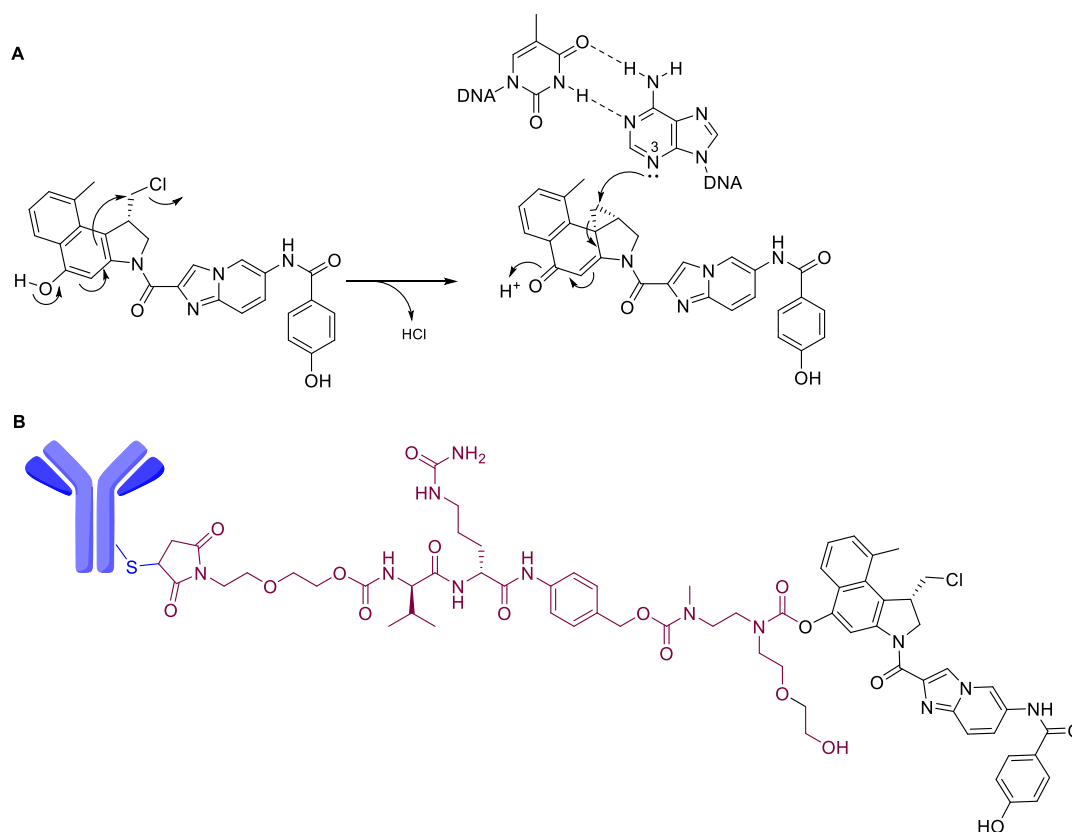


Figure 39. A) Schematic representation of Duocarmycin-based DNA-alkylating agent; B) Chemical structure of SYD985, an ADC currently in clinical trial.

2.1.6.3 Innovative drugs – New payloads for Antibody-Drug Conjugates

There is a need to investigate new payloads for ADCs, since those that have been developed so far involve two unique mechanisms of action. For this reason, the synthesis of new payloads that respond to different action mechanisms has opened a new era for ADCs. Below are summarized some promising examples that have been recently developed.

2.1.6.3.1 Amatoxins

Amatoxins are a group of natural toxins which are present in *Amanita phalloides* mushrooms and are responsible for 95% of all fatal mushroom intoxications.^{132,133} They are potent RNA polymerase II inhibitors and lead cells to apoptosis by

interrupting the transcription and protein synthesis. α -/ β -Amanitin (Figure 40), which represent 90% of all amatoxins, share the same bicyclic octapeptide skeleton of eight L-configured amino acids with several hydroxyl groups in the side chains. The total synthesis of α -Amanitin has opened new possibilities for chemical modification and eventually to its use as payload for the preparation of ADCs.^{134,135} Among the different strategies to use amatoxins as payloads,^{136,137} Heidelberg Pharma developed an amatoxin platform called ATAC (antibody targeted amanitin conjugate), which led recently to the advance of HDP-101 (Figure 40) to phase 1 of clinical trials. Two chemical modifications have been applied to optimize the stability of the α -amanitin analogue, first the removal of the hydroxyl group from tryptophan and second the replacement of the sulfoxide by a thioether group. The payload was conjugated to a Val-Ala-PABC linker through the amide bond of the aspartic acid side chain (Figure 40).¹³⁸

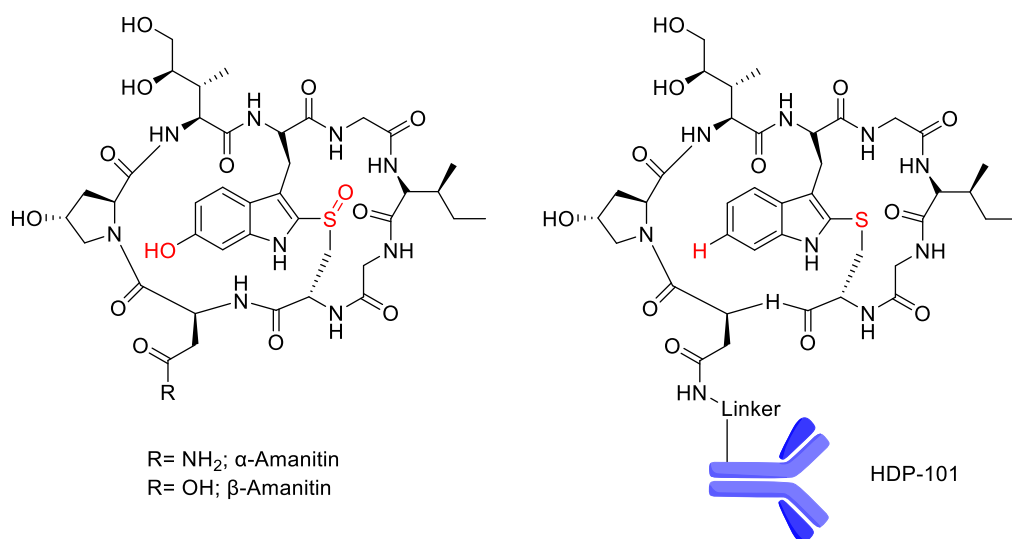


Figure 40. ADC based on amatoxins as payloads.

2.1.6.3.2 NAMPT inhibitors

Recently, Seattle Genetics,¹³⁹ Novartis,¹⁴⁰ and Bayer¹⁴¹ companies have explored the use of NAMPT inhibitors as ADC warheads due to their synthetic chemical ease, high

cytotoxicity in solid and haematological cancer cell lines, and their simple but effective mechanism of action (Figure 41). In general, these ADCs presented good stability, low aggregation, target-dependent efficacy, and potent *in vivo* antitumor activity. At present, there are only three publications¹³⁹⁻¹⁴¹ and few patents published,^{142,143} regarding the use of NAMPT inhibitors as warheads for ADCs. These findings opened the doors for further use of NAMPT inhibitors with high promising *in vitro* and *in vivo* profiles as payloads for the design of potent and effective ADCs.

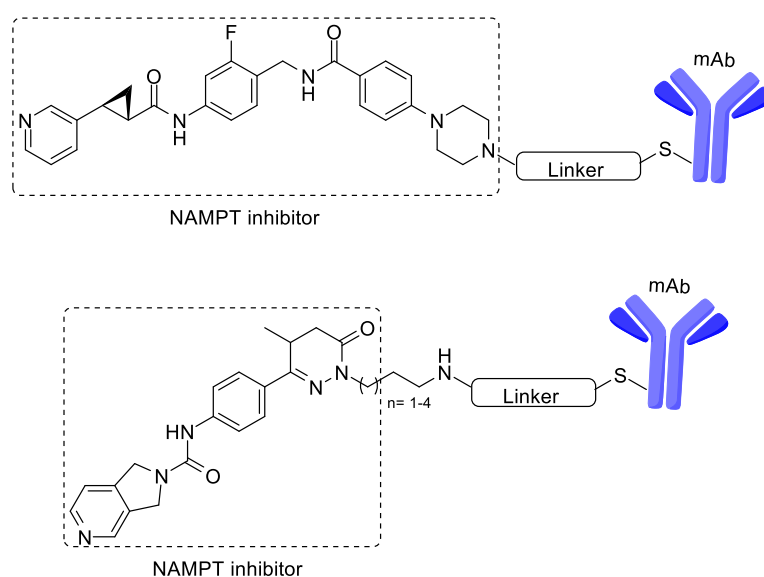


Figure 41. Structure of ADCs incorporating NAMPT inhibitors as payloads.

2.1.7 Bioconjugation strategies

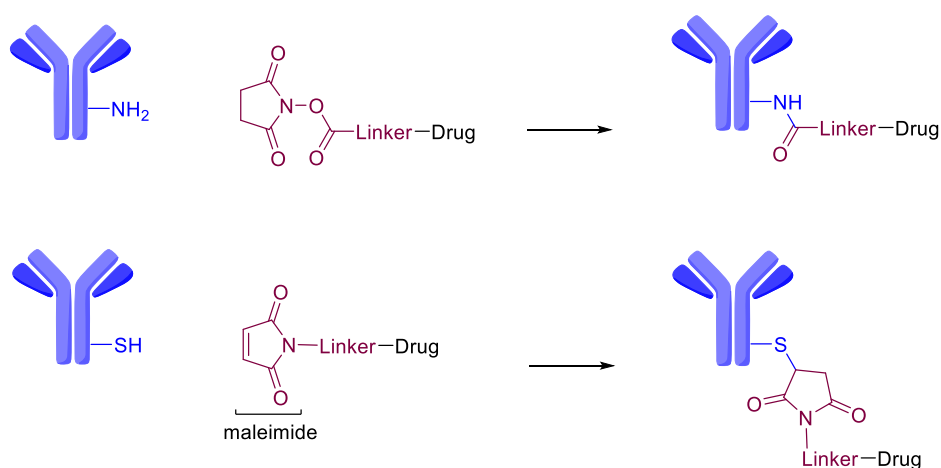
2.1.7.1 Drug-to-antibody ratio (DAR)

Bioconjugation is the synthetic strategy for the incorporation of payloads (drugs) into a mAb through a linker. The drug-to-antibody ratio (DAR) is defined as the number of payloads per mAb. It plays an important role in determining the dose needed to have clinical effect and significantly contributes to the pharmacokinetic profile of an ADC. While a low DAR value can lead to a non-potent but effective ADC, a high DAR value is usually associated with instability of the ADC, toxicity, and fast clearance, often

provoking aggregation, and immunogenic responses. In general, a DAR of 3-4 is used to achieve optimum effect, depending on the potency of the drug.

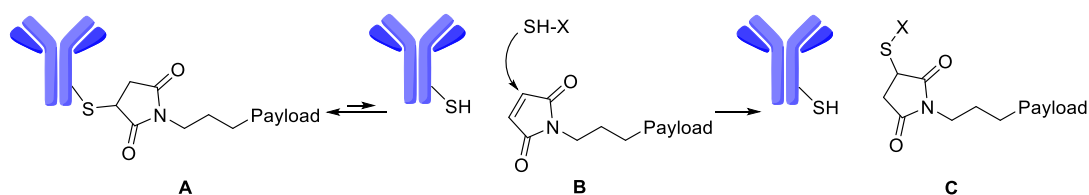
2.1.7.2 Classical chemical bioconjugation

The most common bioconjugation reactions are based on the site-selective modification of the lysine and cysteine residues of the antibody. In the case of lysines, the nucleophilic amino group reacts with active *N*-hydroxysuccinimide esters (NHS) on the linker-payload to form an amide bond. Conjugations *via* the side chain of cysteine residues are also a widely used conjugation strategy in ADCs and it normally implies the reaction of the thiol group with a maleimido moiety of the linker. Usually, in a monoclonal antibody, the thiol groups of Cys are involved in disulfide bridges, typically twelve intrachain and four interchain disulfide bridges. The latter are not critical for the stability of the mAb and can be selectively reduced with dithiothreitol (DTT) or tris(2-carboxyethyl)phosphine (TCEP) to obtain free cysteine residues. Bioconjugation reactions through Cys can produce ADCs with DAR values up to 8 and can be considered a more reproducible method than lysine-based bioconjugation strategies (Scheme 38).



Scheme 38. Lysine and cysteine chemical conjugation.

Currently, in the case of Cys-modification of proteins, maleimides are preferred as chemical handles in the linker because of their unique reactivity in thiol-Michael additions.¹⁴⁴ The two electron-withdrawing groups and the strain of the double bond decrease the energy of the LUMO (lowest unoccupied molecular orbital) synergistically resulting in a potent electrophile towards nucleophilic attack. As a result, maleimides are more reactive Michael acceptors than vinyl sulfones or acrylates.^{145–148} Nevertheless, maleimide-based conjugation faces its own challenges. The resulting thiosuccinimide thioether (ADC A) is in slow equilibrium with the corresponding free maleimide-payload (B) (Scheme 39).¹⁴⁹ An exogenous thiol in plasma, such as the Cys-34 residue of the abundant albumin, can react with B leading to the new bioconjugate C. As a consequence, the original ADC A loses the efficacy because of the partial release of cytotoxic drug before reaching the target cell, which increases off-target toxicities and jeopardizes the overall ADC efficacy.¹⁵⁰



Scheme 39. Loss of efficacy of maleimide-based ADCs.¹⁴⁹

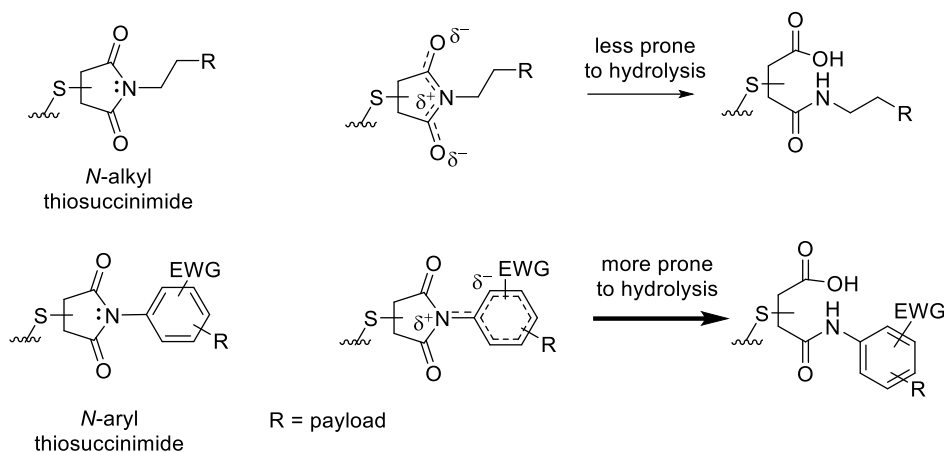
2.1.7.3 New linker technologies

Due to the limitations shown by maleimide, there is an urgent need to find innovative linkers that are more stable in plasma during circulation, thus positively impacting the overall ADC pharmacokinetic profile. Here below, several new linkers are summarized.

2.1.7.3.1 Next-Generation Maleimides (NGM)

2.1.7.3.1.1 N-Aryl maleimides

Dimasi *et al.*¹⁵¹ demonstrated that substitution of the alkyl chain of a maleimide moiety with an aryl group increased thiol addition and thiosuccinimide hydrolysis by increasing the electrophilicity of the maleimide. The resonance structures of the aryl and alkyl thiosuccinimides highlight the character of the partial double bond that shifts from the amide to the aryl moiety, thus increasing the electrophilicity of the carbonyl group. As a result, the aryl thiosuccinimide moiety is more prone to hydrolysis, yielding a more stable intermediate without loss of drug (Scheme 40).



Scheme 40. Hydrolysis of *N*-alkyl vs *N*-aryl thiosuccinimide derivatives.

2.1.7.3.1.2 β -amino maleimides

A strategy based on the incorporation of an amino group close to the carbonyl maleimide moiety to promote an intramolecular-catalysed hydrolysis of the imide function (Figure 42A) has been developed at Genentech company. This catalysis leads to the fast formation of the stable succinamic acid thioether. An ADC prepared with such linker and monomethyl auristatin E (MMAE) as payload, led to improved ADC efficacy and better tolerability in *in vivo* studies (Figure 42B).¹⁵²

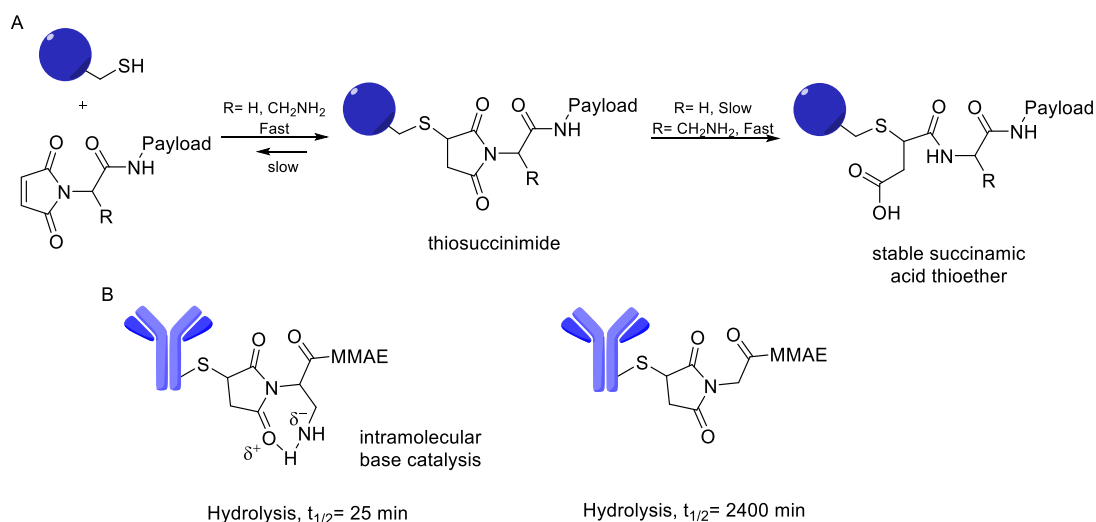


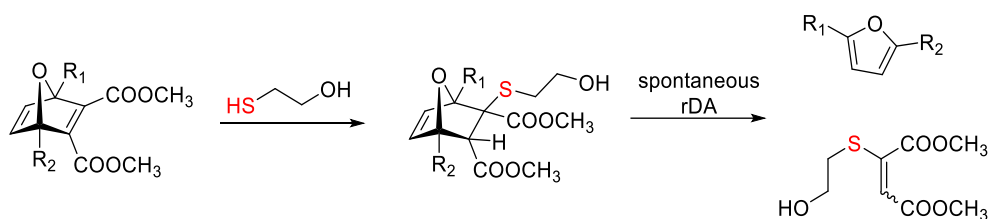
Figure 42. Impact of intramolecular base catalysis in the hydrolysis of the thiosuccinimide moiety.

2.1.7.3.2 Non-classic bioconjugation systems

Although, the next generation maleimides are tackling the major drawbacks of classic maleimides, new site-specific bioconjugation reactions are needed to improve the stability and integrity of the ADC. Recently, several approaches using heteronorbondadiene-based linkers have been described and are summarized in the next section.

2.1.7.3.2.1 Oxanorbornadienes (ONDs)

Finn and co-workers described the selective conjugate addition of 2-mercaptoethan-1-ol to a 7-oxanorbornadienedicarboxylate (OND) to generate an oxanorbornenic adduct that suffered a spontaneous retro Diels-Alder reaction (rDA) reaction to give furan derivatives and thiomaleates (Scheme 41).¹⁵³



Scheme 41. Conjugate addition of thiol to ONDs and subsequent rDA reaction.

To verify whether the ONDs might have an application in the field of thiol-sensitive linkers for targeted drug delivery, functionalized electron-deficient oxanorbornadiene reagents were synthesized to study their ability to release the cargo once they were bioconjugated to circulating albumin.¹⁵⁴ Albumin, which accounts for 90% of plasma thiols in mammals, is an attractive carrier that binds covalently small molecules *in vivo*. In this regard, Finn *et al.* described the first covalent attachment of ONDs to circulating albumin in rodents to modulate the kinetic of the release of gadolinium cargos. The substituents on the bicyclic system (R and R') helped tuning the rate at which the drug was released into the blood (Figure 43).

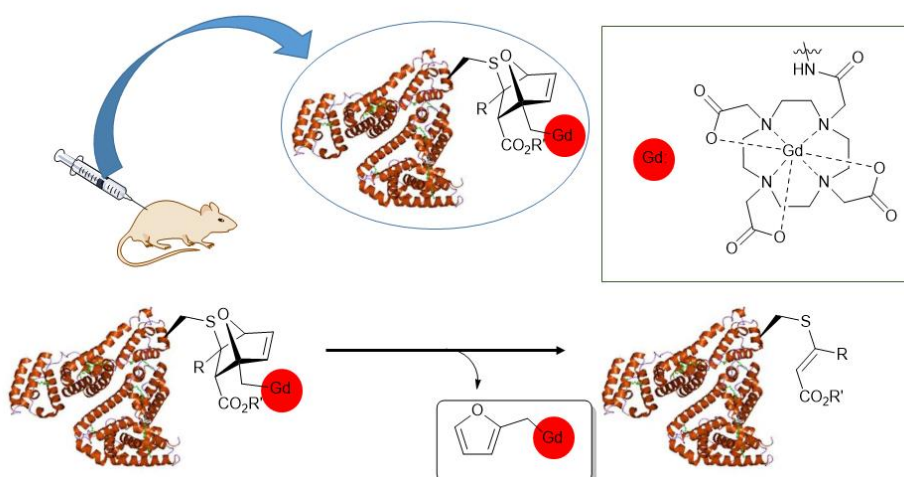
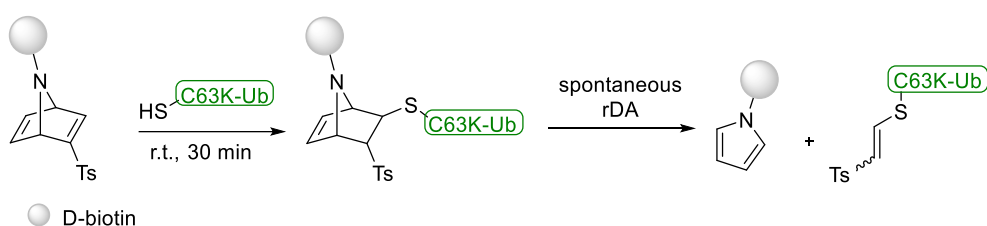


Figure 43. Release of a Gadolinium derivative from an OND conjugated to albumin.

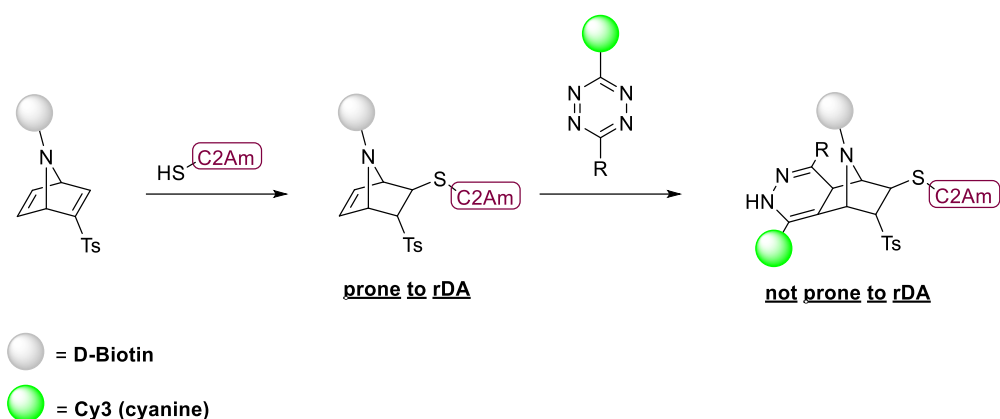
2.1.7.3.2.2 Azanorbornadienic vinyl sulfones

Recently, our research group has developed several [2.2.1]azanorbornadienic vinyl sulfones as versatile reagents for dual bioorthogonal labelling of proteins.¹⁵⁵ These systems present the two essential requirements for this purpose: 1) they are Michael acceptors for the bioconjugation with cysteine residues and, 2) they present an anchor point (N bridge) for the incorporation of an affinity probe. First, the authors used the modified ubiquitin protein (Ub-K63C), which contains a free cysteine residue, to make it react with a biotinylated azanorbornadienic vinyl sulfone. It was observed that, when the cysteine residue of Ub-K63C is bioconjugated to the azanorbornadiene and forms the corresponding azanorbornene, a spontaneous rDA reaction takes place with the release of the Biotin-containing pyrrole (Scheme 42).



Scheme 42. Bioconjugation of Ub-K63C to an azanorbornadienic vinyl sulfone and subsequent spontaneous rDA reaction.

In this work, our research group also carried out the reaction of the C2Am protein with a biotin-containing azanorbornadiene (Scheme 43). The azanorbornene-conjugate formed was stable enough to react with fluorogenic tetrazines *via* a bioorthogonal inverse Electron Demand Diels-Alder (iEDDA) reaction. As a result, a stable compound was formed in which the spontaneous rDA reaction did not occur. Therefore, this azanorbornadienic system can be considered as a versatile tool for dual chemical labelling, allowing the incorporation of two biologically relevant molecules, an affinity probe (biotin) and a fluorogenic probe (Cyanine, Cy3).¹⁵⁵

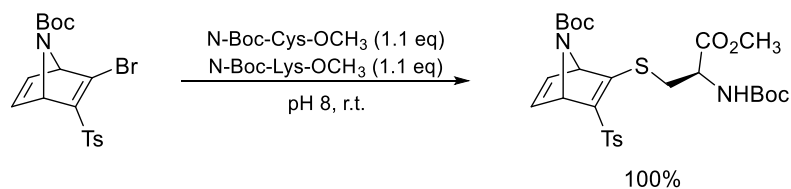


Scheme 43. Dual labelling of protein C2Am by using azanorbornadienic vinyl sulfones as bioconjugation tool.

The above mentioned Oxanorbornadienes (ONDs) and azanorbornadienes (ZNDs) are not suitable for the development of ADCs because they are prone to a spontaneous reaction of rDA after protein bioconjugation, what would lead to partial release of the drug into the blood stream before reaching the tumor site.¹⁵⁶

2.1.7.3.2.3 Azanorbornadienic bromovinyl sulfones

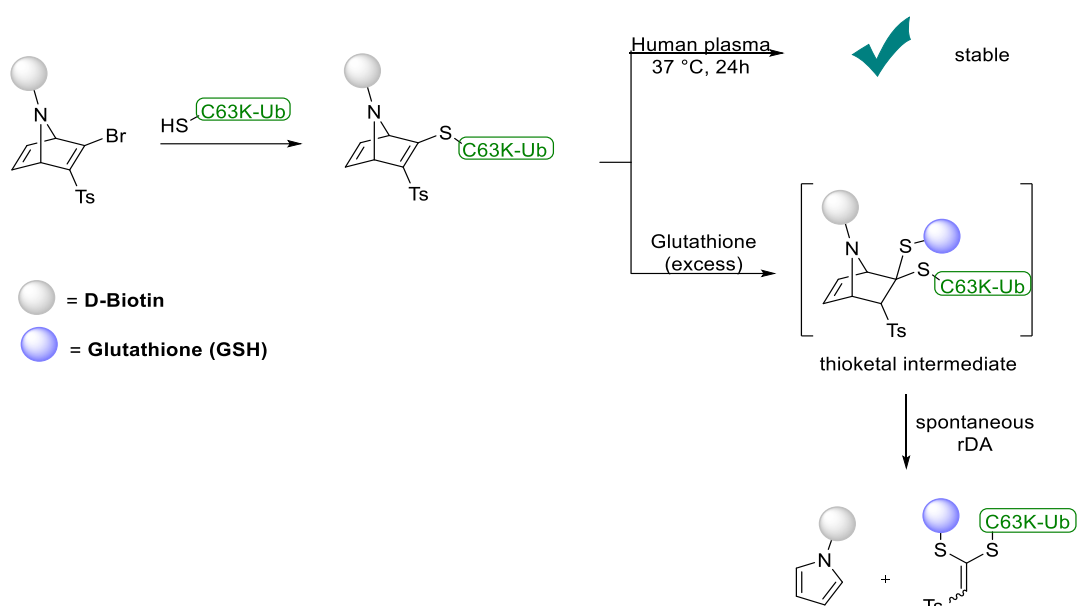
Recently, a new generation of azanorbornadienic systems has been developed in our group. The new compounds contain the functionality bromovinyl sulfone and have proved to be selective for cysteine bioconjugation (Scheme 44).¹⁵⁷ These bicyclic compounds are able to react with the thiol group of Cys residues through a nucleophilic vinylic substitution ($S_NV\sigma$) with bromide as leaving group.^{158–161}



Scheme 44. Competition between Cys and Lys residue for conjugation with [2.2.1]azanobicyclic bromovinyl sulfone.

In a further experiment, the bioconjugation between protein Ub-K63C and the biotinylated azanorbornadienic bromovinyl sulfone was performed (Scheme 45). The

resulting Ub-K63C/azanorbornadiene conjugate was shown to be stable in blood plasma after incubation for 24 h at 37 °C. However, incubation of this conjugate with an excess of glutathione for 1 h resulted in a thioketal intermediate, which evolved to give the pyrrole derivative by a spontaneous rDA. Therefore, the glutathione-sensitive character of these bicyclic systems could find applications in the field of ADCs.



Scheme 45. Stability studies of Ub-K63C-containing azanorbornadienic reagents.

2.2 OBJECTIVES

In order to improve the *in vivo* cytotoxic activity of the NAMPT inhibitors synthesized in Chapter 1, an approach to the preparation of ADCs will be performed. For this purpose, we plan to develop conveniently functionalized new inhibitors based on the structure of inhibitor **47a**, to be used as payloads (Figure 44). As the conjugation of the payload to the linker needs a chemical handle in the molecule, we envisaged the introduction of an amino group (furfurylamine, pyrrolidine/pyrrolidine) in the inhibitor. The amino group can be easily involved in the formation of carbamates and is the most common handle used in ADCs.

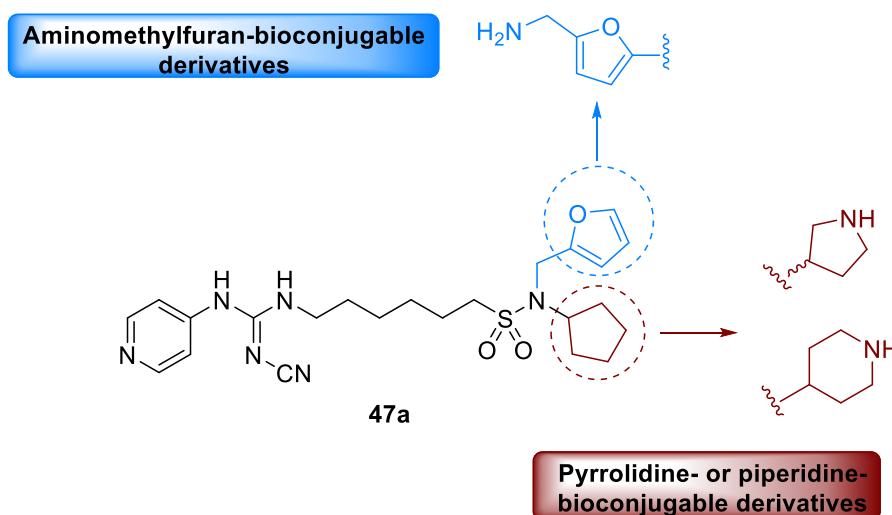
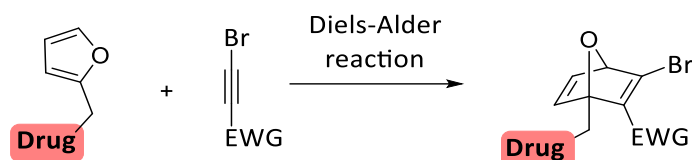


Figure 44. Possible chemical modification to make **47a** a bioconjugable compound for ADC.

Once the best cytotoxic compounds are identified, we envisage the synthesis of ADCs. For that purpose, two different strategies are planned:

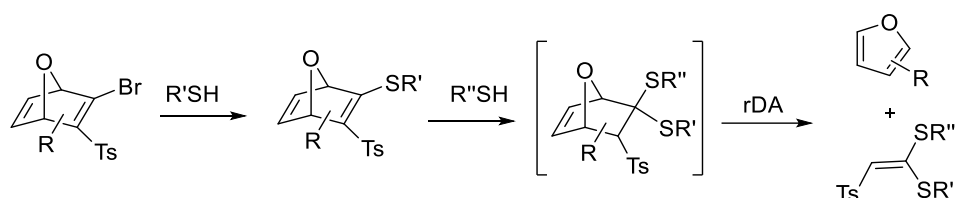
- 1) Incorporation of the payloads into CD138 antibody through an enzymatically cleavable linker following a classical approach.
- 2) Development of a new OND-based linker strategy for the preparation of ADCs that could be used for the drug delivery of furan-tail NAMPT inhibitors. The corresponding NAMPT inhibitor could be incorporated into the OND through a Diels-

Alder reaction with the appropriate alkyne (Scheme 46). The bromovinyl functionality of these systems would allow the incorporation of the payload-linker system into a mAb through site-selective bioconjugation.



Scheme 46. Diels Alder (DA) cycloaddition between activated alkynes and furan-tailed NAMPT inhibitors.

Since the use of the OND-linker strategy is based in the ability of these bicyclic systems to the fragmentation in the presence of glutathione (*via* rDA reaction), we planned to carry out a preliminary study of the fragmentation reaction of differently substituted ONDs in the presence of a model of a biological thiol. For a future application in ADCs, a cytotoxic furan-containing drug (e.g., NAMPT inhibitors) would be released (Scheme 47).



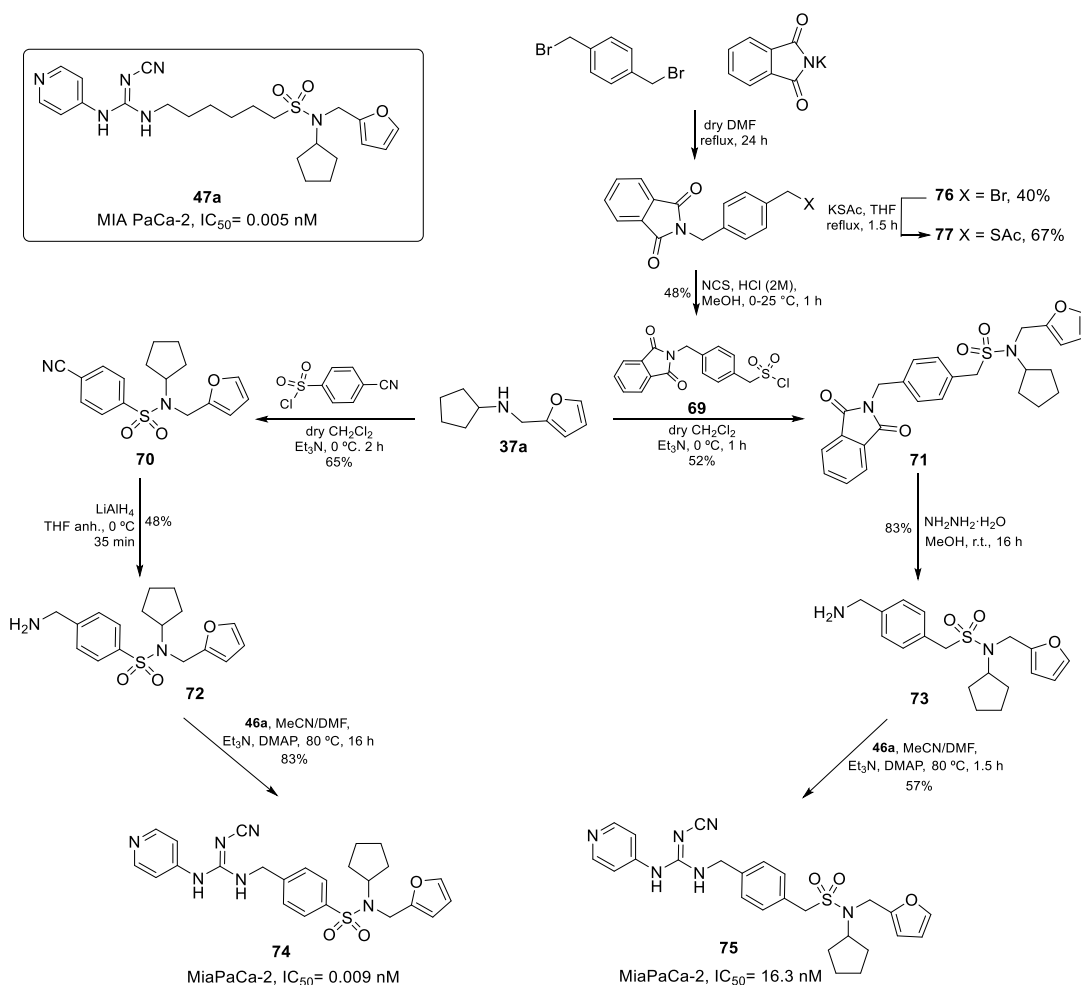
Scheme 47. Proposed study of the thiol-promoted OND fragmentation.

2.3 RESULTS AND DISCUSSION

2.3.1 CHEMISTRY

2.3.1.1 Preparation of new bioconjugable NAMPT inhibitors

To study the influence of the conformational flexibility of the linker in compound **47a** (the most cytotoxic compound towards MIA Paca-2 cells), we addressed the preparation of compounds **74** and **75** (Scheme 48). The synthesis of **74** started by coupling commercially available 4-cyanobenzenesulfonyl chloride with *N*-cyclopentylfurfurylamine **37a**, to yield sulfonamide **70**. Reduction of **70** with LiAlH₄ afforded the corresponding amino compound **72**, which after coupling with phenyl *N*-cyano-*N'*-(pyridin-4-yl)carbamimidate **46a** yielded compound **74** (Scheme 48). In a similar way, reaction of **37a** with sulfonyl chloride **69** afforded sulfonamide **71**. Subsequent deprotection of the phthalimide group by treatment with hydrazine gave the corresponding amino compound **73** that finally reacted with carbamidate **46a** to afford the final compound **75**.



Scheme 48. Synthesis of (pyridin-4-yl)cyanoguanidine-based inhibitors **74** and **75**.

Compounds **74** and **75** were tested *in vitro* for their anti-proliferative activity on MIA PaCa-2 cell line. Compound **74** presented an IC₅₀ value in the picomolar range (same range than **47a**). Surprisingly, the homoanalogue **75** containing an extra methylene group between the sulfonamide and the phenyl ring, showed to be 1800-fold less cytotoxic than **74**, with an IC₅₀ of 16.3 nM. As the synthetic route for the preparation of **74** was considerably shorter than the one for the synthesis of **47a**, compound **74** was selected as the best candidate to design new bioconjugable NAMPT inhibitors. Therefore, based on the structure of **74** we envisioned three possible families of compounds to be used as payloads for ADCs: quaternary pyridinium salts, furfurylamine and pyrrolidine/piperidine derivatives (Figure 45). All these molecules

contain a nucleophilic amino group (or a pyridinic nitrogen) as a handle for the incorporation into the linker.¹⁶²

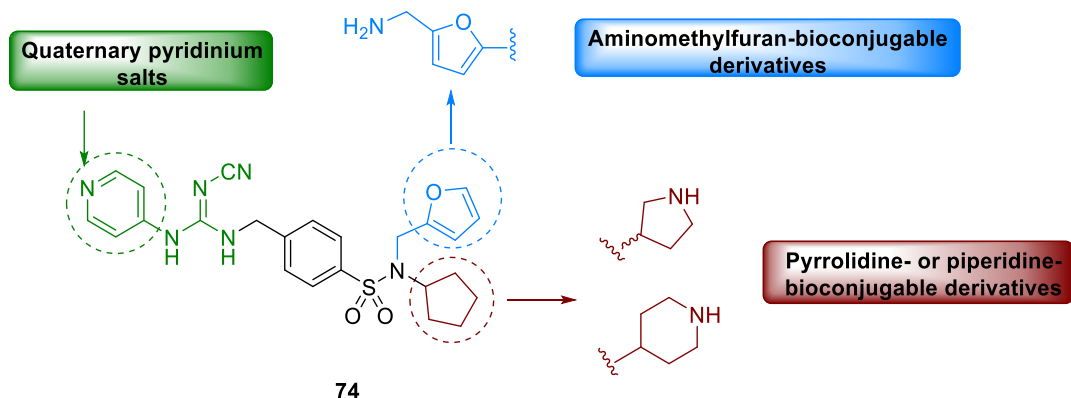
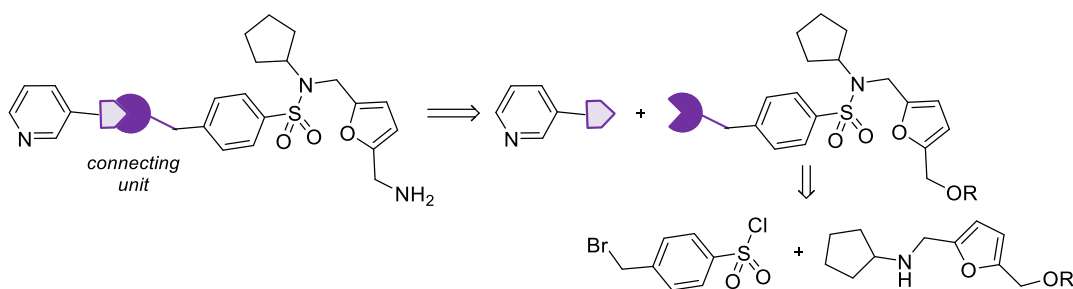


Figure 45. Possible chemical modifications to make **74** a bioconjugable compound for ADC.

Thus, in order to perform SAR studies on this new class of conjugable NAMPT inhibitors, the cyanoguanidine as well as triazole, acrylamide and thiourea groups were chosen as connecting units.

2.3.1.1.1 Preparation of new furfurylamine derivatives

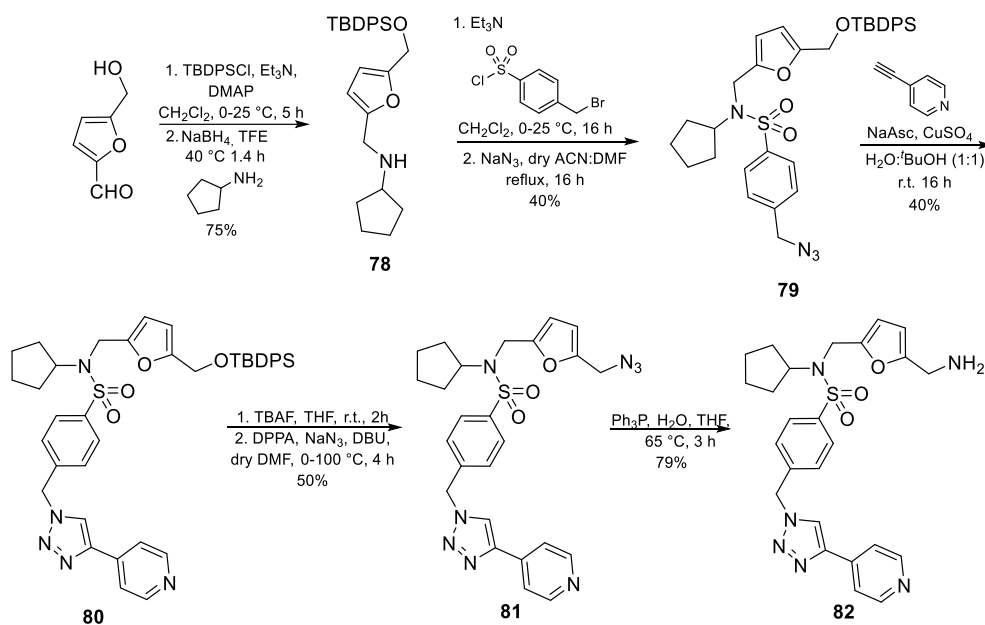
The general structure of this family of compounds and the corresponding retrosynthetic analysis is presented in Scheme 49.



Scheme 49. Retrosynthetic analysis for furfurylamine derivatives.

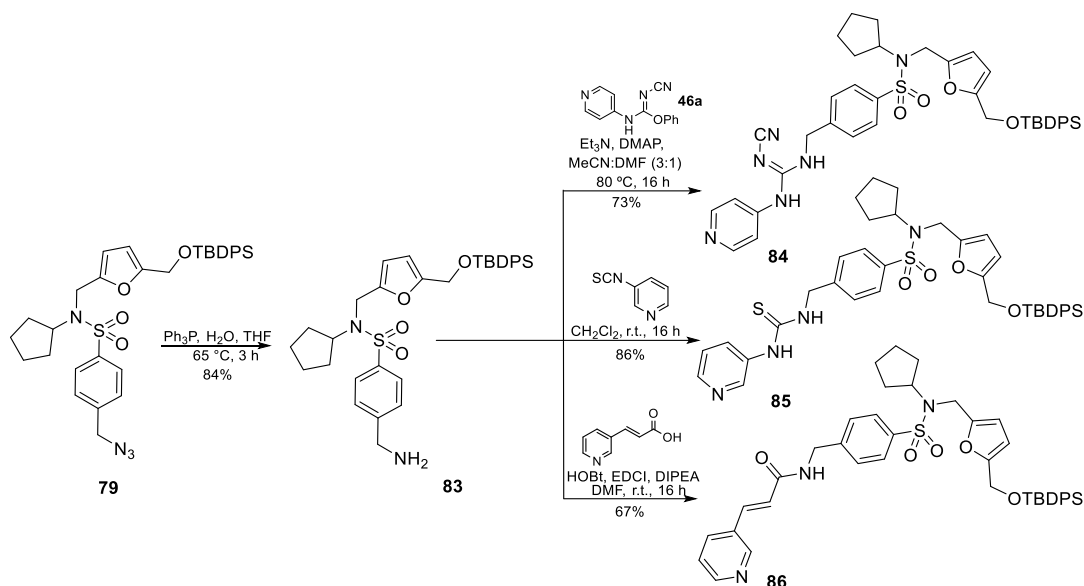
The synthesis of the furfurylamine family (Scheme 50) was carried out starting from 5-hydroxymethylfurfural (5-HMF). Reaction with *tert*-butyl(chloro)diphenylsilane (TBDPSCI) afforded the corresponding *O*-protected intermediate which after

reductive amination with cyclopentylamine gave compound **78**. Subsequent reaction with 4-(bromomethyl)benzenesulfonyl chloride yielded a sulfonamide derivative, that was further transformed into the corresponding azido compound **79** after reaction with sodium azide. CuAAC reaction of **79** with 4-ethynylpyridine in the presence of a catalytic amount of sodium ascorbate and copper (II) sulfate gave triazole derivative **80**. Finally, deprotection with TBAF followed by a Mitsunobu-like reaction with DPPA, sodium azide and DBU and Staudinger reaction afforded amino derivative **82**.



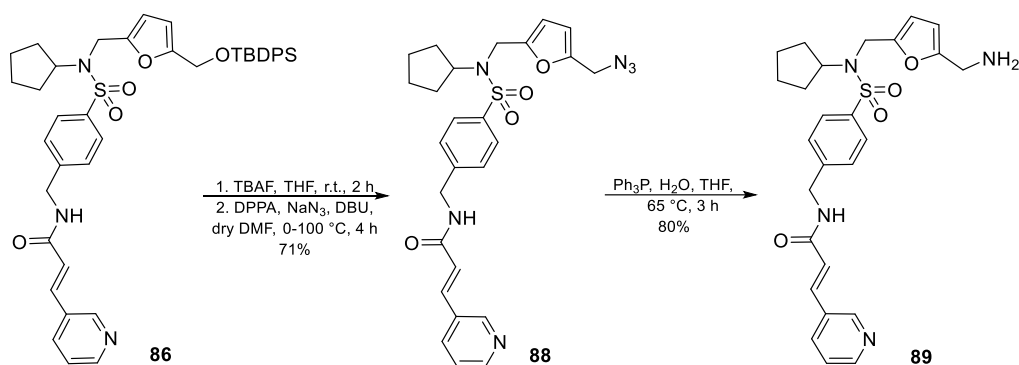
Scheme 50. Synthetic strategy for the preparation of final compound **82**.

The preparation of the cyanoguanidine, thiourea and acrylamide analogues was carried out from azido intermediate **79**. Thus, Staudinger reaction generated the corresponding amino derivative **83**, which was then coupled with compound **46a**, 3-isothiocyanatopyridine and *trans*-3-(3-pyridyl)acrylic acid to give compounds **84**, **85** and **86** respectively (Scheme 51).



Scheme 51. Synthetic strategy for the preparation of cyanoguanidine, thiourea and acrylamide intermediates **84**, **85** and **86**, respectively.

The preparation of the aminomethyl furan derivative **89** (Scheme 47) was achieved from *O*-protected intermediate **86** following the same strategy than for the preparation of **82** (Scheme 52).

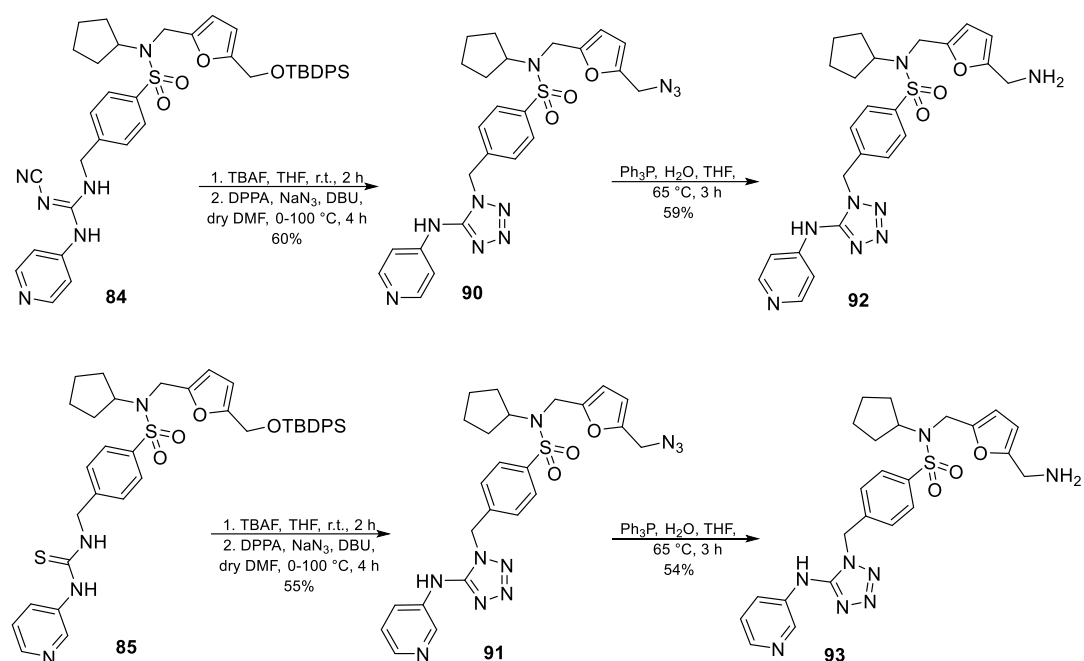


Scheme 52. Synthesis of furfurylamine derivative **89**.

A similar synthetic route starting from cyanoguanidine and thiourea analogues **84** and **85** afforded 4-pyridyl and 3-pyridyl tetrazoles **90** and **91**, respectively. Finally, in a further synthetic step, the azido groups of compounds **90** and **91** were reduced by

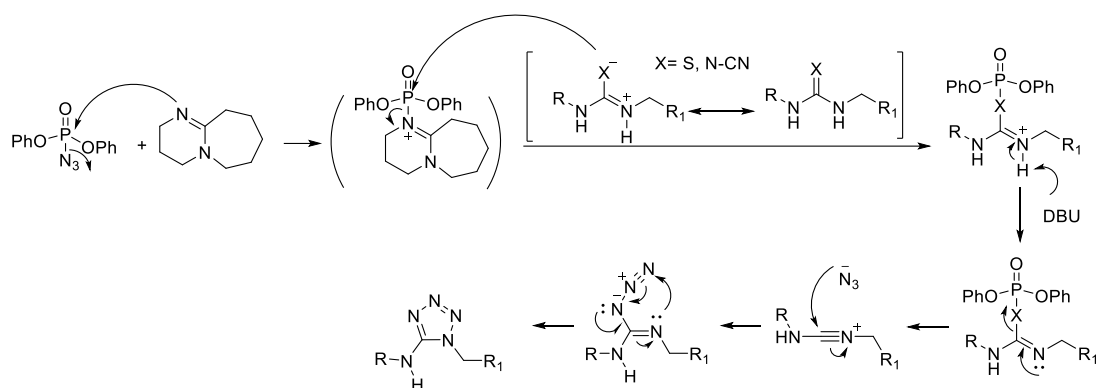
Staudinger reaction to yield the two final compounds **92** and **93** as shown in Scheme 53.

53.



Scheme 53. Synthesis of the final compounds **92** and **93**.

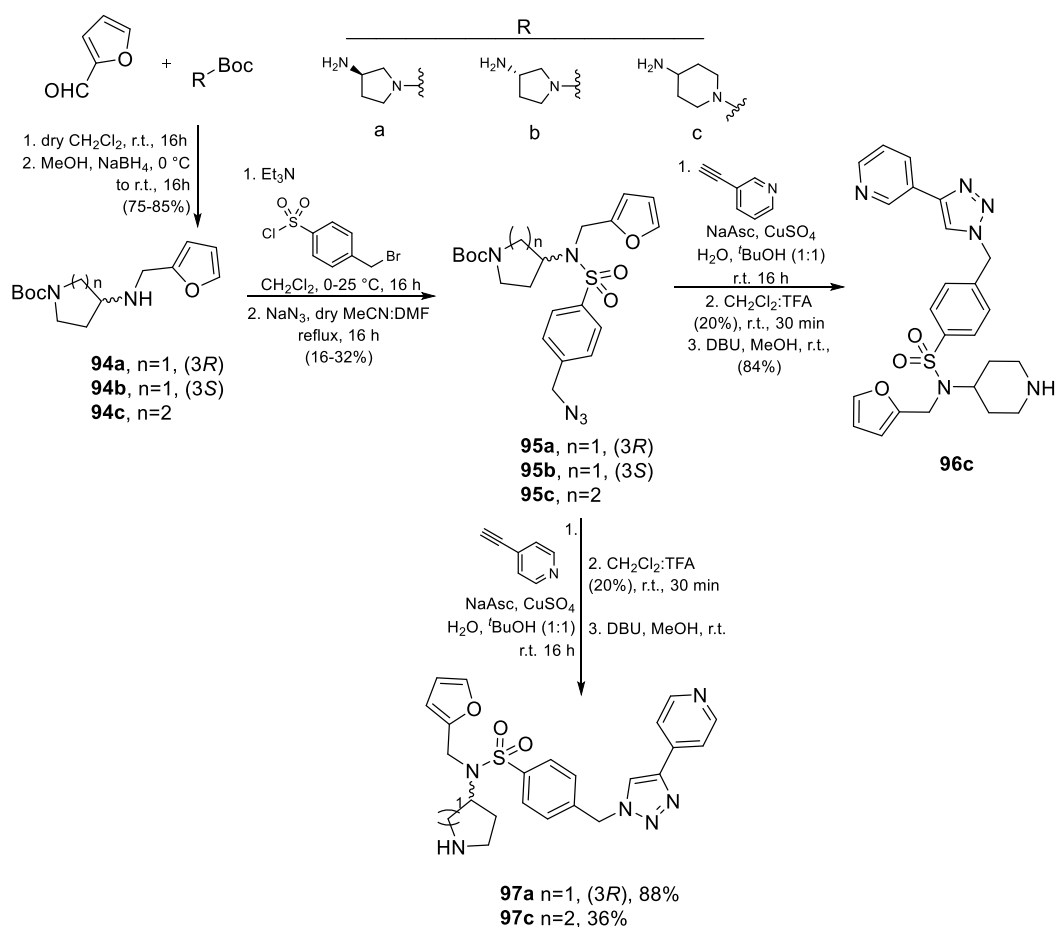
A possible reaction mechanism for the formation of tetrazoles **90** and **91**, is shown in Scheme 54. First, DBU can act as a nucleophilic catalyst to activate DPPA, being N₃ the leaving group. Then, the thiolate or the N (-N-CN) of the cyanoguanidine group attacks the activated DPPA to form a diphenylphosphoryl intermediate. Subsequently, a phosphorous derivative is eliminated to generate a nitrilium ion that is attacked by the free azide anion to form an azidoimine intermediate. Finally, an intramolecular reaction affords the corresponding tetrazole.



Scheme 54. Plausible reaction mechanism for the formation of tetrazole derivatives **90** and **91**.

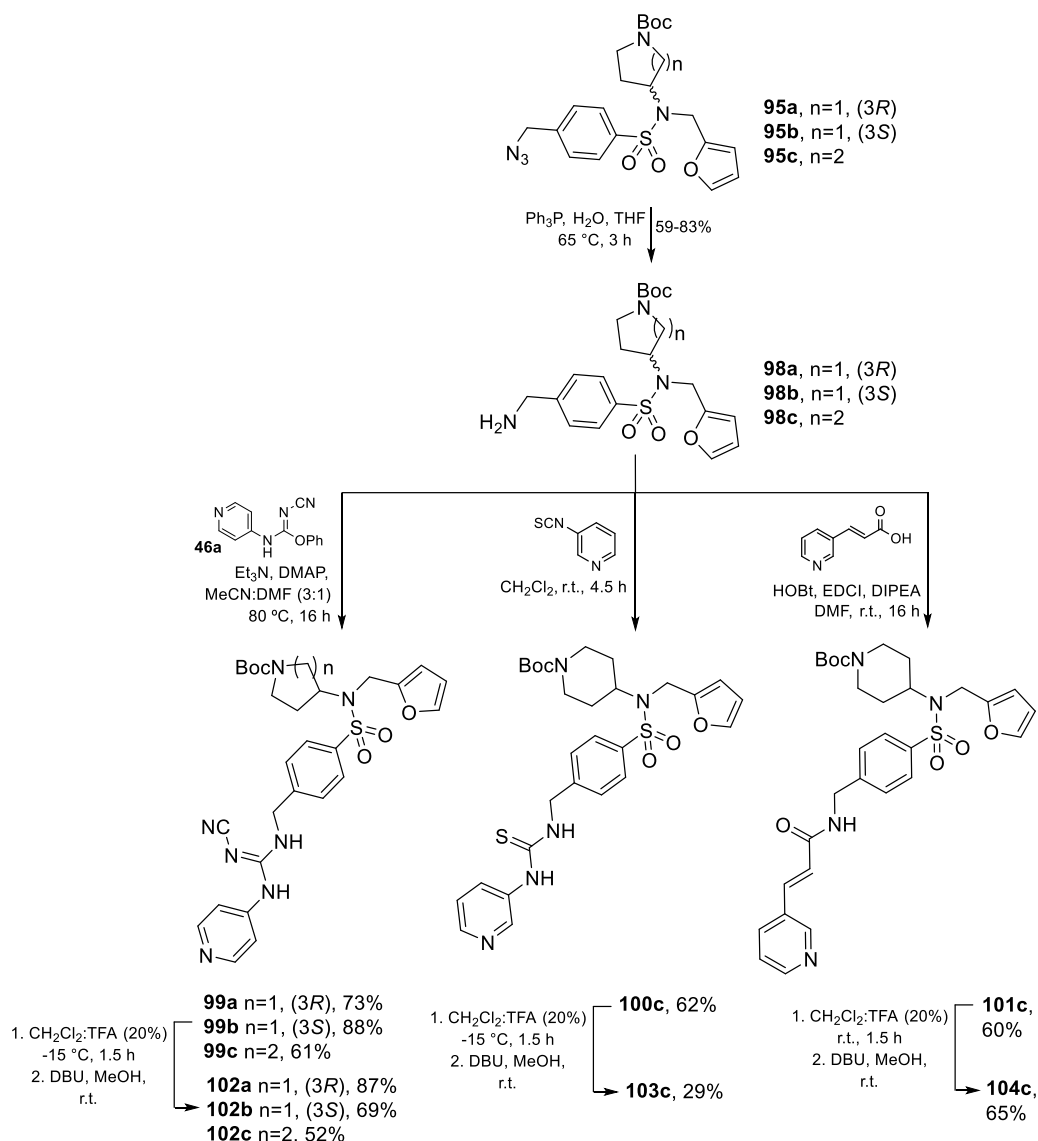
2.3.1.1.2 Preparation of new pyrrolidine and piperidine derivatives

Another possible modification to make **74** a bioconjugable payload was the replacement of the cyclopentyl moiety by either a pyrrolidine or piperidine group. Reductive amination of (*R*)- and (*S*)-*N*-Boc-3-aminopyrrolidine and *N*-Boc-4-aminopiperidine and furfural followed by reaction with 4-(bromomethyl)benzenesulfonyl chloride and subsequent treatment with sodium azide gave the corresponding azido compounds **95a-c**. Then, CuAAC reaction with 3- and 4-ethynylpyridine afforded the triazole intermediates, which after acidic deprotection and neutralization with DBU yielded the final compounds **96c**, **97a** and **97c** (Scheme 55).



Scheme 55. Synthesis of the final compounds **96c**, **97a** and **97c**.

On the other hand, the azido derivatives **95a-c** were reduced *via* Staudinger reaction to yield the corresponding amines **98a-c** (Scheme 56), which were then coupled with **46a**, *trans*-3-(3-pyridyl)acrylic acid and 3-isothiocyanatopyridine to give the corresponding Boc-protected compounds **99a-c** and **100c** and **101c**. Then, reaction of these compounds with 20% TFA in DCM followed by treatment with DBU afforded the final compounds **102a-c**, **103c** and **104c**. The acidic Boc deprotection of cyanoguanidine and thiourea derivatives **99a-c** and **100c** was carried out at low temperature (-15°C) due to the acid-sensitive nature of these moieties.

Scheme 56. Synthesis of the final compounds **102a-c**, **103c** and **104c**.

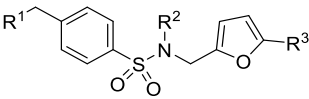
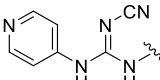
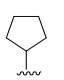
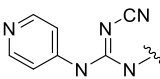
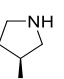
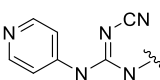
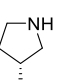
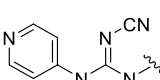
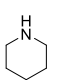
2.3.2 BIOLOGICAL EVALUATION

2.3.2.1 Viability assays on ML2 and RPMI8226 cells

The new compounds prepared as payloads for the incorporation into ADCs were tested *in vitro* for their anti-proliferative activity (Table 6) by Paulina Biniecka, in the group of Dr. M. Duchosal at the Centre Hospitalier Universitaire de Lausanne (CHUV, Lausanne, Switzerland). The compounds were tested in ML2 (acute myeloid leukemia) cell line, and the most promising ones were further evaluated on RPMI826

cell line, which is a multiple myeloma expressing the antigen CD138. Among the furfurylamine derivatives, compound **93** (entry 13), with a tetrazole connecting unit between the pyridine (cap group) and the benzylsulfonamide (spacer group) resulted to be the most cytotoxic compound with IC_{50} of 1.5 and 0.22 nM towards ML2 and RPMI826 cell line, respectively. Piperidine and pyrrolidine derivatives presented in general higher IC_{50} s than the furfurylamine family, indicating that the modification of the cyclopentyl group led to less cytotoxic compounds (e.g., entry 2 vs 3 and 10 vs 11). Finally, it is worth to point out that the position of the N of the pyridine joined to the connecting unit significantly influenced the IC_{50} values, being the compounds containing a 3-pyridine substituent more active than those having the 4-pyridine (entry 6 vs 7 and 12 vs 13).

Table 6. Evaluation of the viability on ML2 and RPMI8226 cells for the new compounds. ML2: acute myeloid leukemia; RPMI8226: multiple myeloma. NA = not available. a) Data are mean \pm SD, $n \geq 3$.

						
Entry	ID	R ¹	R ²	R ³	IC_{50} on ML2 (nM)	IC_{50} on RPMI8226 (nM)
1	FK866	-	-	-	0.2 \pm 0.5	1.1 \pm 0.5
2	74			H	0.53 \pm 0.02	0.21 \pm 0.01
3	102a			H	18 \pm 0.4	NA
4	102b			H	11.5 \pm 2.4	NA
5	102c			H	9 \pm 1	NA

6	82			CH ₂ NH ₂	> 2000	NA
7	96c			H	131±18	NA
8	97a			H	> 2000	NA
9	97c			H	> 2000	NA
10	89			CH ₂ NH ₂	10.67±3	21.42±0.67
11	104c			H	164±15	NA
12	92			CH ₂ NH ₂	169±19	NA
13	93			CH ₂ NH ₂	0.89±0.02	0.22±0.01
14	103c			H	> 2000	NA

2.3.3 PREPARATION OF NAMPT INHIBITOR-BASED ADCs

Compounds **74**, **89** and **93** were selected as payloads for the synthesis of new NAMPT inhibitor-based ADCs (Figure 48). This part of the project was performed during a secondment at Heidelberg Pharma (Germany). The linkers used for the preparation of the ADCs were either available at Heidelberg Pharma or purchased from Iris Biotech GmbH (Germany). Two types of linkers were selected: 1) linker **105** or MC-Val-Ala-PAB-PNP, a classic dipeptide cathepsine-B sensitive linker which has been activated with a *p*-nitrophenyl (PNP) group as appropriate chemical function to form stable carbamates with amines; 2) linkers **106a** and **106b** that are also protease-sensitive linkers that have been modified with a PEG chain to increase the hydrophilicity of the complex linker-drug before bioconjugation with the mAb. Linker **106a** incorporates the dipeptide fragment Ala-Val while linker **106b** incorporates the fragment Ala-Cit as shown in Figure 46.

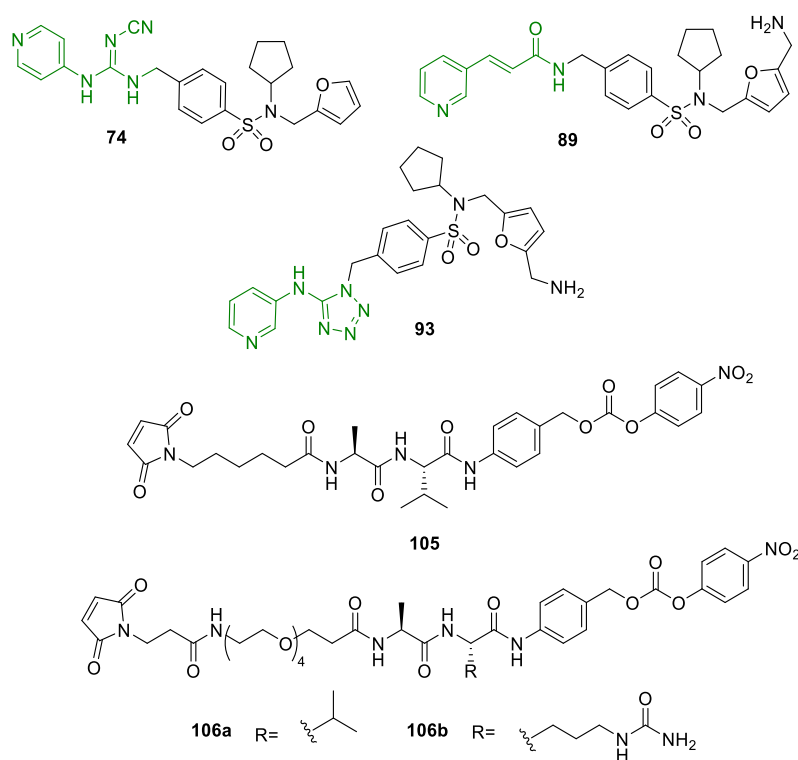


Figure 46. Structures of the selected payloads **74**, **89** and **93** and linkers **105** and **106a-b**.

Five new payload-linkers (**107**, **108a-b** and **109a-b**) were synthesized, combining the linkers **105**, **106a** and **106b** and final compounds **89** and **93** in the presence of DMAP as base (Figure 47).

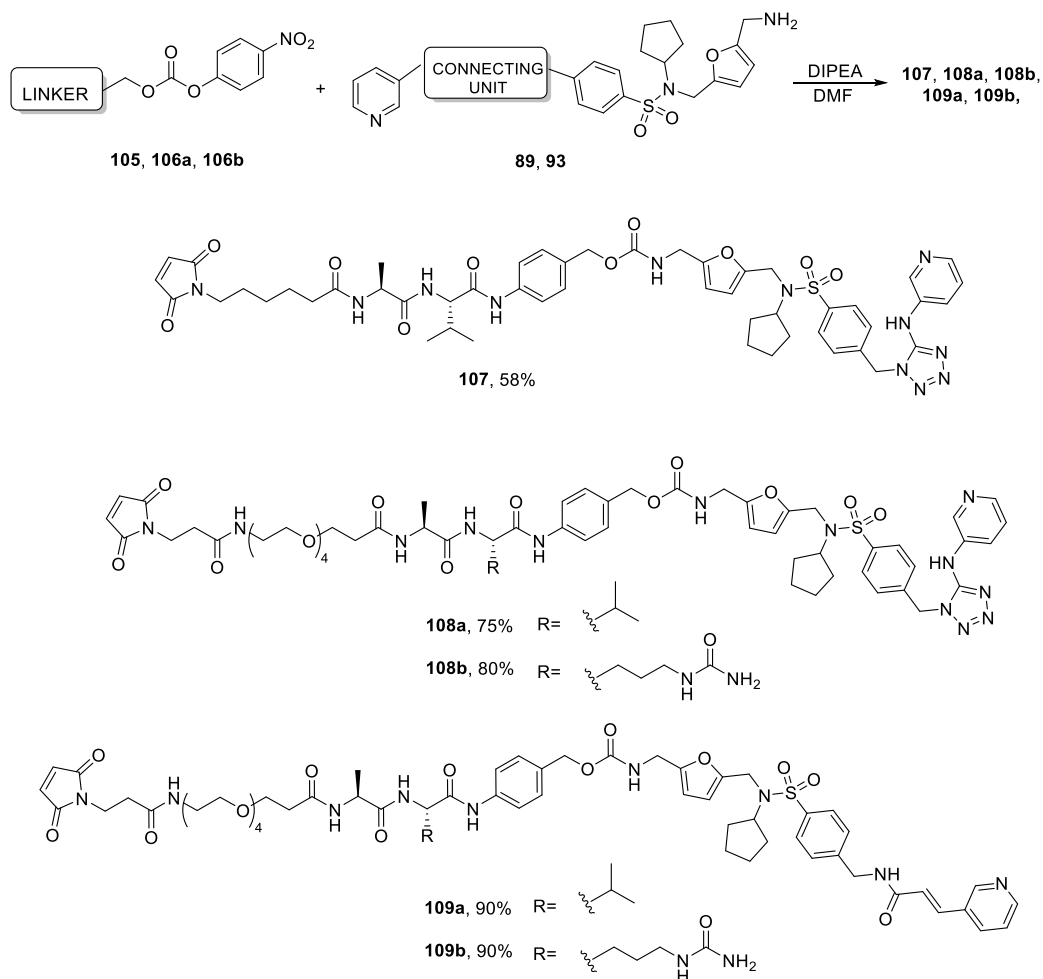
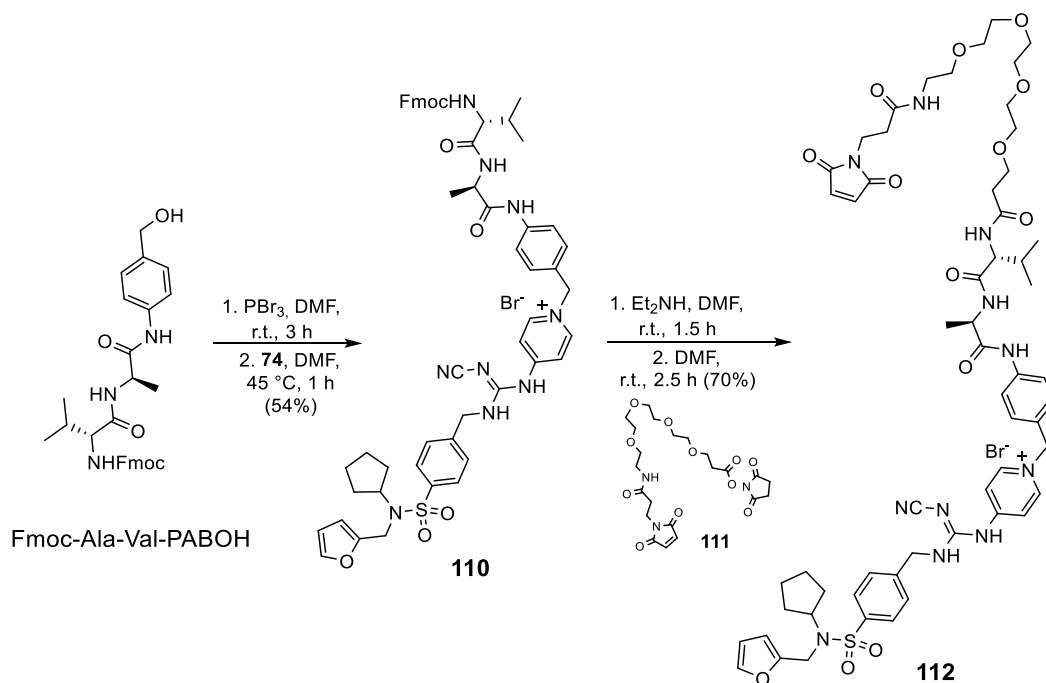


Figure 47. Synthesis of the payload-linkers bearing NAMPT inhibitors.

The linkers **105** and **106a-b** are appropriate for the incorporation of amino-functionalized payloads *via* carbamate ligation. However, for the incorporation of **74** that does not bear an amino group, a modification of linker **106a** was needed. Thus, reaction of Fmoc-Ala-Val-PABOH with PBr_3 afforded the brominated derivative at the benzyl position (Scheme 57). Subsequent alkylation with payload **74** yielded **110** in good yield. Then, Fmoc deprotection with diethylamine followed by coupling with

commercially available PEG4 activated ester **111**, yielded the quaternary pyridinium salt **112** as shown in Scheme 57.



Scheme 57. Synthesis of the linker-payload **112**.

Finally, the bioconjugation reaction between payload-linkers **107**, **108a-b**, **109a-b** and **112** and monoclonal antibody CD138, previously synthesized by Paulina Binięcka at Heidelber Pharma (Germany), was carried out in a buffer solution (pH 7.4) with DMSO as co-solvent (10-20%) as shown in Figure 48. Firstly, the mAb was subjected to treatment with TCEP to reduce the disulfide bonds for the subsequent bioconjugation with the complex payload-linker. Then, the non-reacted thiols were capped with an excess of *N*-ethylmaleimide, which was finally quenched with *N*-acetyl-L-cysteine before purification (PD-10 column) of the resulting solution. Each of the resulting sterilized solutions were then analyzed by the analytical department of Heidelberg Pharma to verify the formation of protein aggregations by SEC-HPLC, and for DAR calculation. The TOF-MS analysis confirmed a high DAR between 7.55 and 8.42 for the corresponding ADCs **113**, **114**, **115a-b** and **116a-b** shown in Figure 48.

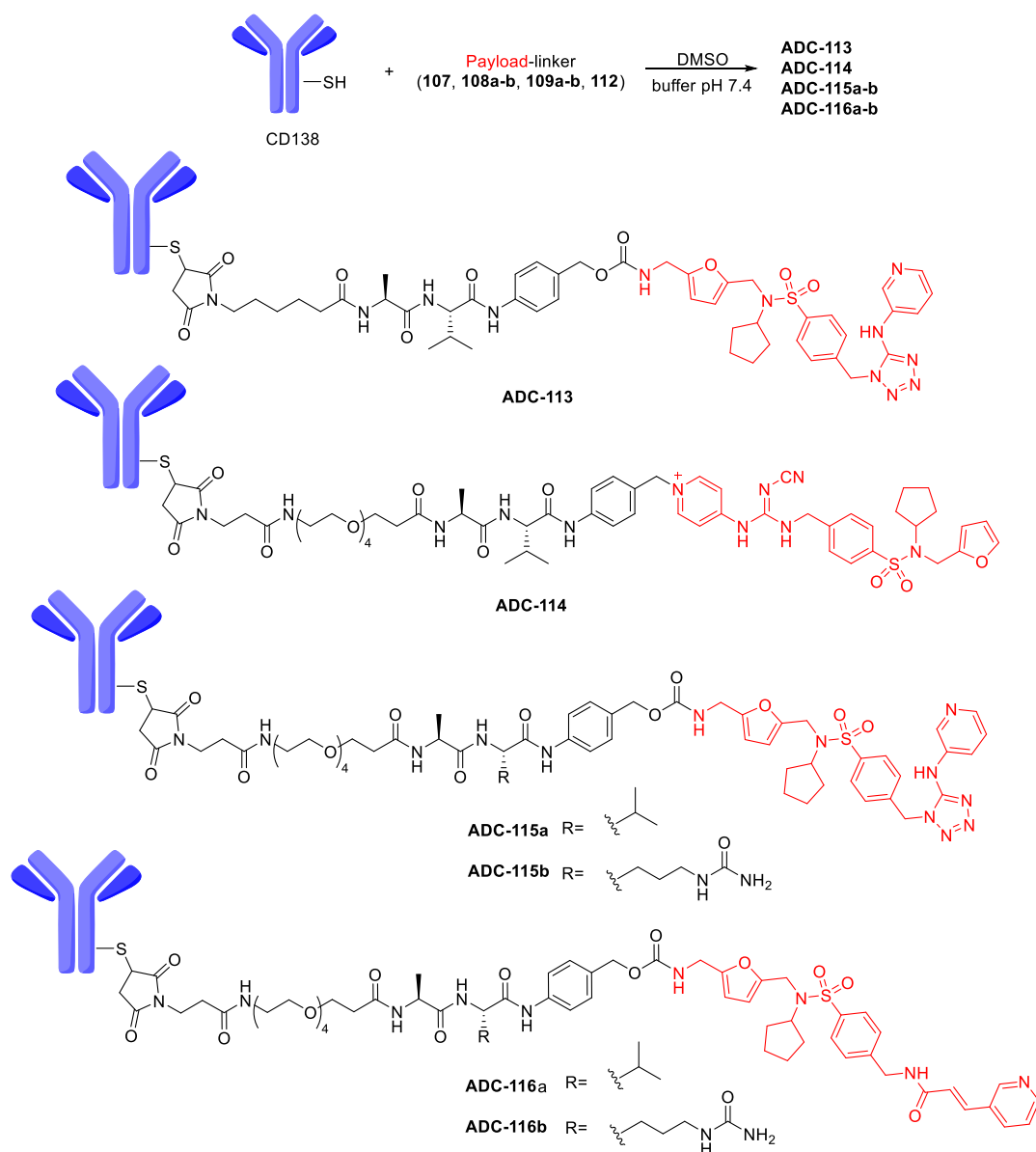
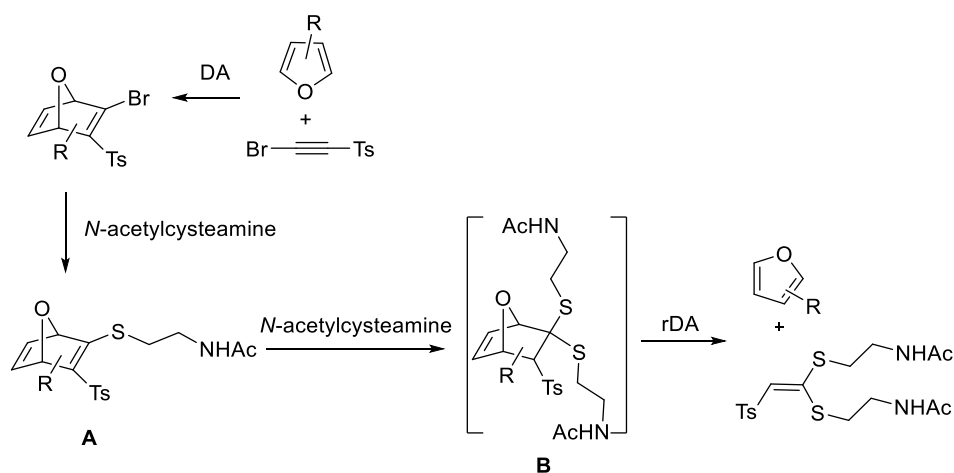


Figure 48. Synthesis of 6 new ADCs bearing NAMPT inhibitors as payloads. PABC= *p*-aminobenzylcarbamate, PAB= *p*-aminobenzyl. **ADC-113**: Val-Ala-PABC-**107** (DAR=7.83); **ADC114**: Val-Ala-PAB-**112** (DAR=7.69); **ADC-115a**: Val-Ala-PABC-**108a** (DAR=7.72); **ADC-115b**: Val-Cit-PABC-**108b** (DAR=7.55); **ADC-116a**: Val-Ala-PABC-**109a** (DAR=8.42); **ADC-116b**: Val-Cit-PABC-**109b** (DAR=8.33).

2.3.4 OXANORBORNADIENES AS PUTATIVE NOVEL LINKERS FOR ADCs

As we have already presented in the Introduction section of this chapter, oxanorbornadienic systems (ONDs) could be used as new linkers for the development of ADCs as they present the requirements to be self-immolative chemical systems programmed to deliver a cytotoxic agent selectively at the tumor site. In this section we will present the synthesis of these bicyclic systems and will explore preliminarily their reactivity towards models of biological thiols. ONDs are usually prepared through Diels-Alder (DA) reaction between furan (or furan derivatives) and electron-deficient alkynes. In case of using substituted furans, a mixture of regioisomeric ONDs would be obtained. As indicated in the introduction section (pag. 148), oxanorbornadienic thiovinyl sulfones are prone to undergo a fragmentation reaction in the presence of an excess of thiols. By analogy, we propose that the related oxanorbornadienic systems could fragment in the same way, that is, a two-reaction sequence that implies a conjugate addition followed by a retro-Diels-Alder (rDA) reaction (Scheme 58).

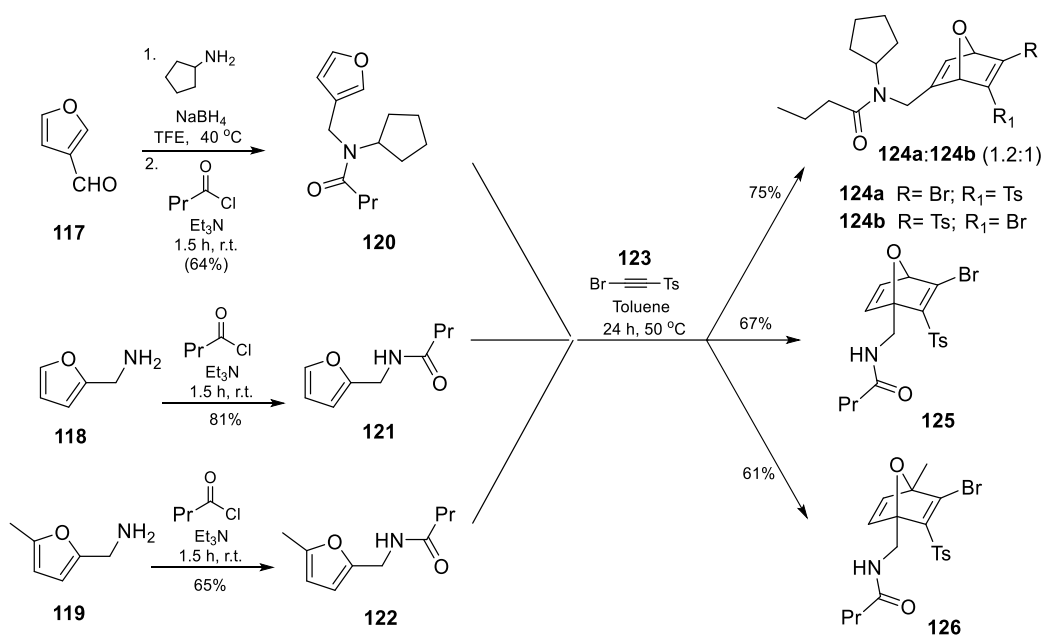


Scheme 58. Cysteamine-promoted fragmentation of ONDs.

This reactivity could find applications in the field of glutathione-sensitive linkers for target drug delivery by exploiting the higher GSH concentration inside the tumor cells compared to its surroundings.¹⁵⁴ The rates at which ONDs can release the active drug can play an important role in the overall efficacy of the ADCs. To explore this possible application, we planned a preliminary study to analyse the kinetic of the fragmentation reaction of several oxanorbornadienic thiovinyl sulfones. The thio-substituent of the OND system **A** (Scheme 58) would mimic the cysteine present on the antibody's surface, while the addition of an excess of *N*-acetylcysteamine would simulate the intracellular reaction of the conjugate antibody-OND with glutathione.

2.3.4.1 Synthesis of oxanorbornadienes

The synthesis of the ONDs used for the kinetic studies started from 3-furancarboxaldehyde **117**, furfurylamine **118**, and 5-methylfurfurylamine **119** (Scheme 59). Firstly, reductive amination between cyclopentylamine and **117** followed by butanoylation of the resulting amine afforded derivative **120** in 64% yield. A Diels-Alder reaction between **120** and alkyne **123**^{163,164} yielded ONDs **124a** and its regioisomer **124b** with an overall yield of 75%. ONDs **125** and **126** shared the same synthetic strategy except that acylated furfurylamines **121** and **122** were used as dienes in the DA reaction. In these cases, only the regioisomers indicated were obtained, as confirmed by 1D NOESY experiments.



Scheme 59. Synthetic route for the preparation of oxanornbornadienes **124a-b**, **125** and **126**.

The high regioselectivity observed in the formation of ONDs **125** and **126** could be attributed to a stabilization of the transition state due to a hydrogen bond between the NH of the amide and the oxygen atoms of the tosyl moiety, as shown in Figure 49.

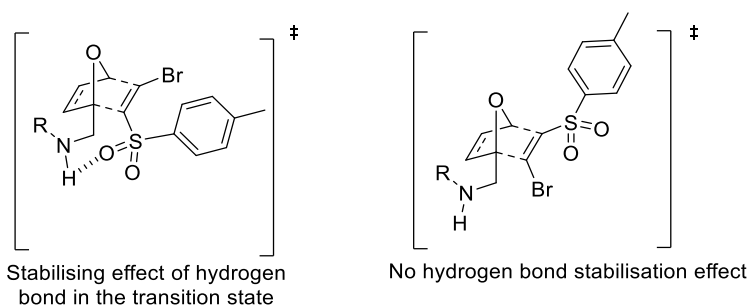
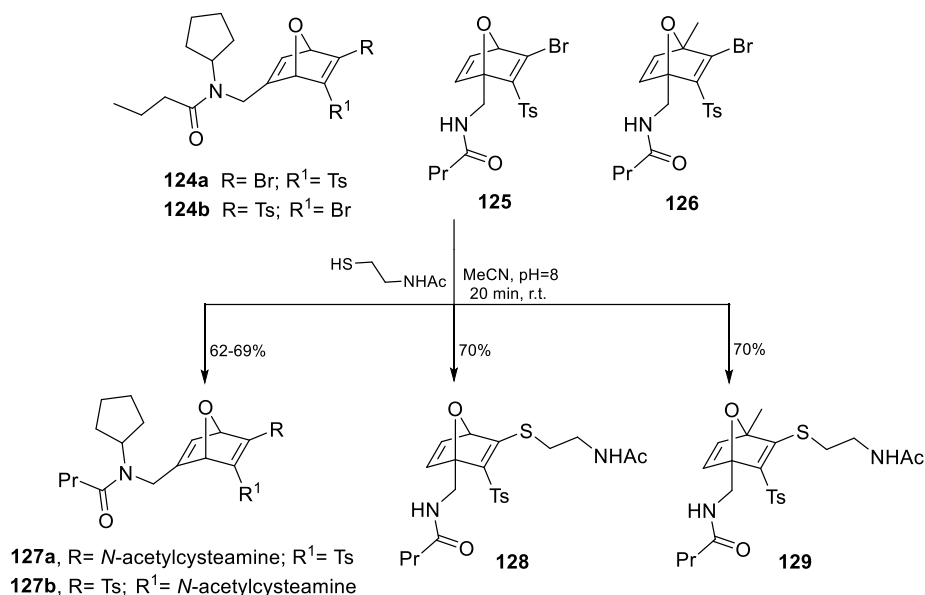


Figure 49. Hypothetic weak stabilisation effect through hydrogen bonding in the transition state of the DA reaction.

2.3.4.2 Kinetic studies of the OND fragmentation

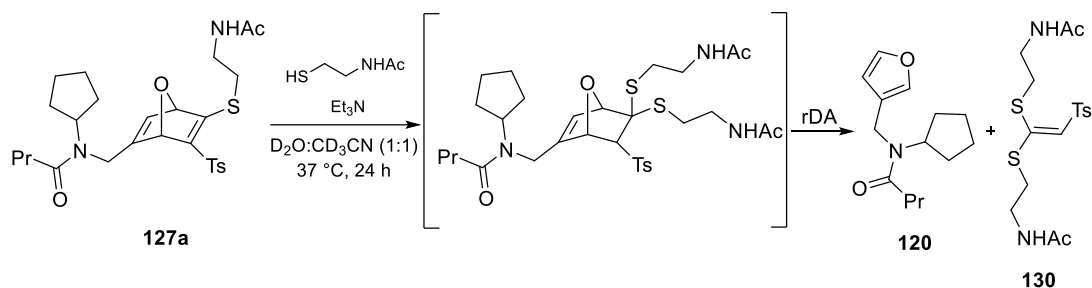
ONDs **124-126** were reacted with *N*-acetylcysteamine in acetonitrile at r.t. and pH 8.0. The reaction takes place through a nucleophilic vinylic substitution mechanism

(S_NV_S), as was previously established with azanorbornadienic analogues.¹⁵⁷ The corresponding oxanorbornadienic thiovinyl sulfones **127-129** were isolated in 62-70% yield (Scheme 60).



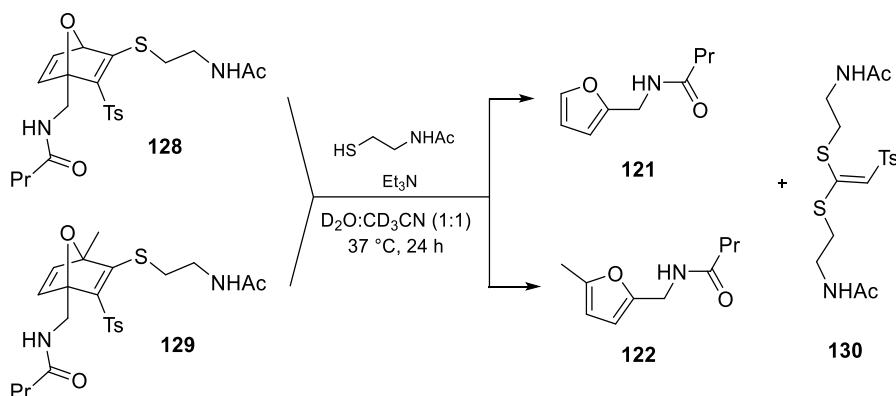
Scheme 60. Thiol substitution on bicyclic systems **124-126**.

To determine the half-life ($t_{1/2}$) of the thiovinyl sulfones we evaluated the tendency of the system to fragmentate after a second addition of thiol. The kinetic studies were carried out on **127-129**, *via* the addition of an excess of *N*-acetylcysteamine. The reactions were carried out at physiological temperature (37 °C) in the presence of 1.0 equiv. of Et₃N and in a deuterated solvent mixture (D₂O:CD₃CN, 1:1) to allow the reactions to be followed by ¹H NMR. ONDs **127a** and **127b** were transformed into furan derivative **120** and alkene **130** through a thioketal intermediate in a two-step reaction sequence (Scheme 61). By ¹H NMR we observed that the rDA reaction is the limiting rate step of the sequence. The formation of the thioketal intermediate occurs within the first 5 min. The rDA step was monitored by NMR during 24 h. The percentage of conversion of ONDs **127a** and **127b** into furan **120** and ketene, *S,S*-acetal **130** was 17.2% and 8.3% after 24 h, respectively.



Scheme 61. Kinetic study of rDA reaction of OND **127a**.

The fragmentation reactions of bicyclic derivatives **128** and **129**, were also monitored by ^1H NMR under the same conditions (Scheme 62). These fragmentations occurred significantly faster than in the case of **127**. The values of $t_{1/2}$ could be determined in both cases. OND **129** showed to be the most sensitive to the fragmentation in the presence of *N*-acetylcysteine ($t_{1/2} = 3.0$ h) in comparison with **128** ($t_{1/2} = 12$ h).



Scheme 62. Kinetic studies of rDA reaction of **128** and **129**.

The fragmentation of OND **129** was also studied at pH 5.9 to mimic the physiological conditions inside the tumor cells. When the reaction was performed in CD_3CN :citrate-phosphate buffer, the value of $t_{1/2}$ was 3.3 h, similar to the value previously determined ($t_{1/2} = 3.0$ h). This study shows that the fragmentation reaction was not strongly affected by the pH, instead, the structural modifications on the bicyclic skeleton were critical for the fragmentation rate. The half-life only increased by 19 minutes when decreasing from pH 12 to pH 5.9 (Figure 50). However, the half-life decreased from

12 to 3.3 hours when adding a methyl group at position 4 of the bicyclic skeleton at the same pH.

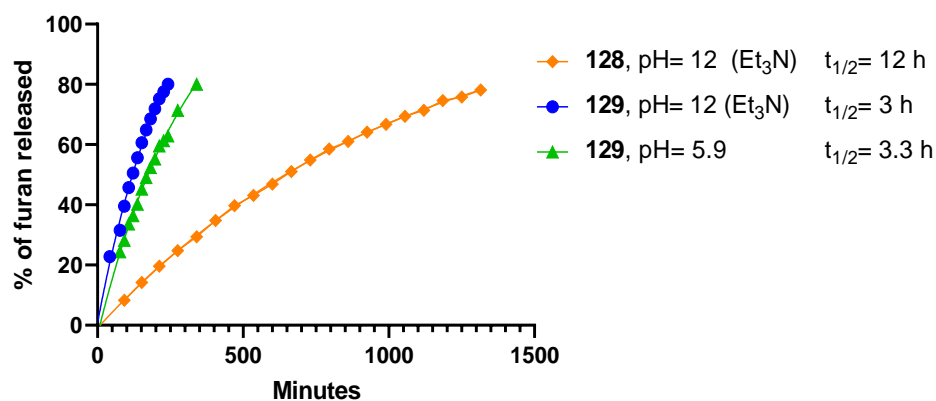
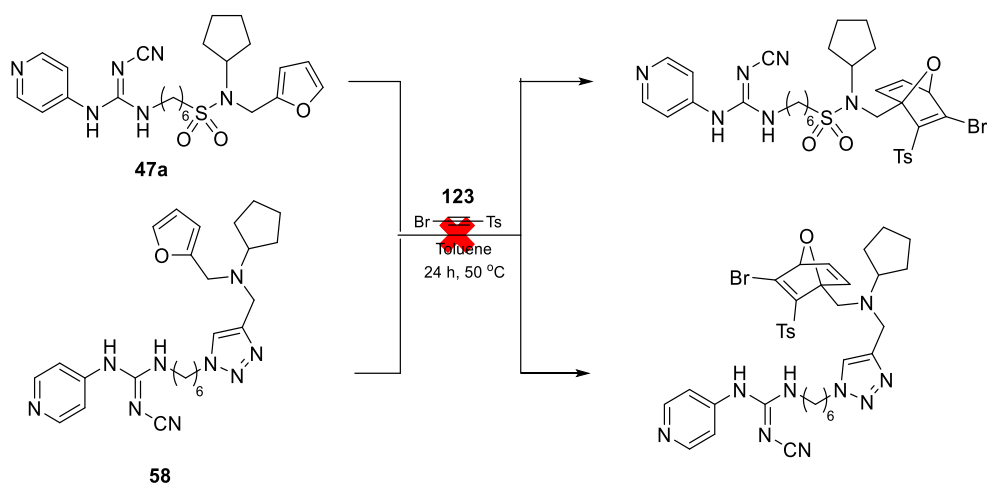


Figure 50. Plots of % conversion of ONDs **128** and **129** into the corresponding furan derivatives vs time (GraphPad Prism) to determine the half-life at 37 °C and different pH.

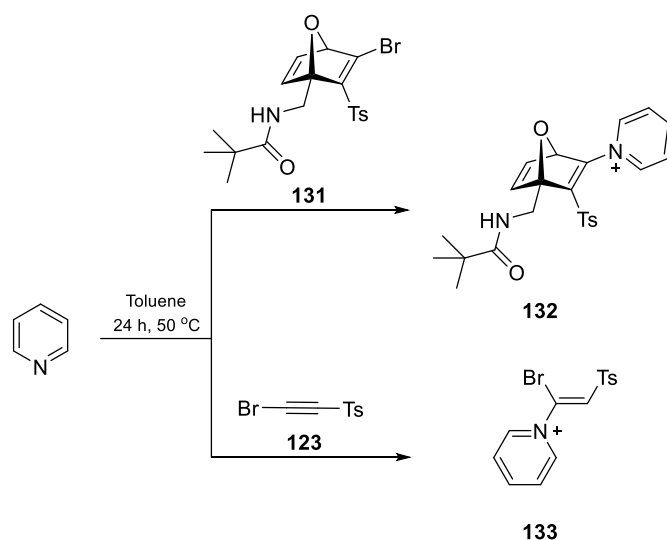
2.3.4.3 Reactivity of electrophilic ONDs and activated alkynes towards pyridine derivatives

The use of ONDs as linkers for ADC applications implies the presence of a furan moiety in the cytotoxic drug to be delivered. This furan moiety will serve as a handle for the OND synthesis *via* a DA reaction with the appropriate alkyne. Thus, the cytotoxic drug and the linker would constitute a unique fragment to be bioconjugated with the mAb. Therefore, we first attempted the DA reaction between activated alkyne **123** and NAMPT inhibitors **47a** and **58** (Scheme 63).



Scheme 63. Attempts to synthesize bioconjugable OND bearing NAMPT inhibitors.

Unfortunately, these reactions afforded a complex mixture of compounds, probably related with the incompatibility between the activated alkyne and the nucleophilic pyridine moiety present in NAMPT inhibitors. The pyridine moiety could also interfere with the resulting oxanorbornadienic bromovinyl sulfone. Thus, stability studies of alkyne **123** and model oxanorbornadienic bromovinyl sulfone **131** in the presence of pyridine under DA reaction conditions (temperature and solvent) were performed (Scheme 64). As anticipated, after 3h of reaction, all the alkyne **123** reacted with pyridine through a conjugate addition to afford pyridinium salt **133**. On the other hand, oxabicyclic **131** afforded **132** through a nucleophilic vinylic substitution (S_NV_S) mechanism. Both results were confirmed by mass spectrometry. It is interesting to point out that when 2-fluoropyridine, a weaker nucleophilic pyridine, was used in the reaction, both substrates (alkyne **123** and oxanorbornadiene **131**) remained stable under the same reaction conditions.



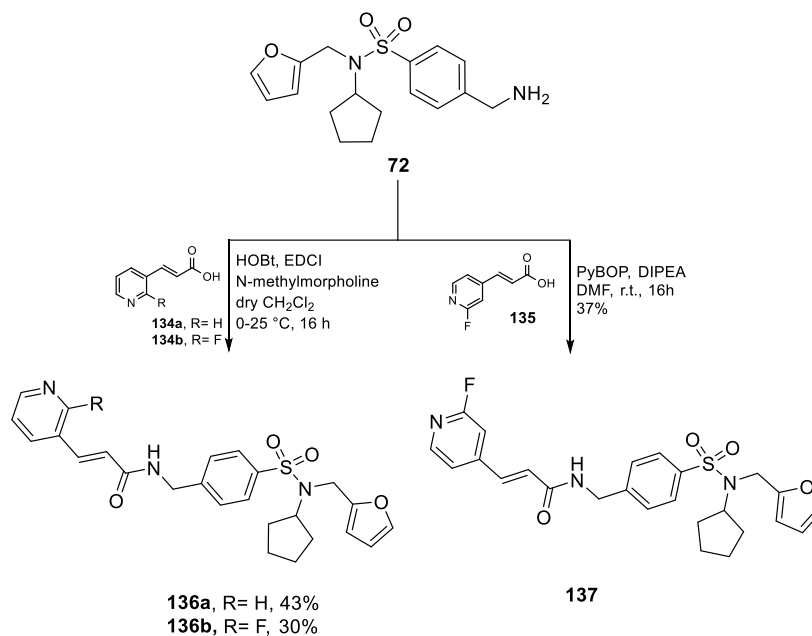
Scheme 64. Reactions of pyridine with alkyne **123** and OND **131**.

2.3.5 SYNTHESIS OF PUTATIVE NAMPT INHIBITORS CONTAINING A FLUOROPYRIDINE MOIETY

2.3.5.1 Acrylamide-containing family

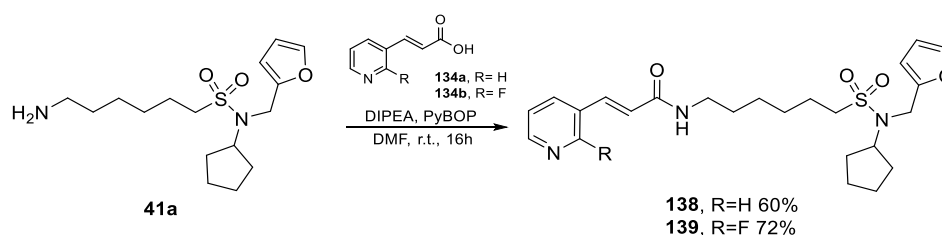
The most relevant cytotoxic compounds prepared in the first chapter of this Thesis present a nucleophilic pyridine moiety which makes these structures incompatible with the incorporation into an OND. To overcome this issue, we envisaged a strategy based on the preparation of NAMPT inhibitors that incorporated a 2-fluoropyridine instead of a pyridine moiety. The electronegative character of fluorine would reduce the nucleophilicity of the contiguous pyridinic nitrogen and would allow the synthesis of the corresponding OND system. Besides, the 2-fluorine substituent will make the pyridine moiety less prone to *in vivo* N-oxidation, which is one of the main limitation of most pyridine-based NAMPT inhibitors.^{25,141} Moreover, to study the influence of the fluorine in terms of cytotoxicity, a series of 2-fluoropyridine- and pyridine-containing molecules were synthesized. Following this strategy, the intermediate **72** was coupled with commercially available carboxylic acid **134a** and the synthesized analogue **134b** to afford amides **136a** and **136b** in moderate yields. Compound **137** was synthesized from the same intermediate **72** and *tert*-butyl-(*E*)-3-(2-fluoropyridin-

4-yl)acrylate **135** (for synthetic details see experimental part) using DIPEA, PyBOP in DMF in 37% yield (Scheme 65).



Scheme 65. Synthetic route to putative NAMPT inhibitors **136a**, **136b** and **137**.

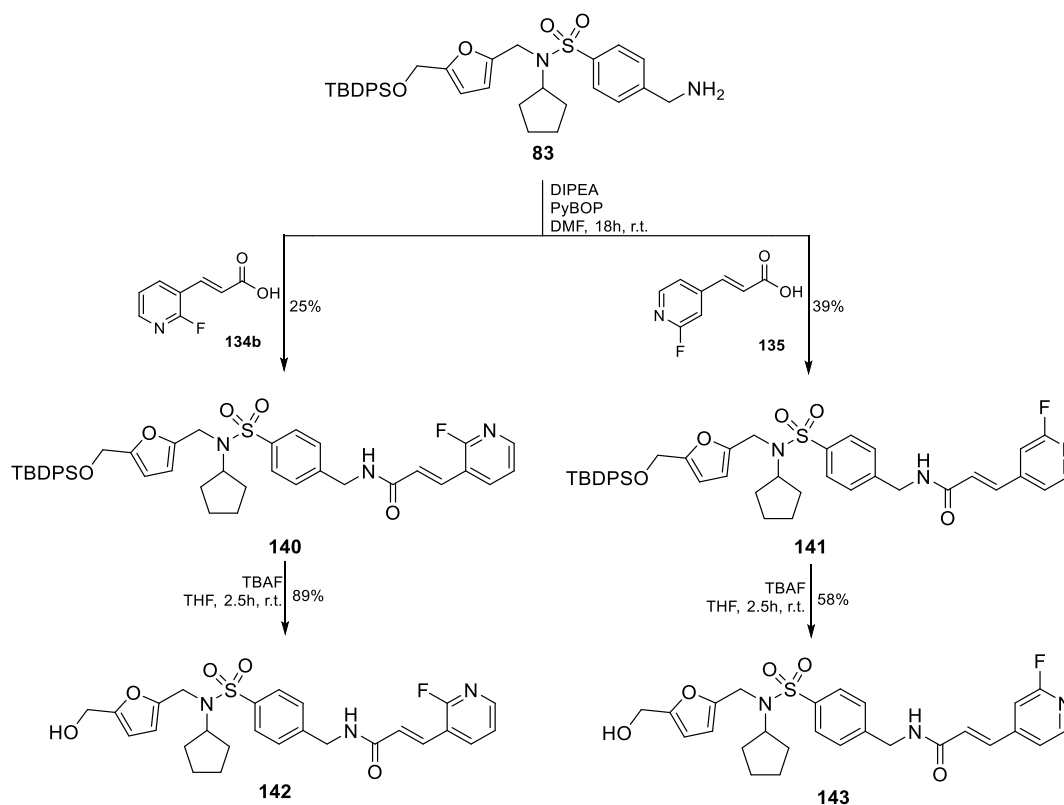
Additionally, compounds **138** and **139**, which present a flexible 6-carbon chain instead of the benzyl group, were synthesized. Reaction of amine **41a** with carboxylic acids **134a** and **134b** using PyBOP and DIPEA in DMF afforded **138** and **139** in good yields (Scheme 66).



Scheme 66. Synthetic route to final compounds **138** and **139**.

To improve the aqueous solubility of the derivatives, compounds **142** and **143**, which present a hydroxymethyl substituent at the furan tail group, were synthesized following a similar synthetic route (Scheme 67). First, the amine **83** was coupled with

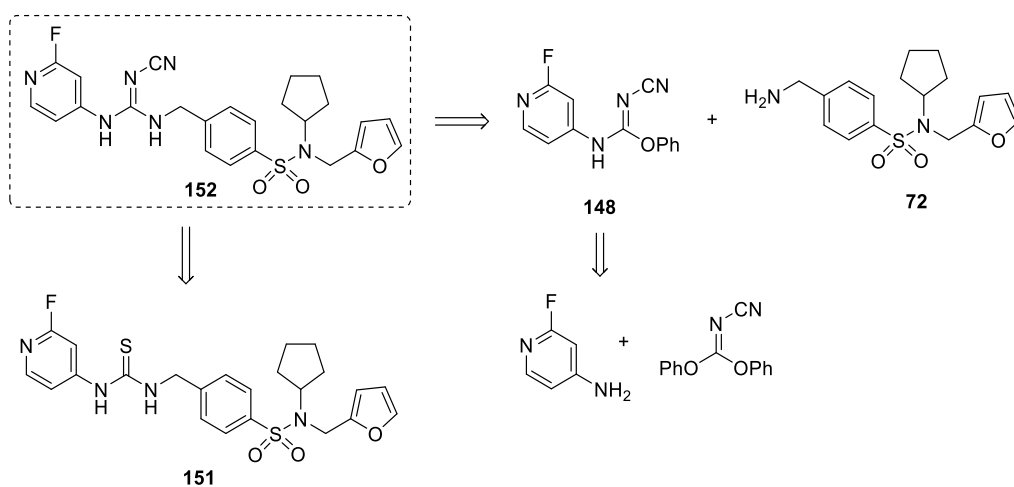
previously synthesised carboxylic acids **134b** and **135** under standard conditions to yield TBDPS-protected derivatives **140** and **141** in moderate yields. Finally, the TBDPS-protecting group was removed using TBAF in THF to afford final compounds **142** and **143**.



Scheme 67. Parallel synthetic routes to final compounds **142** and **143**.

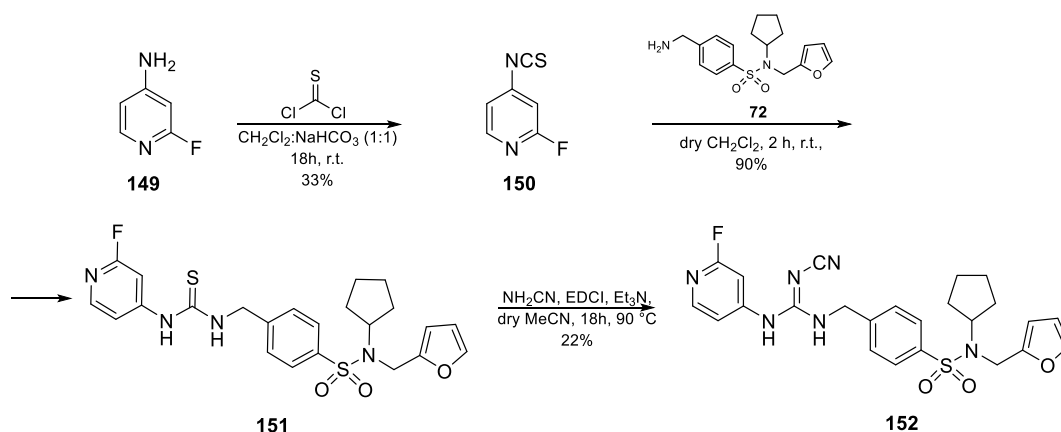
2.3.5.2 Cyanoguanidine-containing family

The synthesis of analogues presenting a 2-fluoropyridine and a cyanoguanidine connecting unit was then attempted. Thus, the preparation of compound **152** would imply the reaction of carbamimidate **148** and previously synthesized amine **72** (Scheme 68). However, all the attempts to obtain **148** by reaction of 4-amino-2-fluoropyridine and diphenyl cyanocarbonimidate were unsuccessful.



Scheme 68. Retrosynthetic analysis for the preparation of **152**.

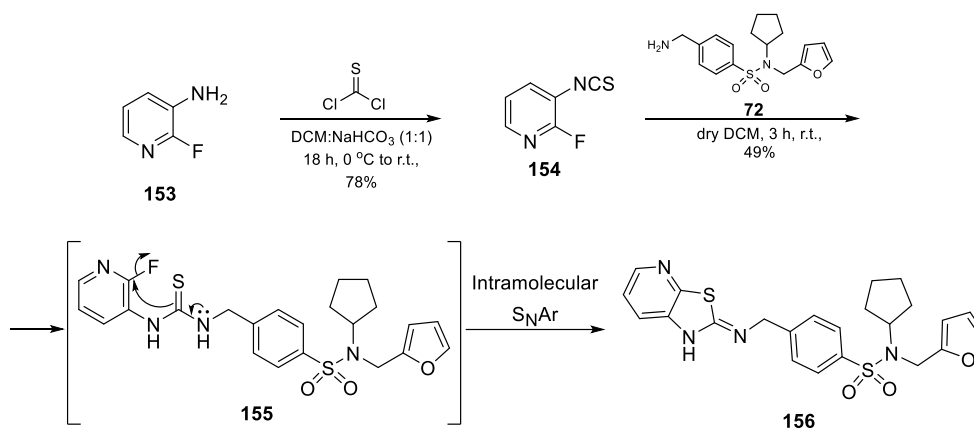
A second approach for the synthesis of cyanoguanidine **152** implied the preparation of thiourea **151**. Thus, reaction of commercial 4-amino-2-fluoropyridine **149** and thiophosgene yielded isothiocyanate **150**, in 33% yield (Scheme 69). Compound **150** was then reacted with amine **72** to form thiourea derivative **151**. Compound **152** was then formed in low yield by reaction of **151** with cyanamide, EDCI and Et₃N in MeCN.



Scheme 69. Synthetic route for the preparation of thiourea- and cyanoguanidine-connected inhibitors **151** and **152**.

The same synthetic strategy was attempted for the preparation of thiourea **155** (Scheme 70), except that commercial 2-fluoro-3-aminopyridine **153** was used as starting material. However, reaction of isothiocyanate **154** with amine **72** did not

afford the expected thiourea **155**. The ^{13}C -NMR spectrum did not show the characteristic signal of the C=S at around 180 ppm nor the C-F splitting. Besides, the HRMS indicated a mass 20 units lower than expected, indicating the loss of HF. Therefore, we concluded that thiourea **155** was short-lived and underwent rapid intramolecular attack via $\text{S}_{\text{N}}\text{Ar}$ (Scheme 70), yielding a fused five-membered cycle **156** after substitution of fluorine. In contrast, the presence of the fluorine atom at *meta* position in the pyridine ring with respect to the thiourea group prevents the intramolecular nucleophilic attack to occur in the case of thiourea **151**.



Scheme 70. Synthetic route to compound **155**, which underwent rapid intramolecular cyclization to form compound **156**.

The HRMS and NMR data of compound **156** were in accordance with the proposed structure. The ^{13}C -NMR spectrum showed two signals at 166.3 and 155.3 ppm that were assigned to both carbon atoms next to the sulfur in the fused five-membered cycle.

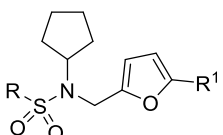
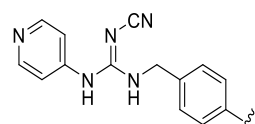
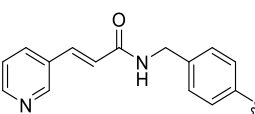
2.3.6 BIOLOGICAL EVALUATION

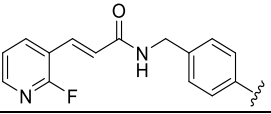
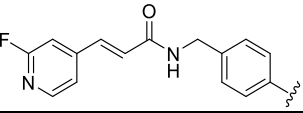
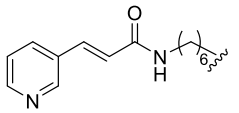
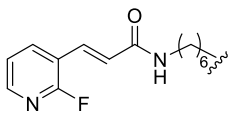
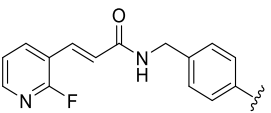
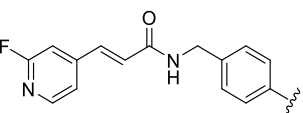
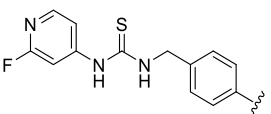
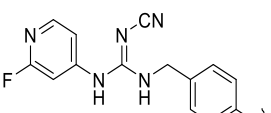
2.3.6.1 *In vitro* viability assays of the newly prepared compounds on MIA PaCa-2 cell line

The new compounds were tested *in vitro* for their anti-proliferative activity by Dr. Irene Caffa, at the Department of Internal Medicine of the University of Genoa (Table

7) in Prof. Alessio Nencioni's laboratory. The analysis of the cytotoxicity of the new 2-fluoro pyridine analogues towards MIA PaCa-2 cell line afforded several conclusions. Compared to **74** (entry 1), the substitution of cyanoguanidine by an acrylamide connecting group led to a dramatic decrease in cytotoxicity (entry 1 vs 2). Besides, the incorporation of a fluorine atom next to the nitrogen of the pyridine diminishes drastically the cytotoxicity towards MIA PaCa-2 cell line in all cases (entry 1 vs 10, entry 2 vs 3/4, entry 5 vs 6, entry 2 vs 7). Additionally, the incorporation of a hydroxymethyl group at C-5 of the furan moiety in the acrylamide family (entry 6 and 8) was analyzed. In both cases, even if the cLogP, which measures how much a compound is hydrophilic, decreased to a value similar to that of **74** (entry 1) none of them reached a good cytotoxicity. Compound **152** (entry 10), with an IC₅₀ of 2.44 nM was identified as the best of the series. The cytotoxicity of this compound is good enough for ADC application and could be considered a good candidate for OND formation and targeted drug delivery strategies.

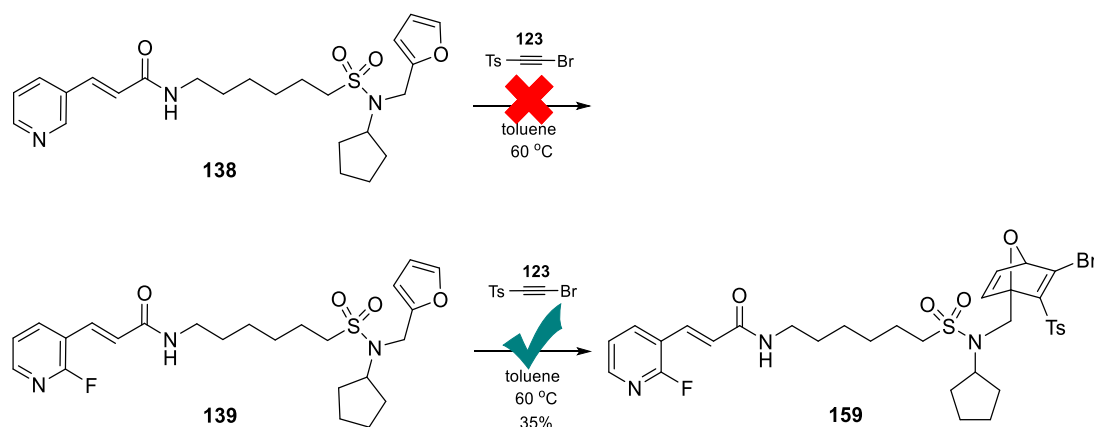
Table 7. Evaluation of the viability on MIA PaCa-2 cell line for the new compounds. MIA PaCa-2= Pancreatic cancer. NA = not available. a) Data are mean \pm SD, n \geq 3. ^a cLogP was calculated using Chemdraw 19.1.

					
Entry	ID	R	R ¹	Viability assay - IC ₅₀ on MIA PaCa-2 cell line (nM)	cLogP ^a
1	74		H	0.009 \pm 0.001	3.1
2	136a		H	21.60 \pm 3.81	3.7

3	136b		H	> 800	3.9
4	137		H	> 800	3.9
5	138		H	10.63±3.49	3.3
6	139		H	109±49	3.5
7	142		CH ₂ OH	> 800	2.9
8	143		CH ₂ OH	> 800	2.9
9	151		H	797±137	4.0
10	152		H	2.44±0.57	3.4

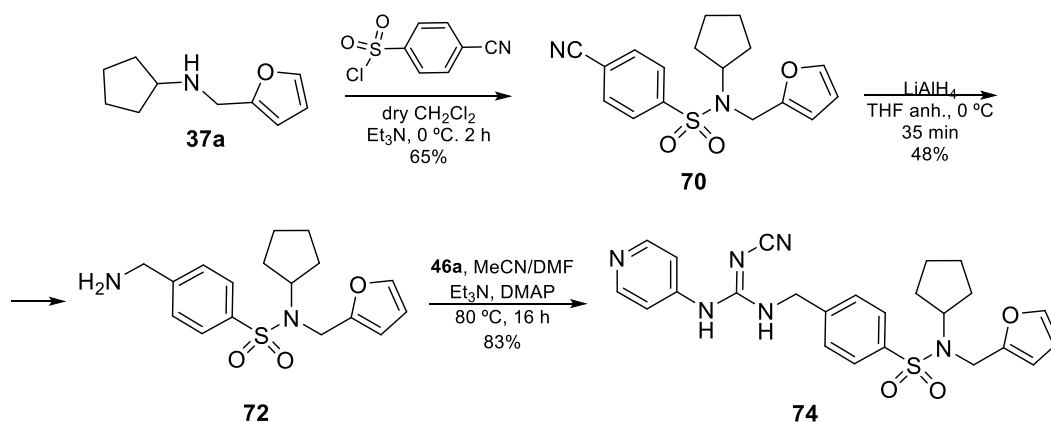
2.3.7 PRELIMINARY DA REACTIONS WITH FURAN-BASED NAMPT INHIBITORS

Diels-Alder reactions between furan-containing NAMPT inhibitors of the acrylamide family (**138** and **139**) and alkyne **123** were subsequently attempted (Scheme 71). The reaction with pyridine containing derivative **138** did not afford the corresponding OND adduct, as previously observed with compounds **47a** and **58** (Scheme 63, pag. 174). However, the DA reaction of 2-fluoropyridine analogue **139** and alkyne **123** yielded the corresponding regioisomeric adducts (3:1 ratio). Only the major regioisomer **159** (Scheme 71) was isolated and characterized. A NOE effect between H-2 of Ts and the contiguous -CH₂- group was observed and confirmed the structure of **159**. This result indicates that less-nucleophilic pyridine containing NAMPT inhibitors can be incorporated into OND systems. Therefore, once the cross-reactivity of pyridine has been overtaken, the preparation of NAMPT inhibitor-based ADCs using ONDs as innovative linkers could be achieved. This strategy is being currently investigated in our group.



Scheme 71. Attempted DA reactions on cytotoxic compounds **138** and **139**.

2.4 EXPERIMENTAL PART

Scheme 72. Synthesis of (pyridin-4-yl)cyanoguanidine-based inhibitor **74**.**4-Cyano-N-cyclopentyl-N-(furan-2-ylmethyl)benzenesulfonamide (70)**

To a solution of **37a** (1.3 g, 7.8 mmol) in 45 mL of dry CH_2Cl_2 at 0°C under argon, Et_3N (2.2 mL, 16 mmol) and 4-cyanobenzenesulfonyl chloride (3.2 g, 16 mmol) in dry CH_2Cl_2 (30 mL) were added dropwise. The mixture was stirred overnight at r.t. The reaction mixture was washed with water (50 mL x 2) and brine (2x 50 mL), dried over anh. Na_2SO_4 and concentrated *in vacuo*. The resulting residue was purified by flash chromatography ($\text{Et}_2\text{O}:\text{Cy}$, 1:2) to give **70** (2.1 g, 80%) as a white solid. ^1H NMR (300 MHz, CDCl_3 , δ ppm) 7.86 – 7.61 (m, 4H, Ph), 7.25 – 7.09 (m, 1H, furan), 6.35 – 6.19 (m, 2H, furan), 4.41 (s, 2H, CH_2 -furan), 4.31 – 4.13 (m, 1H, CH Cyclopentyl), 1.84 – 1.70 (m, 2H, CH_2 Cyclopentyl), 1.69 – 1.43 (m, 6H, 3 CH_2 Cyclopentyl). ^{13}C NMR (75.4 MHz, CDCl_3 , δ ppm) 150.5 (qC, furan), 145.4 (qC, Ph), 142.0 (CH, furan), 132.5 (2 CH, Ph), 127.5 (2 CH, Ph), 117.4 (CN), 115.7 (qC, Ph), 110.6 (CH, furan), 109.5 (CH, furan), 59.5 (CH, Cyclopentyl), 40.1 (CH_2 -furan), 29.5 (2 CH_2 , Cyclopentyl), 23.4 (2 CH_2 , Cyclopentyl). ESI-HRMS m/z calcd for $\text{C}_{17}\text{H}_{18}\text{N}_2\text{O}_3\text{SNa}$ $[\text{M}+\text{Na}]^+$, 353.0930; found, 353.0927.

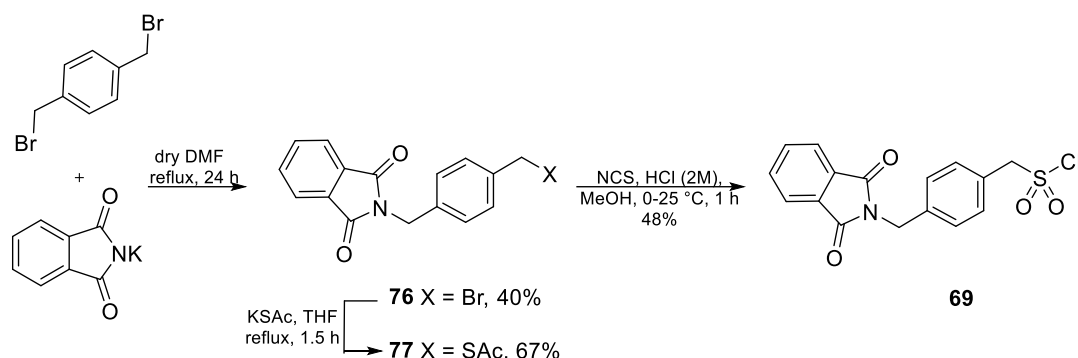
4-(Aminomethyl)-N-cyclopentyl-N-(furan-2-ylmethyl)benzenesulfonamide (72)

A suspension of LiAlH₄ (903 mg, 23.8 mmol) in dry THF (17.7 mL) was cooled at 0 °C. Then, compound **70** (1.97 g, 5.95 mmol) in dry THF (55 mL) was added dropwise under N₂. The mixture was stirred for 30 min at 0 °C. Then, a sat. aq. soln. of Na₂SO₄ was added slowly under vigorous stirring until a white solid was precipitated. After stirring at 20 °C for 10 min, the suspension was filtered on a celite pad, washed with THF, and the solvent evaporated *in vacuo*. The resulting residue was purified by flash chromatography (NH₄OH:MeOH:CH₂Cl₂, 0.1:1:15) to give **72** (1.19 g, 48%) as a light brown oil. ¹H NMR (300 MHz, CDCl₃, δ ppm) 7.69 (d, *J* = 8.4 Hz, 2H, Ph), 7.40 (d, *J* = 8.4 Hz, 2H, Ph), 7.28 (br s, 1H, furan), 6.32 – 6.25 (m, 2H, furan), 4.37 (s, 2H, CH₂-furan), 4.18 (quint, *J* = 8.4 Hz, 1H, Cyclopentyl), 3.95 (s, 2H, CH₂-NH₂), 1.89 (br s, 2H, NH₂), 1.79 – 1.35 (m, 8H, 4 CH₂ Cyclopentyl). ¹³C NMR (75.4 MHz, CDCl₃, δ ppm) 151.7 (qC, furan), 147.4 (qC, Ph), 141.7 (CH, furan), 139.3 (qC, Ph), 127.4 (2 CH, Ph), 127.3 (2 CH, Ph), 110.6 (CH, furan), 108.7 (CH, furan), 59.1 (CH, Cyclopentyl), 45.8 (CH₂-furan), 40.2 (CH₂-NH₂), 29.2 (2 CH₂, Cyclopentyl), 23.4 (2 CH₂, Cyclopentyl). ESI-HRMS *m/z* calcd for C₁₇H₂₂N₂O₃S [M+H]⁺, 335.1424; found, 335.1421.

(*E*)-4-((2-Cyano-3-(pyridin-4-yl)guanidino)methyl)-*N*-cyclopentyl-*N*-(furan-2-ylmethyl)benzenesulfonamide (74**)**

To a solution of compound **46a** (30 mg, 0.12 mmol) in dry MeCN:DMF (2 mL, 3:1), compound **72** (48 mg, 0.14 mmol), Et₃N (48 μL, 0.34 mmol) and DMAP (3 mg, 40 μmol) were added, and the mixture was stirred and heated at 80 °C under argon for 16 h. The reaction mixture was concentrated *in vacuo* and the residue was purified by flash chromatography on silica gel (MeOH:EtOAc, 1:10) to yield **74** (50 mg, 83%) as a white solid. ¹H NMR (300 MHz, DMSO-*d*₆, δ ppm) 9.68 (br s, 1H, NH-Py), 8.49 – 8.27 (m, 3H, 2H Py, NH-CH₂), 7.77 (d, *J* = 8.4 Hz, 2H, Ph), 7.56 – 7.53 (m, 1H, furan), 7.50 (d, *J* = 8.3 Hz, 2H, Ph), 7.29 – 7.08 (m, 2H, Py), 6.43 – 6.35 (m, 1H, furan), 6.34 – 6.25 (m, 1H, furan), 4.57 – 4.55 (m, 2H, CH₂-NH), 4.35 (s, 2H, CH₂-furan), 4.10 (quint, *J* = 8.1 Hz, 1H, CH cyclopentyl), 1.58 – 1.22 (m, 8H, 4 CH₂ cyclopentyl). ¹³C NMR (75.4 MHz, DMSO-*d*₆, δ ppm) 157.8 (C=N), 151.7 (qC, furan), 149.8 (2 CH, Py), 143.2 (2 qC, Py, Ph), 142.2

(CH, furan), 138.9 (qC, Ph), 127.9 (2 CH, Ph), 127.0 (2 CH, Ph), 116.2 (C≡N), 115.0 (2 CH, Py), 110.6 (CH, furan), 108.3 (CH, furan), 58.6 (CH, cyclopentyl), 44.6 (CH₂-NH), 39.9 (CH₂-Furan), 28.4 (2 CH₂, cyclopentyl), 22.9 (2 CH₂, cyclopentyl). ESI-HRMS *m/z* calcd for C₂₄H₂₇N₆O₃S [M+H]⁺, 479.1860; found, 479.1850.



Scheme 73. Synthesis of sulfonyl chloride **69**.

2-(4-(Bromomethyl)benzyl)isoindoline-1,3-dione (**76**)¹⁶⁵

Phthalimide potassium salt (1.0 g, 5.5 mmol) was suspended in dry DMF (6.5 mL) and 1,4-bis(bromomethyl)benzene (2.1 g, 8.1 mmol) was added. The suspension was refluxed for 24 h under argon and the solvent was evaporated under vacuum. The residue was suspended in water (20 mL) and was extracted with EtOAc (3x20 mL). The combined organic phases were dried over Na₂SO₄, filtered, and concentrated *in vacuo*. The crude product was purified by column chromatography on silica gel (EtOAc:Cy, 1:5→1:3) to provide **76** (700 mg, 40%) as a white solid. ¹H NMR (300 MHz, CDCl₃, δ ppm) 7.84 (dd, *J* = 5.7, 3.0 Hz, 2H), 7.71 (dd, *J* = 5.7, 3.0 Hz, 2H), 7.46 - 7.35 (d, *J* = 8.1 Hz, 2H), 7.28 - 7.18 (d, *J* = 8.1 Hz, 2H), 4.80 (s, 2H), 4.40 (s, 2H). ¹H NMR data match with those previously reported for this compound.

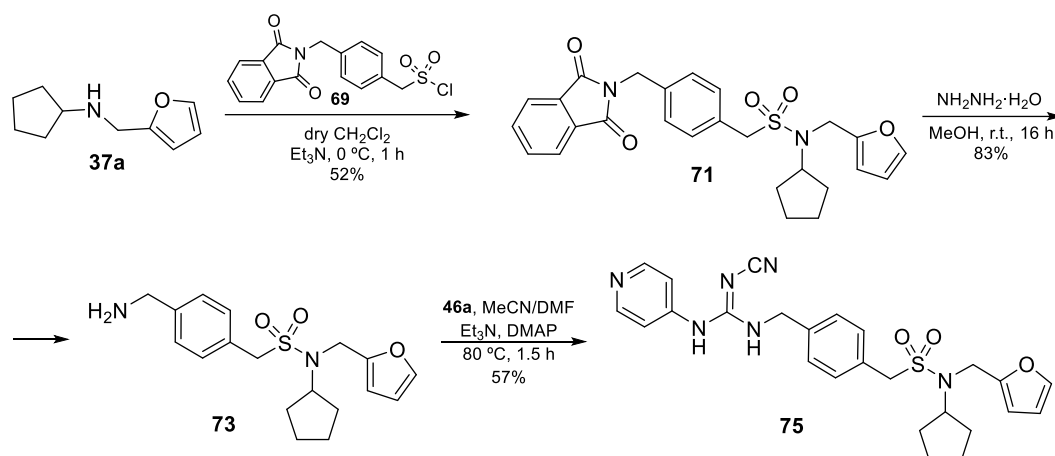
S-(4-((1,3-Dioxoisoindolin-2-yl)methyl)benzyl) ethanethioate (**77**)

To a stirred solution of **76** (422 mg, 1.3 mmol) in THF (16 mL), potassium thioacetate (460 mg, 3.7 mmol) was added in small portions during 20 min and the mixture was refluxed for 1.5 h. Then, the solvent was evaporated *in vacuo*, the resulting residue

was suspended in H₂O and extracted with EtOAc (3x). The combined organic phases were washed with brine, dried over anh. Na₂SO₄ and concentrated in *vacuo*. The crude product was purified by flash chromatography on silica gel (EtOAc:Cy, 1:4) to give **77** (287 mg, 67%) as a white solid. ¹H NMR (300 MHz, CDCl₃, δ ppm) 7.84 (dd, *J* = 5.9, 3.3 Hz, 2H, Phth), 7.70 (dd, *J* = 5.9, 3.3 Hz, 2H, Phth), 7.36 (d, *J* = 8.4 Hz, 2H, Ph), 7.23 (d, *J* = 8.4 Hz, 2H, Ph), 4.82 (s, 2H, CH₂-N), 4.09 (s, 2H, CH₂-S), 2.30 (s, 3H, CH₃). ¹³C NMR (75.4 MHz, CDCl₃, δ ppm) 194.9 (C=O), 167.9 (2 C=O), 137.3 (qC, Phth), 135.4 (qC, Ph), 134.0 (2 CH, Phth), 132.1 (qC, Ph), 129.1 (2 CH, Ph), 128.9 (2 CH, Ph), 123.3 (2 CH, Phth), 41.2 (CH₂-N), 33.1 (CH₂-S), 30.3 (CH₃). ESI-HRMS *m/z* calcd for C₁₈H₁₅NO₃SNa [M+Na]⁺, 348.0665; found, 348.0663.

(4-((1,3-Dioxoisindolin-2-yl)methyl)phenyl)methanesulfonyl chloride (69)

2M HCl (0.5 mL) solution was added to a stirred solution of **77** (287 mg, 0.9 mmol) in MeCN (5 mL) at 0 °C. NCS (507 mg, 3.8 mmol) was added in small portions over 30 min and the reaction mixture was warmed to r.t. and stirred for 1 h. The reaction mixture was quenched with ice-cold water (6 mL) and extracted with Et₂O (x 2). The combined organic layers were washed with sat. aq. soln. of NaHCO₃, H₂O and brine. Then, the organic phase was dried over anh. Na₂SO₄ and concentrated to afford **69** as a white solid that was used in the next step without further purification. ¹H NMR (300 MHz, CDCl₃, δ ppm) 7.85 (dd, *J* = 5.4, 3.0 Hz, 2H), 7.72 (dd, *J* = 5.4, 3.0 Hz, 2H), 7.52 (d, *J* = 8.1 Hz, 2H), 7.43 (d, *J* = 8.4 Hz, 2H), 4.87 (s, 2H), 4.82 (s, 2H).



Scheme 74. Synthesis of (pyridin-4-yl)cyanoguanidine-based inhibitor **75**.

***N*-Cyclopentyl-1-(4-((1,3-dioxoisindolin-2-yl)methyl)phenyl)-*N*-(furan-2-yl)methyl)methanesulfonamide (**71**)**

To a suspension of **37a** (51 mg, 0.3 mmol) in dry CH₂Cl₂ (2 mL), Et₃N (0.12 mL, 0.83 mmol) under argon at 0 °C was added and the mixture was stirred over 3 Å MS. Then, compound **69** (130 mg, 0.37 mmol) in dry CH₂Cl₂ (2 mL) was added over 1 h and the resulting mixture stirred for 1 h at 0 °C. The reaction mixture was quenched with water (15 mL) and extracted with CH₂Cl₂ (15 mL x 3). The combined organic layers were washed with brine, dried over anh. Na₂SO₄ and concentrated. The crude product was purified by flash chromatography on silica gel (EtOAc:Toluene, 1:8) to give **71** (77 mg, 52%) as a white solid. ¹H NMR (300 MHz, CDCl₃, δ ppm) 7.84 (dd, *J* = 5.4, 3.3 Hz, 2H, Phth), 7.71 (dd, *J* = 5.4, 3.3 Hz, 2H, Phth), 7.44-7.34 (m, 2H Ph, 1H furan), 7.17 (d, *J* = 8.4 Hz, 2H, Ph), 6.38 - 6.30 (m, 2H, furan), 4.83 (s, 2H, CH₂-NPhth), 4.25 (s, 2H, CH₂SO₂), 3.98 (s, 2H, CH₂-furan), 3.83 - 3.65 (m, 1H, CH cyclopentyl), 1.70-1.45 (m, 4H, 2 CH₂ cyclopentyl), 1.40-1.31 (m, 4H, 2 CH₂ cyclopentyl). ¹³C NMR (75.4 MHz, CDCl₃, δ ppm) 167.9 (C=O), 151.1 (qC, furan), 142.1 (CH, furan), 136.7 (qC, Phth), 135.1 (qC, Ph), 134.0 (2 CH, Phth), 132.0 (qC, Ph), 129.8 (2 CH, Ph), 128.4 (2 CH, Ph), 123.3 (2 CH, Phth), 110.8 (CH, furan), 109.5 (CH, furan), 60.4 (CH, cyclopentyl), 59.3

(CH₂SO₂), 41.2 (CH₂-NPhth), 39.8 (CH₂-furan), 29.8 (2 CH₂, cyclopentyl), 23.3 (2 CH₂, cyclopentyl).

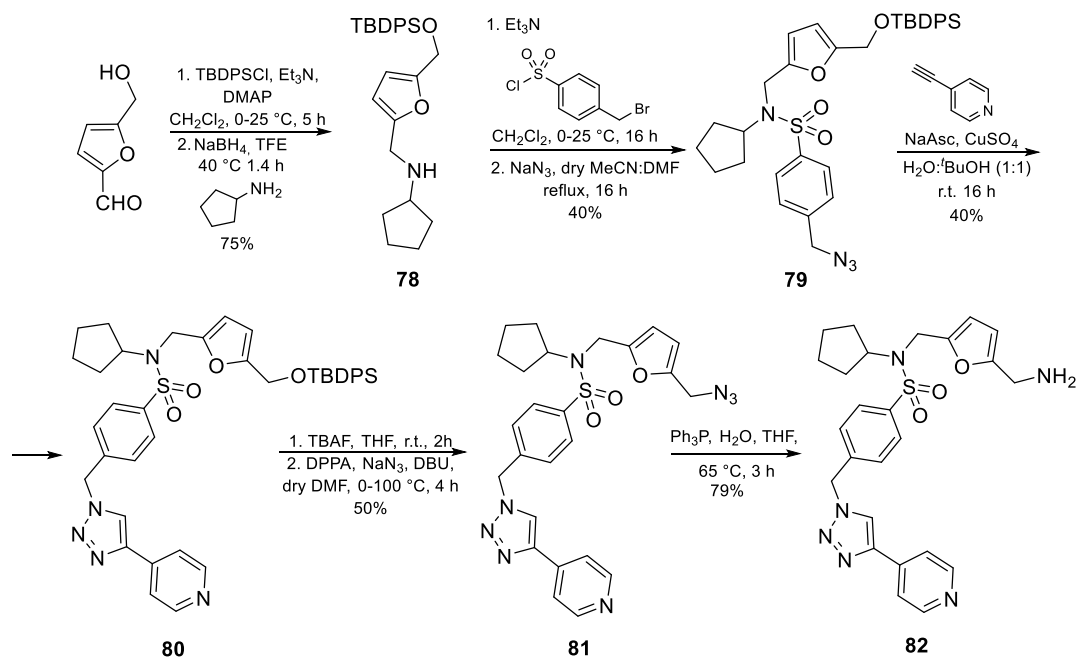
1-(4-(Aminomethyl)phenyl)-N-cyclopentyl-N-(furan-2-ylmethyl)-methanesulfonamide (73)

To a stirred solution of **71** (77 mg, 0.2 mmol) in MeOH (2 mL), NH₂NH₂ (46 μL, 1.0 mmol) was added at 0°C and stirred for 3h. The reaction mixture was warmed to r.t. and stirred overnight. The white precipitate was filtered off and washed with MeOH (20 mL). The solvent was evaporated *in vacuo* and the crude product was dissolved in 2M HCl (10 mL) and washed with Et₂O (x3). The aqueous layer was basified with sat. aq. soln. of NaOH to pH=8 and extracted with EtOAc (10 mL x 3). The organic layers were collected and dried over anh. Na₂SO₄ and concentrated *in vacuo* to yield **73** as a yellow oil (83%). This compound was used in the next step without purification.

(E)-1-(4-((2-Cyano-3-(pyridin-4-yl)guanidino)methyl)phenyl)-N-cyclopentyl-N-(furan-2-ylmethyl)methanesulfonamide (75)

To a solution of compound **46a** (28 mg, 0.12 mmol) in dry MeCN:DMF (3 mL, 3:1), compound **73** (45 mg, 0.13 mmol), Et₃N (48 μL, 0.34 mmol) and DMAP (3 mg, 30 μmol) were added, and the mixture was stirred and heated at 80 °C under argon for 1.5 h. The reaction mixture was concentrated *in vacuo* and the residue was purified by flash chromatography on silica gel (MeOH:EtOAc, 1:8) to yield **75** (26 mg, 57%) as a white solid. ¹H NMR (300 MHz, DMSO-*d*₆, δ ppm) 9.50 (br s, 1H, NH-Py), 8.45 - 8.30 (m, 3H, 2H Py, NH-CH₂), 7.66 - 7.58 (m, 1H, furan), 7.34 - 7.29 (m, 4H, Ph), 7.20 (br s, 2H, Py), 6.45 - 6.37 (m, 1H, furan), 6.35 - 6.27 (m, 1H, furan), 4.57 - 4.55 (m, CH₂-NH), 4.26 (s, 2H, CH₂SO₂), 4.24 (s, 2H, CH₂-furan), 3.89 (quint, *J* = 8.1 Hz, 1H, CH cyclopentyl), 1.70-1.30 (m, 8H, 4 CH₂ cyclopentyl). ¹³C NMR (75.4 MHz, DMSO-*d*₆, δ ppm) 157.4 (C=N), 151.7 (qC, furan), 150.1 (2 CH, Py), 145.7 (qC, Py), 142.4 (CH, furan), 138.1 (qC, Ph), 130.8 (2CH, Ph), 128.6 (qC, Ph), 127.2 (2CH, Ph), 116.2 (C≡N), 114.8 (2 CH, Py), 110.7

(CH, furan), 108.6 (CH, furan), 58.9 (CH, cyclopentyl), 57.0 (CH₂SO₂), 44.7 (CH₂-NH), 35.7 (CH₂-furan), 29.8 (2 CH₂, cyclopentyl), 22.9 (2 CH₂, cyclopentyl). ESI-HRMS *m/z* calcd for C₂₅H₂₉N₆O₃S [M+H]⁺, 493.2015; found, 493.2012.



Scheme 75. Synthetic strategy for the preparation of final compound 82.

***N*-((5-(((*tert*-Butyldiphenylsilyl)oxy)methyl)furan-2-yl)methyl)cyclopentanamine (78)**

To a solution of 5-hydroxymethylfurfural (2 g, 16 mmol) in dry CH₂Cl₂ (60 mL) at 0 °C, TBDPSCI (5.4 mL, 20.9 mmol), Et₃N (2.9 mL, 20.6 mmol) and DMAP (194 mg, 1.6 mmol) were added. The reaction was warmed up to r.t. and stirred for 5 h. The mixture was washed with water (2x) and brine (2x). The organic layer was dried over Na₂SO₄, filtered, and evaporated. The resulting residue (15.9 mmol) was dissolved in trifluoroethanol (30 mL) and was stirred at 40 °C for 10 min. Then, cyclopentylamine (1.3 mL, 13.2 mmol) was added, and the mixture was vigorously stirred for 1 h at 40 °C. After this time, NaBH₄ (995 mg, 26 mmol) was added, and the solution was additionally stirred for 30 min at 40 °C. The mixture was filtered, and the residue was

washed with EtOH (50 mL), and the filtrate dried under high *vacuum*. The crude product was purified by flash chromatography (Et₃N:EtOAc:Cy, 0.1:3:6) to yield **78** (4.3 g, 75%) as a yellow oil. ¹H NMR (300 MHz, CDCl₃, δ ppm) 7.75 – 7.63 (m, 4H, Ph), 7.49 – 7.34 (m, 6H, Ph), 6.09 – 5.99 (m, 2H, furan), 4.62 (s, 2H, CH₂-OTBDPS), 3.71 (s, 2H, CH₂-NH), 3.08 (quint, *J* = 6.6 Hz, 1H, CH cyclopentyl), 1.89 – 1.76 (m, 2H, CH₂ cyclopentyl), 1.76 – 1.45 (m, 4H, 2 CH₂ cyclopentyl), 1.43 – 1.24 (m, 2H, CH₂ cyclopentyl), 1.05 (s, 9H, C(CH₃)₃). ¹³C NMR (75.4 MHz, CDCl₃, δ ppm) 153.9 (qC, Ph), 153.3 (qC, Ph), 135.8 (4 CH, Ph), 133.6 (qC, furan), 129.8 (2 CH, Ph), 127.8 (4 CH, Ph), 108.1 (CH, furan), 107.4 (CH, furan), 59.1 (CH₂-OTBDPS), 58.8 (CH, cyclopentyl), 45.2 (CH₂-NH), 33.2 (2 CH₂, cyclopentyl), 26.9 (C(CH₃)₃), 24.3 (2 CH₂, cyclopentyl), 19.4 (qC, C(CH₃)₃). ESI-HRMS *m/z* calcd for C₂₇H₃₆NO₂Si [M+H]⁺, 434.2503; found, 434.2510.

4-(Azidomethyl)-N-((5-(((*tert*-butyldiphenylsilyl)oxy)methyl)furan-2-yl)methyl)-N-cyclopentylbenzenesulfonamide (79)

To a solution of **78** (4.0 g, 9.2 mmol) in dry CH₂Cl₂ (65 mL) at 0 °C under argon, Et₃N (1.3 mL, 9.2 mmol) and 4-bromobenzenesulfonyl chloride (1.9 g, 7.1 mmol) were added, and the mixture was stirred at r.t. overnight. The reaction mixture was evaporated, dissolved in Et₂O, washed with 1M HCl (3x), H₂O and brine. The organic phase was dried over anhydrous Na₂SO₄, filtered and concentrated under reduced pressure. The crude (5.9 mmol) was dissolved in dry MeCN:DMF (75 mL, 15:1) and NaN₃ (1.1 g, 16.7 mmol) was added. The reaction mixture was heated under reflux for 24 h. The solvent was evaporated, and the mixture was diluted with H₂O and extracted with Et₂O (3x). The organic phases were combined, washed with water (3x), dried over anhydrous Na₂SO₄, filtered and the solvent was removed under vacuum. The resulting residue was purified by flash chromatography (EtOAc:Cy, 1:4) to give **79** (1.74 g, 40%) as a colourless oil. ¹H NMR (300 MHz, CDCl₃, δ ppm) 7.76 – 7.63 (m, 6H, Ph), 7.48 – 7.35 (m, 6H, Ph), 7.35 – 7.28 (m, 2H, Ph), 6.19 (d, *J* = 3.1 Hz, 1H, furan), 6.06 (d, *J* = 3.1 Hz, 1H, furan), 4.51 (s, 2H, CH₂-OTBDPS), 4.35 (s, 2H, CH₂-NSO₂Ar), 4.32 (s, 2H, CH₂-N₃), 4.20 (quint, *J* = 8.7 Hz, 1H, CH cyclopentyl), 1.79 – 1.64 (m, 2H, CH₂

cyclopentyl), 1.65 – 1.54 (m, 2H, CH₂ cyclopentyl), 1.54 – 1.39 (m, 4H, 2 CH₂ cyclopentyl), 1.05 (s, 9H, C(CH₃)). ¹³C NMR (75.4 MHz, CDCl₃, δ ppm) 153.5 (2 qC, Ph), 150.9 (qC, furan), 141.1 (qC, Ph), 139.9 (qC, Ph), 135.7 (4 CH, Ph), 133.5 (qC, furan), 129.9 (2 CH, Ph), 128.3 (4 CH, Ph), 127.8 (2 CH, Ph), 127.7 (2 CH, Ph), 109.8 (CH, furan), 108.5 (CH, furan), 59.3 (CH, cyclopentyl), 58.9 (CH₂-OTBDPS), 54.1 (CH₂-N₃), 40.4 (CH₂-NSO₂Ar), 29.5 (2 CH₂, cyclopentyl), 26.9 (C(CH₃)₃), 23.6 (2 CH₂, cyclopentyl), 19.4 (qC, C(CH₃)₃). ESI-HRMS *m/z* calcd for C₃₄H₄₀N₄O₄SSi [M+Na]⁺, 651.2426; found, 651.2432.

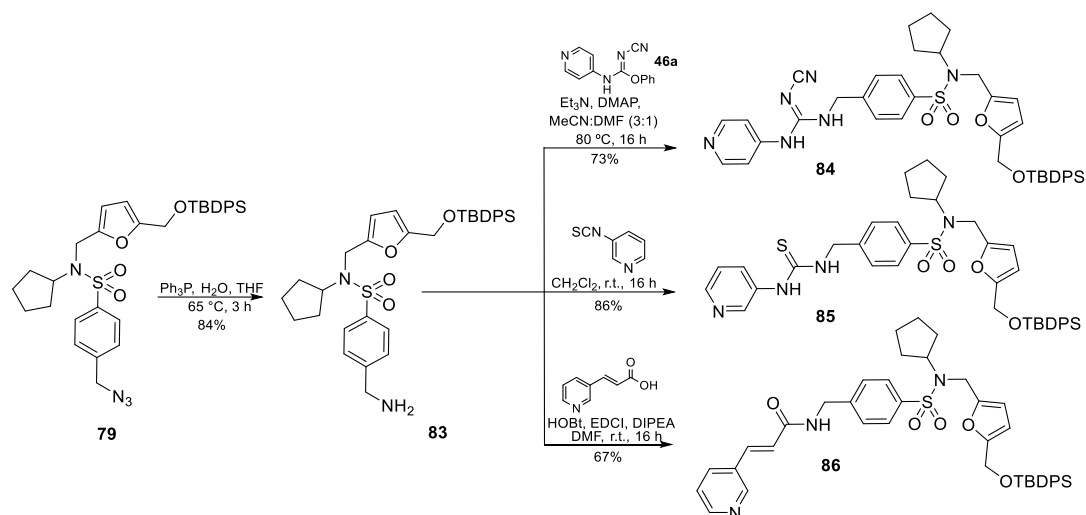
***N*-((5-(((*tert*-Butyldiphenylsilyl)oxy)methyl)furan-2-yl)methyl)-*N*-cyclopentyl-4-((4-(pyridin-4-yl)-1H-1,2,3-triazol-1-yl)methyl)benzenesulfonamide (80)**

To a suspension of azide **79** (200 mg, 300 μmol) and 4-ethynylpyridine (53 mg, 500 μmol) in a mixture of water/*tert*-butanol (1:1) (4 mL), sodium ascorbate (13 mg, 64 μmol) in water (0.25 mL), and CuSO₄ pentahydrate (2 mg, 7 μmol) in water (0.25 mL) were added to the mixture. The resulting solution was vigorously stirred at r.t. overnight. The reaction mixture was concentrated *in vacuo* and the crude was purified by flash chromatography (NH₄OH:MeOH:Et₂O, 0.01:0.5:10) to give **80** (90 mg, 40%) as a colourless oil. ¹H NMR (300 MHz, CDCl₃, δ ppm) 8.63 (br s, 2H, Py), 7.76 (s, 1H, triazole), 7.73 – 7.60 (m, 8H, 6H Ph, 2H Py), 7.47 – 7.32 (m, 6H, Ph), 7.29 – 7.20 (m, 2H, Ph), 6.17 (d, *J* = 3.2 Hz, 1H, furan), 6.04 (d, *J* = 3.1 Hz, 1H, furan), 5.50 (s, 2H, CH₂-triazole), 4.50 (s, 2H, CH₂-OTBDPS), 4.33 (s, 2H, CH₂-NSO₂Ar), 4.16 (quint, *J* = 8.7 Hz, 1H, CH cyclopentyl), 1.78 – 1.65 (m, 2H, CH₂ cyclopentyl), 1.65 – 1.54 (m, 2H, CH₂ cyclopentyl), 1.54 – 1.38 (m, 4H, 2 CH₂ cyclopentyl), 1.03 (s, 9H, C(CH₃)₃). ¹³C NMR (75.4 MHz, CDCl₃, δ ppm) 153.5 (2 qC, Ph), 150.8 (2 CH, Py), 150.6 (qC, furan), 146.0 (qC, triazole), 141.9 (qC, Ph), 138.6 (qC, Ph), 137.7 (qC, Py), 135.7 (4 CH, Ph), 133.4 (qC, furan), 129.9 (2 CH, Ph), 128.3 (4 CH, Ph), 128.0 (2 CH, Ph), 127.8 (2 CH, Ph), 121.3 (CH, triazole), 120.1 (2 CH, Py), 109.8 (CH, furan), 108.6 (CH, furan), 59.4 (CH, cyclopentyl), 58.9 (CH₂-OTBDPS), 53.6 (CH₂-triazole), 40.4 (CH₂-NSO₂Ar), 29.5 (2 CH₂, cyclopentyl), 26.8 (C(CH₃)₃), 23.5 (2 CH₂, cyclopentyl), 19.4 (qC, C(CH₃)₃). ESI-HRMS *m/z* calcd for C₄₁H₄₆N₅O₄SSi [M+H]⁺, 732.3033; found, 732.3034.

***N*-((5-(Aminomethyl)furan-2-yl)methyl)-*N*-cyclopentyl-4-((4-(pyridin-4-yl)-1H-1,2,3-triazol-1-yl)methyl)benzenesulfonamide (**82**)**

To a solution of **80** (90 mg, 109 μmol) in THF (2 mL), TBAF in THF (1M, 160 μL , 160 μmol) was added and the mixture was stirred at r.t. for 2 h. The solvent was removed under reduced pressure and the residue (109 μmol) was dissolved in dry DMF (1 mL) at 0 °C under N_2 . Then, DPPA (72 μL , 0.3 mmol) and DBU (50 μL , 0.3 mmol) were added dropwise. After 30 min of stirring, NaN_3 (22 mg, 0.3 mmol) was added, and the mixture was additionally stirred for 4 h at 100 °C. The solvent was evaporated *in vacuo*, the crude was dissolved in EtOAc, and the organic phase was washed with water and brine, dried over Na_2SO_4 , filtered, and concentrated *in vacuo*. The crude was purified by flash chromatography ($\text{NH}_4\text{OH}:\text{MeOH}:\text{CH}_2\text{Cl}_2$, 0.1:1:10) to yield **81** (31 mg, 50%) as colourless oil. ^1H NMR (300 MHz, CDCl_3 , δ ppm) 8.67 – 8.59 (m, 2H), 7.93 (s, 1H), 7.74 – 7.65 (m, 4H), 7.37 – 7.30 (m, 2H), 6.23 (d, $J = 3.3$ Hz, 1H), 6.19 (d, $J = 3.2$ Hz, 1H), 5.63 (s, 2H), 4.34 (s, 2H), 4.18 (quint, $J = 8.8$ Hz, 1H), 4.09 (s, 2H), 1.79 – 1.66 (m, 2H), 1.66 – 1.54 (m, 2H), 1.54 – 1.36 (m, 4H). ESI-HRMS m/z calcd for $\text{C}_{25}\text{H}_{27}\text{N}_8\text{O}_3\text{S}$ $[\text{M}+\text{H}]^+$, 519.1916; found, 519.1921. To a solution of **81** (30 mg, 58 μmol) in THF (1.0 mL), H_2O (10 μL) and Ph_3P (23 mg, 90 μmol) were added, and the reaction mixture was stirred at 65 °C for 3 h. The resulting residue was evaporated under vacuum and purified by flash chromatography ($\text{NH}_4\text{OH}:\text{MeOH}:\text{EtOAc}$, 0.1:1:5) to yield **82** (22 mg, 79%) as a white solid. ^1H NMR (300 MHz, CD_3OD , δ ppm) 8.67 (s, 1H, triazole), 8.61 – 8.54 (m, 2H, Py), 7.91 – 7.84 (m, 2H, Py), 7.79 (d, $J = 8.4$ Hz, 2H, Ph), 7.50 (d, $J = 8.5$ Hz, 2H, Ph), 6.24 – 6.14 (m, 2H, furan), 5.79 (s, 2H, CH_2 -triazole), 4.38 (s, 2H, CH_2 - NSO_2Ar), 4.21 (quint, $J = 8.4$ Hz, 1H, CH cyclopentyl), 3.72 (s, 2H, CH_2 - NH_2), 1.73 – 1.53 (m, 4H, 2 CH_2 cyclopentyl), 1.53 – 1.37 (m, 4H, 2 CH_2 cyclopentyl). ^{13}C NMR (75.4 MHz, CD_3OD , δ ppm) 154.3 (qC, Ph), 152.7 (qC, furan), 150.8 (2 CH, Py), 146.4 (qC, triazole), 142.4 (qC, Py), 141.4 (qC, furan), 140.3 (2 qC, furan, Ph), 129.7 (2 CH, Ph), 128.9 (2 CH, Ph), 124.8 (CH, triazole), 121.5 (2 CH, Py), 110.6 (CH, furan), 108.8 (CH, furan), 60.7 (CH, cyclopentyl), 54.3 (CH_2 -triazole), 41.3 (CH_2 - NSO_2Ar), 38.7

(CH₂-NH₂), 30.2 (2 CH₂, cyclopentyl), 24.4 (2 CH₂, cyclopentyl). ESI-HRMS *m/z* calcd for C₂₅H₂₉N₆O₃S [M+H]⁺, 493.2012; found, 493.2016.



Scheme 76. Synthetic strategy for the preparation of intermediates **84-86**.

4-(Aminomethyl)-N-((5-(((tert-butyl-diphenylsilyl)oxy)methyl)furan-2-yl)methyl)-N-cyclopentylbenzenesulfonamide (**83**)

To a solution of **79** (1.0 g, 1.6 mmol) in THF (6 mL), H₂O (0.17 mL) and Ph₃P (626 mg, 2.39 mmol) were added. The reaction mixture was stirred at 65 °C for 3 h. The resulting residue was evaporated under vacuum and purified by flash chromatography (NH₄OH:MeOH:Et₂O, 0.1:1:9) to yield **83** (805 mg, 84%) as a white solid. ¹H NMR (300 MHz, CDCl₃, δ ppm) 7.76 – 7.59 (m, 6H), 7.50 – 7.28 (m, 8H), 6.21 (d, *J* = 3.2 Hz, 1H), 6.07 (d, *J* = 3.1 Hz, 1H), 4.56 – 4.50 (m, 2H), 4.35 – 4.28 (m, 2H), 4.26 – 4.12 (m, 1H), 3.85 (s, 2H), 1.79 – 1.63 (m, 2H), 1.63 – 1.53 (m, 2H), 1.53 – 1.38 (m, 4H), 1.04 (s, 9H). ESI-HRMS *m/z* calcd for C₃₄H₄₃N₂O₄SSi [M+H]⁺, 603.2712; found, 603.2707.

(*E*)-N-((5-(((tert-Butyl-diphenylsilyl)oxy)methyl)furan-2-yl)methyl)-4-((2-cyano-3-(pyridin-4-yl)guanidino)methyl)-N-cyclopentylbenzenesulfonamide (**84**)

To a solution of compound **46a** (198 mg, 830 μmol) in dry MeCN:DMF (8 mL, 3:1), amine **83** (600 mg, 995 μmol), Et₃N (0.3 mL, 2.3 mmol) and DMAP (21 mg, 174 μmol) were added, and the mixture was stirred and heated at 80 °C under argon overnight. The reaction mixture was concentrated under vacuum and the residue was purified by flash chromatography (MeOH:EtOAc, 1:9) to give **84** (454 mg, 73%) as a white solid. ¹H NMR (300 MHz, CDCl₃, δ ppm) 8.34 (d, J = 5.9 Hz, 2H, Py), 7.71 – 7.63 (m, 4H, Ph), 7.57 (d, J = 8.4 Hz, 2H, Ph), 7.46 – 7.32 (m, 6H, Ph), 7.27 (d, J = 8.2 Hz, 2H, Ph), 7.10 (d, J = 6.0 Hz, 2H, Py), 6.62 (br s, 1H, NH-CH₂), 6.15 (d, J = 3.2 Hz, 1H, furan), 6.05 (d, J = 3.1 Hz, 1H, furan), 4.59 – 4.43 (m, 4H, CH₂-NH, CH₂-OTBDPS), 4.26 (s, 2H, CH₂-NSO₂Ar), 4.11 (quint, J = 7.1 Hz, 1H, CH cyclopentyl), 1.72 – 1.51 (m, 4H, 2 CH₂ cyclopentyl), 1.51 – 1.33 (m, 4H, 2 CH₂ cyclopentyl), 1.03 (s, 9H, C(CH₃)₃). ¹³C NMR (75.4 MHz, CDCl₃, δ ppm) 158.0 (C=N), 153.5 (2 qC, Ph), 150.9 (qC, furan), 150.8 (2 CH, Py), 144.8 (qC, Py), 141.6 (qC, Ph), 140.3 (qC, Ph), 135.7 (4 CH, Ph), 133.4 (qC, furan), 129.9 (2 CH, Ph), 128.0 (2 CH, Ph), 127.8 (4 CH, Ph), 127.6 (2 CH, Ph), 116.9 (C \equiv N), 116.3 (2 CH, Py), 109.6 (CH, furan), 108.6 (CH, furan), 59.3 (CH, cyclopentyl), 58.9 (CH₂-OTBDPS), 45.5 (CH₂-NH), 40.4 (CH₂-NSO₂Ar), 29.3 (2 CH₂, cyclopentyl), 26.8 (C(CH₃)₃), 23.5 (2 CH₂, cyclopentyl), 19.3 (qC, C(CH₃)₃). ESI-HRMS m/z calcd for C₄₁H₄₇N₆O₄SSi [M+H]⁺, 747.3154; found, 747.3143.

***N*-((5-(((*tert*-Butyldiphenylsilyl)oxy)methyl)furan-2-yl)methyl)-*N*-cyclopentyl-4-((3-(pyridin-3-yl)thioureido)methyl)benzenesulfonamide (85)**

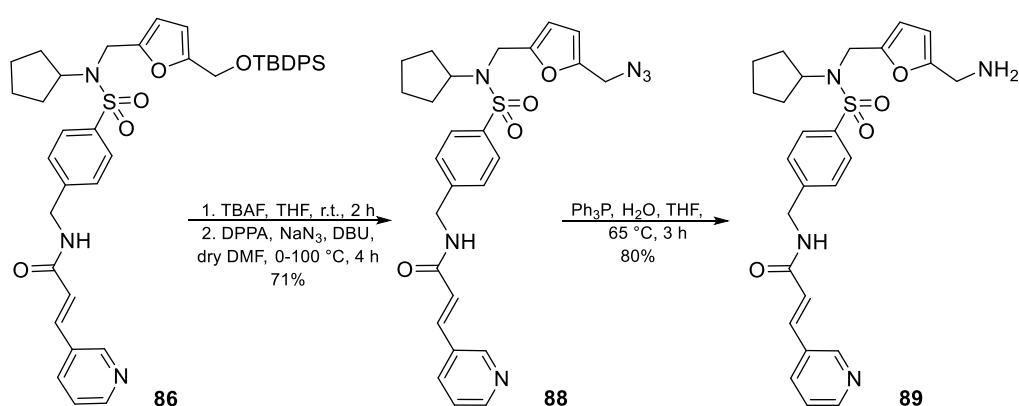
To a solution of **83** (500 mg, 830 μmol) in anhydrous CH₂Cl₂ (20 mL), 3-Pyridyl isothiocyanate (230 μL , 2 mmol) and Et₃N (290 μL , 2 mmol) were added. After stirring at r.t. for 16 h, the solvent was removed under *vacuo* and the resulting residue was purified by flash chromatography (Acetone:Et₂O, 1:5) to give **85** (524 mg, 86%) as a white solid. ¹H NMR (300 MHz, CDCl₃, δ ppm) 8.49 – 8.44 (m, 1H, Py), 8.43 – 8.37 (m, 1H, Py), 8.08 (br s, 1H, NH-Py), 7.89 – 7.79 (m, 1H, Py), 7.74 – 7.60 (m, 4H, Ph), 7.60 – 7.48 (m, 2H, Ph), 7.48 – 7.33 (m, 6H, Ph), 7.33 – 7.19 (m, 3H, 2H Ph, 1H Py), 6.89 – 6.72 (m, 1H, NH-CH₂), 6.14 (d, J = 3.2 Hz, 1H, furan), 6.04 (d, J = 3.1 Hz, 1H, furan),

4.86 (d, $J = 5.6$ Hz, 2H, $\underline{\text{C}}\text{H}_2\text{-NH}$), 4.52 (s, 2H, $\text{CH}_2\text{-OTBDPS}$), 4.27 (s, 2H, $\text{CH}_2\text{-NSO}_2\text{Ar}$), 4.19 – 4.04 (m, 1H, CH cyclopentyl), 1.74 – 1.53 (m, 4H, 2 CH_2 cyclopentyl), 1.53 – 1.34 (m, 4H, 2 CH_2 cyclopentyl), 1.03 (s, 9H, $\text{C}(\underline{\text{C}}\text{H}_3)_3$). ^{13}C NMR (75.4 MHz, CDCl_3 , δ ppm) 182.3 (C=S), 153.6 (2 qC, Ph), 150.8 (qC, furan), 147.4 (CH, Py), 146.1 (CH, Py), 142.6 (qC, Ph), 139.7 (qC, Ph), 135.7 (4 CH, Ph), 134.4 (qC, Py), 133.5 (qC, furan), 132.5 (CH, Py), 129.9 (2 CH, Ph), 128.1 (2 CH, Ph), 127.8 (4 CH, Ph), 127.4 (2 CH, Ph), 124.1 (CH, Py), 109.6 (CH, furan), 108.6 (CH, furan), 59.4 (CH, cyclopentyl), 58.9 ($\underline{\text{C}}\text{H}_2\text{-OTBDPS}$), 48.3 ($\text{CH}_2\text{-NH}$), 40.5 ($\text{CH}_2\text{-NSO}_2\text{Ar}$), 29.4 (2 CH_2 , cyclopentyl), 26.9 ($\text{C}(\underline{\text{C}}\text{H}_3)_3$), 23.5 (2 CH_2 , cyclopentyl), 19.4 (qC, $\underline{\text{C}}(\text{CH}_3)_3$). ESI-HRMS m/z calcd for $\text{C}_{40}\text{H}_{47}\text{N}_4\text{O}_4\text{S}_2\text{Si}$ [$\text{M}+\text{H}$] $^+$, 739.2800; found, 739.2803.

(*E*)-*N*-(4-(*N*-((5-(((*tert*-Butyldiphenylsilyl)oxy)methyl)furan-2-yl)methyl)-*N*-cyclopentylsulfamoyl)benzyl)-3-(pyridin-3-yl)acrylamide (86**)**

Under N_2 atmosphere, HOBt hydrate (99 mg, 700 μmol), EDCI (128 mg, 800 μmol) and (*E*)-3-(3-pyridyl)acrylic acid (100 mg, 700 μmol) were added sequentially to a cooled solution of **83** (268 mg, 400 μmol) in dry CH_2Cl_2 (3 mL). After stirring at 0 °C for 10 min *N*-methyilmorpholine (140.0 μL , 1.2 mmol) was added dropwise under stirring. The mixture was then warmed to r.t. and was stirred overnight. A sat. aq. sol. of NaHCO_3 (6 mL) was added and stirred vigorously for 5 min. The aqueous layer was extracted with CH_2Cl_2 (x3). The combined organic extracts were washed with brine and dried over anh. Na_2SO_4 . The solvent was evaporated in *vacuo* and the residue was purified by flash chromatography (Acetone:Et₂O, 1:5) to give **86** (220 mg, 67%) as a white solid. ^1H NMR (300 MHz, CDCl_3 , δ ppm) 8.72 – 8.64 (m, 1H, Py), 8.58 – 8.50 (m, 1H, Py), 7.81 – 7.72 (m, 1H, Py), 7.71 – 7.56 (m, 7H, $\text{CH}=\underline{\text{C}}\text{H}\text{-Py}$, 6H Ph), 7.47 – 7.33 (m, 6H, Ph), 7.33 – 7.26 (m, 3H, 1H Py, 2H Ph), 6.62 – 6.43 (m, 2H, $\text{CH}=\underline{\text{C}}\text{H}\text{-CO}$, $\text{NH}\text{-CH}_2$), 6.19 (d, $J = 3.1$ Hz, 1H, furan), 6.05 (d, $J = 3.1$ Hz, 1H, furan), 4.63 – 4.44 (m, 4H, $\text{CH}_2\text{-OTBDPS}$, $\underline{\text{C}}\text{H}_2\text{-NH}$), 4.30 (s, 2H, $\text{CH}_2\text{-NSO}_2\text{Ar}$), 4.23 – 4.05 (m, 1H, CH cyclopentyl), 1.76 – 1.61 (m, 2H, CH_2 cyclopentyl), 1.61 – 1.51 (m, 2H, CH_2 cyclopentyl), 1.51 – 1.35 (m, 4H, 2 CH_2 cyclopentyl), 1.03 (s, 9H, $\text{C}(\underline{\text{C}}\text{H}_3)_3$). ^{13}C NMR (75.4 MHz, CDCl_3 , δ ppm)

165.4 (C=O), 153.5 (2 qC, Ph), 151.1 (qC, furan), 150.4 (CH, Py), 149.1 (CH, Py), 143.1 (qC, Ph), 140.0 (qC, Ph), 138.1 (CH=C_H-Py), 135.7 (4 CH, Ph), 134.8 (CH, Py), 133.5 (qC, furan), 130.8 (qC, Py), 129.9 (2 CH, Ph), 128.1 (2 CH, Ph), 127.8 (4 CH, Ph), 127.5 (2 CH, Ph), 123.9 (CH, Py), 122.6 (CH=C_H-CO), 109.6 (CH, furan), 108.6 (CH, furan), 59.3 (CH, cyclopentyl), 58.9 (C_H2-OTBDPS), 43.2 (CH₂-NH), 40.4 (CH₂-NSO₂Ar), 29.4 (2 CH₂, cyclopentyl), 26.9 (C(CH₃)₃), 23.5 (2 CH₂, cyclopentyl), 19.4 (qC, C(CH₃)₃). ESI-HRMS m/z calcd for C₄₂H₄₈N₃O₅Si [M+H]⁺, 734.3084; found, 734.3078.

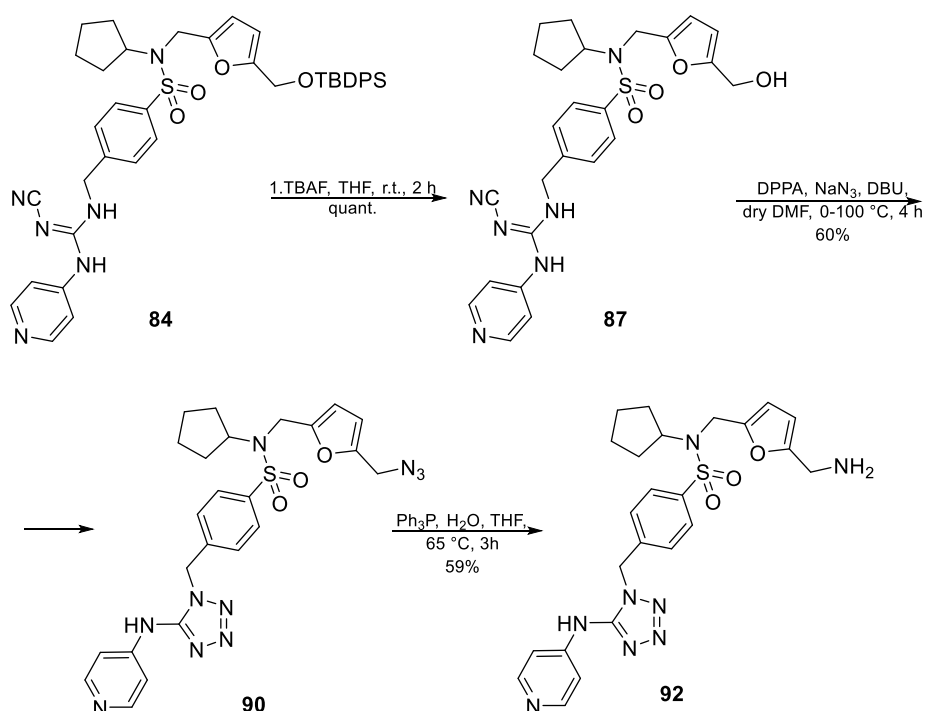


Scheme 77. Synthesis of furfurylamine derivative **89**.

(E)-N-(4-(N-((5-(Azidomethyl)furan-2-yl)methyl)-N-cyclopentylsulfamoyl)benzyl)-3-(pyridin-3-yl)acrylamide (89**)**

To a solution of **86** (199 mg, 271 μ mol) in THF (4.4 mL), TBAF 1M in THF (350 μ L, 350 μ mol) was added. After stirring at r.t. for 2 h, the solvent was removed under reduced pressure and the resulting residue (271 μ mol) was dissolved in dry DMF (3 mL) at 0 °C under N₂, and DPPA (160 μ L, 700 μ mol) and DBU (110 μ L, 730 μ mol) were added dropwise. NaN₃ (47 mg, 730 μ mol) was added after 30 min and the mixture was stirred for 4 h at 100 °C. The solvent was evaporated in *vacuo*, the crude was dissolved in EtOAc and was washed with water and brine. The organic phase was dried over anh. Na₂SO₄, filtered and concentrated in *vacuo*. The crude was purified by flash chromatography (Acetone:Et₂O, 2:5) to yield **88** (100 mg, 71%) as a colourless oil. ESI-HRMS m/z calcd for C₂₆H₂₉N₆O₄S [M+H]⁺, 521.1962; found, 521.1966. To a solution of

88 (100 mg, 192 μmol) in THF (3 mL), H_2O (21 μL) and Ph_3P (76 mg, 290 μmol) were added. The reaction mixture was stirred at 65 $^\circ\text{C}$ for 1 h. After evaporation under *vacuum*, the resulting residue was purified by flash chromatography ($\text{NH}_4\text{OH}:\text{MeOH}:\text{EtOAc}$, 0.1:2:10) to yield **89** (76 mg, 80%) as a sticky white solid. ^1H NMR (300 MHz, CD_3OD , δ ppm) 8.79 – 8.67 (m, 1H, Py), 8.57 – 8.47 (m, 1H, Py), 8.13 – 8.00 (m, 1H, Py), 7.78 – 7.69 (m, 2H, Ph), 7.62 (d, $J = 16.0$ Hz, 1H, $\text{CH}=\underline{\text{C}}\text{H-Py}$), 7.53 – 7.42 (m, 3H, 1H Py, 2H Ph), 6.80 (d, $J = 15.9$ Hz, 1H, $\text{CH}=\underline{\text{C}}\text{H-CO}$), 6.19 (d, $J = 3.2$ Hz, 1H, furan), 6.12 (d, $J = 3.2$ Hz, 1H, furan), 4.58 (s, 2H, $\text{CH}_2\text{-Ph}$), 4.39 (s, 2H, $\text{CH}_2\text{SO}_2\text{Ar}$), 4.21 (quint, $J = 7.9$ Hz, 1H, CH cyclopentyl), 3.64 (s, 2H, $\underline{\text{C}}\text{H}_2\text{-NH}_2$), 1.72 – 1.55 (m, 4H, 2 CH_2 cyclopentyl), 1.55 – 1.36 (m, 4H, 2 CH_2 cyclopentyl). ^{13}C NMR (75.4 MHz, CD_3OD , δ ppm) 167.8 (C=O), 156.6 (qC, Ph), 152.1 (qC, furan), 150.9 (CH, Py), 149.8 (CH, Py), 145.1 (qC, Ph), 141.1 (qC, Ph), 138.2 ($\text{CH}=\underline{\text{C}}\text{H-Py}$), 136.3 (CH, Py), 132.8 (2 qC, furan, Ph), 129.0 (2 CH Ph, 1qC Py), 128.5 (2 CH, Ph), 125.5 (CH, Py), 124.4 ($\text{CH}=\underline{\text{C}}\text{H-CO}$), 110.4 (CH, furan), 107.5 (CH, furan), 60.6 (CH, cyclopentyl), 43.8 ($\underline{\text{C}}\text{H}_2\text{-Ph}$), 41.3 ($\text{CH}_2\text{SO}_2\text{Ar}$), 39.3 ($\text{CH}_2\text{-NH}_2$), 30.1 (2 CH_2 , cyclopentyl), 24.4 (2 CH_2 , cyclopentyl). ESI-HRMS m/z calcd for $\text{C}_{26}\text{H}_{29}\text{N}_6\text{O}_4\text{S}$ [$\text{M}+\text{H}$] $^+$, 495.2060; found, 495.2061.



Scheme 78. Synthesis of furfurylamine derivative **92**.

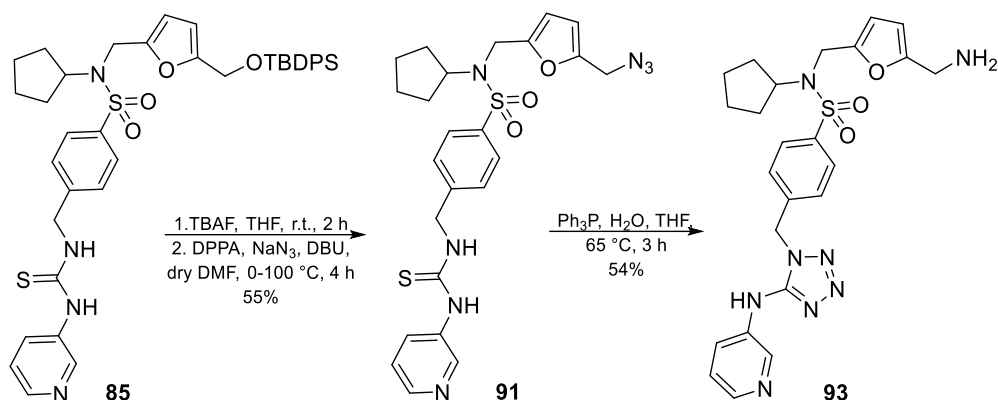
(E)-4-((2-Cyano-3-(pyridin-4-yl)guanidino)methyl)-N-cyclopentyl-N-((5-(hydroxymethyl)furan-2-yl)methyl)benzenesulfonamide (87**)**

To a solution of **84** (132 mg, 177 μmol) in THF (2.9 mL), TBAF 1M in THF (230 μL , 230 μmol) was added. After stirring at r.t. for 2 h, the solvent was removed under reduced pressure and the resulting residue was purified by column chromatography on silica gel (MeOH:EtOAc, 1:5) to yield **87** (89 mg, 99%) as a white solid. ^1H NMR (300 MHz, CD_3OD , δ ppm) 8.49 – 8.24 (m, 2H, Py), 7.85 – 7.67 (m, 2H, Ph), 7.59 – 7.42 (m, 2H, Ph), 7.37 – 7.21 (m, 2H, Py), 6.30 – 6.10 (m, 2H, furan), 4.64 (s, 2H, $\text{CH}_2\text{-NH}$), 4.40 (s, 4H, $\text{CH}_2\text{-OH}$, $\text{CH}_2\text{-NSO}_2\text{Ar}$), 4.19 (quint, $J = 8.5$ Hz, 1H, CH cyclopentyl), 1.71 – 1.55 (m, 4H, 2 CH_2 cyclopentyl), 1.55 – 1.38 (m, 4H, 2 CH_2 cyclopentyl). ^{13}C NMR (75.4 MHz, CD_3OD , δ ppm) 159.7 (C=N), 155.6 (qC, furan), 152.8 (qC, furan), 150.5 (2 CH, Py), 144.1 (qC, Ph), 141.3 (qC, Ph), 129.1 (2 CH, Ph), 128.6 (2 CH, Ph), 117.4 (C \equiv N), 116.7 (2 CH, Py), 110.4 (CH, furan), 109.3 (CH, furan), 60.6 (CH, cyclopentyl), 57.3 ($\text{CH}_2\text{-OH}$),

46.2 (CH₂-NH), 41.3 (CH₂-NSO₂Ar), 30.1 (2 CH₂, cyclopentyl), 24.4 (2 CH₂, cyclopentyl). ESI-HRMS *m/z* calcd for C₂₅H₂₉N₆O₄S [M+H]⁺, 509.1960; found, 509.1966.

***N*-((5-(Aminomethyl)furan-2-yl)methyl)-*N*-cyclopentyl-4-((5-(pyridin-4-ylamino)-1H-tetrazol-1-yl)methyl)benzenesulfonamide (92)**

To a solution of **87** (89 mg, 180 μmol) in dry DMF (2 mL) at 0 °C under N₂, DPPA (115 μL, 520 μmol) and DBU (80 μL, 520 μmol) were added dropwise. NaN₃ (34 mg, 520 μmol) was added after 30 min and the mixture was stirred for 4 h at 100 °C. The solvent was evaporated *in vacuo*, the crude was dissolved in EtOAc, and the organic phase was washed with water and brine. The solvent was dried over anh. Na₂SO₄, filtered and concentrated *in vacuo*. The crude was purified by flash chromatography (MeOH:EtOAc, 1:9) to yield **90** (56 mg, 60%) as a colourless oil. ESI-HRMS *m/z* calcd for C₂₄H₂₇N₁₀O₃S [M+H]⁺, 535.1976; found, 535.1983. To a solution of compound **90** (56 mg, 105 μmol) in THF (2.0 mL), H₂O (12 μL) and Ph₃P (42 mg, 160 μmol) were added. The reaction mixture was stirred at 65 °C for 3 h. After evaporation under vacuum, the resulting residue was purified by flash chromatography (NH₄OH:MeOH:EtOAc, 0.1:2:10) to yield **92** (31 mg, 59%) as a white solid. ¹H NMR (300 MHz, CD₃OD, δ ppm) 8.30 – 8.15 (m, 2H, Py), 7.80 – 7.70 (m, 2H, Ph), 7.61 – 7.49 (m, 2H, Py), 7.43 – 7.32 (m, 2H, Ph), 6.15 (d, *J* = 3.2 Hz, 1H, furan), 6.08 (d, *J* = 3.2 Hz, 1H, furan), 5.68 (s, 2H, CH₂-tetrazole), 4.36 (s, 2H, CH₂-NSO₂Ar), 4.19 (quint, *J* = 8.1 Hz, 1H, CH cyclopentyl), 3.61 (s, 2H, CH₂-NH₂), 1.70 – 1.51 (m, 4H, 2 CH₂ cyclopentyl), 1.51 – 1.33 (m, 4H, 2 CH₂ cyclopentyl). ¹³C NMR (75.4 MHz, CD₃OD, δ ppm) 156.2 (qC, tetrazole), 154.9 (qC, Py), 152.0 (qC, furan), 148.0 (2 CH Py, 1 qC furan), 142.3 (qC, Ph), 140.8 (qC, Ph), 129.1 (2 CH, Ph), 128.8 (2 CH, Ph), 113.9 (2 CH, Py), 110.5 (CH, furan), 107.6 (CH, furan), 60.6 (CH, cyclopentyl), 49.5 (CH₂-tetrazole), 41.3 (CH₂-NSO₂Ar), 39.2 (CH₂-NH₂), 30.1 (2 CH₂, cyclopentyl), 24.4 (2 CH₂, cyclopentyl). ESI-HRMS *m/z* calcd for C₂₄H₂₉N₈O₃S [M+H]⁺, 509.2074; found, 509.2078.

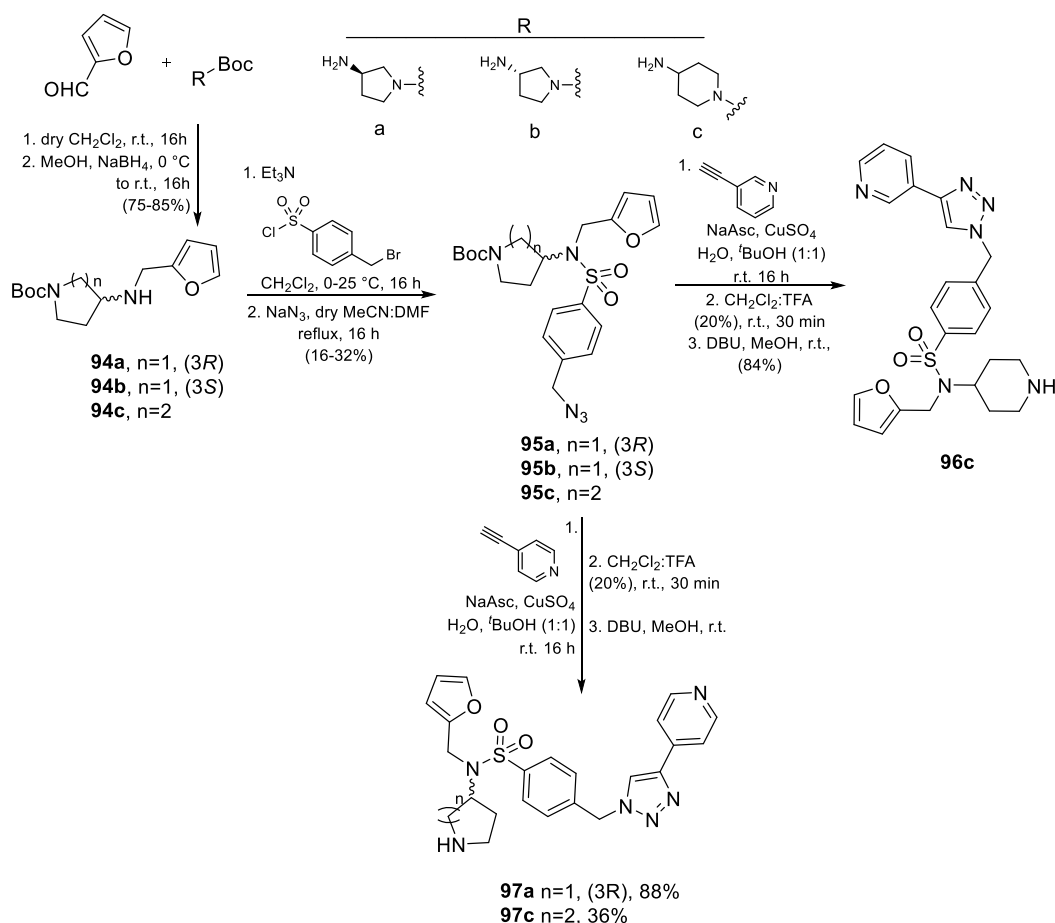


Scheme 79. Synthesis of furfurylamine derivative **93**.

***N*-((5-(Aminomethyl)furan-2-yl)methyl)-*N*-cyclopentyl-4-((5-(pyridin-3-ylamino)-1H-tetrazol-1-yl)methyl)benzenesulfonamide (**93**)**

To a solution of **85** (524 mg, 709 μmol) in THF (12 mL), TBAF in THF (1M, 922 μL , 922 μmol) was added. After stirring at r.t. for 1 h, the solvent was removed under reduced pressure and the resulting residue (709 μmol) was dissolved in dry DMF (8.5 mL) at 0 °C under N_2 , and DPPA (440 μL , 2 mmol) and DBU (310 μL , 2 mmol) were added dropwise. NaN_3 (132 mg, 2 mmol) was added after 30 min and the mixture was stirred for 4 h at 100 °C. The solvent was evaporated in *vacuo*, the crude was dissolved in EtOAc, and the organic phase was washed with water and brine. The solvent was dried over anh. Na_2SO_4 and concentrated in *vacuo*. The crude was purified by flash chromatography (Acetone:Et₂O, 1:1) to yield **91** (192 mg, 55%) as a colourless oil. ESI-HRMS m/z calcd for $\text{C}_{24}\text{H}_{27}\text{N}_{10}\text{O}_3\text{S}$ $[\text{M}+\text{H}]^+$, 535.1980; found, 535.1983. To a solution of **91** (160 mg, 300 μmol) in THF (6 mL), H_2O (30 μL) and Ph_3P (118 mg, 449 μmol) were added. The reaction mixture was stirred at 65 °C for 1 h. After evaporation under vacuum, the resulting residue was purified by flash chromatography ($\text{NH}_4\text{OH}:\text{MeOH}:\text{EtOAc}$, 0.1:1:9) to yield **93** (82 mg, 54%) as a white solid. ^1H NMR (300 MHz, CD_3OD , δ ppm) 8.86 – 8.71 (m, 1H, Py), 8.28 – 8.14 (m, 2H, Py), 7.88 – 7.77 (m, 2H, Ph), 7.50 – 7.38 (m, 3H, 1H Py, 2H Ph), 6.45 (d, $J = 3.3$ Hz, 1H, furan), 6.31 (d, $J = 3.3$ Hz, 1H, furan), 5.77 (s, 2H, CH_2 -tetrazole), 4.39 (s, 2H, CH_2 -NSO₂Ar), 4.20 (quint, J

= 8.1 Hz, 1H, CH cyclopentyl), 4.09 (s, 2H, CH₂-NH₂), 1.67 – 1.47 (m, 4H, 2 CH₂ cyclopentyl), 1.47 – 1.33 (m, 4H, 2 CH₂ cyclopentyl). ¹³C NMR (75.4 MHz, CD₃OD, δ ppm) 155.0 (qC, tetrazole), 154.1 (qC, Py), 147.5 (qC, furan), 144.0 (2 CH Py, 1 qC furan), 141.9 (qC, Ph), 140.9 (qC, Ph), 140.5 (CH, Py), 129.3 (2 CH, Ph), 128.9 (2 CH, Ph), 127.2 (2 CH, Py), 125.5 (CH, Py), 112.9 (CH, furan), 110.8 (CH, furan), 60.7 (CH, cyclopentyl), 49.5 (CH₂-tetrazole), 41.4 (CH₂-NSO₂Ar), 36.9 (CH₂-NH₂), 30.1 (2 CH₂, cyclopentyl), 24.4 (2 CH₂, cyclopentyl). ESI-HRMS *m/z* calcd for C₂₄H₂₈N₈O₃Na [M+Na]⁺, 531.1893; found, 531.1897.



Scheme 80. Synthesis of the final compounds **96c**, **97a** and **97c**.

***tert*-Butyl-(S)-3-((furan-2-ylmethyl)amino)pyrrolidine-1-carboxylate (**94a**)**

A solution of furfural (900 μ L, 11 mmol) and *tert*-butyl-(*S*)-3-aminopyrrolidine-1-carboxylate (1.8 mL, 11 mmol) was stirred in dry CH_2Cl_2 (25 mL) over molecular sieves 3 Å at r.t. for 24 h. The reaction mixture was concentrated in *vacuo* and the residue dissolved in CH_3OH (25 mL). NaBH_4 (823 mg, 22 mmol) was added to the mixture at 0°C. The reaction was warmed to r.t. and stirred overnight. The solvent was removed, and the residue suspended in water and extracted with EtOAc (3x). The organic phases were extracted with 1M HCl (3x), and the aq. phases were adjusted to pH 10 with a sat. aq. sol. of NaOH. The aq. phase was extracted with EtOAc (3x), and the organic phases were washed with H_2O , brine and dried over anh. Na_2SO_4 . The solvent was filtered, and evaporated to obtain **94a** (2.46 g, 85%) as a yellow oil that was used in the next step without further purification. ^1H NMR (300 MHz, CDCl_3 , δ ppm, mixture of rotamers) 7.40 – 7.30 (m, 2H, furan), 6.35 – 6.23 (m, 2H, furan), 6.23 – 6.10 (m, 2H, furan), 3.78 (s, 4H, 2 CH_2 -furan), 3.60 – 3.38 (m, 4H, 1 CH_2 pyrrolidine rotamer A, 1 CH_2 pyrrolidine rotamer B), 3.38 – 3.21 (m, 4H, CH_2 pyrrolidine rotamer B, CH pyrrolidine rotamer A, CH pyrrolidine rotamer B), 3.20 – 2.95 (m, 2H, CH_2 pyrrolidine rotamer B), 2.11 – 1.91 (m, 2H, CH_2 pyrrolidine rotamer A), 1.78 – 1.62 (m, 2H, CH_2 pyrrolidine rotamer B), 1.57 (br s, 2H, 2 NH), 1.44 (s, 18H, 2 Boc). ^{13}C NMR (75.4 MHz, CDCl_3 , δ ppm, mixture of rotamers) 154.7, 153.6, 142.1, 110.3, 107.2, 79.3, 56.9, 56.0, 52.0, 51.4, 44.7, 44.5, 44.2, 32.1, 31.4, 28.6. ESI-HRMS m/z calcd for $\text{C}_{14}\text{H}_{23}\text{N}_2\text{O}_3$ $[\text{M}+\text{H}]^+$, 267.1706; found, 267.1703.

***tert*-Butyl-(*R*)-3-((furan-2-ylmethyl)amino)pyrrolidine-1-carboxylate (94b)**

The synthesis of **94b** followed the same procedure as **94a**, except that the starting material was *tert*-butyl-(*R*)-3-aminopyrrolidine-1-carboxylate. Yield= 85%, orange oil. Compound **94b** showed NMR spectra identical to those of its enantiomer **94a**. ESI-HRMS m/z calcd for $\text{C}_{14}\text{H}_{23}\text{N}_2\text{O}_3$ $[\text{M}+\text{H}]^+$, 267.1705; found, 267.1703.

4-[(Furan-2-ylmethyl)amino]piperidin-1-carboxylic acid *tert*-butyl ester (94c)¹⁶⁶

The synthesis of **94c** followed the same procedure as **94a**, except that the starting material was *tert*-butyl 4-amino-1-piperidinecarboxylate. Yield= 75%, colourless oil. ^1H NMR (300 MHz, CDCl_3 , δ ppm) 7.42 – 7.31 (m, 1H), 6.36 – 6.24 (m, 1H), 6.21 – 6.07 (m, 1H), 4.01 (br d, 2H), 3.81 (s, 2H), 2.86 – 2.70 (m, 2H), 2.70 – 2.55 (m, 1H), 1.91 – 1.70 (m, 2H), 1.44 (s, 9H), 1.36 – 1.17 (m, 2H). ^1H NMR data match with those previously reported for this compound.

***tert*-Butyl-(S)-3-((4-(azidomethyl)-N-(furan-2-ylmethyl)phenyl)sulfonamido)pyrrolidine-1-carboxylate (95a)**

To a solution of **94a** (635 mg, 2.4 mmol) in dry CH_2Cl_2 (17 mL) at 0 °C under argon, Et_3N (330 μL , 2.4 mmol) and 4-(bromomethyl)benzenesulfonyl chloride (494 mg, 1.8 mmol) were added and the mixture was stirred at r.t. overnight. The reaction mixture was evaporated, dissolved in EtOAc, washed with 1M HCl (3x), H_2O and brine (3x), dried over anhydrous Na_2SO_4 , filtered and concentrated under reduced pressure. The residue (327 mg, 720 μmol) was dissolved in dry MeCN:DMF (8.5 mL, 15:1). NaN_3 (120 mg, 1.9 mmol) was added, and the mixture was heated under reflux for 24 h. The solvent was evaporated, and the mixture was diluted with 5 mL of H_2O and extracted with EtOAc (3x). The combined organic extracts were washed with water (3x), dried over anhydrous Na_2SO_4 , filtered and the solvent was removed under *vacuum*. The resulting residue was purified by flash chromatography (EtOAc:Cy, 1:3) to give **95a** (210 mg, 19%) as a colourless oil. ^1H NMR (300 MHz, CDCl_3 , δ ppm, mixture of rotamers) 7.68 (d, $J = 8.3$ Hz, 4H, Ph), 7.38 (d, $J = 7.9$ Hz, 4H, Ph), 7.28 – 7.21 (m, 2H, furan), 6.36 – 6.20 (m, 4H, furan), 4.54 – 4.30 (m, 10H, 2 CH_2 -furan, 2 CH_2 - N_3 , CH pyrrolidine rotamer A, CH pyrrolidine rotamer B) 3.56 – 3.35 (m, 4H, CH_2 pyrrolidine rotamer A, 1 CH_2 pyrrolidine rotamer B), 3.36 – 3.04 (m, 4H, CH_2 pyrrolidine rotamer A, CH_2 pyrrolidine rotamer B), 2.08 – 1.87 (m, 4H, CH_2 pyrrolidine rotamer A, CH_2 pyrrolidine rotamer B), 1.42 (s, 18H, 2 Boc). ^{13}C NMR (75.4 MHz, CDCl_3 , δ ppm, mixture of rotamers) 154.3, 150.4, 142.4, 140.5, 140.3, 128.5, 127.6, 110.7, 109.4, 79.8, 56.2, 54.0, 48.0, 46.9,

44.0, 43.7, 40.5, 29.6, 28.5, 28.4. ESI-HRMS m/z calcd for $C_{21}H_{27}N_5O_5Na$ $[M+Na]^+$, 484.1627; found, 484.1625.

***tert*-Butyl-(*R*)-3-((4-(azidomethyl)-*N*-(furan-2-ylmethyl)phenyl)sulfonamido)pyrrolidine-1-carboxylate (**95b**)**

The synthesis of **95b** followed the same procedure as **95a**, except that the starting material was **94b**. Yield= 16%, colourless oil. Compound **95b** showed NMR spectra identical to those of its enantiomer **95a**. ESI-HRMS m/z calcd for $C_{21}H_{27}N_5O_5Na$ $[M+Na]^+$, 484.1627; found, 484.1625.

***tert*-Butyl-4-((4-(azidomethyl)-*N*-(furan-2-ylmethyl)phenyl)sulfonamido)piperidine-1-carboxylate (**95c**)**

The synthesis of **95c** followed the same procedure as **95a**, except that the starting material was **94c**. Yield= 32%, yellow oil. 1H NMR (300 MHz, $CDCl_3$, δ ppm) 7.74 – 7.61 (m, 2H, Ph), 7.43 – 7.31 (m, 2H, Ph), 7.31 – 7.18 (m, 1H, furan), 6.36 – 6.15 (m, 2H, furan), 4.41 (s, 4H, CH_2-N_3 , CH_2 -furan), 4.23 – 3.97 (m, 2H, CH_2 piperidine), 3.81 (quint, $J = 8.1$ Hz, 1H, CH piperidine), 2.75 – 2.51 (m, 2H, CH_2 piperidine), 1.64 – 1.48 (m, 4H, 2 CH_2 piperidine), 1.42 (s, 9H, $C(CH_3)_3$). ^{13}C NMR (75.4 MHz, $CDCl_3$, δ ppm) 154.6 (C=O), 150.7 (qC, furan), 142.2 (CH, furan), 141.2 (qC, Ph), 140.1 (qC, Ph), 128.5 (2 CH, Ph), 127.5 (2 CH, Ph), 110.7 (CH, furan), 109.5 (CH, furan), 79.9 ($C(CH_3)_3$), 56.5 (CH, piperidine), 54.0 (CH_2-N_3), 43.62 (2 CH_2 , piperidine), 39.9 (CH_2 -furan), 30.6 (2 CH_2 , piperidine), 28.5 ($C(CH_3)_3$). ESI-HRMS m/z calcd for $C_{22}H_{29}N_5O_5SNa$ $[M+Na]^+$, 498.1777; found, 498.1782.

***N*-(Furan-2-ylmethyl)-*N*-(piperidin-4-yl)-4-((4-(pyridin-3-yl)-1H-1,2,3-triazol-1-yl)methyl)benzenesulfonamide (**96c**)**

Compound **95c** (95 mg, 200 μ mol) and 3-ethynylpyridine (66 mg, 640 μ mol) were suspended in a 1:1 mixture of water/*tert*-butanol (3 mL). Sodium ascorbate (16 mg,

80 μmol), and CuSO_4 pentahydrate (1 mg, 4 μmol) in water (0.5 mL) were added and the mixture was stirred at r.t. overnight. The solvent was concentrated *in vacuo*, the crude (68 mg, 120 μmol) was dissolved in 20% TFA/ CH_2Cl_2 (250 μL TFA, 1 mL CH_2Cl_2) at 0 °C and the mixture was stirred at 0 °C for 1 h. The solvent was evaporated, and the residue was dissolved in MeOH, DBU was added and was stirred for 1 min. Then, the mixture was evaporated, and the resulting residue was purified by flash chromatography ($\text{NH}_4\text{OH}:\text{MeOH}:\text{EtOAc}$, 0.1:1:2) to give **96c** (47 mg, 84%) as a white solid. ^1H NMR (300 MHz, CD_3OD , δ ppm) 9.08 – 8.91 (m, 1H, Py), 8.54 (s, 1H, triazole), 8.50 (dd, $J = 4.9, 1.6$ Hz, 1H, Py), 8.26 (dt, $J = 8.0, 1.9$ Hz, 1H, Py), 7.84 – 7.66 (m, 2H, Ph), 7.57 – 7.41 (m, 3H, 1H Py, 2H Ph), 7.37 – 7.23 (m, 1H, furan), 6.33 – 6.20 (m, 2H, furan), 5.75 (s, 2H, CH_2 -triazole), 4.45 (s, 2H, CH_2 -furan), 3.77 (tt, $J = 11.9, 4.1$ Hz, 1H, CH piperidine), 2.96 (d, $J = 12.6$ Hz, 2H, CH_2 piperidine), 2.50 (td, $J = 12.5, 2.7$ Hz, 2H, CH_2 piperidine), 1.61 (qd, $J = 12.2, 4.1$ Hz, 2H, CH_2 piperidine), 1.54 – 1.41 (m, 2H, CH_2 piperidine). ^{13}C NMR (75.4 MHz, CD_3OD , δ ppm) 152.6 (qC, furan), 149.7 (CH, Py), 147.3 (CH, Py), 145.9 (qC, triazole), 143.3 (CH, furan), 142.9 (qC, Ph), 141.4 (qC, Ph), 134.9 (CH, Py), 129.7 (2 CH, Ph), 128.7 (2 CH, Ph), 128.5 (qC, Py), 125.6 (CH, Py), 123.5 (CH, triazole), 111.5 (CH, furan), 110.2 (CH, furan), 57.7 (CH, piperidine), 54.3 (CH_2 -triazole), 46.7 (2 CH_2 , piperidine), 40.9 (CH_2 -furan), 32.3 (2 CH_2 , piperidine). ESI-HRMS m/z calcd for $\text{C}_{24}\text{H}_{27}\text{N}_6\text{O}_3\text{S}$ $[\text{M}+\text{H}]^+$, 479.1859; found, 479.1860.

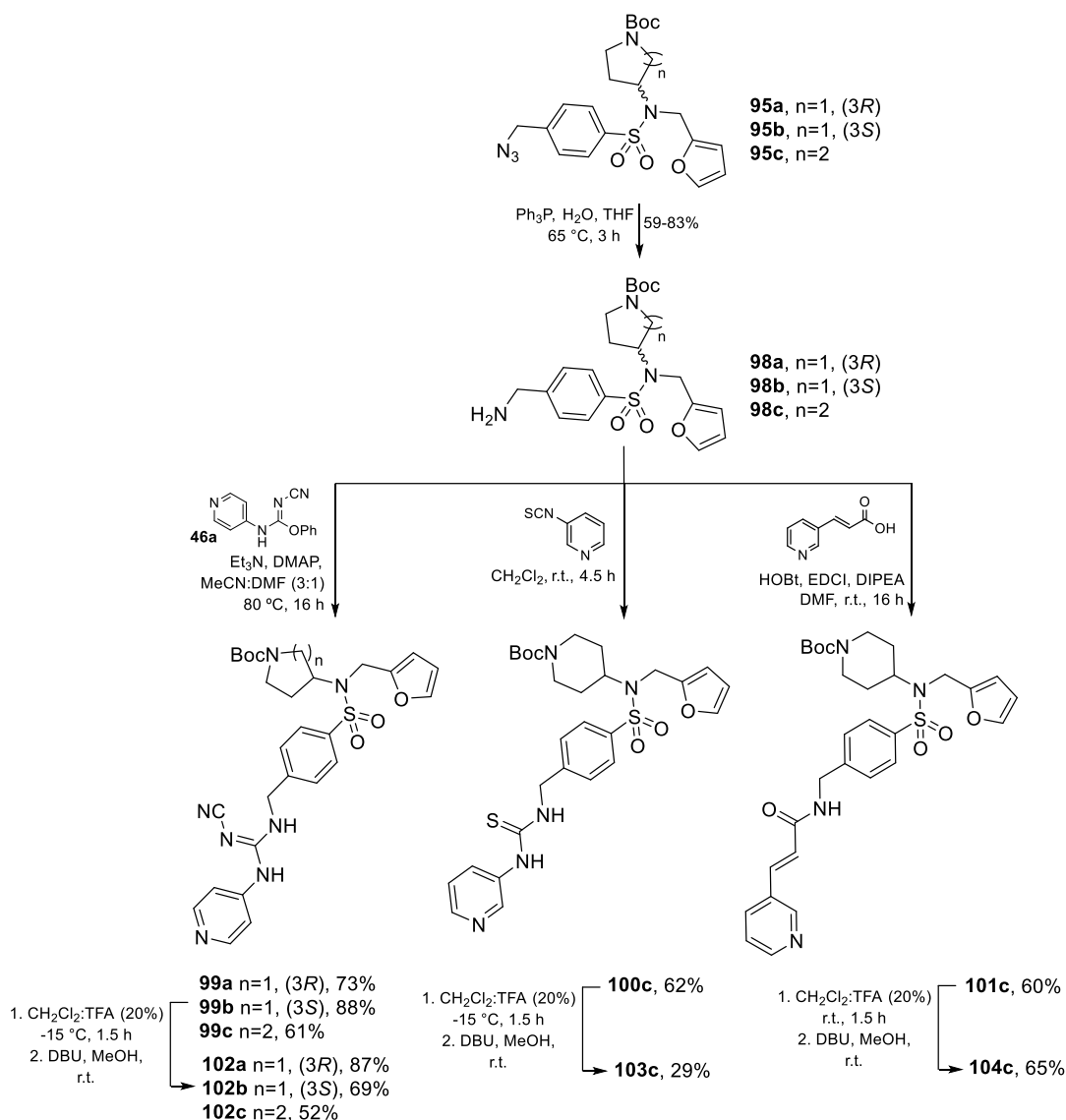
(S)-N-(Furan-2-ylmethyl)-4-((4-(pyridin-4-yl)-1H-1,2,3-triazol-1-yl)methyl)-N-(pyrrolidin-3-yl)benzenesulfonamide (97a)

The synthesis of **97a** followed the same procedure as **96c**, except that the starting materials were azide **95a** and 4-ethynylpyridine. Yield= 88%, light-yellow solid. ^1H NMR (300 MHz, CD_3OD , δ ppm) 8.65 (s, 1H, triazole), 8.61 – 8.51 (m, 2H, Py), 7.92 – 7.83 (m, 2H, Py), 7.82 – 7.72 (m, 2H, Ph), 7.57 – 7.44 (m, 2H, Ph), 7.36 – 7.24 (m, 1H, furan), 6.34 – 6.23 (m, 2H, furan), 5.78 (s, 2H, CH_2 -triazole), 4.56 – 4.32 (m, 3H, CH_2 -furan, CH pyrrolidine), 3.04 – 2.88 (m, 2H, CH_2 pyrrolidine), 2.88 – 2.61 (m, 2H, CH_2 pyrrolidine), 1.99 – 1.64 (m, 2H, CH_2 pyrrolidine). ^{13}C NMR (75.4 MHz, CD_3OD , δ ppm)

152.3 (qC, furan), 150.8 (2 CH, Py), 146.4 (qC, triazole), 143.4 (CH, furan), 142.0 (qC, Py), 141.6 (qC, Ph), 140.3 (qC, Ph), 129.8 (2 CH, Ph), 128.9 (2 CH, Ph), 124.8 (CH, triazole), 121.4 (2 CH, Py), 111.6 (CH, furan), 110.2 (CH, furan), 59.4 (CH, pyrrolidine), 54.3 (CH₂-triazole), 49.7 (CH₂, pyrrolidine), 46.2 (CH₂, pyrrolidine), 41.7 (CH₂-furan), 29.9 (CH₂, pyrrolidine). ESI-HRMS *m/z* calcd for C₂₁H₂₇N₅O₅SNa [M+Na]⁺, 484.1627; found, 484.1625.

***N*-(Furan-2-ylmethyl)-*N*-(piperidin-4-yl)-4-((4-(pyridin-4-yl)-1H-1,2,3-triazol-1-yl)methyl)benzenesulfonamide (97c)**

The synthesis of **97c** followed the same procedure as **96c**, except that the starting materials were azide **95c** and 4-ethynylpyridine. Yield= 36%, white solid. ¹H NMR (300 MHz, CDCl₃, δ ppm) 8.69 – 8.57 (m, 2H, Py), 7.89 (s, 1H, triazole), 7.76 – 7.60 (m, 4H, 2H Py, 2H Ph), 7.34 – 7.27 (m, 2H, Ph), 7.23 – 7.17 (m, 1H, furan), 6.24 (s, 2H, furan), 5.63 (s, 2H, CH₂-triazole), 4.42 (s, 2H, CH₂-furan), 3.85 – 3.63 (m, 1H, CH piperidine), 3.38 (br s, 1H, NH), 3.16 – 2.99 (m, 2H, CH₂ piperidine), 2.67 – 2.42 (m, 2H, CH₂ piperidine), 1.74 – 1.48 (m, 4H, 2 CH₂ piperidine). ¹³C NMR (75.4 MHz, CDCl₃, δ ppm) 150.8 (qC, furan), 150.6 (2 CH, Py), 146.1 (qC, triazole), 142.2 (qC, Py), 142.1 (CH, furan), 138.8 (qC, Ph), 137.7 (qC, Ph), 128.3 (2 CH, Ph), 127.8 (2 CH, Ph), 121.4 (CH, triazole), 120.0 (CH, Py), 110.7 (CH, furan), 109.5 (CH, furan), 56.5 (CH, piperidine), 53.6 (CH₂-triazole), 46.0 (2 CH₂, piperidine), 39.8 (CH₂-furan), 31.5 (CH₂, piperidine). ESI-HRMS *m/z* calcd for C₂₄H₂₇N₆O₃S [M+H]⁺, 479.1854; found, 479.1860.

Scheme 81. Synthesis of the final compounds **102a-c**, **103c** and **104c**.

(*S,E*)-4-((2-Cyano-3-(pyridin-4-yl)guanidino)methyl)-*N*-(furan-2-ylmethyl)-*N*-(pyrrolidin-3-yl)benzenesulfonamide (102a**)**

To a solution of **95a** (106 mg, 230 μ mol) in THF (1 mL), H₂O (25 μ L) and Ph₃P (90 mg, 340 μ mol) were added. The reaction mixture was stirred at 65 °C for 3 h. The resulting residue was evaporated under vacuum and purified by flash chromatography (NH₄OH:MeOH:Et₂O, 0.1:1:9) to yield **98a** (98 mg, 80%) as a colourless oil. ESI-HRMS m/z calcd for C₂₁H₂₉N₃O₅SNa [M+Na]⁺, 458.1719; found, 458.1720. Compound **46a**

(36 mg, 150 μmol) was dissolved in dry MeCN:DMF (4 mL, 3:1), and **98a** (78 mg, 180 μmol), Et₃N (60 μL , 420 μmol) and DMAP (4.0 mg, 31 μmol) were added, and the mixture was stirred at 80 °C under argon overnight. The reaction mixture was concentrated under vacuum and the residue was purified by flash chromatography (MeOH:EtOAc, 1:5) to give **99a** (63 mg, 73%) as a colourless oil. ESI-HRMS m/z calcd for C₂₈H₃₄N₇O₅S [M+H]⁺, 580.2337; found, 580.2337. Compound **99a** (48 mg, 83 μmol) was dissolved in 20 % TFA/CH₂Cl₂ (250 μL TFA, 1 mL CH₂Cl₂) at -20 °C and the mixture was stirred at -20 °C for 10 min. Et₃N (2.3 mL) was added to the mixture, and it was stirred for 10 min at -20 °C. Then, EtOAc was added, and the organic phase was washed with brine, dried over Na₂SO₄, filtered, and evaporated in vacuo. The residue was dissolved in MeOH (1 mL), DBU was added, and the solvent was evaporated in vacuo. The resulting residue was purified by flash chromatography (NH₄OH:MeOH:EtOAc, 0.1:1:2) to give **102a** (34 mg, 87%) as a light-yellow solid. ¹H NMR (300 MHz, CD₃OD, δ ppm) 8.43 – 8.31 (m, 2H, Py), 7.75 (d, J = 8.4 Hz, 2H, Ph), 7.52 (d, J = 8.4 Hz, 2H, Ph), 7.41 – 7.32 (m, 1H, furan), 7.32 – 7.23 (m, 2H, Py), 6.41 – 6.23 (m, 2H, furan), 4.64 (s, 2H, CH₂-Ph), 4.58 – 4.37 (m, 3H, CH₂-furan, CH pyrrolidine), 3.08 – 2.94 (m, 2H, CH₂, pyrrolidine), 2.94 – 2.65 (m, 2H, CH₂, pyrrolidine), 1.96 – 1.71 (m, 2H, CH₂, pyrrolidine). ¹³C NMR (75.4 MHz, CD₃OD, δ ppm) 159.6 (C=N), 152.4 (qC, furan), 150.5 (2 CH, Py), 148.5 (qC, Py), 144.6 (qC, Ph), 143.5 (CH, furan), 140.7 (qC, Ph), 129.2 (2 CH, Ph), 128.6 (2 CH, Ph), 117.4 (C \equiv N), 116.7 (2 CH, Py), 111.6 (CH, furan), 110.2 (CH, furan), 59.1 (CH pyrrolidine), 49.3 (CH₂, pyrrolidine), 46.2 (CH₂, pyrrolidine), 46.1 (CH₂-Ph), 41.8 (CH₂-furan), 29.6 (CH₂, pyrrolidine). ESI-HRMS m/z calcd for C₂₃H₂₆N₇O₃S [M+H]⁺, 480.1808; found, 480.1812.

(*R,E*)-4-((2-Cyano-3-(pyridin-4-yl)guanidino)methyl)-*N*-(furan-2-ylmethyl)-*N*-(pyrrolidin-3-yl)benzenesulfonamide (102b)

The synthesis of **102b** followed the same procedure as **102a**, except that the starting material was azide **95b**. Yield (3 steps)= 36%, white solid. Compound **102b** showed

NMR spectra identical to those of its enantiomer **102a**. ESI-HRMS m/z calcd for $C_{23}H_{26}N_7O_3S$ $[M+H]^+$, 480.1805; found, 480.1812.

(E)-4-((2-Cyano-3-(pyridin-4-yl)guanidino)methyl)-N-(furan-2-ylmethyl)-N-(piperidin-4-yl)benzenesulfonamide (102c)

The synthesis of **102c** followed the same procedure as **102a**, except that the starting material was azide **95c**. Yield (3 steps)= 27%, white solid. 1H NMR (300 MHz, CD_3OD , δ ppm) 8.45 – 8.32 (m, 2H, Py), 7.74 (d, $J = 8.4$ Hz, 2H, Ph), 7.49 (d, $J = 8.4$ Hz, 2H, Ph), 7.39 – 7.31 (m, 1H, furan), 7.31 – 7.22 (m, 2H, Py), 6.37 – 6.24 (m, 2H, furan), 4.63 (s, 2H, CH_2 -Ph), 4.47 (s, 2H, CH_2 -furan), 3.77 (quint, $J = 8.1$ Hz, 1H, CH piperidine), 3.08 – 2.89 (m, 2H, CH_2 piperidine), 2.62 – 2.44 (m, 2H, CH_2 piperidine), 1.63 (qd, $J = 12.3$, 4.2 Hz, 2H, CH_2 piperidine), 1.55 – 1.43 (m, 2H, CH_2 piperidine). ^{13}C NMR (75.4 MHz, CD_3OD , δ ppm) 159.7 (C=N), 152.7 (qC, furan), 150.5 (2 CH, Py), 148.6 (qC, Py), 144.3 (qC, Ph), 143.3 (CH, furan), 141.8 (qC, Ph), 129.1 (2 CH, Ph), 128.4 (2 CH, Ph), 117.5 (C \equiv N), 116.8 (2 CH, Py), 111.6 (CH, furan), 110.1 (CH, furan), 57.5 (CH, piperidine), 46.6 (2 CH_2 , piperidine), 46.2 (CH_2 -Ph), 40.9 (CH_2 -furan), 32.1 (2 CH_2 , piperidine). ESI-HRMS m/z calcd for $C_{24}H_{28}N_7O_3S$ $[M+H]^+$, 494.1965; found, 494.1965.

N-(Furan-2-ylmethyl)-N-(piperidin-4-yl)-4-((3-(pyridin-3-yl)thioureido)methyl)benzenesulfonamide (103c)

To a solution of **98c** (72 mg, 160 μ mol) in anhydrous CH_2Cl_2 (3.5 mL), 3-Pyridyl isothiocyanate (45 μ L, 400 μ mol) and Et_3N (56 μ L, 400 μ mol) were added. After stirring at r.t. for 3 h, the solvent was removed under *vacuo* and the resulting residue was purified by flash chromatography (acetone: Et_2O , 1:5) to give **100c** (58 mg, 62%) as a white solid. ESI-HRMS m/z calcd for $C_{28}H_{36}N_5O_5S_2$ $[M+H]^+$, 586.2154; found, 586.2152. Compound **100c** (58 mg, 99 μ mol) was dissolved in 20 % TFA/ CH_2Cl_2 (250 μ L TFA, 1 mL CH_2Cl_2) at 0 °C and the mixture was stirred at 0 °C for 10 min. Et_3N (2.3 mL) was added to the mixture, and it was stirred for 10 min at 0 °C. Then, $EtOAc$ was

added, and the organic phase was washed with brine, dried over Na₂SO₄, filtered, and evaporated in *vacuo*. The residue was dissolved in MeOH and DBU (18 μL, 118 μmol) was added, and the solvent was evaporated in *vacuo*. The resulting residue was purified by flash chromatography (NH₄OH:MeOH:EtOAc, 0.1:1:3) to give **103c** (14 mg, 29%) as a white solid. ¹H NMR (300 MHz, CD₃OD, δ ppm) 8.62 (dd, *J* = 2.6, 0.7 Hz, 1H, Py), 8.30 (dd, *J* = 4.8, 1.5 Hz, 1H, Py), 8.03 (ddd, *J* = 8.3, 2.6, 1.4 Hz, 1H, Py), 7.72 (d, *J* = 8.5 Hz, 2H, Ph), 7.50 (d, *J* = 8.6 Hz, 2H, Ph), 7.41 (ddd, *J* = 8.2, 4.8, 0.8 Hz, 1H, Py), 7.38 – 7.35 (m, 1H, furan), 6.39 – 6.25 (m, 2H, furan), 4.91 (s, 2H, CH₂-Ph), 4.48 (s, 2H, CH₂-furan), 3.81 (tt, *J* = 11.9, 4.0 Hz, 1H, CH piperidine), 3.14 – 3.00 (m, 2H, CH₂ piperidine), 2.62 (td, *J* = 12.6, 2.8 Hz, 2H, CH₂ piperidine), 1.69 (qd, *J* = 12.4, 4.2 Hz, 2H, CH₂ piperidine), 1.62 – 1.47 (m, 2H, CH₂ piperidine). ¹³C NMR (75.4 MHz, CD₃OD, δ ppm) 184.1 (C=S), 152.7 (qC, furan), 146.1 (2 CH, Py), 145.4 (qC, Py), 143.4 (CH, furan), 141.2 (qC, Ph), 138.2 (qC, Ph), 133.6 (CH, Py), 129.1 (2 CH, Ph), 128.2 (2 CH, Ph), 125.0 (CH, Py), 111.6 (CH, furan), 110.2 (CH, furan), 56.9 (CH, piperidine), 48.3 (CH₂-Ph), 46.3 (2 CH₂, piperidine), 40.9 (CH₂-furan), 31.5 (2 CH₂, piperidine). ESI-HRMS *m/z* calcd for C₂₃H₂₈N₅O₃S₂ [M+H]⁺, 486.1624; found, 486.1628.

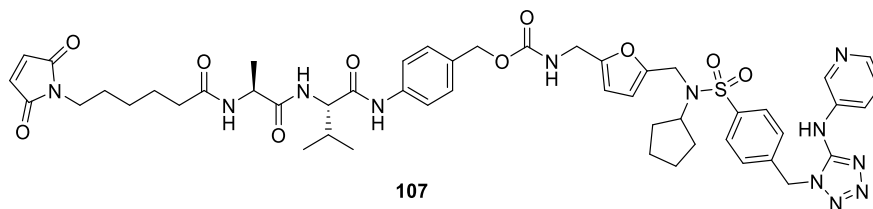
(*E*)-*N*-(4-(*N*-(Furan-2-ylmethyl)-*N*-(piperidin-4-yl)sulfamoyl)benzyl)-3-(pyridin-3-yl)acrylamide (104c)

Under N₂ atmosphere, HOBT hydrate (33 mg, 240 μmol), EDCI (46 mg, 240 μmol) and (*E*)-3-(3-pyridyl)acrylic acid (36 mg, 240 μmol) were added sequentially to a cooled solution of **98c** (72 mg, 160 μmol) in dry CH₂Cl₂ (1 mL). After stirring at 0 °C for 10 min, *N*-methyilmorpholine (50 μL, 450 μmol) was added dropwise under stirring at 0 °C. The mixture was then allowed to reach r.t. under stirring overnight. A sat. aq. sol. of NaHCO₃ (2 mL) was added and stirred vigorously for 5 min. The aqueous layer was extracted with CH₂Cl₂ (x3). The combined organic extracts were washed with brine and dried over anh. Na₂SO₄. The solvent was evaporated in *vacuo* and the residue purified by flash chromatography (Acetone:Et₂O, 2:5) to give **101c** (56 mg, 60%) as a white solid. ESI-HRMS *m/z* calcd for C₃₀H₃₇N₄O₆S [M+H]⁺, 581.2432; found, 581.2428.

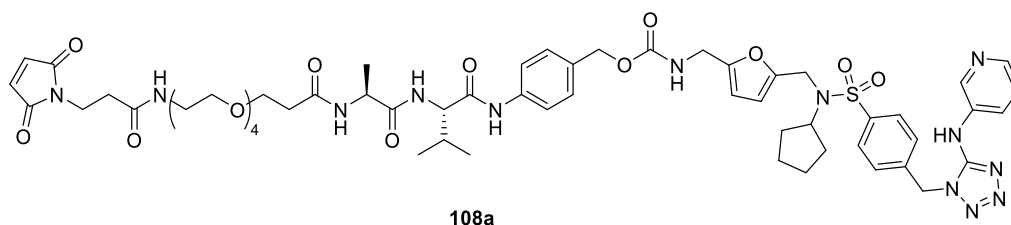
Compound **101c** (56 mg, 96 μmol) was dissolved in 20 % TFA/ CH_2Cl_2 (0.25 mL TFA, 1.0 mL CH_2Cl_2) at 0 °C and the mixture was stirred at 0 °C for 10 min. Et_3N (2.3 mL) was added to the mixture, and it was stirred for 10 min at 0 °C. Then, EtOAc was added, and the organic phase was washed with water and brine, dried over Na_2SO_4 , filtered, and evaporated *in vacuo*. The residue was dissolved in CH_2Cl_2 (1 mL), DBU was added, and the solvent was evaporated *in vacuo*. The resulting residue was purified by flash chromatography ($\text{NH}_4\text{OH}:\text{MeOH}:\text{EtOAc}$, 0.1:1:1) to give **104c** (30 mg, 65%) as a white solid. ^1H NMR (300 MHz, CD_3OD , δ ppm) 8.79 – 8.67 (m, 1H, Py), 8.52 (dd, $J = 4.9, 1.6$ Hz, 1H, Py), 8.06 (dt, $J = 8.1, 1.9$ Hz, 1H, Py), 7.72 (d, $J = 8.4$ Hz, 2H, Ph), 7.61 (d, $J = 15.9$ Hz, 1H, $\text{CH}=\underline{\text{C}}\text{-Py}$), 7.52 – 7.42 (m, 3H, 2 CH Ph, 1H Py), 7.40 – 7.32 (m, 1H, furan), 6.80 (d, $J = 15.9$ Hz, 1H, $\text{CH}=\underline{\text{C}}\text{-CO}$), 6.37 – 6.28 (m, 2H, furan), 4.58 (s, 2H, $\text{CH}_2\text{-Ph}$), 4.47 (s, 2H, $\text{CH}_2\text{-furan}$), 3.75 (tt, $J = 11.9, 4.1$ Hz, 1H, CH piperidine), 3.05 – 2.91 (m, 2H, CH_2 piperidine), 2.52 (td, $J = 12.5, 2.7$ Hz, 2H, CH_2 piperidine), 1.62 (qd, $J = 12.2, 4.1$ Hz, 2H, CH_2 piperidine), 1.55 – 1.43 (m, 2H, CH_2 piperidine). ^{13}C NMR (75.4 MHz, CD_3OD , δ ppm) 167.8 (C=O), 152.8 (qC, furan), 150.9 (CH, Py), 149.8 (CH, Py), 145.1 (qC, Ph), 143.3 (CH, furan), 141.6 (qC, Ph), 138.2 ($\text{CH}=\underline{\text{C}}\text{-Py}$), 136.3 (CH, Py), 132.8 (qC, Py), 129.1 (2 CH, Ph), 128.3 (2 CH, Ph), 125.6 (CH, Py), 124.4 ($\text{CH}=\underline{\text{C}}\text{-CO}$), 111.6 (CH, furan), 110.1 (CH, furan), 57.6 (CH, piperidine), 46.7 (2 CH_2 , piperidine), 43.8 ($\text{CH}_2\text{-Ph}$), 40.8 ($\text{CH}_2\text{-furan}$), 32.2 (2 CH_2 , piperidine). ESI-HRMS m/z calcd for $\text{C}_{25}\text{H}_{29}\text{N}_4\text{O}_4\text{S}$ $[\text{M}+\text{H}]^+$, 481.1902; found, 481.1904.

General Procedure 1 (GP1): synthesis of payloads-linkers

The payload (1 eq) was dissolved in dry DMF under Ar. The linker (1.6 eq) and DIPEA (6 eq) were added to the mixture and the reaction was stirred between 3 and 16 h at r.t. Then, the crude was purified by reversed-phase chromatography ($\text{H}_2\text{O}+0.05\%$ TFA to 100% MeCN) to yield the corresponding payload-linker.

Payload-linker (**107**)

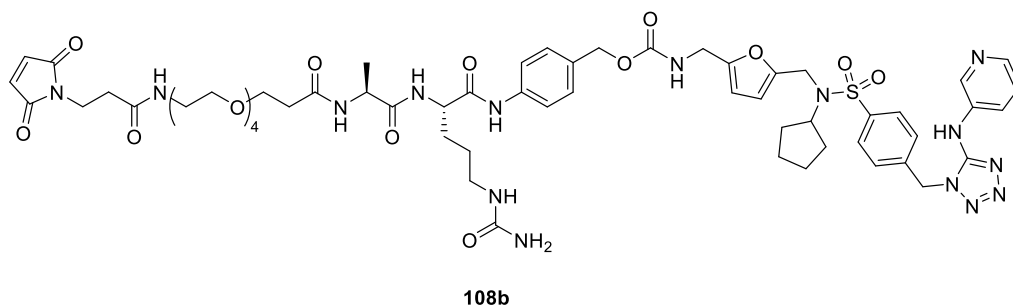
The synthesis of the payload-linker **107** was carried out following the general procedure 1 (GP1), starting from payload **93** and linker **105**. Yield: 58%, white solid. ^1H NMR (500 MHz, $\text{DMSO-}d_6$, δ ppm) 10.34 (s, 1H), 9.92 (br s, 1H), 9.03 (br s, 1H), 8.42 (br s, 2H), 8.13 (d, $J = 7.0$ Hz, 1H), 7.79 (d, $J = 8.3$ Hz, 2H), 7.76 – 7.70 (m, 1H), 7.70 – 7.62 (m, 1H), 7.57 (d, $J = 8.6$ Hz, 2H), 7.44 (d, $J = 8.1$ Hz, 2H), 7.27 (d, $J = 8.4$ Hz, 2H), 6.99 (s, 2H), 6.21 – 6.14 (m, 1H), 6.14 – 6.05 (m, 1H), 5.87 – 5.74 (m, 2H), 4.95 (s, 2H), 4.39 (quint, $J = 7.1$ Hz, 1H), 4.30 (s, 2H), 4.25 – 4.13 (m, 1H), 4.13 – 4.02 (m, 2H), 3.36 (t, $J = 7.1$ Hz, 2H), 2.25 – 2.06 (m, 2H), 2.06 – 1.92 (m, 1H), 1.54 – 1.39 (m, 7H), 1.39 – 1.23 (m, 7H), 1.20 – 1.16 (m, 2H), 1.05 – 0.65 (m, 6H). ^{13}C NMR (126 MHz, $\text{DMSO-}d_6$, δ ppm) 172.3, 171.1, 171.0, 171.0, 156.1, 152.0, 152.0, 150.7, 140.0, 139.4, 138.7, 138.1, 134.4, 131.7, 128.6, 128.4, 128.1, 127.4, 125.7, 118.9, 109.1, 107.4, 65.2, 58.7, 57.5, 49.0, 48.1, 37.3, 37.0, 34.9, 30.4, 28.4, 27.7, 25.8, 24.9, 22.9, 19.2, 18.2, 17.9. ESI-HRMS m/z calcd for $\text{C}_{50}\text{H}_{61}\text{N}_{12}\text{O}_{10}\text{S}$ $[\text{M}+\text{H}]^+$, 1021.4339; found, 1021.4349.

Payload-linker (**108a**)

The synthesis of the payload-linker **108a** was carried out following the general procedure 1 (GP1), starting from payload **93** and linker **106a**. Yield: 75%, white solid. ^1H NMR (500 MHz, $\text{DMSO-}d_6$, δ ppm) 9.91 (s, 1H), 8.90 (br s, 1H), 8.89 – 8.82 (m, 1H),

8.69 – 8.64 (m, 1H), 8.30 – 8.22 (m, 1H), 8.16 (d, $J = 7.0$ Hz, 1H), 8.04 – 7.96 (m, 1H), 7.87 (d, $J = 8.5$ Hz, 1H), 7.79 (d, $J = 8.1$ Hz, 1H), 7.75 (d, $J = 8.1$ Hz, 1H), 7.71 – 7.63 (m, 2H), 7.62 – 7.49 (m, 4H), 7.47 (d, $J = 8.1$ Hz, 1H), 7.30 – 7.21 (m, 2H), 6.99 (s, 1H), 7.08 – 6.68 (m, 1H), 6.23 – 6.17 (m, 1H), 6.14 – 6.08 (m, 1H), 4.96 (s, 2H), 4.56 – 4.46 (m, 2H), 4.39 (quint, $J = 7.0$ Hz, 1H), 4.30 (s, 1H), 4.21 (dd, $J = 8.7, 6.7$ Hz, 1H), 4.09 (d, $J = 6.2$ Hz, 2H), 3.64 – 3.56 (m, 4H), 3.55 – 3.43 (m, 13H), 3.36 (t, $J = 5.9$ Hz, 3H), 3.23 – 3.12 (m, 2H), 2.46 (t, $J = 6.9$ Hz, 1H), 2.42 – 2.17 (m, 3H), 2.02 – 1.90 (m, 1H), 1.55 – 1.43 (m, 3H), 1.41 – 1.25 (m, 7H), 1.05 – 0.65 (m, 6H). ^{13}C NMR (126 MHz, DMSO- d_6 , δ ppm) 171.1, 170.9, 170.7, 170.3, 169.5, 169.1, 164.6, 164.5, 158.4, 158.2, 156.1, 151.9, 150.8, 146.6, 144.2, 138.7, 138.7, 138.6, 135.0, 134.5, 131.8, 131.7, 128.6, 128.5, 128.0, 127.8, 127.0, 125.1, 118.9, 109.0, 107.4, 69.8, 69.7, 69.5, 69.5, 69.0, 66.9, 65.2, 58.6, 57.5, 49.0, 42.0, 38.5, 37.3, 35.9, 34.1, 33.9, 30.6, 28.4, 22.9, 19.1, 18.1, 17.9. ESI-HRMS m/z calcd for $\text{C}_{55}\text{H}_{75}\text{N}_{13}\text{O}_{15}\text{SNa}$ $[\text{M}+\text{Na}]^+$, 1248.5116; found, 1248.5119.

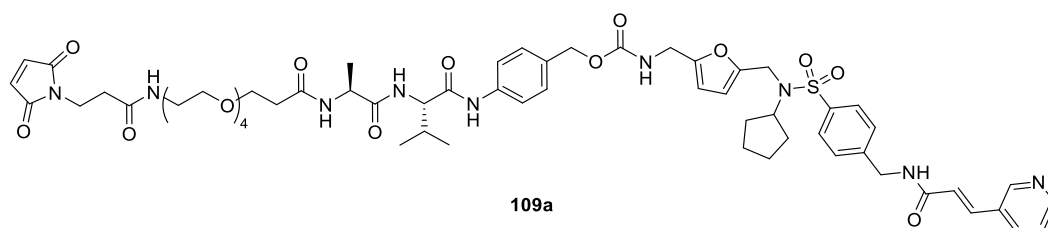
Payload-linker (**108b**)



The synthesis of the payload-linker **108b** was carried out following the general procedure 1 (GP1), starting from payload **93** and linker **106b**. Yield: 80%, white solid. ^1H NMR (500 MHz, DMSO- d_6 , δ ppm) 10.39 (s, 1H), 9.97 (s, 1H), 9.06 (s, 1H), 8.55 – 8.33 (m, 2H), 8.16 – 8.07 (m, 1H), 8.05 – 7.98 (m, 1H), 7.86 (t, $J = 8.9$ Hz, 2H), 7.83 – 7.74 (m, 2H), 7.59 (d, $J = 8.2$ Hz, 2H), 7.45 (d, $J = 8.1$ Hz, 2H), 7.30 – 7.24 (m, 2H), 7.00 (s, 1H), 6.21 – 6.14 (m, 1H), 6.12 – 6.05 (m, 1H), 5.84 – 5.75 (m, 2H), 4.96 (s, 2H), 4.39

(q, $J = 8.0$ Hz, 1H), 4.31 (s, 1H), 4.26 – 4.21 (m, 1H), 4.10 – 4.04 (m, 2H), 3.65 – 3.57 (m, 4H), 3.53 – 3.45 (m, 12H), 3.41 – 3.34 (m, 2H), 3.20 – 3.13 (m, 2H), 3.09 – 2.92 (m, 2H), 2.47 (t, $J = 6.9$ Hz, 8H), 2.44 – 2.31 (m, 2H), 2.03 – 1.93 (m, 1H), 1.76 – 1.65 (m, 1H), 1.65 – 1.56 (m, 2H), 1.54 – 1.41 (m, 5H), 1.41 – 1.23 (m, 5H), 1.05 – 0.65 (m, 6H). ^{13}C NMR (126 MHz, DMSO- d_6 , δ ppm) 171.6, 171.2, 171.0, 170.8, 170.0, 159.4, 159.0, 152.5, 151.1, 139.8, 139.1, 138.7, 135.0, 129.1, 128.9, 128.6, 127.9, 126.4, 119.4, 109.5, 107.8, 70.2, 70.0, 69.9, 69.5, 67.4, 65.7, 59.1, 58.0, 53.6, 48.6, 39.0, 37.8, 36.4, 34.5, 34.4, 31.0, 29.7, 28.9, 27.2, 23.4, 19.6, 18.6. ESI-HRMS m/z calcd for $\text{C}_{61}\text{H}_{82}\text{N}_{15}\text{O}_{16}\text{SNa}$ $[\text{M}+\text{Na}]^+$, 1334.5594; found, 1334.5599.

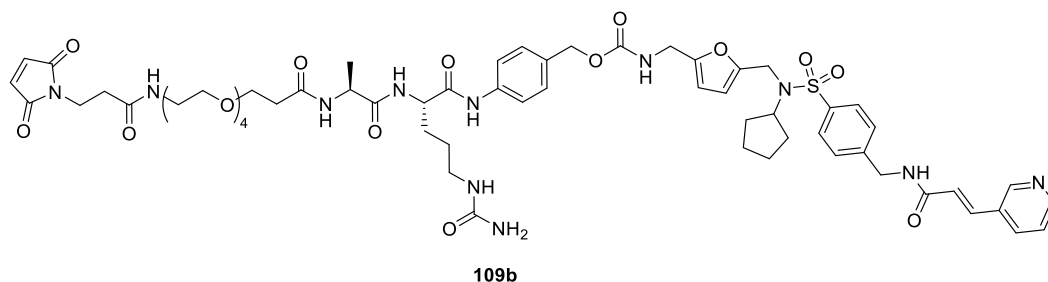
Payload-linker (**109a**)



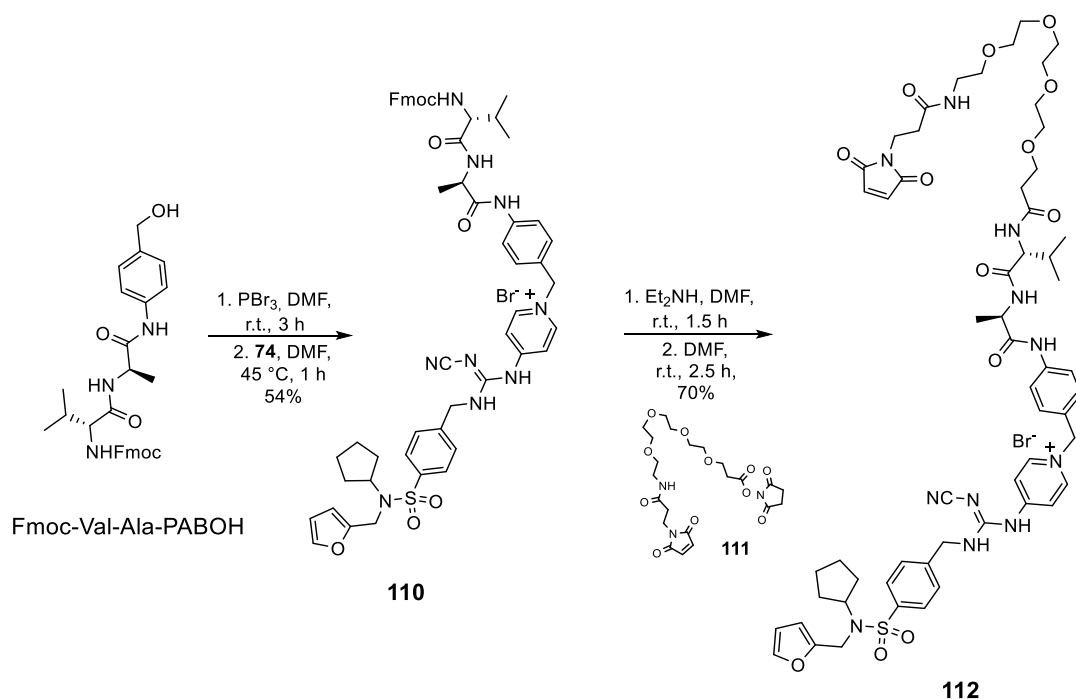
The synthesis of the payload-linker **109a** was carried out following the general procedure 1 (GP1), starting from payload **89** and linker **106a**. Yield: 90%, white solid. ^1H NMR (500 MHz, DMSO- d_6 , δ ppm) 9.91 (s, 1H), 8.90 (br s, 1H), 8.89 – 8.82 (m, 1H), 8.72 – 8.62 (m, 1H), 8.30 – 8.21 (m, 1H), 8.16 (d, $J = 7.0$ Hz, 1H), 8.04 – 7.96 (m, 1H), 7.87 (d, $J = 8.5$ Hz, 1H), 7.79 (d, $J = 8.1$ Hz, 1H), 7.75 (d, $J = 8.1$ Hz, 1H), 7.71 – 7.63 (m, 2H), 7.60 – 7.55 (m, 3H), 7.52 (d, $J = 8.4$ Hz, 1H), 7.47 (d, $J = 8.1$ Hz, 1H), 7.31 – 7.21 (m, 2H), 6.99 (s, 1H), 6.88 (d, $J = 15.9$ Hz, 1H), 6.22 – 6.16 (m, 1H), 6.14 – 6.08 (m, 1H), 4.96 (s, 2H), 4.55 – 4.48 (m, 2H), 4.39 (quint, $J = 7.0$ Hz, 1H), 4.30 (s, 1H), 4.24 – 4.17 (m, 1H), 4.14 – 4.07 (m, 2H), 3.63 – 3.56 (m, 3H), 3.53 – 3.42 (m, 12H), 3.41 – 3.33 (m, 2H), 3.20 – 3.11 (m, 2H), 2.46 (t, $J = 6.9$ Hz, 1H), 2.42 – 2.16 (m, 3H), 2.01 – 1.91 (m, 1H), 1.54 – 1.44 (m, 3H), 1.41 – 1.23 (m, 7H), 1.05 – 0.65 (m, 6H). ^{13}C NMR (126 MHz, DMSO- d_6 , δ ppm) 171.1, 170.9, 170.7, 170.3, 169.5, 164.5, 151.9, 150.8, 146.6, 144.2, 138.7, 135.0, 134.5, 131.8, 128.6, 128.5, 128.0, 127.8, 127.0, 125.1, 118.9, 109.0,

107.4, 69.8, 69.7, 69.5, 69.0, 66.9, 65.2, 58.6, 57.5, 49.0, 42.0, 38.5, 37.3, 35.9, 34.1, 33.9, 30.6, 28.4, 22.9, 19.1, 18.1, 17.9. ESI-HRMS m/z calcd for $C_{60}H_{77}N_9O_{16}SNa$ $[M+Na]^+$, 1234.5096; found, 1234.5101.

Payload-linker (**109b**)



The synthesis of the payload-linker **109b** was carried out following the general procedure 1 (GP1), starting from payload **89** and linker **106b**. Yield: 90%, white solid. 1H NMR (500 MHz, $DMSO-d_6$, δ ppm) 9.97 (s, 1H), 8.92 (s, 1H), 8.90 – 8.82 (m, 1H), 8.72 – 8.65 (m, 1H), 8.33 – 8.24 (m, 1H), 8.15 – 8.07 (m, 1H), 8.04 – 7.96 (m, 1H), 7.86 (d, J = 8.7 Hz, 1H), 7.79 (d, J = 8.1 Hz, 1H), 7.75 (d, J = 8.2 Hz, 1H), 7.72 – 7.65 (m, 2H), 7.63 – 7.55 (m, 3H), 7.52 (d, J = 8.4 Hz, 1H), 7.47 (d, J = 8.1 Hz, 1H), 7.30 – 7.22 (m, 2H), 6.99 (s, 1H), 6.89 (d, J = 15.9 Hz, 1H), 6.22 – 6.17 (m, 1H), 6.14 – 6.09 (m, 1H), 4.96 (s, 2H), 4.58 – 4.48 (m, 2H), 4.43 – 4.35 (m, 1H), 4.30 (s, 1H), 4.27 – 4.20 (m, 1H), 4.12 – 4.06 (m, 2H), 3.65 – 3.55 (m, 4H), 3.53 – 3.43 (m, 13H), 3.41 – 3.33 (m, 3H), 3.21 – 3.12 (m, 2H), 3.08 – 2.89 (m, 2H), 2.52 – 2.42 (m, 7H), 2.42 – 2.17 (m, 3H), 2.03 – 1.91 (m, 1H), 1.76 – 1.64 (m, 1H), 1.64 – 1.55 (m, 2H), 1.55 – 1.41 (m, 4H), 1.41 – 1.21 (m, 5H), 1.05 – 0.65 (m, 6H). ^{13}C NMR (126 MHz, $DMSO-d_6$, δ ppm) 171.1, 170.7, 170.6, 170.3, 169.5, 164.5, 159.0, 158.5, 150.8, 144.2, 138.6, 134.8, 134.5, 132.0, 128.6, 128.1, 127.8, 127.0, 125.2, 118.9, 109.0, 107.4, 69.8, 69.7, 69.5, 69.0, 66.9, 65.2, 58.6, 57.5, 53.1, 42.0, 38.5, 37.3, 35.9, 34.1, 33.9, 32.6, 30.6, 29.3, 28.4, 26.8, 22.9, 19.2, 18.1. ESI-HRMS m/z calcd for $C_{63}H_{83}N_{11}O_{17}SNa$ $[M+Na]^+$, 1320.5561; found, 1320.5581.



Scheme 82. Synthetic route for the preparation of the linker-payload **112**.

Pyridinium salt (**110**)

To the solution of Fmoc-Val-Ala-PABOH (500 mg, 970 μmol) in anh. DMF (7.5 mL) at 0°C was added slowly a 1M solution of PBr_3 in CH_2Cl_2 (970 μL , 970 μmol) during 10 min. After 3 h, the solvent was evaporated under *vacuum* and the crude was dissolved in EtOAc and washed with water. The organic phase was then dried (Na_2SO_4), filtered and concentrated under *vacuum* affording the corresponding bromo derivative that was used in the next step without further purification. ESI-HRMS m/z calcd for $\text{C}_{30}\text{H}_{32}\text{N}_3\text{O}_4^{79}\text{BrNa}$ [$\text{M}+\text{Na}$] $^+$, 600.1469; found, 600.1468 and calc. for $\text{C}_{30}\text{H}_{32}\text{N}_3\text{O}_4^{81}\text{BrNa}$ [$\text{M}+\text{Na}$] $^+$, 602.1447; found, 602.1448. The crude (173 μmol) was dissolved in DMF (0.6 mL) and **74** (42 mg, 86 μmol) was added to the mixture. The reaction was heated at 45°C for 2h, then the solvent was evaporated, and the crude was purified by reversed phase prep-HPLC to yield **110** (67 mg, 54%) as a white solid. ^1H NMR (300 MHz, $\text{DMSO}-d_6$, δ ppm) 10.13 (s, 1H), 9.41 (br s, 1H), 8.76 (d, $J = 7.3$ Hz, 2H), 8.20 (d, $J = 6.8$ Hz, 1H), 7.88 (d, $J = 7.5$ Hz, 2H), 7.82 – 7.69 (m, 4H), 7.69 – 7.57

(m, 4H), 7.56 – 7.46 (m, 3H), 7.45 – 7.36 (m, 5H), 7.36 – 7.26 (m, 2H), 6.42 – 6.34 (m, 1H), 6.33 – 6.25 (m, 1H), 5.56 (s, 2H), 4.71 – 4.56 (m, 3H), 4.46 – 4.17 (m, 7H), 4.10 (quint, $J = 8.6$ Hz, 2H), 3.98 – 3.84 (m, 1H), 2.05 – 1.91 (m, 2H), 1.56 – 1.42 (m, 4H), 1.38 – 1.25 (m, 4H), 1.30 (d, $J = 7.0$ Hz, 2H), 0.87 (dd, $J = 9.1, 6.7$ Hz, 6H). ^{13}C NMR (75.4 MHz, DMSO- d_6 , δ ppm) 171.4, 171.1, 156.1, 153.1, 151.7, 144.4, 143.9, 143.8, 142.2, 140.7, 139.8, 139.2, 129.3, 129.2, 128.1, 127.6, 127.1, 127.0, 125.3, 120.1, 119.5, 115.0, 110.6, 108.4, 65.7, 61.0, 59.9, 58.6, 49.1, 46.7, 45.1, 39.9, 30.4, 28.4, 22.9, 19.1, 18.2, 17.9. ESI-HRMS m/z calcd for $\text{C}_{54}\text{H}_{58}\text{N}_9\text{O}_7\text{S}$ $[\text{M}]^+$, 976.4161; found, 976.4174.

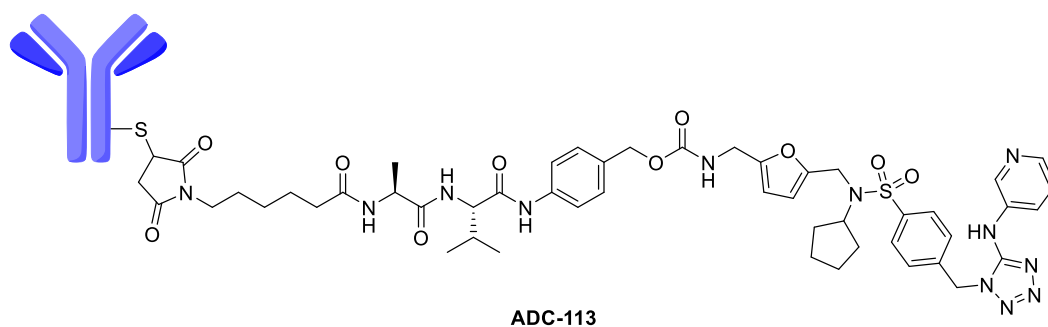
Payload-linker (**112**)

Compound **110** (55 mg, 56 μmol) was dissolved in DMF (4 mL) and diethylamine (58 μL , 560 μmol) was added to the mixture. The reaction was stirred at r.t. for 1.5 h, then the solvent was evaporated to obtain the amine derivative that was used directly in the next step without further purification. The crude (56 μmol) was dissolved in DMF (2 mL) and Mal-dPEG(4)-NHS **111** (34 mg, 56 μmol), and DIPEA (23 μL , 133 μmol) were added to the mixture. The reaction was stirred for 2.5 h at r.t. and the solvent was evaporated. The crude was purified by reversed phase prep-HPLC to yield **112** (53 mg, 70%) as a white solid. ^1H NMR (500 MHz, DMSO- d_6 , δ ppm) 10.02 (s, 1H), 9.34 (br s, 1H), 8.81 – 8.66 (m, 2H), 8.23 – 8.14 (m, 1H), 8.06 – 7.94 (m, 1H), 7.94 – 7.79 (m, 2H), 7.77 (d, $J = 8.1$ Hz, 1H), 7.64 (d, $J = 8.6$ Hz, 2H), 7.59 (t, $J = 7.8$ Hz, 2H), 7.55 – 7.53 (m, 1H), 7.51 (d, $J = 8.2$ Hz, 1H), 7.41 (d, $J = 8.3$ Hz, 2H), 6.99 (s, 1H), 6.42 – 6.34 (m, 1H), 6.35 – 6.22 (m, 1H), 5.55 (s, 2H), 4.72 – 4.58 (m, 2H), 4.40 – 4.28 (m, 3H), 4.23 – 4.15 (m, 1H), 4.10 (q, $J = 8.3$ Hz, 1H), 3.69 – 3.54 (m, 6H), 3.54 – 3.44 (m, 13H), 3.44 – 3.30 (m, 3H), 3.20 – 3.11 (m, 2H), 2.45 (t, $J = 6.9$ Hz, 1H), 2.42 – 2.16 (m, 4H), 1.99 – 1.89 (m, 1H), 1.53 – 1.40 (m, 3H), 1.37 – 1.26 (m, 3H), 1.29 (d, $J = 7.0$ Hz, 2H), 1.05 – 0.65 (m, 6H). ^{13}C NMR (126 MHz, DMSO- d_6 , δ ppm) 175.9, 174.9, 174.5, 171.4, 170.9, 170.7, 170.3, 169.5, 169.2, 169.1, 158.2, 157.9, 151.7, 144.4, 142.3, 139.8, 139.2, 134.5, 129.3, 129.2, 128.3, 128.1, 127.2, 127.1, 119.5, 115.7, 115.0,

110.6, 108.4, 78.7, 69.8, 69.7, 69.5, 69.0, 66.9, 60.9, 59.6, 58.6, 57.4, 49.1, 45.1, 38.5, 35.9, 34.7, 34.1, 33.9, 30.6, 28.4, 22.9, 22.4, 19.1, 18.1, 17.8. ESI-HRMS m/z calcd for $C_{57}H_{74}N_{11}O_{13}S [M]^+$, 1152.5166; found, 1152.5183.

General Procedure 2 (GP2): synthesis of ADCs

The antibody solution was prepared by taking 10 mg of the Ab in a PBS solution at 5.0 mg/mL. The antibody was uncapped by reaction with Tris-(2-carboxyethyl)-phosphine hydrochloride (TCEP, 40 eq, 50 mM in H_2O) by incubating the solution for 3 h at 37°C on a shaking platform. Then, two dialysis were performed after 4 and 16 h, to filter off the excess of TCEP. The dialysis was achieved at 4 °C in a 3 L PBS solution (1 mM EDTA) at pH 7.4 by using a Slide-A-Lyzer Dialysis Cassette 20'000 MWCO (Molecular Weight Cut Off). Subsequently, the conjugation with the payloads occurred adding a freshly prepared solution of payload-linkers (**107**, **108a-b**, **109a-b** or **112**) (20 eq, 10 μ g/ μ L in DMSO) to the antibody solution and incubating the resulting mixture for 1h at r.t. on a shaking platform. The remaining free thiols on the antibody were capped by adding a freshly prepared solution of *N*-ethylmaleimide (12 eq, 100 mM in DMSO) and the resulting mixture was incubated for 1 h at r.t. on a shaking platform. Then, the resulting excess of *N*-ethylmaleimide were quenched by reaction with a freshly prepared solution of *N*-acetyl-L-cysteine (40 eq, 100 mM in H_2O). The solution was incubated for 15 min at r.t. on a shaking platform and then it was centrifuged at full speed for 5 minutes. Then, the supernatant was taken and purified with a PD-10 column (GE Healthcare Life Sciences) by gravity. The protein-containing fractions were identified by using Bradford reagent and it was then measured their protein content (≥ 0.1 mg/mL) using NanoDrop. The fractions were collected, dialysed with a Slide-A-Lyzer Dialysis Cassettes 20'000 MWCO and adjusted to a protein concentration of 5.0 mg/mL.

ADC-113

ADC-113 was synthesized following the general procedure 2 (GP2), starting from the mAb CD138 and the payload-linker **107**. DAR= 7.83.

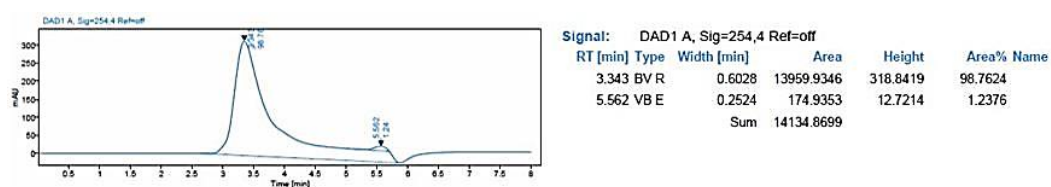
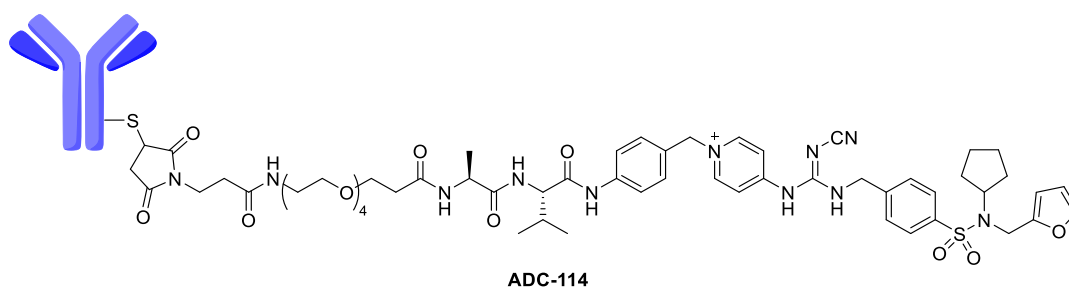


Figure 51. SEC-HPLC analysis at 254 nm of **ADC-113**.

ADC-114

ADC-114 was synthesized following the general procedure 2 (GP-2), starting from the mAb CD138 and the payload-linker **112**. DAR= 7.69.

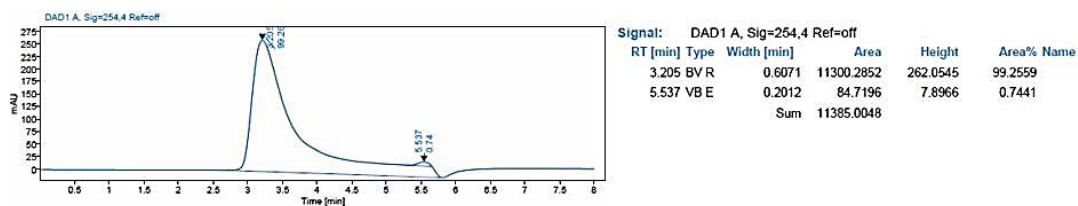
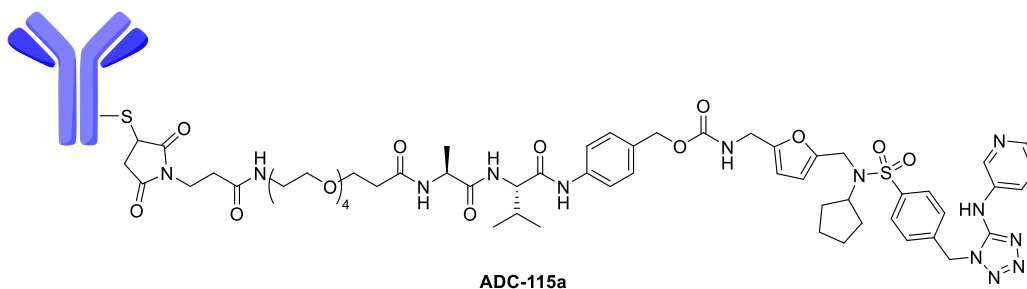


Figure 52. SEC-HPLC analysis at 254 nm of ADC-114.

ADC-115a



ADC-115a was synthesized following the general procedure 2 (GP-2), starting from the mAb CD138 and the payload-linker **108a**. DAR 7.72.

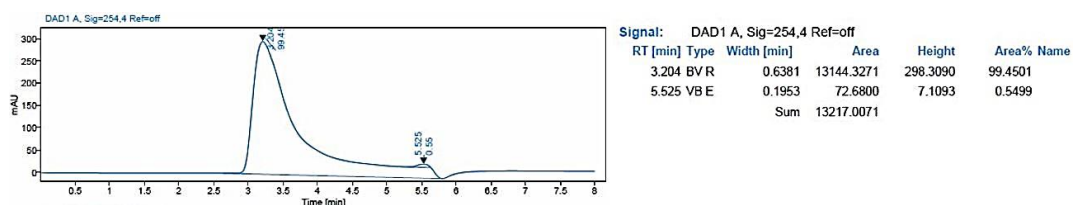
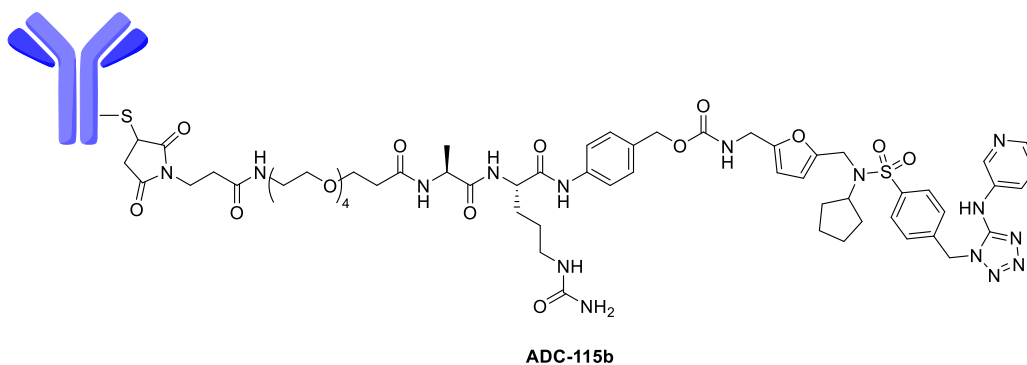


Figure 53. SEC-HPLC analysis at 254 nm of ADC-115a.

ADC-115b



ADC-115b was synthesized following the general procedure 2 (GP-2), starting from the mAb CD138 and the payload-linker **108b**. DAR= 7.55.

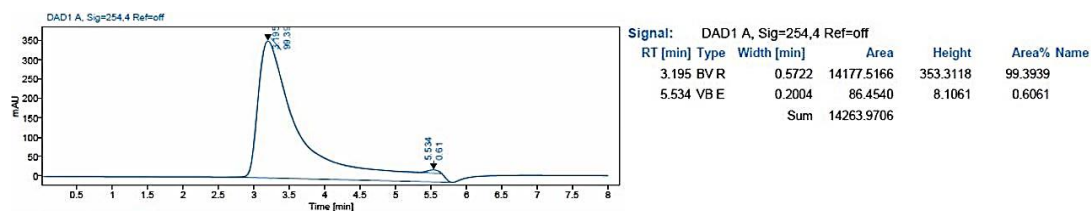
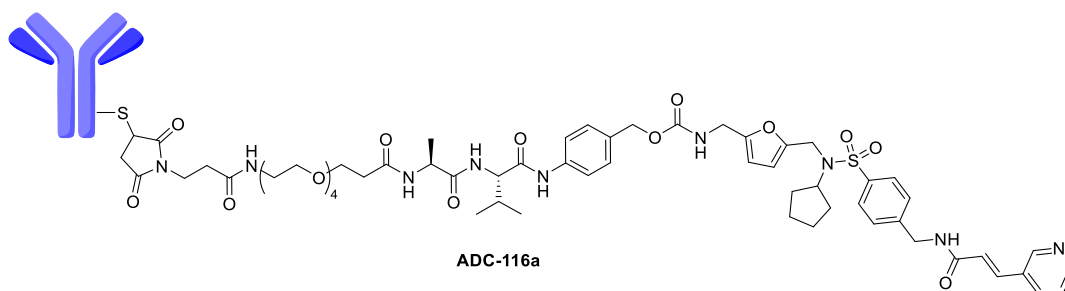


Figure 54. SEC-HPLC analysis at 254 nm of **ADC-115b**.

ADC-116a



ADC-116a was synthesized following the general procedure 2 (GP-2), starting from the mAb CD138 and the payload-linker **109a**. DAR= 8.52.

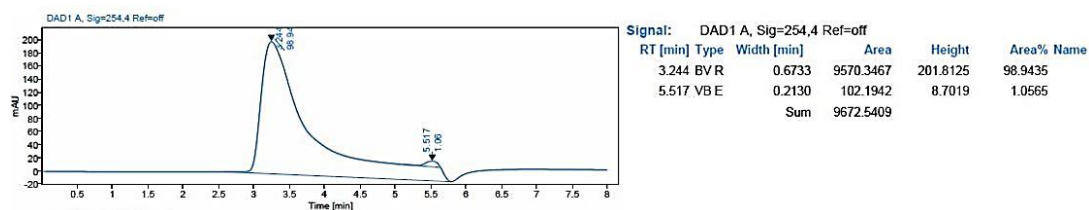
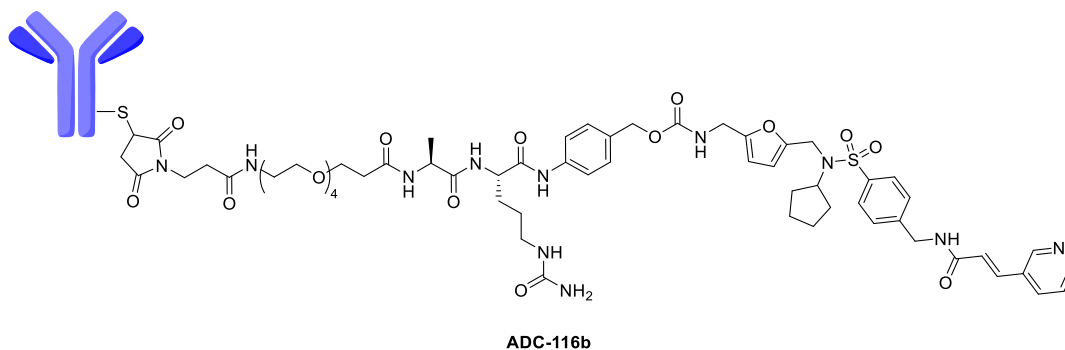


Figure 55. SEC-HPLC analysis at 254 nm of **ADC-116a**.

ADC-116b

ADC-116b was synthesized following the general procedure 2 (GP-2), starting from the mAb CD138 and the payload-linker **109b**. DAR= 8.33.

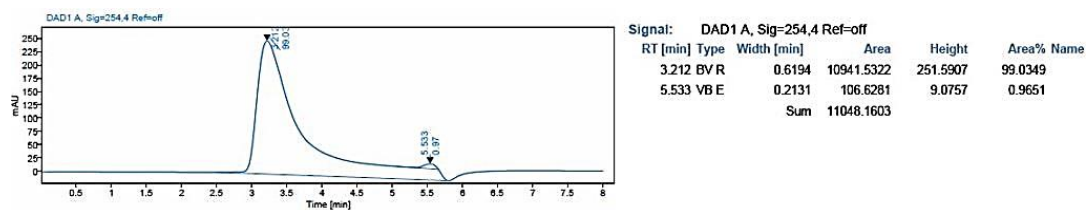
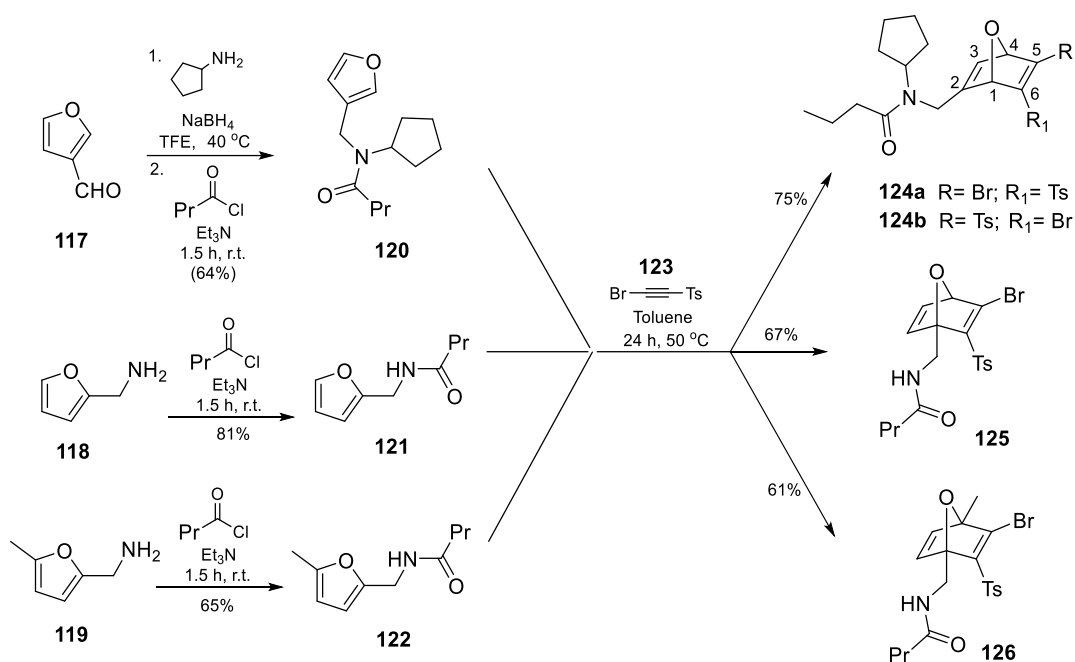


Figure 56. SEC-HPLC analysis at 254 nm of **ADC-116b**.



Scheme 83. Synthetic route for the preparation of oxanorbornadienes **124-126**.

***N*-Cyclopentyl-*N*-(furan-3-ylmethyl)butyramide (**120**)**

A solution of 3-furancarboxaldehyde **117** (3.7 g, 38.8 mmol) in 2,2,2-trifluoroethanol (80 mL) was stirred at 40 °C for 5 min under argon. Cyclopentylamine (3.5 mL, 35.2 mmol) was added, and the mixture was stirred for 30 min., followed by the addition of NaBH₄ (2.7 g, 70.5 mmol) and a further 30 min of stirring at 40 °C. Then, the mixture was filtered through celite, the residue was washed with ethanol and the solvent was evaporated to yield the amine derivative (5.82 g, 35.2 mmol) as a brown oil, which was dissolved in dry CH₂Cl₂ (83.0 mL) under Ar atmosphere and the reaction was cooled to 0 °C. Butyryl chloride (7.3 mL, 70.4 mmol) and triethylamine (7.1 mL, 70.4 mmol) were added and the reaction was stirred for 1.5 h at r.t.. Then, the reaction mixture was diluted with CH₂Cl₂, it was washed with a 1M HCl and subsequently with a sat. aq. sol. of NH₄Cl. The organic phase was separated, dried with anhydrous Na₂SO₄, filtered, and concentrated *in vacuo*. The residue was purified by column chromatography on silica gel (Et₂O: Cy, 1:6 → 1:2) to yield compound **120** (5.31 g, 64 %) as a sticky yellow solid. ¹H NMR (300 MHz, CDCl₃, δ ppm, mixture of rotamers)

7.45 – 7.18 (m, 4H, furan), 6.39 – 6.19 (m, 2H, furan), 4.91 – 4.66 (m, 1H, CH cyclopentyl rotamer A), 4.33 – 4.08 (m, 5H, CH cyclopentyl rotamer B, 2 CH₂-N), 2.46 – 2.17 (m, 4H, 2 CH₂-C=O), 1.89 – 1.37 (m, 20H, 8 CH₂ cyclopentyl, 2 CH₂-CH₃), 1.05 – 0.79 (m, 6H, 2 CH₃-CH₂). ¹³C NMR (75.4 MHz, CDCl₃, δ ppm, mixture of rotamers) 176.8, 173.3, 143.7, 142.6, 140.3, 139.5, 123.9, 110.9, 109.2, 77.4, 58.9, 55.9, 40.0, 36.6, 35.8, 30.1, 29.3, 23.9, 19.1, 19.0, 18.4, 14.1, 13.8, 13.7. ESI-HRMS *m/z* calcd for C₁₄H₂₁NO₂Na [M+Na], 258.1470; found, 258.1465.

***N*-(Furan-2-ylmethyl)butyramide (121)**

Furfurylamine **118** (1.8 mL, 20.6 mmol) was dissolved in dry CH₂Cl₂ (50 mL) under Ar atmosphere and the reaction was cooled to 0 °C. Butyryl chloride (4.3 mL, 41.2 mmol) and triethylamine (5.7 mL, 41.2 mmol) were added and the reaction was stirred for 1.5 h at r.t.. Then, the reaction mixture was diluted with CH₂Cl₂, it was washed with 1M HCl and subsequently with a sat. aq. sol. of NH₄Cl. The organic phase was separated, dried with anhydrous Na₂SO₄, and concentrated *in vacuo*. The residue was purified by column chromatography on silica gel (EtOAc:Cy, 1:3 → 2:1) to yield compound **121** (2.8 g, 81 %) as a white solid. ¹H NMR (300 MHz, CDCl₃, δ ppm) 7.36 – 7.28 (m, 1H, furan), 6.35 – 6.25 (m, 1H, furan), 6.23 – 6.15 (m, 1H, furan), 6.07 (br s, 1H, NH), 4.40 (d, *J* = 5.4 Hz, 2H, CH₂-NH), 2.16 (t, *J* = 7.5 Hz, 2H, CH₂-CH₂-CH₃), 1.64 (sept, *J* = 7.4 Hz, 2H, CH₂-CH₂-CH₃), 0.91 (t, *J* = 7.4 Hz, 3H, CH₃). ¹³C NMR (75 MHz, CDCl₃, δ ppm) 173.0 (C=O), 151.6 (qC, furan), 142.2 (CH, furan), 110.5 (CH, furan), 107.4 (CH, furan), 38.5 (CH₂-CH₂-CH₃), 36.5 (CH₂-NH), 19.1 (CH₂-CH₂-CH₃), 13.8 (CH₃). ESI-HRMS *m/z* calcd for C₉H₁₃NO₂ [M+H]⁺, 190.0836; found, 190.0838.

***N*-((5-Methylfuran-2-yl)methyl)butyramide (122)¹⁶⁷**

The synthesis of compound **122** followed the same procedure as **121**, except that the starting material was amine **119**. Yield= 65%. ¹H NMR (300 MHz, CDCl₃, δ ppm) 6.15 – 5.98 (m, 1H, furan), 5.90 – 5.82 (m, 2H, furan, NH), 4.35 (d, *J* = 5.3 Hz, 2H CH₂-NH),

2.24 (s, 3H, CH₃ furan), 2.15 (t, $J = 7.5$ Hz, 2H, CH₂-CH₂-CH₃), 1.65 (sept, $J = 7.4$ Hz, 2H, CH₂-CH₂-CH₃), 0.93 (t, $J = 7.4$ Hz, 3H, CH₂-CH₂-CH₃). NMR data match with those previously reported for this compound.

***p*-Tolyl [2-Bromoethynyl] sulfone (**123**)¹⁶⁴**

A mixture of AlCl₃ (14.6 g, 109.7 mmol) and tosyl chloride (20.9 g, 109.7 mmol) was dissolved in dry CH₂Cl₂ (100 mL) and stirred under argon atmosphere for 20 min at r.t. After this time, the crude was filtered through a celite pad, and the resultant liquid was added dropwise to a solution of commercial bis(trimethylsilyl) acetylene (22.6 mL, 99.8 mmol) in dry CH₂Cl₂ (100 mL) at 0 °C for 1 h. After the addition, the reaction was allowed to warm at r.t. overnight. Once the reaction has finished, the crude was poured into a solution of HCl in cold water (20%). The organic layer was washed with an aqueous solution of HCl (1M), with brine, and dried over anhydrous Na₂SO₄. The solvent was removed under reduced pressure and the resultant solid was recrystallized from cyclohexane affording the trimethyl(tosylethynyl)silane as derivative a light brown powder. Part of the crude (31.7 mmol) was dissolved in acetone (200 mL), NBS (6.2 g, 34.9 mmol) and silver nitrate (540 mg, 3 mmol) were added. Then, the reaction was protected from light and stirred at r.t. for 50 min. The mixture was filtered over a celite pad, and the solvent was removed under reduced pressure. The product was purified by recrystallization in cyclohexane affording **123** (8.21 g, 42%) as yellow crystals.

ONDs 124a-b

To a solution of compound **120** (4.5 g, 19.1 mmol) in toluene (150 mL), **123** (5.5 g, 21.0 mmol) was added. The mixture was stirred at 50 °C for 24 h, concentrated *in vacuo* and purified by column chromatography on silica gel (Et₂O: Cy, 1:2 → 4:1) to yield two regioisomers: **124a** (3.38 g, orange foam), and **124b** (2.89 g, yellow foam). The overall yield was 75%. Regioisomer **124a**: ¹H NMR (300 MHz, CDCl₃, δ ppm, mixture of rotamers) 7.93 – 7.75 (m, 4H, Ts), 7.47 – 7.29 (m, 4H, Ts), 6.76 – 6.51 (m,

2H, 2 H-3), 5.55 – 5.16 (m, 4H, 2 H-1, 2 H-4), 4.89 – 4.71 (m, 2H, 2 CH cyclopentyl), 4.35 – 4.04 (m, 4H, 2 CH₂-N), 2.45 (s, 6H, 2 CH₃ Ts), 2.25 – 1.96 (m, 4H, 2 CH₂-CH₂-CH₃), 1.93 – 1.17 (m, 20H, 8 CH₂ cyclopentyl, 2 CH₂-CH₃), 1.07 – 0.82 (m, 6H, 2 CH₃-CH₂). ¹³C NMR (75.4 MHz, CDCl₃, δ ppm, mixture of rotamers) 173.8, 159.8, 150.3, 147.2, 133.8, 132.9, 130.3, 128.0, 91.0, 87.0, 58.9, 55.5, 43.0, 39.7, 35.6, 30.4, 23.8, 21.9, 19.0, 14.1. ESI-HRMS *m/z* calcd for C₂₃H₂₉⁸¹BrNO₄S [M+H]⁺, 496.0975; found, 496.0971; *m/z* calcd for C₂₃H₂₉⁷⁹BrNO₄S [M+H]⁺, 494.0995; found, 494.0993. Regioisomer **124b**: ¹H NMR (300 MHz, CDCl₃, δ ppm, mixture of rotamers) 7.78 (d, *J* = 8.3 Hz, 4H, Ts), 7.34 (d, *J* = 8.0 Hz, 4H, Ts), 6.58 (s, 2H, 2 H-3), 5.66 – 5.10 (m, 4H, 2 H-1, 2 H-4), 4.76 – 4.62 (m, 2H, 2 CH cyclopentyl), 4.38 – 3.79 (m, 4H, 2 CH₂-N), 2.44 (s, 6H, 2 CH₃ Ts), 2.38 – 2.30 (m, 4H, 2 CH₂-CH₂-CH₃), 1.86 – 1.18 (m, 20H, 8 CH₂ cyclopentyl, 2 CH₂-CH₃), 1.04 – 0.83 (m, 6H, 2 CH₃-CH₂); ¹³C NMR (75.4 MHz, CDCl₃, δ ppm, mixture of rotamers) 173.4, 156.0, 145.7, 145.2, 136.1, 130.1, 127.8, 92.1, 85.6, 58.8, 55.6, 39.2, 35.9, 35.6, 29.9, 29.6, 23.7, 23.4, 21.3, 18.7, 14.1. ESI-HRMS *m/z* calcd for C₂₃H₂₉⁷⁹BrNO₄S [M+H]⁺, 494.0995; found, 494.0993; *m/z* calcd for C₂₃H₂₉⁸¹BrNO₄S [M+H]⁺, 496.0975; found, 496.0972.

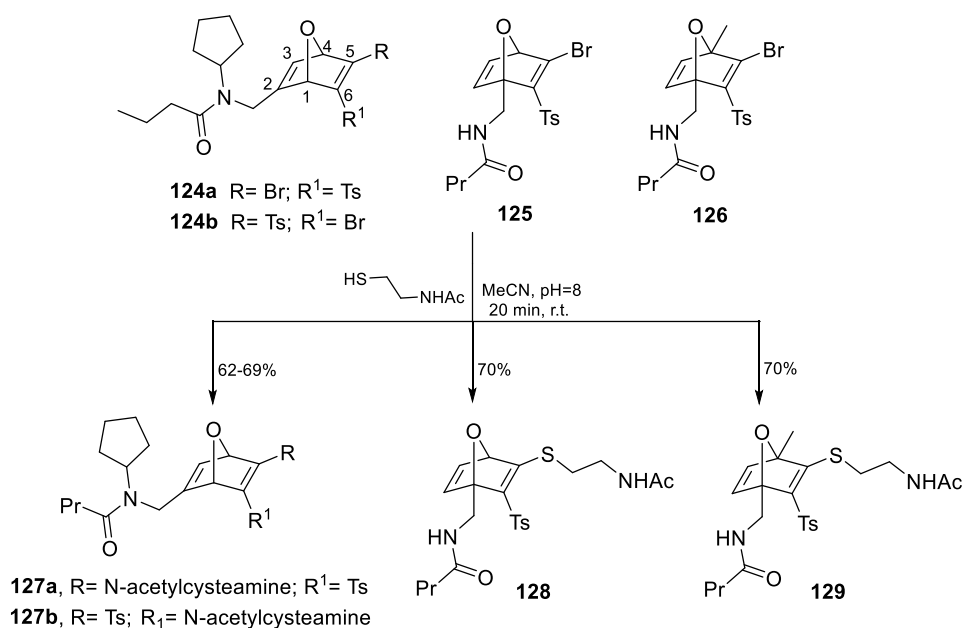
(rac)-N-(((1S,4R)-3-Bromo-2-tosyl-7-oxabicyclo[2.2.1]hepta-2,5-dien-1-yl)methyl)butyramide (125)

To a solution of compound **121** (1.8 g, 10.8 mmol) in toluene (24 mL), **123** (558 mg, 2.2 mmol) was added and the mixture was stirred at 50 °C for 24 h. Then, the solvent was concentrated *in vacuo* and purified by column chromatography on silica gel (Et₂O:Cy, 1:3 → 1:1) to yield compound **125** (615 mg, 67%) as a light-brown sticky solid. ¹H NMR (300 MHz, CDCl₃, δ ppm) 7.73 (d, *J* = 8.4 Hz, 2H, Ts), 7.36 (d, *J* = 7.9 Hz, 2H, Ts), 6.93 (dd, *J* = 5.2, 1.8 Hz, 1H, OND), 6.62 (d, *J* = 5.2 Hz, 1H, OND), 6.09 (br s, 1H, NH), 5.30 (d, *J* = 1.9 Hz, 1H, OND), 4.56 (dd, *J* = 15.0, 8.3 Hz, 1H, CH_a-NH), 3.65 (dd, *J* = 15.0, 3.9 Hz, 1H, CH_b-NH), 2.45 (s, 3H, CH₃ Ts), 2.21 – 2.08 (m, 2H, CH₂-CH₂-CH₃), 1.64 (sept, *J* = 7.4 Hz, 2H, CH₂-CH₂-CH₃), 0.93 (t, *J* = 7.4 Hz, 3H, CH₃). ¹³C NMR (75.4 MHz, CDCl₃, δ ppm) 173.3 (C=O), 149.4 (qC, OND), 149.3 (qC, OND), 145.8 (qC,

Ts), 143.9 (CH, OND), 140.8 (CH, OND), 135.3 (qC, Ts), 130.3 (2 CH, Ts), 127.9 (2 CH, Ts), 97.5 (qC, OND), 89.3 (CH, OND), 38.8 ($\underline{\text{C}}\text{H}_2\text{-CH}_2\text{-CH}_3$), 38.3 (CH₂-NH), 21.9 (CH₃ Ts), 19.2 (CH₂- $\underline{\text{C}}\text{H}_2\text{-CH}_3$), 13.9 (CH₃). ESI-HRMS m/z calcd for C₁₈H₂₀NO₄⁷⁹BrSNa [M+Na], 448.0187; found, 448.0189; m/z calcd for C₁₈H₂₀NO₄⁸¹BrSNa [M+Na], 450.0165; found, 450.0167.

***N*-(((1*S*,4*R*)-3-Bromo-4-methyl-2-tosyl-7-oxabicyclo[2.2.1]hepta-2,5-dien-1-yl)methyl)butyramide (126)**

To a solution of **122** (1.3 g, 7.4 mmol) in toluene (20 mL), **123** (2.9 g, 11.1 mmol) was added and mixture was stirred at 45 °C for 16 h. Then, the formed precipitate was triturated with toluene and dried over high *vacuum* to give **126** (2.0 g, 61%) as a white solid. ¹H NMR (300 MHz, CDCl₃, δ ppm) 7.73 (d, J = 8.3 Hz, 2H, Ts), 7.35 (d, J = 8.0 Hz, 2H, Ts), 6.71 – 6.51 (m, 2H, OND), 6.06 (br s, 1H, NH), 4.51 (dd, J = 15.0, 8.2 Hz, 1H, $\underline{\text{C}}\text{H}_a\text{-NH}$), 3.62 (dd, J = 15.0, 3.9 Hz, 1H, $\underline{\text{C}}\text{H}_b\text{-NH}$), 2.43 (s, 3H, CH₃ Ts), 2.14 (t, J = 7.5 Hz, 2H, $\underline{\text{C}}\text{H}_2\text{-CH}_2\text{-CH}_3$), 1.76 – 1.54 (m, 5H, CH₃ OND, CH₂- $\underline{\text{C}}\text{H}_2\text{-CH}_3$), 0.92 (t, J = 7.4 Hz, 3H, CH₂-CH₂- $\underline{\text{C}}\text{H}_3$). ¹³C NMR (75 MHz, CDCl₃, δ ppm) 173.3 (C=O), 153.4 (qC, OND), 150.2 (qC, OND), 145.6 (qC, Ts), 144.8 (CH, OND), 144.0 (CH, OND), 135.4 (qC, Ts), 130.2 (2 CH, Ts), 127.8 (2 CH, Ts), 96.3 (qC, OND), 95.1 (qC, OND), 38.7 ($\underline{\text{C}}\text{H}_2\text{-CH}_2\text{-CH}_3$), 38.4 (CH₂-NH), 21.9 (CH₃ Ts), 19.2 (CH₂- $\underline{\text{C}}\text{H}_2\text{-CH}_3$), 15.6 (CH₃, OND), 13.8 (CH₂-CH₂- $\underline{\text{C}}\text{H}_3$). ESI-HRMS m/z calcd for C₁₉H₂₂NO₄⁷⁹BrSNa [M+Na], 462.0342; found, 462.0345; m/z calcd for C₁₈H₂₀NO₄⁸¹BrSNa [M+Na], 464.0319; found, 464.0325.



Scheme 84. Thiol substitution on bicyclic systems **124-126**.

***N*-(((1*S*,4*R*)-5-((2-Acetamidoethyl)thio)-6-tosyl-7-oxabicyclo[2.2.1]hepta-2,5-dien-2-yl)methyl)-*N*-cyclopentylbutyramide (**127a**)**

To a solution of compound **124a** (900 mg, 1.8 mmol) in acetonitrile (145 mL) was added *N*-acetylcysteamine (197 mg, 1.7 mmol) in acetonitrile (5.9 mL) and a phosphate-buffered saline (pH=8, 80 mL). After 20 min., the reaction was evaporated, the crude was diluted with EtOAc and washed with water. The organic phase was separated, and the aqueous phase was extracted with EtOAc (3x), was dried with anhydrous Na₂SO₄, and concentrated *in vacuo*. The residue was purified by column chromatography on silica gel (MeOH:Et₂O, 1:60 → 1:5) to obtain compound **127a** (545 mg, 62%) as an orange oil. ¹H NMR (300 MHz, CD₃CN, δ ppm, mixture of rotamers) 7.99 – 7.83 (m, 4H, Ts), 7.59 – 7.42 (m, 4H, Ts), 6.89 – 6.54 (m, 2H, 2 H-3), 6.08 – 5.83 (m, 4H, 2 H-1, 2 H-4), 4.87 – 4.61 (m, 2H, 2 CH cyclopentyl), 4.41 – 4.17 (m, 4H, 2 CH₂-N), 4.01 – 3.68 (m, 4H, 2 CH₂-CH₂-CH₃), 3.48 – 3.31 (m, 4H, 2 CH₂-NH), 3.29 – 3.00 (m, 4H, 2 CH₂-S), 2.53 (s, 6H, 2 CH₃ Ts), 1.94 (s, 6H, 2 CH₃ Ac), 1.82 – 1.26 (m, 20H, 8 CH₂ cyclopentyl, 2 CH₂-CH₂-CH₃), 1.11 – 0.85 (m, 6H, 2 CH₃-CH₂); ¹³C NMR

(75.4 MHz, CD₃CN, δ ppm, mixture of rotamers) 171.8, 160.0, 155.4, 139.6, 132.7, 130.8, 127.4, 117.9, 87.6, 86.3, 55.7, 43.1, 40.8, 35.5, 31.7, 29.7, 24.0, 22.5, 21.3, 19.2, 13.8. ESI-HRMS m/z calcd for C₂₇H₃₇N₂O₅S₂ [M+H]⁺, 533.2138; found, 533.2140.

***N*-(((1*S*,4*R*)-6-((2-Acetamidoethyl)thio)-5-tosyl-7-oxabicyclo[2.2.1]hepta-2,5-dien-2-yl)methyl)-*N*-cyclopentylbutyramide (127b)**

The synthesis of compound **127b** followed the same procedure as **127a**, except that the starting material was OND **124b**. Yield= 69%, yellow oil. ¹H NMR (300 MHz, CD₃CN, δ ppm, mixture of rotamers) 7.76 – 7.62 (m, 4H, Ts), 7.40 (d, J = 8.0 Hz, 4H, Ts), 6.80 (s, 2H, 2 NH), 6.47 (s, 2H, 2 H-6), 5.92 – 5.71 (m, 2H, 2 H-3), 5.58 – 5.32 (m, 4H, 2 H-1, 2 H-4), 4.64 – 4.54 (m, 2H, 2 CH cyclopentyl) 4.35 – 4.02 (m, 4H, 2 CH₂-N), 3.86 (m, 4H, 2 CH₂-CH₂-CH₃), 3.52 – 3.15 (m, 4H, 2 CH₂-NH), 3.07 – 2.79 (m, 4H, 2 CH₂-S), 2.42 (s, 6H, 2 CH₃ Ts), 1.85 (s, 6H, 2 CH₃-Ac), 1.71 – 1.16 (m, 20H, 8 CH₂ cyclopentyl, 2 CH₂-CH₂-CH₃), 1.03 – 0.76 (m, 6H, 2 CH₃-CH₂); ¹³C NMR (75.4 MHz, CD₃CN, δ ppm, mixture of rotamers) 174.0, 171.2, 167.0, 156.0, 137.4, 131.0, 127.8, 88.5, 86.1, 59.4, 40.5, 36.0, 32.6, 24.2, 22.9, 21.6, 19.6, 14.2. ESI-HRMS m/z calcd for C₂₇H₃₇N₂O₅S₂ [M+H]⁺, 533.2138; found, 533.2141.

***N*-(((1*S*,4*R*)-3-((2-Acetamidoethyl)thio)-2-tosyl-7-oxabicyclo[2.2.1]hepta-2,5-dien-1-yl)methyl)butyramide (128)**

The synthesis of compound **128** followed the same procedure as **127a**, except that the starting material was OND **125**. Yield= 70%, white solid. ¹H NMR (300 MHz, CD₃CN, δ ppm) 7.68 (d, J = 8.3 Hz, 2H, Ts), 7.40 (d, J = 7.9 Hz, 2H, Ts), 6.91 (ddd, J = 5.3, 2.0, 0.8 Hz, 1H, OND), 6.71 (br s, 1H, NH), 6.58 (d, J = 5.3 Hz, 1H, OND), 6.40 (br s, 1H, NH-CH₂-OND), 5.94 (d, J = 2.0 Hz, 1H, OND), 4.35 (dd, J = 15.0, 7.7 Hz, 1H, Ha-NH), 3.43 (dd, J = 14.9, 4.2 Hz, 1H, Hb-NH), 3.38 – 3.29 (m, 2H, CH₂-NHAc), 3.21 – 2.96 (m, 2H, CH₂-S), 2.42 (s, 3H, CH₃ Ts), 2.05 (t, J = 7.4 Hz, 2H, CH₂-CH₂-CH₃), 1.87 (s, 3H, CH₃ Ac), 1.53 (sept, J = 7.3 Hz, 2H, CH₂-CH₂-CH₃), 0.87 (t, J = 7.4 Hz, 3H, CH₂-CH₂-CH₃).

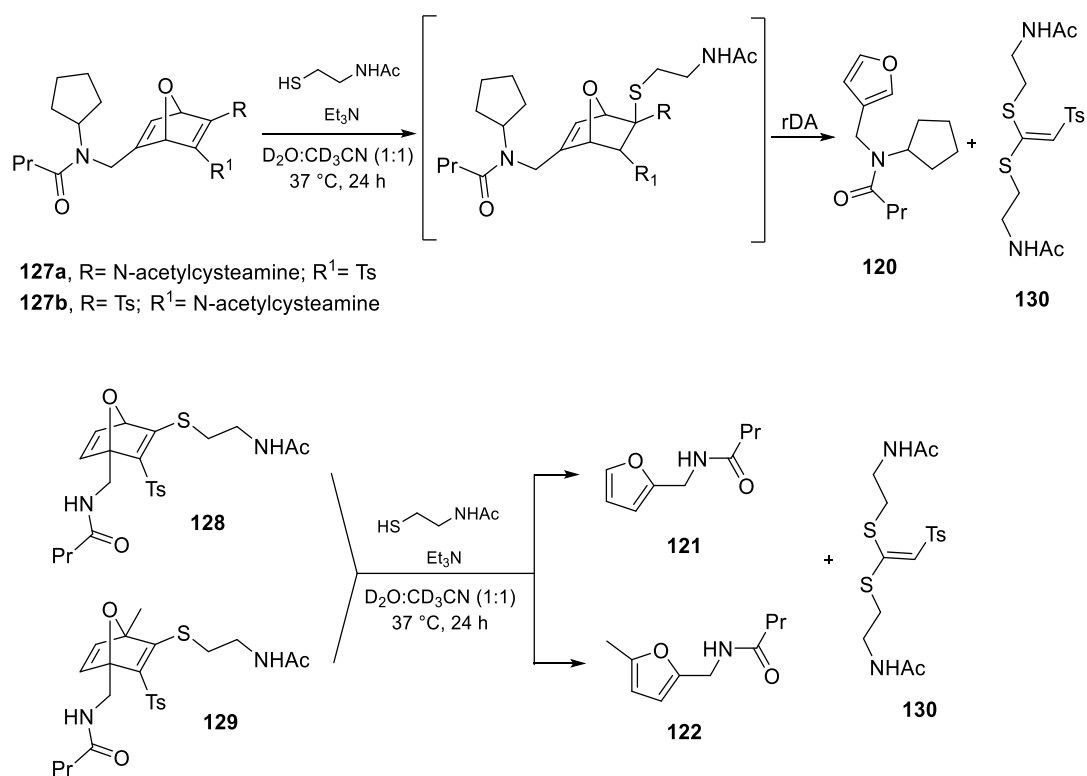
^{13}C NMR (75.4 MHz, CD_3CN , δ ppm) 173.8 (C=O), 172.8 (C=O), 171.4 (qC, OND), 146.1 (qC, Ts), 144.5 (CH, OND), 141.2 (CH, OND), 138.7 (qC, OND), 138.0 (qC, Ts), 131.0 (2 CH, Ts), 127.7 (2 CH, Ts), 97.8 (qC, OND), 86.2 (CH, C-4), 41.1 ($\underline{\text{C}}\text{H}_2\text{-NHAc}$), 38.8 (2 CH, CHa, CHb), 38.7 ($\underline{\text{C}}\text{H}_2\text{-CH}_2\text{-CH}_3$), 32.0 ($\text{CH}_2\text{-S}$), 23.0 (CH_3 , Ac), 21.7 (CH_3 , Ts), 19.8 ($\text{CH}_2\text{-}\underline{\text{C}}\text{H}_2\text{-CH}_3$), 14.0 ($\text{CH}_2\text{-CH}_2\text{-}\underline{\text{C}}\text{H}_3$). ESI-HRMS m/z calcd for $\text{C}_{22}\text{H}_{28}\text{N}_2\text{O}_5\text{S}_2\text{Na}$ [M+Na], 487.1328; found 487.1332.

***N*-(((1*S*,4*R*)-3-((2-Acetamidoethyl)thio)-4-methyl-2-tosyl-7-oxabicyclo[2.2.1]hepta-2,5-dien-1-yl)methyl)butyramide (129)**

The synthesis of compound **129** followed the same procedure as **127a**, except that the starting material was OND **126**. Yield= 70%, white solid. ^1H NMR (300 MHz, CDCl_3 , δ ppm) 7.73 (d, $J = 8.3$ Hz, 2H, Ts), 7.35 (d, $J = 8.0$ Hz, 2H, Ts), 6.67 – 6.64 (m, 2H, OND), 6.64 – 6.58 (m, 1H, NH Ac), 5.97 – 5.85 (m, 1H, NH), 4.49 (dd, $J = 14.8, 7.8$ Hz, 1H, $\underline{\text{C}}\text{H}_a\text{-NH}$), 3.59 (dd, $J = 14.8, 4.0$ Hz, 1H, $\underline{\text{C}}\text{H}_b\text{-NH}$), 3.52 – 3.26 (m, 2H, $\underline{\text{C}}\text{H}_2\text{-NHAc}$), 3.17 – 2.99 (m, 2H, $\text{CH}_2\text{-S}$), 2.43 (s, 3H, CH_3 Ts), 2.10 (t, $J = 7.5$ Hz, 2H, $\underline{\text{C}}\text{H}_2\text{-CH}_2\text{-CH}_3$), 1.96 (s, 3H, CH_3 Ac), 1.75 (s, 3H, CH_3 OND), 1.61 (sept, $J = 7.4$ Hz, 3H, $\text{CH}_2\text{-}\underline{\text{C}}\text{H}_2\text{-CH}_3$), 0.91 (t, $J = 7.4$ Hz, 3H, $\text{CH}_2\text{-CH}_2\text{-}\underline{\text{C}}\text{H}_3$). ^{13}C NMR (75.4 MHz, CDCl_3 , δ ppm) 173.2 (C=O), 170.7 (C=O), 168.4 (qC, OND), 151.0 (qC, OND), 145.2 (qC, Ts), 144.6 (CH, OND), 144.5 (CH, OND), 136.8 (qC, Ts), 130.2 (2 CH, Ts), 127.4 (2 CH, Ts), 96.3 (qC, OND), 95.5 (qC, OND), 39.8 ($\underline{\text{C}}\text{H}_2\text{-NHAc}$), 38.7 ($\underline{\text{C}}\text{H}_2\text{-CH}_2\text{-CH}_3$), 38.6 (2 CH, CHa, CHb), 33.5 ($\text{CH}_2\text{-S}$), 23.3 (CH_3 , Ac), 21.8 (CH_3 , Ts), 19.2 ($\text{CH}_2\text{-}\underline{\text{C}}\text{H}_2\text{-CH}_3$), 16.3 (CH_3 OND), 13.8 ($\text{CH}_2\text{-CH}_2\text{-}\underline{\text{C}}\text{H}_3$). ESI-HRMS m/z calcd for $\text{C}_{23}\text{H}_{30}\text{N}_2\text{O}_5\text{S}_2\text{Na}$ [M+Na], 501.1487; found, 501.1488.

General procedure for rDA at pH 12

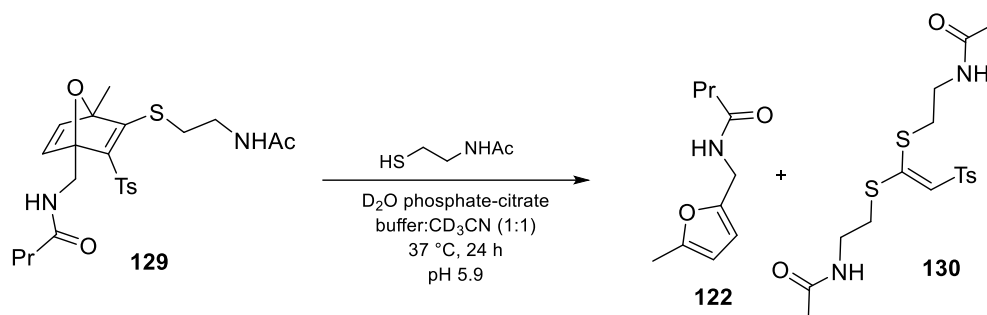
To a solution of the OND (1 eq) in D_2O : CD_3CN (0.2 mL) in an NMR tube, was added *N*-acetylcysteamine (4 eq) in D_2O : CD_3CN (0.2 mL) and Et_3N (4 eq) in D_2O : CD_3CN (0.2 mL). The reaction was left at 37 °C and was checked by NMR every 15-60 min for 24 h to monitor the rate of formation of the corresponding furan derivative.



Scheme 85. Kinetic studies of rDA reaction of **127-129**.

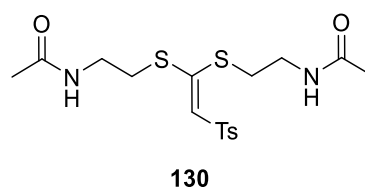
General procedure for rDA at pH 5.9

To a solution of a phosphate-citrate buffer:CD₃CN (1:1, 0.2 mL) in an NMR tube, OND (1 eq) in a phosphate-citrate buffer: CD₃CN (1:1) (0.2 mL) and *N*-acetylcysteamine (4 eq) in a phosphate-citrate buffer: CD₃CN (0.2 mL) were added. The reaction was left at 37 °C and was checked by NMR after 1 hour and every subsequent 15 mins. The deuterated phosphate-citrate buffer was freshly prepared by adding K₂HPO₄ (178 mg), citric acid (96 mg) and NaOH (6 mg) in D₂O (10 mL).

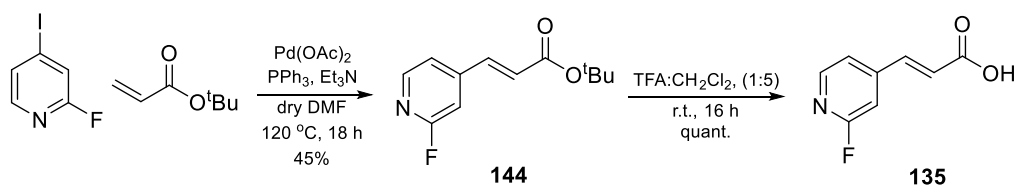


Scheme 86. Kinetic studies of rDA reaction of **129** at pH 5.9.

***N,N'*-(((2-Tosylethene-1,1-diyl)bis(sulfanediyl))bis(ethane-2,1-diyl))diacetamide (**130**)**



^1H NMR (300 MHz, CDCl_3 , δ ppm) 7.84 (d, $J = 8.3$ Hz, 2H, Ts), 7.33 (d, $J = 8.0$ Hz, 2H, Ts), 6.95 – 6.75 (m, 2H, 2 NH), 6.60 (s, 1H, $\text{CH}=\text{CS}$), 3.42 (q, $J = 6.0$ Hz, 2H, $\text{CH}_2\text{-NH}$), 3.35 (q, $J = 6.2$ Hz, 2H, $\text{CH}_2\text{-NH}$), 3.09 (t, $J = 6.2$ Hz, 2H, $\text{CH}_2\text{-S}$), 3.01 (t, $J = 6.2$ Hz, 2H, $\text{CH}_2\text{-S}$), 2.42 (s, 3H, CH_3 Ts), 1.98 (s, 3H, CH_3 Ac), 1.95 (s, 3H, CH_3 Ac). ESI-LRMS m/z 439.08 [M+Na].



Scheme 87. Synthesis of carboxylic acid derivative **135**.

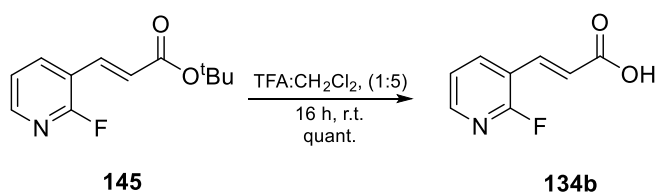
(*E*)-*tert*-Butyl 3-(2-fluoropyridin-4-yl)acrylate (144**)**

Palladium (II) acetate (40 mg, 179 μmol), triphenylphosphine (94 mg, 359 μmol), triethylamine (1.25 mL, 8.97 mmol) and *tert*-butyl acrylate (2.6 mL, 17.9 mmol) were

added to a solution of 2-fluoro-4-iodopyridine (400 mg, 1.8 mmol) in dry DMF (4.4 mL). The reaction mixture was heated under argon at 120 °C for 18 h. After cooling to r.t., H₂O was added, and the aq. phase was extracted EtOAc (3x). The combined organic phases were dried with Na₂SO₄, filtered, and concentrated *in vacuo*. The resulting crude was purified by column chromatography on silica gel (EtOAc:Cy, 1:30 → 1:20), yielding compound **144** (179 mg, 45%) as a yellow solid. ¹H NMR (300 MHz, CDCl₃, δ ppm) 8.22 (d, *J* = 5.2 Hz, 1H, Py), 7.47 (d, *J* = 16.0 Hz, 1H, CH=CHCO₂^tBu), 7.24 (d, *J* = 5.3 Hz, 1H, Py), 6.97 (s, 1H, Py), 6.51 (d, *J* = 16.0 Hz, 1H, CH=CHCO₂^tBu), 1.53 (s, 9H, (CH₃)₃-C); ¹³C NMR (75.4 MHz, CDCl₃, δ ppm) 165.0 (C=O), 164.6 (d, ¹*J*_{C,F} = 239 Hz, C-F Py), 148.6 – 148.4 (d, ³*J*_{C,F} = 15.1 Hz, CH Py), 147.7 (d, ⁴*J*_{C,F} = 8.3 Hz, qC Py), 139.3 (CH=CHCO₂^tBu), 126.3 (CH=CHCO₂^tBu), 119.6 (CH, Py), 107.9 (d, ²*J*_{C,F} = 37.7 Hz, CH Py), 81.7 ((CH₃)₃-C), 28.2 (3 CH₃, ^tBu). ESI-HRMS *m/z* calcd for C₁₂H₁₅FNO₂ [M+H]⁺, 224.1081; found, 224.1080.

(*E*)-3-(2-Fluoropyridin-4-yl)acrylic acid (**135**)

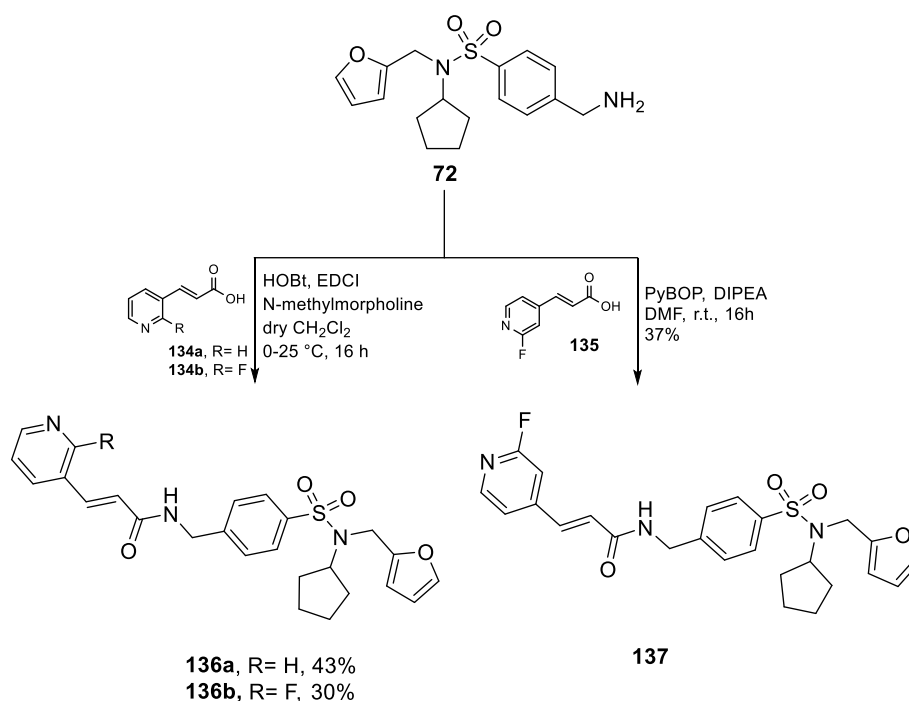
A solution of **144** (185 mg, 829 μmol) in dry DCM (6.2 mL) was treated with TFA (1.6 mL, 19.9 mmol) and the resulting solution was stirred under argon for 18 h at r.t. Then, the reaction was evaporated *in vacuo*, and co-evaporated with toluene to yield compound **135** as a white solid which was used in the next step without any further purification. ESI-HRMS *m/z* calcd for C₈H₇FNO₂[M+H]⁺, 168.0455; found, 168.0454.



Scheme 88. Synthesis of carboxylic acid derivative **134b**.

(*E*)-3-(2-Fluoropyridin-3-yl)acrylic acid (**134b**)

A solution of **145**²⁴ (260 mg, 1.2 mmol) in dry DCM (8.7 mL) was treated with TFA (2.2 mL, 27.8 mmol) and the resulting solution was stirred under argon for 18 h at r.t. Then, the reaction mixture was evaporated *in vacuo*, and co-evaporated with toluene to yield compound **134b** as a white solid which was used in the next step without any further purification. ESI-HRMS *m/z* calcd for C₈H₇FNO₂ [M+H]⁺, 168.0455; found 168.0454.



Scheme 89. Synthesis of final compounds **136a-b** and **137**.

(E)-N-(4-(N-Cyclopentyl-N-(furan-2-ylmethyl)sulfamoyl)benzyl)-3-(pyridin-3-yl)acrylamide (136a**)**

Under N₂ atmosphere, HOBT (121 mg, 897 μmol), EDCI (172 mg, 897 μmol) and **134a** (134 mg, 897 μmol) were added sequentially to a cooled solution of **72** (200 mg, 598 μmol) in dry CH₂Cl₂ (3.2 mL). After stirring at 0 °C for 10 min, N-methylmorpholine (184 μL, 1.7 mmol) was added dropwise under stirring at 0 °C. The mixture was cooled to r.t. and it was stirred overnight. A sat. aq. sol. of NaHCO₃ (6.3 mL) was added and stirred vigorously for 5 min. The aqueous layer was extracted with CH₂Cl₂ (3x), and

the combined organic extracts were washed with brine and dried over anhydrous Na_2SO_4 . Then, the solvent was evaporated *in vacuo* and the residue purified by column chromatography on silica gel (MeOH:EtOAc, 1:80 \rightarrow 1:20) to give compound **136a** (121 mg, 43%) as a white solid. ^1H NMR (300 MHz, CDCl_3 , δ ppm) 8.58 (s, 1H, Py), 8.45 (d, $J = 5.6$ Hz, 1H, Py), 7.74 – 7.63 (m, 1H, Py), 7.59 – 7.45 (m, 3H, C-CH=CH, 1H furan, 1H Py), 7.34 – 7.08 (m, 4H, Ph), 6.64 – 6.60 (m, 1H, NH), 6.46 (d, $J = 15.7$ Hz, 1H, CH=CH-CO), 6.25 – 6.09 (m, 2H, furan), 4.52 (d, $J = 6.0$ Hz, 2H, NH-CH₂-C), 4.25 (s, 2H, N-CH₂-CO), 4.13 – 3.95 (m, 1H, CH cyclopentyl), 1.82 – 1.01 (m, 8H, 4 CH₂ cyclopentyl); ^{13}C NMR (75.4 MHz, CDCl_3 , δ ppm) 165.5 (C=O), 151.5 (qC, furan), 150.6 (CH, Py), 149.3 (CH, Py), 143.3 (qC, Ph), 142.0 (CH, Ph), 139.8 (CH, furan), 138.2 (qC, Ph), 134.7 (CH, Py), 130.7 (qC, Py), 128.1 (2 CH, Ph), 127.5 (C-CH=CH, 1 CH Py), 123.9 (CH, Ph), 122.6 (CH=CH-CO), 110.7 (CH, furan), 108.9 (CH, furan), 59.3 (CH, cyclopentyl), 43.2 (NH-CH₂-C), 40.3 (N-CH₂-CO), 29.4 (2 CH₂, cyclopentyl), 23.6 (2 CH₂, cyclopentyl). ESI-MS m/z calc for $\text{C}_{25}\text{H}_{28}\text{N}_3\text{O}_4\text{S}$ $[\text{M}+\text{H}]^+$, 466.1795; found, 466.1790.

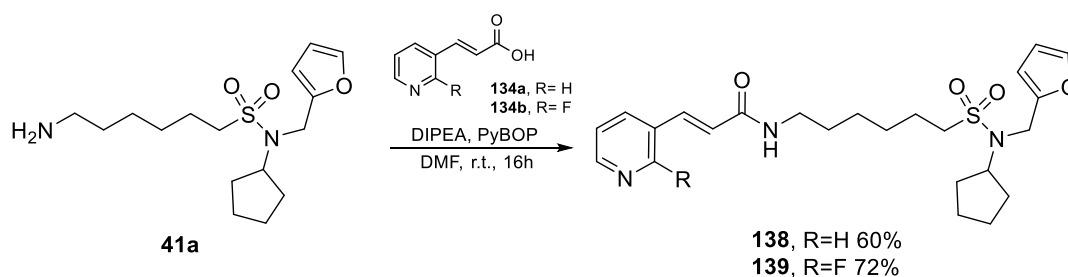
(E)-N-(4-(N-Cyclopentyl-N-(furan-2-ylmethyl)sulfamoyl)benzyl)-3-(2-fluoropyridin-3-yl)acrylamide (136b)

The synthesis of compound **136b** followed the same procedure as **136a**, except that the starting material was carboxylic acid derivative **134b**. Column chromatography (acetone:Et₂O, 1:80 \rightarrow 1:20), yield= 30%, yellow solid. ^1H NMR (300 MHz, CDCl_3 , δ ppm) 8.18 (d, $J = 5.4$ Hz, 1H, Py), 7.92 – 7.87 (m, 1H, Py), 7.74 – 7.50 (m, 3H, C-CH=CH, 1H furan, 1H Py), 7.37 – 7.32 (m, 2H, Ph), 7.29 – 7.19 (m, 2H, Ph), 6.70 (d, $J = 15.8$ Hz, 1H, CH=CH-CO), 6.53 – 6.38 (m, 1H, NH), 6.35 – 6.18 (m, 2H, furan), 4.62 (m, 2H, $J = 5.2$ Hz, NH-CH₂-C), 4.35 (s, 2H, N-CH₂-CO), 4.27 – 4.02 (m, 1H, CH cyclopentyl), 1.76 – 1.32 (m, 8H, 4 CH₂ cyclopentyl); ^{13}C NMR (75.4 MHz, CDCl_3 , δ ppm) 165.5 (C=O), 161.4 (d, $^1J_{\text{C,F}} = 244$ Hz, C-F Py), 151.6 (CH, furan), 148.1 (d, $^3J_{\text{C,F}} = 15.1$ Hz, CH Py), 143.0 (qC, Ph), 142.6 (qC, Ph), 142.0 (CH, furan), 140.5 (CH, Py), 140.0 (CH, Ph), 133.6 (CH, Py), 128.1 (C-CH=CH), 127.6 (2 CH, Ph), 125.4 (CH=CH-CO), 122.0 (CH, Ph), 117.9 (d, $^2J_{\text{C,F}} = 26.4$ Hz, qC Py), 110.7 (CH, furan), 108.9 (CH, furan), 59.3 (CH, cyclopentyl), 43.3 (NH-

$\underline{\text{C}}\text{H}_2\text{-C}$), 40.3 (N- $\underline{\text{C}}\text{H}_2\text{-CO}$), 29.4 (2 CH_2 , cyclopentyl), 23.6 (2 CH_2 , cyclopentyl). ESI-HRMS m/z calcd for $\text{C}_{25}\text{H}_{27}\text{FN}_3\text{O}_4\text{S}$ $[\text{M}+\text{H}]^+$, 484.1701; found, 484.1703.

(E)-N-(4-(N-Cyclopentyl-N-(furan-2-ylmethyl)sulfamoyl)benzyl)-3-(2-fluoropyridin-4-yl)acrylamide (137)

To a solution of **72** (110 mg, 329 μmol) in DMF (2 mL), was added DIPEA (275 μL , 1.6 mmol), **135** (66 mg, 395 μmol) and PyBOP (257 mg, 493 μmol). The resulting mixture was stirred overnight at r.t., and then the solvent was evaporated, and the crude dissolved in EtOAc, washed with HCl 1 M, a sat. aq. sol. of NaHCO_3 and H_2O . The organic phase was dried over anhydrous Na_2SO_4 , concentrated *in vacuo* and then purified by column chromatography on silica gel (acetone:Et₂O, 1:120 \rightarrow 1:90) to yield compound **137** (58.5 mg, 37 %) as a white solid. ^1H NMR (300 MHz, CDCl_3 , δ ppm) 8.13 (d, $J = 5.4$ Hz, 1H, Py), 7.59 – 7.38 (m, 3H, 2H Ph, 1H furan), 7.31 – 7.12 (m, 4H, 2H Ph, CO- $\underline{\text{C}}\text{H}=\underline{\text{C}}\text{H}$, 1H Py), 7.11 – 6.98 (m, 1H, NH), 6.95 (s, 1H, Py), 6.73 (d, $J = 15.7$ Hz, 1H, CO- $\underline{\text{C}}\text{H}=\underline{\text{C}}\text{H}$), 6.29 – 6.12 (m, 2H, furan), 4.67 – 4.40 (m, 2H, $\underline{\text{C}}\text{H}_2\text{-NH}$), 4.29 (s, 2H, $\text{CH}_2\text{-furan}$), 4.14 – 3.98 (m, 1H, CH cyclopentyl), 1.76 – 1.22 (m, 8H, 4(CH_2) cyclopentyl); ^{13}C NMR (75.4 MHz, CDCl_3 , δ ppm) 165.0 (C=O), 164.5 ($^1J_{\text{C,F}} = 239$ Hz, C-F Py), 151.4 (qC, furan), 148.3 (d, $^3J_{\text{C,F}} = 15.1$ Hz, CH Py), 143.2 (qC, Ph), 142.1 (CO- $\underline{\text{C}}\text{H}=\underline{\text{C}}\text{H}$), 139.4 (qC, Ph), 137.3 (CH, furan), 128.0 (2 CH, Ph), 127.3 (2 CH, Ph), 126.6 (CO- $\underline{\text{C}}\text{H}=\underline{\text{C}}\text{H}$), 119.9 (d, $^4J_{\text{C,F}} = 3.77$ Hz, CH, Py), 110.7 (CH, furan), 108.9 (CH, furan), 107.6 (d, $^2J_{\text{C,F}} = 37.7$ Hz, CH, Py), 59.3 (CH, cyclopentyl), 43.1 ($\text{CH}_2\text{-NH}$), 40.4 (OC- $\text{CH}_2\text{-CN}$), 29.3 (2 CH_2 , cyclopentyl), 23.5 (2 CH_2 , cyclopentyl). ESI-HRMS m/z calcd for $\text{C}_{25}\text{H}_{27}\text{FN}_3\text{O}_4\text{S}$ $[\text{M}+\text{H}]^+$, 484.1701; found, 484.1704.



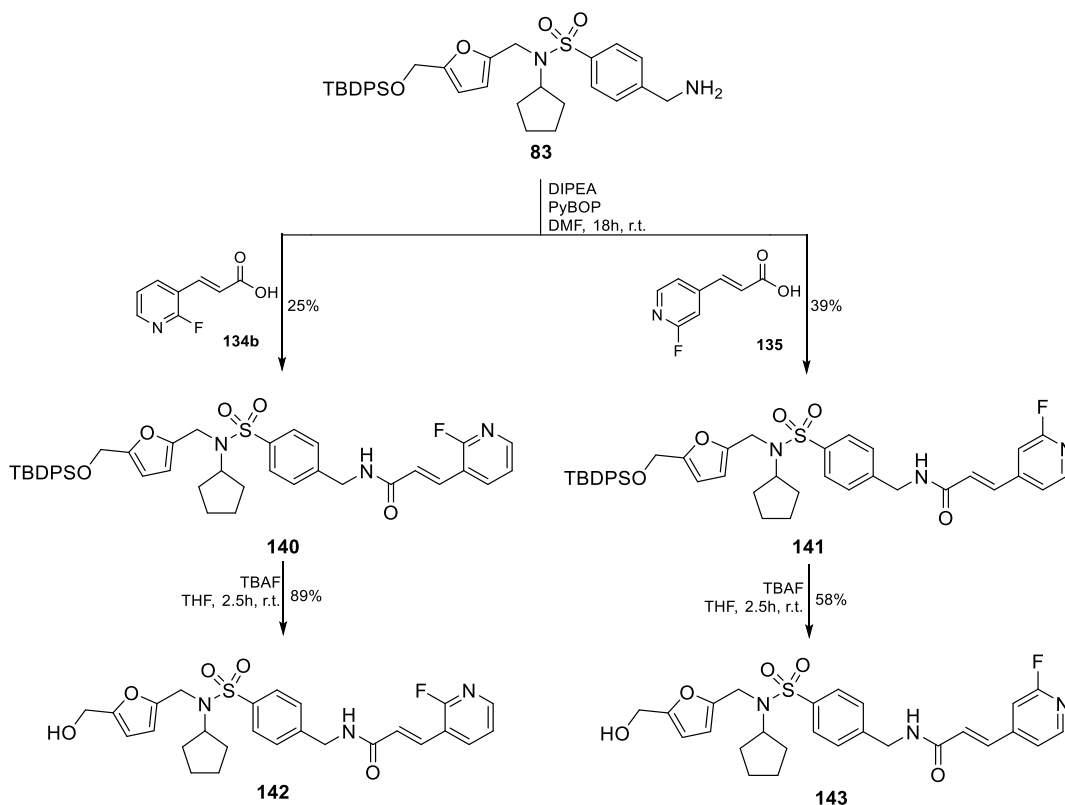
Scheme 90. Synthesis of final compounds **138** and **139**.

(E)-N-(6-(N-Cyclopentyl-N-(furan-2-ylmethyl)sulfamoyl)hexyl)-3-(pyridin-3-yl)acrylamide (138**)**

The synthesis of compound **138** followed the same procedure as **137**, except that the starting material was carboxylic acid **134a** and amine **41a**. Column chromatography (Acetone:Et₂O, 1:8 → 1:2), yield= 60%, white solid. ¹H NMR (300 MHz, CDCl₃, δ ppm) 8.73 (d, *J* = 2.2 Hz, 1H, Py), 8.54 (dd, *J* = 4.9, 1.6 Hz, 1H, Py), 7.78 (dt, *J* = 8.0, 1.9 Hz, 1H, Py), 7.59 (d, *J* = 15.7 Hz, 1H, CH=CH-Py), 7.35 (dd, *J* = 1.9, 0.9 Hz, 1H, furan), 7.30 (dd, *J* = 7.9, 4.8 Hz, 1H, Py), 6.51 (d, *J* = 15.7 Hz, 1H, CH=CH), 6.35 – 6.25 (m, 2H, furan), 6.12 (br t, 1H, NH, amide), 4.35 (s, 2H, CH₂-furan), 4.14 (quint, *J* = 8.5 Hz, 1H, CH, cyclopentyl), 3.36 (q, *J* = 6.9 Hz, 2H, NH-CH₂), 2.82 – 2.71 (m, 2H, SCH₂), 1.93 – 1.80 (m, 2H, CH₂, cyclopentyl), 1.80 – 1.48 (m, 10H, CH₂, cyclopentyl/hexyl), 1.45 – 1.20 (m, 4H, CH₂, hexyl). ¹³C NMR (75.4 MHz, CDCl₃, δ ppm) 165.3 (C=O), 151.4 (qC, furan), 150.2 (CH, Py), 149.1 (CH, Py), 142.2 (CH, furan), 137.1 (CH, alkene), 134.7 (CH, Py), 131.0 (qC, Py), 123.9 (CH, Py), 123.3 (CH, alkene), 110.8 (CH, furan), 109.2 (CH, furan), 59.3 (CH, cyclopentyl), 53.2 (SCH₂) 40.0 (CH₂-furan), 39.6 (NH-CH₂), 30.0 (2 CH₂, cyclopentyl), 29.3 (CH₂, hexyl), 27.9 (CH₂, hexyl), 26.4 (CH₂, hexyl), 23.5 (2 CH₂, cyclopentyl), 23.3 (CH₂, hexyl). ESI-HRMS *m/z* calcd for C₂₄H₃₄N₃O₄S [M+H]⁺, 460.2270; found, 460.2264.

(E)-N-(6-(N-Cyclopentyl-N-(furan-2-ylmethyl)sulfamoyl)hexyl)-3-(2-fluoropyridin-3-yl)acrylamide (139**)**

The synthesis of compound **139** followed the same procedure as **137**, except that the starting material was carboxylic acid **134b** and amine **41a**. Column chromatography (Acetone:Et₂O, 1:24 → 1:12), yield= 72%, white solid. ¹H NMR (300 MHz, CDCl₃, δ ppm) 8.15 (br t, *J* = 4.7, 1H, Py), 7.87 (ddd, *J* = 9.6, 7.5, 2.0 Hz, 1H, Py), 7.58 (d, *J* = 15.8 Hz, 1H, CH=CH-Py), 7.36 (dd, *J* = 1.8, 0.9 Hz, 1H, furan), 7.21 (ddd, *J* = 7.4, 4.8, 1.8 Hz, 1H, Py), 6.63 (d, *J* = 15.8 Hz, 1H, CH=CH), 6.36 – 6.26 (m, 2H, furan), 6.01 (br t, 1H, NH, acrylamide), 4.36 (s, 2H, CH₂-furan), 4.14 (quint, *J* = 8.3 Hz, 1H, CH, cyclopentyl), 3.37 (q, *J* = 6.9 Hz, 2H, NH-CH₂), 2.82 – 2.71 (m, 2H, SCH₂), 1.93 – 1.48 (m, 12H, CH₂, cyclopentyl, hexyl), 1.56 – 1.16 (m, 4H, CH₂ hexyl). ¹³C NMR (75.4 MHz, CDCl₃, δ ppm) 165.3 (C=O), 161.4 (d, ¹*J*_{C,F} = 244.5 Hz, CF, Py), 151.4 (qC, furan), 147.7 (CH, Py) 142.2 (CH, furan), 140.5 (CH, Py), 132.6 (d, *J*_{C,F} = 4.3 Hz, CH=CH), 126.1 (d, ¹*J*_{C,F} = 8.0 Hz, CH=CH), 122.0 (CH, Py), 118.3 (qC, Py), 110.8 (CH, furan), 109.2 (CH, furan), 59.3 (CH, cyclopentyl), 53.2 (SCH₂), 40.0 (CH₂-furan), 39.6 (NH-CH₂), 30.0 (2 CH₂, cyclopentyl), 29.3 (CH₂, hexyl), 27.9 (CH₂, hexyl), 26.4 (CH₂, hexyl), 23.6 (2 CH₂, cyclopentyl), 23.4 (CH₂, hexyl). ESI-HRMS *m/z* calcd for C₂₄H₃₂N₃O₄SNa [M+Na], 500.1995; found, 500.1987.



Scheme 91. Parallel synthetic routes to inhibitors **142** and **143**.

(E)-N-(4-(N-Cyclopentyl-N-((5-(hydroxymethyl)furan-2-yl)methyl)sulfamoyl)benzyl)-3-(2-fluoropyridin-3-yl)acrylamide (142**)**

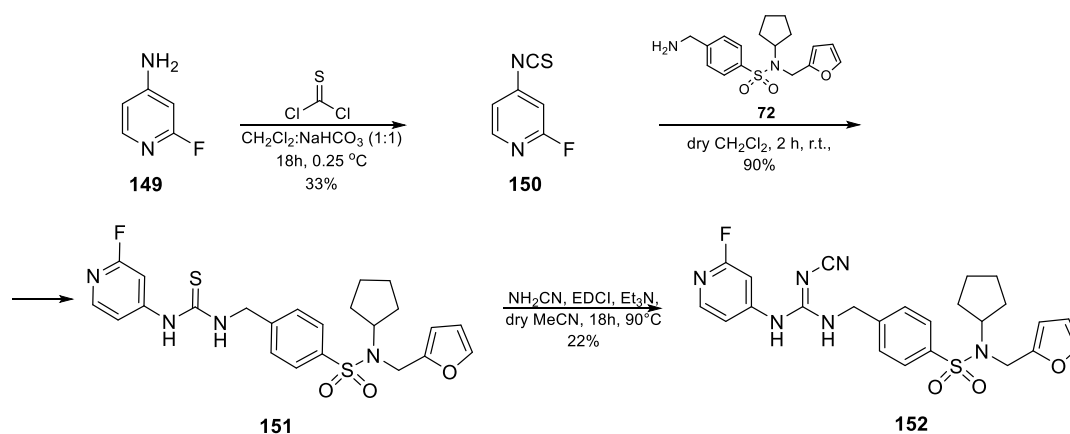
To a solution of **83** (90 mg, 149 μmol) in DMF (1.75 mL), was added DIPEA (125 μL , 717 μmol), **134b** (32 mg, 194 μmol) and PyBOP (117 mg, 224 μmol) and the resulting mixture was stirred overnight at r.t. Then, the solvent was evaporated *in vacuo*, the crude was dissolved in EtOAc and was washed with HCl 1 M, with sat. aq. sol. of NaHCO_3 and H_2O . The organic phase was dried over anhydrous Na_2SO_4 , concentrated *in vacuo* and then purified by column chromatography on silica gel (acetone: Et_2O , 1:90) to yield compound **140** (28.4 mg, 25%) as a white solid. ESI-HRMS m/z calcd for $\text{C}_{42}\text{H}_{46}\text{FN}_3\text{O}_5\text{SSiNa}$ [$\text{M}+\text{Na}$], 774.2804; found, 774.2810. To a solution of **140** (28 mg, 37 μmol) in THF (1 mL), TBAF (484 μL , 48 μmol , 1M in THF) was added and the resulting mixture was stirred at r.t. for 2.5 h. Then, the solvent was removed under

reduced pressure and the resulting residue was purified by column chromatography on silica gel (acetone:Et₂O, 1:40 → 1:5) to yield compound **142** (16.9 mg, 89%) as a pale green oil. ¹H NMR (300 MHz, CDCl₃, δ ppm) 8.17 (m, 1H, Py), 7.94 – 7.83 (m, 1H, Py), 7.73 – 7.53 (m, 3H, 2H Ph, 1H Py), 7.34 – 7.13 (m, 3H, 2H Ph, CO-CH=CH), 6.84 (t, *J* = 6.0 Hz, 1H, NH), 6.73 (d, *J* = 15.8 Hz, 1H, CO-CH=CH), 6.19 – 6.04 (m, 2H, furan), 4.67 – 4.46 (m, 2H, CH₂-NH), 4.38 (s, 2H, CH₂-furan), 4.33 (s, 2H, CH₂-OH), 4.29 – 4.10 (m, 1H, CH cyclopentyl), 2.23 – 2.03 (m, 1H, OH), 1.81 – 1.45 (m, 8H, 4 CH₂ cyclopentyl). ¹³C NMR (75.4 MHz, CDCl₃, δ ppm) 165.7 (C=O), 163.8 (d, ¹*J*_{C,F} = 242 Hz, C-F Py), 153.9 (qC, furan), 150.8 (qC, furan), 148.0 (d, ³*J*_{C,F} = 16.6 Hz, CH Py), 142.7 (qC, Ph), 140.7 (qC, Py), 133.5 (qC, Ph), 127.7 (2 CH, Ph), 127.5 (2 CH, Ph), 125.6 (CO-CH=CH), 122.1 (qC, Py), 122.1 (CO-CH=CH), 109.9 (CH, furan), 108.5 (CH, furan), 59.4 (CH, cyclopentyl), 57.3 (CH₂-furan), 43.4 (CH₂-NH), 40.3 (CH₂-OH), 29.6 (2 CH₂, cyclopentyl), 23.5 (2 CH₂, cyclopentyl). ESI-HRMS *m/z* calcd for C₂₆H₂₈FN₃O₅Na [M+Na], 536.1626; found 536.1627.

(*E*)-*N*-(4-(*N*-Cyclopentyl-*N*-((5-(hydroxymethyl)furan-2-yl)methyl)sulfamoyl)benzyl)-3-(2-fluoropyridin-4-yl)acrylamide (143**)**

The synthesis of compound **143** followed the same procedure as **142**, except that the starting material was carboxylic acid **135**. Yield= 23% (2 steps), yellow oil. ¹H NMR (300 MHz, CDCl₃, δ ppm) 8.19 (d, *J* = 5.2 Hz, 1H, Py), 7.64 – 7.49 (m, 2H, Ph), 7.38 – 7.20 (m, 4H, 2H Ph, CO-CH=CH, 1H Py), 7.10 (br t, 1H, NH), 7.02 – 6.88 (m, 1H, Py), 6.72 (d, *J* = 15.7 Hz, 1H, CO-CH=CH), 6.22 – 6.00 (m, 2H, furan), 4.60 – 4.53 (m, 2H, CH₂-NH), 4.37 (s, 2H, CH₂-furan), 4.32 (s, 2H, CH₂-OH), 4.29 – 4.21 (m, 1H, CH cyclopentyl), 2.45 – 2.34 (m, 1H, OH), 1.79 – 1.33 (m, 8H, 4 CH₂ cyclopentyl). ¹³C NMR (75.4 MHz, CDCl₃, δ ppm) 164.6 (d, ¹*J*_{C,F} = 238 Hz, C-F Py), 165.1 (C=O), 154.0 (qC, furan), 150.8 (qC, furan), 148.2 (d, ³*J*_{C,F} = 21.9 Hz, CH Py), 142.7 (CO-CH=CH), 140.0 (qC, Ph), 137.5 (qC, Ph), 127.5 (2 CH, Ph), 127.2 (2 CH, Ph), 126.4 (CO-CH=CH), 119.9 (qC, Py), 109.9 (CH furan), 108.5 (CH furan), 107.7 (d, ²*J*_{C,F} = 38.5 Hz, CH Py), 59.4 (CH, cyclopentyl), 57.3 (CH₂-furan), 43.3 (CH₂-NH), 40.3 (CH₂-OH), 29.6 (2 CH₂,

cyclopentyl), 23.5 (2 CH₂, cyclopentyl). ESI-HRMS *m/z* calcd for C₂₆H₂₈FN₃O₅Na [M+Na], 536.1626; found, 536.1624.



Scheme 92. Synthesis of thiourea- and cyanoguanidine-based final compounds **151** and **152**.

2-Fluoro-4-isothiocyanatopyridine (**150**)

2-Fluoro-4-aminopyridine **149** (800 mg, 7 mmol) was dissolved in a 1:1 mixture of CH₂Cl₂ and sat. aq. sol. of NaHCO₃ (20 mL), and thiophosgene (985 mg, 8.56 mmol) was added dropwise at 0 °C and the mixture was stirred at r.t. overnight. Then, the reaction was filtered, the aqueous layer was extracted with CH₂Cl₂ (3x), and the combined organic layers were dried with anh. Na₂SO₄, filtered and concentrated *in vacuo*. The residue was purified by column chromatography on silica gel (EtOAc:Cy, 1:30 → 1:15) to yield compound **150** (364 mg, 33%) as a yellow oil. ¹H NMR (300 MHz, CDCl₃, δ ppm) 8.21 (d, *J* = 5.4 Hz, 1H), 7.02 (d, *J* = 5.4, 1H), 6.74 (s, 1H). ¹³C NMR (75.4 MHz, CDCl₃, δ ppm) 165.1 (d, ¹*J*_{C,F} = 240 Hz, C-F), 149.6 (d, ³*J*_{C,F} = 16.6 Hz, CH), 144.7 (qC), 142.8 (NCS), 119.0 (d, ⁴*J*_{C,F} = 5.28 Hz, CH), 106.6 (d, ²*J*_{C,F} = 40.7 Hz, CH). ESI-HRMS *m/z* calcd for C₆H₄FN₂S [M+H]⁺, 155.0074; found, 155.0070.

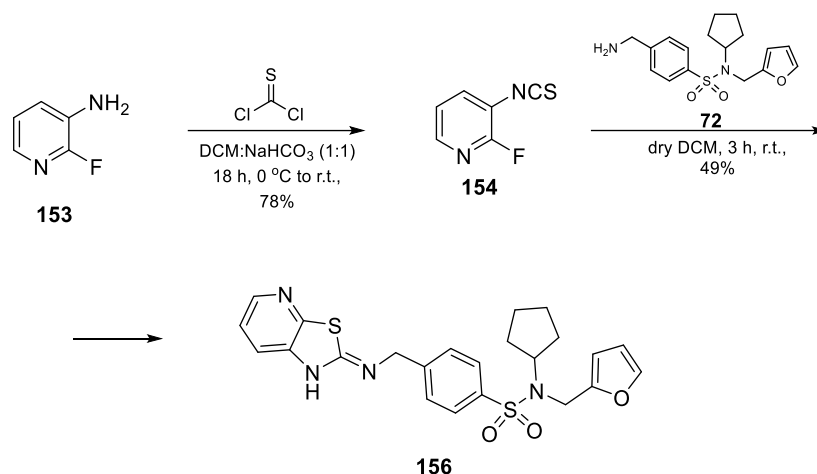
N-Cyclopentyl-4-((3-(2-fluoropyridin-4-yl)thioureido)methyl)-*N*-(furan-2-ylmethyl)benzenesulfonamide (**151**)

Compound **150** (253 mg, 1.6 mmol) was added to a solution of **72** (220 mg, 657 μmol) in dry CH_2Cl_2 (12 mL) and the resulting mixture was stirred at r.t. for 1 h. Then, the solvent was removed *in vacuo* and the resulting residue was purified by column chromatography on silica gel (EtOAc:Cy, 1:4 \rightarrow 1:1) to yield compound **151** (288 mg, 90%) as a colourless oil. ^1H NMR (300 MHz, CDCl_3 , δ ppm) 8.71 (s, 1H, NH), 8.00 (d, $J = 5.7$ Hz, 1H, Py), 7.58 – 7.50 (m, 1H, Py), 7.50 – 7.40 (m, 3H, 2H Ph, NH), 7.36 (d, $J = 5.7$ Hz, 1H, Py), 7.34 – 7.26 (m, 2H, Ph), 7.27 – 7.21 (m, 1H, furan), 6.35 – 6.06 (m, 2H, furan), 4.92 (d, $J = 5.5$ Hz, 2H, NH- $\underline{\text{CH}_2}$), 4.32 (s, 2H, CH_2 -furan), 4.16 – 3.98 (m, 1H, CH cyclopentyl), 1.71 – 1.28 (m, 8H, 4 CH_2 cyclopentyl). ^{13}C NMR (75.4 MHz, CDCl_3 , δ ppm) 180.9 (C=S), 164.6 (d, $^1J_{\text{C,F}} = 236$ Hz, C-F Py) 150.8 (qC, furan), 147.6 (d, $^3J_{\text{C,F}} = 16.6$ Hz, CH Py), 143.0 (qC, Ph), 142.4 (CH, furan), 138.7 (qC, Ph), 128.3 (2 CH, Ph), 127.2 (2 CH, Ph), 113.3 (d, $^4J_{\text{C,F}} = 3.8$ Hz, CH Py), 110.8 (CH, furan), 109.0 (CH, furan), 100.0 (d, $^2J_{\text{C,F}} = 43.0$ Hz, CH Py), 59.5 (CH, cyclopentyl), 47.5 (NH- $\underline{\text{CH}_2}$), 40.5 ($\underline{\text{CH}_2}$ -furan), 29.4 (2 CH_2 , cyclopentyl), 23.6 (2 CH_2 , cyclopentyl). ESI-HRMS m/z calcd for $\text{C}_{23}\text{H}_{26}\text{FN}_4\text{O}_3\text{S}_2$ $[\text{M}+\text{H}]^+$, 489.1425; found, 489.1414.

(E)-4-((2-Cyano-3-(2-fluoropyridin-4-yl)guanidino)methyl)-N-cyclopentyl-N-(furan-2-ylmethyl)benzenesulfonamide (152)

To a solution of **152** (115 mg, 235 μmol) in dry acetonitrile (3 mL) was added EDCI (54.1 mg, 282 μmol), triethylamine (31.0 mg, 306 μmol) and cyanamide (14.8 mg, 353 μmol) under nitrogen atmosphere. The reaction was stirred at r.t. for 1 h, refluxed overnight and concentrated to dryness. The residue was purified by column chromatography on silica gel (EtOAc:Cy, 1:1 \rightarrow 3:1) to give compound **152** (26 mg, 22%) as a white solid. ^1H NMR (300 MHz, CDCl_3 , δ ppm) 8.80 (s, 1H, NH), 7.97 (d, $J = 5.5$ Hz, 1H, Py), 7.55 (d, $J = 8.1$ Hz, 2H, Ph), 7.33 (d, $J = 8.1$ Hz, 2H, Ph), 7.03 (d, $J = 5.5$ Hz, 1H, Py), 6.89 (s, 1H, Py), 6.32 – 6.14 (m, 2H, furan), 4.62 (d, 2H, $J = 5.5$ Hz, NH- $\underline{\text{CH}_2}$), 4.31 (s, 2H, CH_2 -furan), 4.22 – 4.00 (m, 1H, CH cyclopentyl), 1.79 – 1.15 (m, 8H, 4 CH_2 , cyclopentyl). ^{13}C NMR (75.4 MHz, CDCl_3 , δ ppm) 165.2 (d, $^1J_{\text{CF}} = 237$ Hz, C-F Py), 158.0 (C=N), 151.7 (qC, furan), 148.8 (d, $^3J_{\text{CF}} = 17.3$ Hz, CH Py), 142.0 (qC, Ph), 140.6

(qC, Ph), 128.6 (CH, Ph), 128.1 (2 CH, Ph), 114.1 (CH, Py), 111.3 (CH, furan), 109.5 (CH, furan), 101.3 (d, $^2J_{CF} = 43.0$ Hz, CH Ph), 59.9 (CH, cyclopentyl), 46.2 (NH-CH₂), 40.9 (CH₂-furan), 29.9 (2 CH₂, cyclopentyl), 24.1 (2 CH₂, cyclopentyl). ESI-HRMS m/z calcd for C₂₄H₂₆FN₆O₃S [M+H]⁺, 497.1764; found, 497.1766.



Scheme 93. Synthetic route to compound **156**.

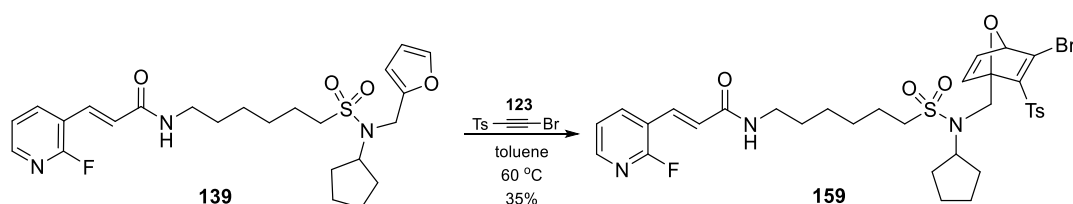
2-Fluoro-3-isothiocyanatopyridine (**154**)

The synthesis of **154** followed the same procedure as **150**, except that the starting material was 2-fluoro-3-aminopyridine **153**. Column chromatography (EtOAc:Cy, 1:10 → 1:4), yield= 78%, light-green oil. ¹H NMR (300 MHz, CDCl₃, δ ppm) 8.14 – 7.95 (m, 1H), 7.63 – 7.47 (m, 1H), 7.23 – 7.09 (m, 1H). ¹³C NMR (75.4 MHz, CDCl₃, δ ppm) 158.8 (d, $^1J_{C,F} = 242$ Hz, C-F), 144.8 (d, $^3J_{C,F} = 13.6$ Hz, CH), 135.7 (CH), 134.2 (NCS), 122.1 (CH), 117.3 (d, $^2J_{C,F} = 30.2$ Hz, qC). ESI-HRMS m/z calcd for C₆H₄FN₂S [M+H]⁺, 155.0074; found, 155.0071.

(Z)-N-Cyclopentyl-N-(furan-2-ylmethyl)-4-((thiazolo[5,4-b]pyridin-2(1H)-ylideneamino)methyl)benzenesulfonamide (**156**)

The synthesis of **156** followed the same procedure as **151**, except that the starting material was isothiocyanate **154**. Column chromatography (EtOAc:Cy, 1:4 → 1:1),

yield= 78%, white solid. ^1H NMR (300 MHz, CDCl_3 , δ ppm) 8.28 – 8.09 (m, 1H, Py), 7.77 – 7.56 (m, 3H, 2H Ph, 1H Py), 7.51 – 7.33 (m, 2H, Ph), 7.30 – 7.16 (m, 3H, 1H furan, 1H Py, NH), 6.34 – 6.16 (m, 2H, furan), 4.75 (s, 2H, NH-CH_2), 4.36 (s, 2H, CH_2 -furan), 4.27 – 4.03 (m, 1H, CH cyclopentyl), 1.80 – 1.34 (m, 8H, 4 CH_2 cyclopentyl). ^{13}C NMR (75.4 MHz, CDCl_3 , δ ppm) 166.3 (C=N), 155.3 (qC, Py), 153.5 (qC, furan), 146.5 (qC, Ph), 143.2 (CH, Py), 142.2 (CH, furan), 142.1 (qC, Ph), 140.6 (qC, Py), 128.1 (2 CH, Ph), 127.8 (2 CH, Ph), 125.3 (CH, Py), 121.6 (CH, Py), 110.8 (CH, furan), 109.1 (CH, furan), 59.4 (CH, cyclopentyl), 48.1 (NH-CH_2), 40.4 (CH_2 -furan), 29.5 (2 CH_2 , cyclopentyl), 23.7 (2 CH_2 , cyclopentyl). ESI-HRMS m/z calcd for $\text{C}_{23}\text{H}_{25}\text{N}_4\text{O}_3\text{S}_2$ [$\text{M}+\text{H}$] $^+$, 469.1363; found, 469.1368.



Scheme 94. Synthesis of OND 159.

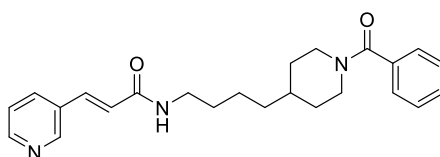
OND 159

To a mixture of compound **139** (30 mg, 63 μmol) in toluene (0.6 mL) at 60 °C, **123** (57 mg, 220 μmol) was added to form a pale-yellow solution which was stirred for 60 h at 60 °C. Then, the solvent was evaporated under *vacuum*, and the crude was purified by column chromatography (Acetone: Et_2O , 1:20 \rightarrow 1:12) to yield compound **159** (32 mg, 35%). ^1H NMR (300 MHz, CDCl_3 , δ ppm) 8.16 (br t, $J = 4.9$ Hz, 1H, Py), 7.90 (ddd, $J = 9.5, 7.5, 2.0$ Hz, 1H, Py), 7.74 (d, $J = 8.3$ Hz, 2H, Ts), 7.59 (d, $J = 15.8$ Hz, 1H, CH=CH), 7.34 (d, $J = 8.1$ Hz, 2H, Ts), 7.21 (ddd, $J = 7.1, 4.9, 1.8$ Hz, 1H, Py), 7.11 (d, $J = 5.3$ Hz, 1H, CH OND), 6.81 (br d, $J = 5.3$ Hz, 1H, CH OND), 6.62 (d, $J = 15.8$ Hz, 1H, CH=CH), 5.99 (t, $J = 5.4$ Hz, 1H, NH), 5.28 (d, $J = 1.9$ Hz, 1H, CH OND), 4.77 (d, $J = 16.6$ Hz, 1H, N- CH_2), 3.85 (quint, $J = 8.4$ Hz, 1H, CH cyclopentyl), 3.70 (d, $J = 16.5$ Hz, 1H, N- CH_2), 3.40 (m, 2H, NH-CH_2), 3.13 – 2.90 (m, 2H, CH_2S), 2.42 (s, 3H, CH_3 Ts), 1.91 – 1.20 (m,

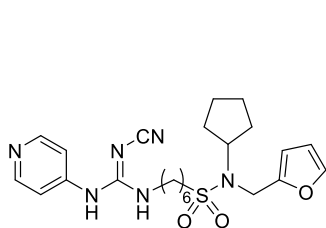
16H, 8 CH₂, 4 CH₂ hexyl, 4 CH₂ cyclopentyl). ¹³C NMR (75.4 MHz, CDCl₃, δ ppm) 165.3 (C=O), 161.4 (d, ¹J_{C,F} = 244.5 Hz, CF Py), 150.1 (qC, OND), 147.8 (CH, Py), 145.7 (qC, Ts), 145.1 (CH, OND), 140.2 (CH, Py), 139.3 (CH, OND), 135.4 (qC, Ph), 132.5 (CH=CH), 131.1 (qC, Py), 130.2 (2 CH, Ts), 129.0 (qC, OND), 127.7 (2 CH, Ts), 126.0 (CH=CH), 125.6 (CH, OND), 122.0 (CH, Py), 118.3 (qC, Py), 98.4 (qC, OND), 89.0 (CH, OND), 60.7 (CH, cyclopentyl), 52.1 (CH₂S), 44.1 (N-CH₂), 39.6 (NH-CH₂), 30.9 (CH₂, cyclopentyl), 30.5 (CH₂, hexyl), 29.3 (CH₂, hexyl), 29.2 (CH₂, cyclopentyl), 27.9 (CH₂, hexyl), 26.4 (CH₂, cyclopentyl), 23.4 (CH₂, cyclopentyl), 23.2 (CH₂, hexyl), 21.9 (CH₃, Ts). ESI-HRMS *m/z* calcd for C₃₃H₃₉⁷⁹BrFN₃O₆S₂Na [M+Na]⁺, 758.1320; found, 758.1340; calcd for C₃₃H₃₉⁸¹BrFN₃O₆S₂Na [M+Na]⁺, 760.1302; found, 758.1319.

CONCLUSIONS

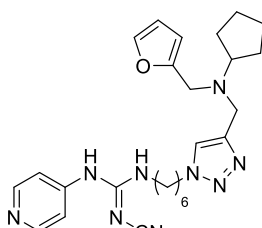
1. Several families of furan-containing NAMPT inhibitors have been prepared and biologically evaluated. Structure-activity-relationship (SAR) studies allowed the selection and optimization of promising drug candidates. Among them, compounds **47a**, **58** and **74** were the most potent NAMPT inhibitors. Particularly, **47a** showed an inhibition potency ($IC_{50} = 3.5$ nM) similar to that of **FK866** ($IC_{50} = 3.3$ nM), which is the reference compound in the field of NAMPT inhibition. Surprisingly, **47a** was 500-fold more cytotoxic in MIA PaCa-2 pancreatic cell line (IC_{50} of 5.0 μ M) than **FK866** (IC_{50} of 2.4 nM), indicating that another mechanism in addition to NAMPT inhibition should be responsible for its antitumor effect. This compound was also more cytotoxic than **FK866** on other five hematological cancer cell lines. Thus, compounds **47a**, **58** and **74** can be considered as promising lead compounds to develop more potent and efficient NAMPT inhibitors.



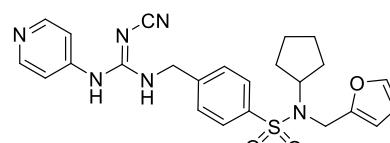
1 (FK866)
MIA PaCa-2, $IC_{50} = 2.4$ nM



47a
MIA PaCa-2, $IC_{50} = 0.005$ nM



58
MIA PaCa-2, $IC_{50} = 2.81$ nM

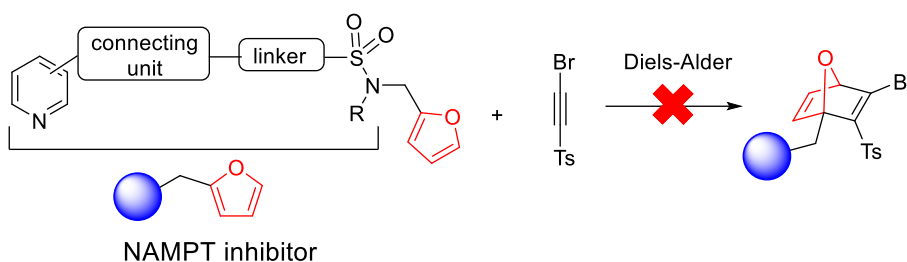


74
MIA PaCa-2, $IC_{50} = 0.009$ nM

2. Compounds **47a** and **58** were assayed *in vivo* in xenograft mouse models and showed less cytotoxicity than **FK866**. This discrepancy between *in vitro* and *in vivo* results can be due to problems of cell permeability or pharmacokinetic issues of the new synthesized compounds. To overcome this limitation, functionalization of the

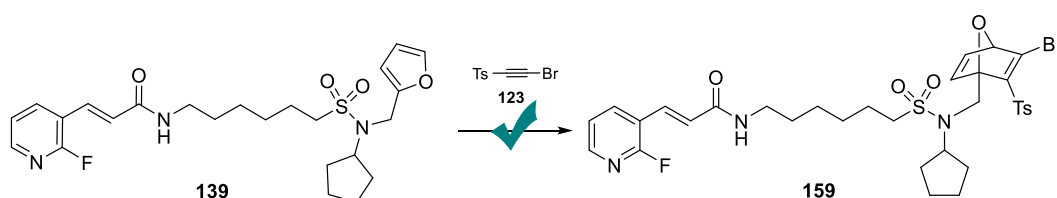
most promising candidates for their incorporation as payloads into an ADC was performed. The new functionalized inhibitors were linked through a peptide linker to antibody CD138 to efficiently afford six NAMPT-inhibitor based ADCs (currently under biological evaluation).

3. The furan moiety of the new NAMPT inhibitors developed in this Thesis, was exploited as a handle for their incorporation into bioconjugable oxanorbornadienic (OND) systems. Attempts to incorporate the inhibitors into ONDs through Diels-Alder reaction failed due to secondary reactions of the pyridine moiety of the inhibitors and the alkyne/bromovinyl sulfone.

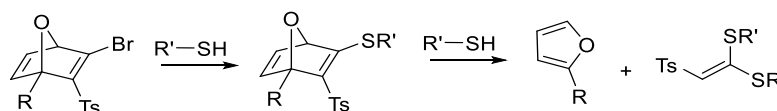


4. NAMPT inhibitors containing non-nucleophilic pyridine (2-fluoropyridine) were prepared and evaluated towards MIA PaCa-2 pancreatic cell line. Although these new derivatives were less cytotoxic than the non-fluorinated analogues, they still present enough activity (cytotoxicity in the low nanomolar range) for ADC applications.

5. Diels-Alder reaction of 2-fluoropyridine analogue **139** and alkyne **123** yielded the corresponding OND adducts, what confirms that less-nucleophilic pyridine containing NAMPT inhibitors can be incorporated into OND systems.



6. Preliminary studies on the reactivity of oxanorbornadienic thiovinyl sulfones have shown that they are sensitive to the fragmentation in the presence of an excess of thiol. This interesting reactivity makes these systems useful as thiol-sensitive cleavable linkers in general strategies of drug delivery and ADC development.



We are aware that in the field of NAMPT inhibitors, the use of this strategy limits the presence of pyridine in the inhibitor, being 2-fluoropyridine (non-nucleophilic pyridine) the more convenient. However, the incorporation of other furan-containing cytotoxic compounds into bioconjugable oxanorbornadienic systems could be of interest and find applications not only for NAMPT inhibitor-based ADCs but also in other general furan-based drug delivery strategies.

MATERIALS AND METHODS

Solvent evaporations were performed under reduced pressure at 25-40 °C. Reactions under anhydrous atmosphere were performed using commercial N₂ (“U” quality) and commercial Ar (“N-48” quality). Thin layer chromatography (TLC) was performed with qualitative purposes on aluminium silica gel plates (Merck Silica gel 60 F254) with detection by UV light (λ 254 nm) and charring with *p*-anisaldehyde, KMnO₄, ninhydrin, vanillin, phosphomolybdic acid, ethanolic H₂SO₄ (10%) or with Pancaldi reagent [(NH₄)₆MoO₄, Ce(SO₄)₂, H₂SO₄, H₂O]. Purifications were carried out either by chromatography column using silica gel 60 (Merck, 40-63 and 63-200 μ m), Sephadex LH-20 (25-100 μ m) eluting by gravity or by flash chromatography (Puriflash PF420, Interchim) with the solvent mixtures indicated in each case. ¹H- and ¹³C-NMR spectra were recorded with a Bruker AMX300, AMX500 or Avance AV-300 spectrometer in the CITIUS of the University of Seville. CDCl₃, CD₃OD, D₂O and DMSO-d₆ were used as solvents at room temperature except when indicated. Chemical shifts are given in ppm and coupling constants (*J*) in Hz. All the assignments were confirmed by 2D spectra (COSY and HSCQ). HMBC and NOE experiments were performed when necessary. Mass spectra (low and high resolution) were registered on a Micromass AutoSpeQ, Orbitrap Elite or Q-Exactive in the CITIUS of the University of Seville. Chemical ionization (CI) was used in Micromass AutoSpeQ and electrospray ionization (ESI) was used in Orbitrap Elite and Q- Exactive. In the case of low-resolution mass spectra, mass to charge ratio (*m/z*) is presented for the most abundant peaks. For high resolution mass spectra, *m/z* is presented for the molecular ion, whose value is compared with the calculated one considering the most abundant isotopes. The HPLC analysis were performed on a Thermo UltiMate 3000 instrument with Accucore C18 column (2.1 mm X 150 mm) at the department of Organic Chemistry at the University of Seville. Mobile phase consisted in solvent A (H₂O, 0.1% TFA) and solvent B (MeCN). The samples were eluted with a linear gradient from 95% A and 5% B to 0% A and

100% B, between 15 and 40 min. All chromatograms were registered at 254 nm wavelength.

At Heidelberg Pharma, solvents and reagents were purchased from commercial vendors and used without further purification. ESI-MS studies were performed using a Thermo Orbitrap LTQ XL™ mass spectrometer (Thermo Scientific™) connected to an Agilent 1200 series high performance liquid chromatography (HPLC) system (isocratic mode; mobile phase composition: MeOH:MeCN:H₂O, 40:40:20; flow rate: 0.25 mL/min) at Heidelberg Pharma Research GmbH, dept. of Bioanalytic. Analytical thin layer chromatography (TLC) was performed on POLYGRAM® SIL G/UV polyester pre-coated plates (40x80 mm, 0.20 mm silica gel 60) and compounds visualization was accomplished with UV light, 1% cinnamaldehyde, ninhydrin or Vaughn's staining reagents depending on the functional groups to be detected. Flash chromatography was carried out by using Teledyne ISCO CombiFlash® RF system on Silica RediSep® Rf disposable columns. All the compounds at Heidelberg Pharma, were purified by preparative RP-HPLC (VWR LaPrep Sigma LP1200 pumps, VWR LaPrep Sigma 3101 UV detector; column: Phenomenex Luna® 10 µm C18(2) 100Å, 250 x 21.2 mm) and analysed by analytical RP-HPLC (VWR HITACHI Chromaster 5110 binary HPLC pump, VWR HITACHI Chromaster 5430 diode array detector (DAD); column: Phenomenex Luna® 10 µm C18(2) 100Å, 250 x 4.6 mm). ADCs were purified by preparative size exclusion fast-protein liquid chromatography (SEC-HPLC, ÄKTA™ Start system) and analysed by analytical SEC (Knauer PLATINblue HPLC with DAD, column: Tosoh Bioscience TSKgel® UP-SW3000, 2 µm, 4.6 mm ID x 30 cm). ADCs were concentrated by using Amicon® Ultra-15 Centrifugal Filters MWCO 50000 (Millipore) and filtered through disposable sterile Millex®-GV syringe filters (Millipore). Concentration measurements were carried out with Thermo Fisher Scientific NanoDrop™ 2000 136 Experimental part spectrophotometer (λ = 280, 310 nm, sample size 2 µL).

Cell lines and reagents

MIA PaCa-2 and MDA-MB-231 were purchased from ATCC (LGC Standards S.r.l., Milan, Italy) and maintained in RPMI1640 medium supplemented with 10% FBS, penicillin (50U/mL) and streptomycin (50µg/mL) (Thermofisher, Italy). Five hematological cell lines (ML2 – Acute myeloid leukemia, Jurkat – Acute lymphoblastic leukemia, Namalwa – Burkitt lymphoma, RPMI8226 – Multiple Myeloma and NB4 – acute myeloid leukemia M3) were purchased from DSMZ (German Collection of Microorganisms and Cell Cultures) or ATCC. The cell lines were cultured in RPMI medium (Invitrogen AG, 61870-01) supplemented with 10% heat inactivated fetal calf serum (Amimed, 2-01F30-I) and 1% penicillin/streptomycin at 37°C (Amimed, 4-01F00-H) in a humidified atmosphere of 95% air and 5% CO₂. **FK866** was obtained from the NIMH Chemical Synthesis and Drug Supply Program.

Cell viability assay

2x10³ MIA PaCa-2 or MDA-MB-231 cells were plated in 96 well plates and let adhere overnight. 24 h later cells were treated with the analogues of **FK866**. Viability was determined 72 h after. The culture plates were fixed with cold 3% trichloroacetic acid at 4°C for 30 minutes, washed with cold water and dried overnight. Finally, the plates were stained with 0.4% sulforodhamine B (SRB) in 1% acetic acid, washed four times with 1% acetic acid to remove unbound dye, dried overnight and then the stain was extracted with 10 mM Tris Base and the absorbance was read at 560 nm.

Measurement of intracellular NAD⁺ levels

MIA PaCa-2 or MDA-MB-231 cells were plated at a density of 3 x 10⁴ cells/well in 24-well plates. After 24 h, cells were treated (or not) with the different compounds and cultured for further 24h (in the time course experiments, cells were cultured for further 24h, 48h and 72h). Cells were harvested and lysed in 0.1 mL 0.6 M perchloric acid. Intracellular NAD⁺ levels were determined as previously reported¹⁶⁸ and ATP

levels were quantified by a commercially available ATP determination kit (Invitrogen, Carlsbad, CA) following the manufacturer's instruction. Luminescence was measured using a FLUOstar OPTIMA (BMG Labtech, Ortenberg, Germany) and ATP concentrations in the samples were calculated from the ATP standard curve.

Determination of NAMPT inhibition

NAMPT inhibition was determined as previously reported.¹⁶⁹ Briefly, 10 ng of recombinant human NAMPT protein (#ab198090, Abcam, Cambridge, UK) were incubated in 40 μ L reaction buffer (0.4 mM PRPP, 2 mM ATP, 0.02% BSA, 2 mM DTT, 12 mM $MgCl_2$ and 50 mM Tris-HCl) in eppendorf tubes, in the presence or absence of the different compounds. After a 5 min incubation at 37°C, 9.0 μ L of NAM (0.2 μ M final concentration) were added and the reaction was stopped after 15 min, by heating samples at 95°C for 1 min. Samples were then cooled to 0°C and NMN was detected by adding 20 μ L of 20% acetophenone and 20 μ L KOH (2M) into each tube. The mixture was vortexed and kept at 0°C for 3 min; 90 μ L of 88% formic acid were then added and the tubes were incubated at 37°C for 10 minutes. Finally, 100 μ L of the mixture was transferred into a flat-bottom 96-well plate and the fluorescence (excitation 382 nm, emission 445 nm) was measured using a CLARIOstar®Plus (BMG Labtech).

Flow cytometry analyses

The cytotoxic and cellular effects of **47a**, **49a** and **58** on malignant cell lines were evaluated using a Beckman Coulter Cytomics FC500 flow cytometer (Beckman Coulter International S.A.). The measured parameters included cell death, MMP assessments and ROS production.

Cell death analysis

To assess cell death, cells were stained with ANNEXIN-V (ANXN, eBioscience, BMS306FI/300) and 7-aminoactinomycin D (7AAD, Immunotech, A07704) as described by the manufacturer and analyzed using flow cytometry. Dead cells were identified as 7AAD⁺ and early apoptotic cells as ANXN⁺ 7AAD⁻.

Assessment of Mitochondrial Membrane Potential (MMP)

ML2, Jurkat and RPMI8226 cells were incubated with NAMPT inhibitors for up to 96h. At each time point, cells were stained with Tetramethylrhodamine, methyl ester (TMRM, ThermoFisher Scientific, T668) according to the manufacturer's protocol. TMRM is a cell-permeant dye that accumulates in the active mitochondria, showing red-orange fluorescence, detected by flow cytometer. The amount of the dye is directly proportional to the amount of live cells with active mitochondria. The graphs depict the percentage of cells losing MMP over time.

Detection of cellular and mitochondrial ROS

Intracellular levels of H₂O₂, mitochondrial and cytosolic superoxide anions were determined in NAMPT inhibitor-treated and control hematological cell lines by flow cytometry. The cell permeant specific fluorescent probes were used, i.e., dihydroethidium (DHE, Marker Gene Technologies, M1241), MitoSOX (Molecular Probes, M36008) and 6-carboxy-2',7'-dichlorodihydrofluorescein diacetate ester (carboxy-H₂DCFDA; Molecular Probes, C-400). DHE is oxidized intracellularly to ethidium by superoxide anions giving bright red fluorescence. MitoSOX, is selectively targeted to mitochondria, where it is oxidized by ROS and exhibits red fluorescence. Instead, carboxy-H₂DCFDA is hydrolyzed yielding a polar non-fluorescent product (DCFH), which in the presence of hydrogen peroxide is then oxidized to green fluorescent dichlorofluorescein (DCF). Cells were stained separately with 5 μM of

TMRM and H2DCFDA dyes and 10 μM of DHE in PBS, incubated in the dark at 37 °C for 15 min. Then, the cell suspension was analyzed using flow cytometry.

Determination of intracellular NAD⁺ and ATP contents

Cells ($1 \times 10^6/\text{mL}$) in log growth phase were seeded in 6-well plate in presence or absence of NAMPT inhibitors. At each time point 800 μL of cells was centrifuged at 900 g (2000 rpm) for 5 min and washed with cold PBS. Then, supernatant was discarded, and cells were re-suspended in 300 μL of lysis buffer (NaHCO_3 20mM and Na_2CO_3 100mM) and kept at -80°C for at least 4 h before analysis. Total NAD⁺ content was measured in cell lysates using a biochemical assay described previously.¹⁷⁰ Briefly, cell lysates (20 μL) were plated in a 96-well flat bottom plate. A standard curve was generated using a 1:3 serial dilution in lysis buffer of a β -NAD stock solution. Cycling buffer (160 μL) was added into each well and the plate was incubated for 5 min at 37°C. Then, pre-warmed at 37°C ethanol (20 μL) was added into each well and the plate was incubated for an additional 5 min at 37°C. The absorbance was measured in a kinetic mode at 570 nm after 5, 10, 15, 20, and 30 min at 37°C on a spectrophotometer. The amount of NAD⁺ in each sample was normalized to the protein content for each test sample at each time point. Total ATP cell content was quantified using the ATP determination Kit (Life Technologies, A22066) according to manufacturer's instructions.

Xenograft studies

The *in vivo* evaluation of compounds **47a** and **58** was carried out using a xenograft model of human acute myeloid leukemia. Non-leaky C.B.-17 SCID mice (8 weeks old; Iffa Credo, L'Arbresle, France) were bred and housed in micro-isolator cages in a specific pathogen-free room within the animal facilities at the University Hospital of Lausanne. Animals were allowed to acclimatize to their new environment for 1 week prior to use. All animals were handled according to the respective institutional

regulations after approval of the animal ethic committee of the University of Lausanne. Manipulations were performed under a laminar flow hood under sterile conditions. ML-2 cells (AML, 2×10^7) were injected subcutaneously into the mouse right flank. Once the tumor reached a volume of 100 mm^3 , mice were randomly subdivided into four groups. The treatment groups included: (i) vehicle ($n = 3$), (ii) **47a** ($n = 4$), (iii) **58** ($n = 4$) and finally (iv) **FK866** ($n = 4$). The compounds were administered intraperitoneally (10 mg/kg body weight) in 200 μL 0.9 % saline, twice a day for 4 days, repeated weekly over 3 weeks. Vehicle (control) group was treated only with 200 μL 0.9 % saline. All animals were monitored daily for any signs of illness and sacrificed immediately if tumor has reached a size of 1000 mm^3 . Statistical analysis of mice survival was done using Log-rank (Mantel-Cox) test and GraphPad Prism software. (Version 9.10, GraphPad Software, San Diego, CA).

REFERENCES

- (1) Galli, U.; Travelli, C.; Massarotti, A.; Fakhfour, G.; Rahimian, R.; Tron, G. C.; Genazzani, A. A. Medicinal Chemistry of Nicotinamide Phosphoribosyltransferase (NAMPT) Inhibitors. *J. Med. Chem.* **2013**, *56* (16), 6279–6296.
- (2) Hasmann, M.; Schemainda, I. FK866, a Highly Specific Noncompetitive Inhibitor of Nicotinamide Phosphoribosyltransferase, Represents a Novel Mechanism for Induction of Tumor Cell Apoptosis. *Cancer Res.* **2003**, *63* (21), 7436–7442.
- (3) Ghanem, M. S.; Monacelli, F.; Nencioni, A. Advances in NAD-Lowering Agents for Cancer Treatment. *Nutrients* **2021**, *13*, 1665.
- (4) Higginson, C. J.; Eno, M. R.; Khan, S.; Cameron, M. D.; Finn, M. G. Albumin-Oxanorbornadiene Conjugates Formed Ex Vivo for the Extended Circulation of Hydrophilic Cargo. *ACS Chem. Biol.* **2016**, *11* (8), 2320–2327.
- (5) Sanhueza, C. A.; Baksh, M. M.; Thuma, B.; Roy, M. D.; Dutta, S.; Prévile, C.; Chrunyk, B. A.; Beaumont, K.; Dullea, R.; Ammirati, M.; Liu, S.; Gebhard, D.; Finley, J. E.; Salatto, C. T.; King-Ahmad, A.; Stock, I.; Atkinson, K.; Reidich, B.; Lin, W.; Kumar, R.; Tu, M.; Menhaji-Klotz, E.; Price, D. A.; Liras, S.; Finn, M. G.; Mascitti, V. Efficient Liver Targeting by Polyvalent Display of a Compact Ligand for the Asialoglycoprotein Receptor. *J. Am. Chem. Soc.* **2017**, *139* (9), 3528–3536.
- (6) Pfeiffer, T.; Schuster, S.; Bonhoeffer, S. Cooperation and Competition in the Evolution of ATP-Producing Pathways. *Science (80-.)*. **2001**, *292* (5516), 504–507.
- (7) Savitz, J. The Kynurenine Pathway : A Fi Nger in Every Pie. *Mol Psychiatry* **2020**, *25*, 131–147.
- (8) Franco, J.; Piacente, F.; Walter, M.; Fratta, S.; Ghanem, M.; Benzi, A.; Caffa, I.; Kurkin, A. V.; Altieri, A.; Herr, P.; Martínez-Bailén, M.; Robina, I.; Bruzzone, S.; Nencioni, A.; Del Rio, A. Structure-Based Identification and Biological Characterization of New NAPRT Inhibitors. *Pharmaceuticals* **2022**, *15* (7), 1–15.
- (9) Galli, U.; Colombo, G.; Travelli, C.; Tron, G. C.; Genazzani, A. A.; Grolla, A. A. Recent Advances in NAMPT Inhibitors: A Novel Immunotherapeutic Strategy. *Front. Pharmacol.* **2020**, *11*, 1–20.

- (10) Sampath, D.; Zabka, T. S.; Misner, D. L.; O'Brien, T.; Dragovich, P. S. Inhibition of Nicotinamide Phosphoribosyltransferase (NAMPT) as a Therapeutic Strategy in Cancer. *Pharmacol. Ther.* **2015**, *151*, 16–31.
- (11) Heske, C. M. Beyond Energy Metabolism: Exploiting the Additional Roles of NAMPT for Cancer Therapy. *Front. Oncol.* **2020**, *9* (1), 1514.
- (12) Sethi, C. J. K.; Genazzani, A. A.; Piemonte, U. Extracellular Nicotinamide Phosphoribosyltransferase, a New Cancer Metabokine Tables of Links. **2016**.
- (13) Takahashi, R.; Nakamura, S.; Nakazawa, T.; Minoura, K.; Yoshida, T.; Nishi, Y.; Kobayashi, Y.; Ohkubo, T. Structure and Reaction Mechanism of Human Nicotinamide Phosphoribosyltransferase. *J. Biochem.* **2010**, *147* (1), 95–107.
- (14) Khan, J. A.; Tao, X.; Tong, L. Molecular Basis for the Inhibition of Human NMPRTase, a Novel Target for Anticancer Agents. *Nat. Struct. Mol. Biol.* **2006**, *13* (7), 582–588.
- (15) Khan, J. A.; Tao, X.; Tong, L. Molecular Basis for the Inhibition of Human NMPRTase, a Novel Target for Anticancer Agents. *Nat. Struct. Mol. Biol.* **2006**, *13* (7), 582–588.
- (16) Wang, T.; Zhang, X.; Bheda, P.; Revollo, J. R.; Imai, S. I.; Wolberger, C. Structure of Nampt/PBEF/Visfatin, a Mammalian NAD⁺ Biosynthetic Enzyme. *Nat. Struct. Mol. Biol.* **2006**, *13* (7), 661–662.
- (17) Burgos, E. S.; Schramm, V. L. Weak Coupling of ATP Hydrolysis to the Chemical Equilibrium of Human Nicotinamide Phosphoribosyltransferase. *Biochemistry* **2008**, *47* (42), 11086–11096.
- (18) Burgos, E. S.; Ho, M. C.; Almo, S. C.; Schramm, V. L. A Phosphoenzyme Mimic, Overlapping Catalytic Sites and Reaction Coordinate Motion for Human NAMPT. *Proc. Natl. Acad. Sci. U. S. A.* **2009**, *106* (33), 13748–13753.
- (19) Holen, K.; B. Saltz, L.; Hollywood, E.; Burk, K.; Hanauske, A.-R. The Pharmacokinetics, Toxicities, and Biologic Effects of FK866, a Nicotinamide Adenine Dinucleotide Biosynthesis Inhibitor. *Invest New Drugs* **2008**, *26*, 45–51.
- (20) Schou, C.; Ottosen, E. R.; Petersen, H. J.; Björkling, F.; Latini, S.; Hjarnaa, P. V.; Bramm, E.; Binderup, L. Novel Cyanoguanidines. *Bioorg. Med. Chem. Lett.* **1997**, *7* (24), 3095–3100.
- (21) Neggers, J. E.; Kwanten, B.; Dierckx, T.; Noguchi, H.; Voet, A.; Bral, L.; Minner, K.; Massant, B.; Kint, N.; Delforge, M.; Vercruysse, T.; Baloglu, E.; Senapedis,

- W.; Jacquemyn, M.; Daelemans, D. Target Identification of Small Molecules Using Large-Scale CRISPR-Cas Mutagenesis Scanning of Essential Genes. *Nat. Commun.* **2018**, *9* (1), 1–14.
- (22) Korotchkina, L.; Kazyulkin, D.; Komarov, P. G.; Polinsky, A.; Andrianova, E. L.; Joshi, S.; Gupta, M.; Vujcic, S.; Kononov, E.; Toshkov, I.; Tian, Y.; Krasnov, P.; Chernov, M. V.; Veith, J.; Antoch, M. P.; Middlemiss, S.; Somers, K.; Lock, R. B.; Norris, M. D.; Henderson, M. J.; Haber, M.; Chernova, O. B.; Gudkov, A. V. OT-82, a Novel Anticancer Drug Candidate That Targets the Strong Dependence of Hematological Malignancies on NAD Biosynthesis. *Leukemia* **2020**, *34* (7), 1828–1839.
- (23) Sampath, D.; Zabka, T. S.; Misner, D. L.; O'Brien, T.; Dragovich, P. S. Inhibition of Nicotinamide Phosphoribosyltransferase (NAMPT) as a Therapeutic Strategy in Cancer. *Pharmacol. Ther.* **2015**, *151*, 16–31.
- (24) Bai, J. F.; Majjigapu, S. R.; Sordat, B.; Poty, S.; Vogel, P.; Elías-Rodríguez, P.; Moreno-Vargas, A. J.; Carmona, A. T.; Caffa, I.; Ghanem, M.; Khalifa, A.; Monacelli, F.; Cea, M.; Robina, I.; Gajate, C.; Mollinedo, F.; Bellotti, A.; Nahimana, A.; Duchosal, M.; Nencioni, A. Identification of New FK866 Analogues with Potent Anticancer Activity against Pancreatic Cancer. *Eur. J. Med. Chem.* **2022**, *239* (5), 114504.
- (25) Travelli, C.; Aprile, S.; Rahimian, R.; Grolla, A. A.; Rogati, F.; Bertolotti, M.; Malagnino, F.; Di Paola, R.; Impellizzeri, D.; Fusco, R.; Mercalli, V.; Massarotti, A.; Stortini, G.; Terrazzino, S.; Del Grosso, E.; Fakhfour, G.; Troiani, M. P.; Alisi, M. A.; Grosa, G.; Sorba, G.; Canonico, P. L.; Orsomando, G.; Cuzzocrea, S.; Genazzani, A. A.; Galli, U.; Tron, G. C. Identification of Novel Triazole-Based Nicotinamide Phosphoribosyltransferase (NAMPT) Inhibitors Endowed with Antiproliferative and Antiinflammatory Activity. *J. Med. Chem.* **2017**, *60* (5), 1768–1792.
- (26) Mitchell, S. R.; Larkin, K.; Grieselhuber, N. R.; Lai, T. H.; Cannon, M.; Orwick, S.; Sharma, P.; Asemelash, Y.; Zhang, P.; Goettl, V. M.; Beaver, L.; Mims, A.; Pudevalli, V. K.; Blachly, J. S.; Lehman, A.; Harrington, B.; Henderson, S.; Breitbach, J. T.; Williams, K. E.; Dong, S.; Baloglu, E.; Senapedis, W.; Kirschner, K.; Sampath, D.; Lapalombella, R.; Byrd, J. C. Selective Targeting of NAMPT by KPT-9274 in Acute Myeloid Leukemia. *Blood Adv.* **2019**, *3* (3), 242–255.
- (27) You, H.; Youn, H. S.; Im, I.; Bae, M. H.; Lee, S. K.; Ko, H.; Eom, S. H.; Kim, Y. C. Design, Synthesis and X-Ray Crystallographic Study of NAMPTase Inhibitors as Anti-Cancer Agents. *Eur. J. Med. Chem.* **2011**, *46* (4), 1153–1164.
- (28) Christensen, M. K.; Erichsen, K. D.; Olesen, U. H.; Tjørnelund, J.; Fristrup, P.;

- Thougaard, A.; Nielsen, S. J.; Sehested, M.; Jensen, P. B.; Loza, E.; Kalvinsh, I.; Garten, A.; Kiess, W.; Björkling, F. Nicotinamide Phosphoribosyltransferase Inhibitors, Design, Preparation, and Structure-Activity Relationship. *J. Med. Chem.* **2013**, *56* (22), 9071–9088.
- (29) Palacios, D. S.; Meredith, E. L.; Kawanami, T.; Adams, C. M.; Chen, X.; Darsigny, V.; Palermo, M.; Baird, D.; George, E. L.; Guy, C.; Tierney, L.; Thigale, S.; Wang, L.; Weihofen, W. A. Scaffold Morphing Identifies 3-Pyridyl Azetidine Ureas as Inhibitors of Nicotinamide Phosphoribosyltransferase (NAMPT). *ACS Med. Chem. Lett.* **2019**, *10*, 1524–1529.
- (30) Colombano, G.; Travelli, C.; Galli, U.; Caldarelli, A.; Chini, M. G.; Canonico, P. L.; Sorba, G.; Bifulco, G.; Tron, G. C.; Genazzani, A. A.; Avogadro, O. A. A Novel Potent Nicotinamide Phosphoribosyltransferase Inhibitor Synthesized via Click Chemistry. *J. Med. Chem.* **2010**, *53* (2), 616–623.
- (31) Galli, U.; Ercolano, E.; Carraro, L.; Blasi Roman, C. R.; Sorba, G.; Canonico, P. L.; Genazzani, A. A.; Tron, G. C.; Billington, R. A. Synthesis and Biological Evaluation of Isosteric Analogues of FK866, an Inhibitor of NAD Salvage. *ChemMedChem* **2008**, *3* (5), 771–779.
- (32) Wilsbacher, J. L.; Cheng, M.; Cheng, D.; Trammell, S. A. J.; Shi, Y.; Guo, J.; Koeniger, S. L.; Kovar, P. J.; He, Y.; Selvaraju, S.; Heyman, H. R.; Sorensen, B. K.; Clark, R. F.; Hansen, T. M.; Longenecker, K. L.; Raich, D.; Korepanova, A. V.; Cepa, S.; Towne, D. L.; Abraham, V. C.; Tang, H.; Richardson, P. L.; McLoughlin, S. M.; Badagnani, I.; Curtin, M. L.; Michaelides, M. R.; Maag, D.; Buchanan, F. G.; Chiang, G. G.; Gao, W.; Rosenberg, S. H.; Brenner, C.; Tse, C. Discovery and Characterization of Novel Nonsubstrate and Substrate NAMPT Inhibitors. *Mol. Cancer Ther.* **2017**, *16* (7), 1236–1245.
- (33) Oh, A.; Ho, Y. C.; Zak, M.; Liu, Y.; Chen, X.; Yuen, P. W.; Zheng, X.; Liu, Y.; Dragovich, P. S.; Wang, W. Structural and Biochemical Analyses of the Catalysis and Potency Impact of Inhibitor Phosphoribosylation by Human Nicotinamide Phosphoribosyltransferase. *ChemBioChem* **2014**, *15* (8), 1121–1130.
- (34) Vogel, Pierre; Duchosal, Michel; Aimable, Nahimana; Inmaculada, Robina; Mollinedo, Faustino; Nencioni, A. Piperidine Derivatives for Use in the Treatment of Pancreatic Cancer. WO 2018/ 024907 A1, International Application n° PCT/EP2017/069870., 2018.
- (35) Ronchetti, R.; Moroni, G.; Carotti, A.; Gioiello, A.; Camaioni, E. Recent Advances in Urea- And Thiourea-Containing Compounds: Focus on Innovative Approaches in Medicinal Chemistry and Organic Synthesis. *RSC Med. Chem.* **2021**, *12* (7), 1046–1064.

- (36) Zheng, X.; Bauer, P.; Baumeister, T.; Buckmelter, A. J.; Caligiuri, M.; Clodfelter, K. H.; Han, B.; Ho, Y. C.; Kley, N.; Lin, J.; Reynolds, D. J.; Sharma, G.; Smith, C. C.; Wang, Z.; Dragovich, P. S.; Oh, A.; Wang, W.; Zak, M.; Gunzner-Toste, J.; Zhao, G.; Yuen, P. W.; Bair, K. W. Structure-Based Identification of Ureas as Novel Nicotinamide Phosphoribosyltransferase (Nampt) Inhibitors. *J. Med. Chem.* **2013**, *56* (12), 4921–4937.
- (37) Jakobsen, C. M.; Denmeade, S. R.; Isaacs, J. T.; Gady, A.; Olsen, C. E.; Christensen, S. B. Design, Synthesis, and Pharmacological Evaluation of Thapsigargin Analogues for Targeting Apoptosis to Prostatic Cancer Cells. *J. Med. Chem.* **2001**, *44* (26), 4696–4703.
- (38) Moore, Z.; Chakrabarti, G.; Luo, X.; Ali, A.; Hu, Z.; Fattah, F. J.; Vemireddy, R.; DeBerardinis, R. J.; Brekken, R. A.; Boothman, D. A. NAMPT Inhibition Sensitizes Pancreatic Adenocarcinoma Cells to Tumor-Selective, PAR-Independent Metabolic Catastrophe and Cell Death Induced by β -Lapachone. *Cell Death Dis.* **2015**, *6* (1), 1–10.
- (39) Nahimana, A.; Attinger, A.; Aubry, D.; Greaney, P.; Ireson, C.; Thougard, A. V.; Tjørnelund, J.; Dawson, K. M.; Dupuis, M.; Duchosal, M. A. The NAD Biosynthesis Inhibitor APO866 Has Potent Antitumor Activity against Hematologic Malignancies. *Blood* **2009**, *113* (14), 3276–3286.
- (40) Nishida, T.; Naguro, I.; Ichijo, H. NAMPT-Dependent NAD⁺ Salvage Is Crucial for the Decision between Apoptotic and Necrotic Cell Death under Oxidative Stress. *Cell Death Discov.* **2022**, *8* (1).
- (41) Ginet, V.; Puyal, J.; Rummel, C.; Aubry, D.; Breton, C.; Cloux, A. J.; Majjigapu, S. R.; Sordat, B.; Vogel, P.; Bruzzone, S.; Nencioni, A.; Duchosal, M. A.; Nahimana, A. A Critical Role of Autophagy in Antileukemia/Lymphoma Effects of APO866, an Inhibitor of NAD Biosynthesis. *Autophagy* **2014**, *10* (4), 603–617.
- (42) Cloux, A. J.; Aubry, D.; Heulot, M.; Widmann, C.; ElMokh, O.; Piacente, F.; Cea, M.; Nencioni, A.; Bellotti, A.; Bouzourène, K.; Pellegrin, M.; Mazzolai, L.; Duchosal, M. A.; Nahimana, A. Reactive Oxygen/Nitrogen Species Contribute Substantially to the Antileukemia Effect of APO866, a NAD Lowering Agent. *Oncotarget* **2019**, *10* (62), 6723–6738.
- (43) David, O.; Meester, W. J. N.; Bieräugel, H.; Schoemaker, H. E.; Hiemstra, H.; Van Maarseveen, J. H. Intramolecular Staudinger Ligation: A Powerful Ring-Closure Method to Form Medium-Sized Lactams. *Angew. Chemie - Int. Ed.* **2003**, *42* (36), 4373–4375.
- (44) Trinh, P. N. H.; Chong, D. J. W.; Leach, K.; Hill, S. J.; Tyndall, J. D. A.; May, L. T.;

- Vernall, A. J.; Gregory, K. J. Development of Covalent, Clickable Probes for Adenosine A1 and A3 Receptors. *J. Med. Chem.* **2021**, *64* (12), 8161–8178.
- (45) Thomas, J. R.; Liu, X.; Hergenrother, P. J. Size-Specific Ligands for RNA Hairpin Loops. *J. Am. Chem. Soc.* **2005**, *127* (36), 12434–12435.
- (46) Giroud, M.; Ivkovic, J.; Martignoni, M.; Fleuti, M.; Trapp, N. Inhibition of the Cysteine Protease Human Cathepsin L by Triazine Nitriles: Amide ... Heteroarene π -Stacking Interactions and Chalcogen Bonding in the S3 Pocket. *ChemMedChem* **2017**, *12*, 257–270.
- (47) Kong, X.; He, Z.; Zhang, Y.; Mu, L.; Liang, C.; Chen, B.; Jing, X.; Cammidge, A. N. LETTERS A Mesogenic Triphenylene-Perylene- Triphenylene Triad. *Society* **2011**, // (c), 2009–2012.
- (48) Tauk, L.; Schröder, A. P.; Decher, G.; Giuseppone, N. Hierarchical Functional Gradients of PH-Responsive Self-Assembled Monolayers Using Dynamic Covalent Chemistry on Surfaces. *Nat. Chem.* **2009**, *1* (8), 649–656.
- (49) Hizartzidis, L.; Tarleton, M.; Gordon, C. P.; McCluskey, A. Chemoselective Flow Hydrogenation Approaches to Isoindole-7-Carboxylic Acids and 7-Oxa-Bicyclo[2.2.1]Heptanes. *RSC Adv.* **2014**, *4* (19), 9709–9722.
- (50) O'Brien-Brown, J.; Jackson, A.; Reekie, T. A.; Barron, M. L.; Werry, E. L.; Schiavini, P.; McDonnell, M.; Munoz, L.; Wilkinson, S.; Noll, B.; Wang, S.; Kassiou, M. Discovery and Pharmacological Evaluation of a Novel Series of Adamantyl Cyanoguanidines as P2X7 Receptor Antagonists. *Eur. J. Med. Chem.* **2017**, *130*, 433–439.
- (51) Vicens, L.; Olivo, G.; Costas, M. Remote Amino Acid Recognition Enables Effective Hydrogen Peroxide Activation at a Manganese Oxidation Catalyst. *Angew. Chemie - Int. Ed.* **2022**, *61* (7).
- (52) Tagmose, T. M.; Schou, S. C.; Mogensen, J. P.; Nielsen, F. E.; Arkhammar, P. O. G.; Wahl, P.; Hansen, B. S.; Worsaae, A.; Boonen, H. C. M.; Antoine, M. H.; Lebrun, P.; Hansen, J. B. Arylcyanoguanidines as Activators of Kir6.2/SUR1KATP Channels and Inhibitors of Insulin Release. *J. Med. Chem.* **2004**, *47* (12), 3202–3211.
- (53) Romuald, C.; Busseron, E.; Coutrot, F. Very Contracted to Extended Co - Conformations with or without Oscillations in Two- and Three-Station [2]Daisy Chains. *J. Org. Chem.* **2010**, *75* (19), 6516–6531.
- (54) Curtin, M. L.; Heyman, H. R.; Clark, R. F.; Sorensen, B. K.; Doherty, G. A.;

- Hansen, T. M.; Frey, R. R.; Sarris, K. A.; Aguirre, A. L.; Shrestha, A.; Tu, N.; Woller, K.; Pliushchev, M. A.; Sweis, R. F.; Cheng, M.; Wilsbacher, J. L.; Kovar, P. J.; Guo, J.; Cheng, D.; Longenecker, K. L.; Raich, D.; Korepanova, A. V.; Soni, N. B.; Algire, M. A.; Richardson, P. L.; Marin, V. L.; Badagnani, I.; Vasudevan, A.; Buchanan, F. G.; Maag, D.; Chiang, G. G.; Tse, C.; Michaelides, M. R. SAR and Characterization of Non-Substrate Isoindoline Urea Inhibitors of Nicotinamide Phosphoribosyltransferase (NAMPT). *Bioorganic Med. Chem. Lett.* **2017**, *27* (15), 3317–3325.
- (55) R. Lee Webb, C. S. L. Diphenyl Cyanocarbonimidate. A Versatile Synthone for the Construction of Heterocyclic Systems. *J. Heterocycl. Chem.* **1982**, *19*, 1205.
- (56) Khongorzul, P.; Ling, C. J.; Khan, F. U.; Ihsan, A. U.; Zhang, J. Antibody-Drug Conjugates: A Comprehensive Review. *Mol. Cancer Res.* **2020**, *18* (1), 3–19.
- (57) Fu, Z.; Li, S.; Han, S.; Shi, C.; Zhang, Y. Antibody Drug Conjugate : The “ Biological Missile ” for Targeted Cancer Therapy. *Signal Transduct. Target. Ther.* **2022**, *7* (93).
- (58) Sheyi, R.; de la Torre, B. G.; Albericio, F. Linkers: An Assurance for Controlled Delivery of Antibody-Drug Conjugate. *Pharmaceutics* **2022**, *14* (2), 396.
- (59) Yasunaga, M.; Manabe, S.; Tarin, D.; Matsumura, Y. Cancer-Stroma Targeting Therapy by Cytotoxic Immunoconjugate Bound to the Collagen 4 Network in the Tumor Tissue. *Bioconjug. Chem.* **2011**, *22* (9), 1776–1783.
- (60) Dal Corso, A.; Cazzamalli, S.; Gébleux, R.; Mattarella, M.; Neri, D. Protease-Cleavable Linkers Modulate the Anticancer Activity of Noninternalizing Antibody-Drug Conjugates. *Bioconjug. Chem.* **2017**, *28* (7), 1826–1833.
- (61) Capone, E.; Lamolinara, A.; Pastorino, F.; Gentile, R.; Ponziani, S.; Di Vittorio, G.; D’agostino, D.; Bibbò, S.; Rossi, C.; Piccolo, E.; Iacobelli, V.; Lattanzio, R.; Panella, V.; Sallese, M.; De Laurenzi, V.; Giansanti, F.; Sala, A.; Iezzi, M.; Ponzoni, M.; Ippoliti, R.; Iacobelli, S.; Sala, G. Targeting Vesicular Lgals3bp by an Antibody-Drug Conjugate as Novel Therapeutic Strategy for Neuroblastoma. *Cancers (Basel)*. **2020**, *12* (10), 1–18.
- (62) Casi, G.; Neri, D. Noninternalizing Targeted Cytotoxics for Cancer Therapy. *Mol. Pharm.* **2015**, *12* (6), 1880–1884.
- (63) Dean, A. Q.; Luo, S.; Twomey, J. D.; Zhang, B. Targeting Cancer with Antibody-Drug Conjugates: Promises and Challenges. *MAbs* **2021**, *13* (1).
- (64) Drago, J. Z.; Modi, S.; Chandarlapaty, S. Unlocking the Potential of Antibody–

- Drug Conjugates for Cancer Therapy. *Nat. Rev. Clin. Oncol.* **2021**, *18* (6), 327–344.
- (65) Chiu, M. L.; Goulet, D. R.; Teplyakov, A.; Gilliland, G. L. Antibody Structure and Function: The Basis for Engineering Therapeutics. *Antibodies* **2019**, *8* (4), 55.
- (66) Lewis Phillips, G. D.; Li, G.; Dugger, D. L.; Crocker, L. M.; Parsons, K. L.; Mai, E.; Blättler, W. A.; Lambert, J. M.; Chari, R. V. J.; Lutz, R. J.; Wong, W. L. T.; Jacobson, F. S.; Koeppen, H.; Schwall, R. H.; Kenkare-Mitra, S. R.; Spencer, S. D.; Sliwkowski, M. X. Targeting HER2-Positive Breast Cancer with Trastuzumab-DM1, an Antibody-Cytotoxic Drug Conjugate. *Cancer Res.* **2008**, *68* (22), 9280–9290.
- (67) Wong, P. T.; Choi, S. K. Mechanisms of Drug Release in Nanotherapeutic Delivery Systems. *Chem. Rev.* **2015**, *115* (9), 3388–3432.
- (68) Wu, G.; Fang, Y. Z.; Yang, S.; Lupton, J. R.; Turner, N. D. Glutathione Metabolism and Its Implications for Health. *J. Nutr.* **2004**, *134* (3), 489–492.
- (69) Kellogg, B. A.; Garrett, L.; Kovtun, Y.; Lai, K. C.; Leece, B.; Miller, M.; Payne, G.; Steeves, R.; Whiteman, K. R.; Widdison, W.; Xie, H.; Singh, R.; Chari, R. V. J.; Lambert, J. M.; Lutz, R. J. Disulfide-Linked Antibody-Maytansinoid Conjugates: Optimization of in Vivo Activity by Varying the Steric Hindrance at Carbon Atoms Adjacent to the Disulfide Linkage. *Bioconjug. Chem.* **2011**, *22* (4), 717–727.
- (70) Hong, E. E.; Erickson, H.; Lutz, R. J.; Whiteman, K. R.; Jones, G.; Kovtun, Y.; Blanc, V.; Lambert, J. M. Design of Coltuximab Ravtansine, a CD19-Targeting Antibody-Drug Conjugate (ADC) for the Treatment of B-Cell Malignancies: Structure-Activity Relationships and Preclinical Evaluation. *Mol. Pharm.* **2015**, *12* (6), 1703–1716.
- (71) Talele, T. T. Natural-Products-Inspired Use of the Gem -Dimethyl Group in Medicinal Chemistry. *J. Med. Chem.* **2018**, *61* (6), 2166–2210.
- (72) Dubowchik, G. M.; Mosure, K.; Knipe, J. O.; Firestone, R. A. Cathepsin B-Sensitive Dipeptide Prodrugs. 2. Models of Anticancer Drugs Paclitaxel (Taxol®), Mitomycin C and Doxorubicin. *Bioorganic Med. Chem. Lett.* **1998**, *8* (23), 3347–3352.
- (73) Wang, Y.; Fan, S.; Zhong, W.; Zhou, X.; Li, S. Development and Properties of Valine-Alanine Based Antibody-Drug Conjugates with Monomethyl Auristatin E as the Potent Payload. *Int. J. Mol. Sci.* **2017**, *18* (9).

- (74) Jeffrey, S. C.; Nguyen, M. T.; Andreyka, J. B.; Meyer, D. L.; Doronina, S. O.; Senter, P. D. Dipeptide-Based Highly Potent Doxorubicin Antibody Conjugates. *Bioorganic Med. Chem. Lett.* **2006**, *16* (2), 358–362.
- (75) Tang, Y.; Tang, F.; Yang, Y.; Zhao, L.; Zhou, H.; Dong, J.; Huang, W. Real-Time Analysis on Drug-Antibody Ratio of Antibody-Drug Conjugates for Synthesis, Process Optimization, and Quality Control. *Sci. Rep.* **2017**, *7* (1), 2–11.
- (76) Nagornov, K. O.; Gasilova, N.; Kozhinov, A. N.; Virta, P.; Holm, P.; Menin, L.; Nesatyy, V. J.; Tsybin, Y. O. Drug-to-Antibody Ratio Estimation via Proteoform Peak Integration in the Analysis of Antibody-Oligonucleotide Conjugates with Orbitrap Fourier Transform Mass Spectrometry. *Anal. Chem.* **2021**, *93* (38), 12930–12937.
- (77) Graaf, M. De; Boven, E.; Scheeren, H. W.; Haisma, H. J.; Pinedo, H. M. Beta-Glucuronidase-Mediated Drug Release. *Curr. Pharm. Des.* **2002**, *8*, 1391–1403.
- (78) Brot, F. E.; Bell, C. E.; Sly, W. S. Purification and Properties of B-Glucuronidase from Human Placenta. *Biochemistry* **1978**, *17* (3), 385–391.
- (79) Tranoy-Opalinski, I.; Legigan, T.; Barat, R.; Clarhaut, J.; Thomas, M.; Renoux, B.; Papot, S. β -Glucuronidase-Responsive Prodrugs for Selective Cancer Chemotherapy: An Update. *Eur. J. Med. Chem.* **2014**, *74*, 302–313.
- (80) Jeffrey, S. C.; Andreyka, J. B.; Bernhardt, S. X.; Kissler, K. M.; Kline, T.; Lenox, J. S.; Moser, R. F.; Nguyen, M. T.; Okeley, N. M.; Stone, I. J.; Zhang, X.; Senter, P. D. Development and Properties of β -Glucuronide Linkers for Monoclonal Antibody-Drug Conjugates. *Bioconjug. Chem.* **2006**, *17* (3), 831–840.
- (81) Burke, P. J.; Senter, P. D.; Meyer, D. W.; Miyamoto, J. B.; Anderson, M.; Toki, B. E.; Manikumar, G.; Wani, M. C.; Kroll, D. J.; Jeffrey, S. C. Design, Synthesis, and Biological Evaluation of Antibody-Drug Conjugates Comprised of Potent Camptothecin Analogues. *Bioconjug. Chem.* **2009**, *20* (6), 1242–1250.
- (82) Jeffrey, S. C.; De Brabander, J.; Miyamoto, J.; Senter, P. D. Expanded Utility of the β -Glucuronide Linker: ADCs That Deliver Phenolic Cytotoxic Agents. *ACS Med. Chem. Lett.* **2010**, *1* (6), 277–280.
- (83) Joubert, N.; Beck, A.; Dumontet, C.; Denevault-sabourin, C. Antibody – Drug Conjugates : The Last Decade. *Pharmaceuticals* **2020**, *13*, 245.
- (84) Peters, C.; Brown, S. Antibody–Drug Conjugates as Novel Anti-Cancer Chemotherapeutics. *Biosci. Rep.* **2015**, *35* (e00225).
- (85) Beck, A.; Goetsch, L.; Dumontet, C.; Corvaia, N. Strategies and Challenges for

- the next Generation of Antibody–Drug Conjugates. *Nat. Publ. Gr.* **2017**.
- (86) Pettit, G. R.; Kamano, Y.; Herald, C. L.; Tuinman, A. A.; Boettner, F. E.; Kizu, H.; Schmidt, J. M.; Baczynskyj, L.; Tomer, K. B.; Bontems, R. J. The Isolation and Structure of a Remarkable Marine Animal Antineoplastic Constituent : Dolastatin 10. *J. Am. Chem. Soc.* **1987**, *109* (22), 6883–6885.
- (87) Bai, R.; Pettit, G. R.; Hamel, E. Binding of Dolastatin 10 to Tubulin at a Distinct Site for Peptide Antimitotic Agents Near the Exchangeable Nucleotide and Vinca Alkaloid Sites. *J. Biol. Chem.* **1990**, *265* (28), 17141–17149.
- (88) Cormier, A.; Marchand, M.; Ravelli, R. B. G.; Knossow, M. Structural Insight into the Inhibition of Tubulin by Vinca Domain Peptide Ligands. *EMBO Rep.* **2008**, *9* (11), 1101–1106.
- (89) Gao, G.; Wang, Y.; Hua, H.; Li, D.; Tang, C. Marine Antitumor Peptide Dolastatin 10: Biological Activity, Structural Modification and Synthetic Chemistry. *Mar. Drugs* **2021**, *19* (363).
- (90) Myyazaki, K.; Kobayashi, M.; Natsume, T.; Gondo, M.; Mikami, T.; Sakakibara, K.; Tsukagoshi, S. Synthesis and Antitumor Activity of Novel Dolastatin 10 Analogs. *Chem. Pharm. Bull.* **1995**, *43* (10), 1706–1718.
- (91) Doronina, S. O.; Toki, B. E.; Torgov, M. Y.; Mendelsohn, B. A.; Cervený, C. G.; Chace, D. F.; Deblanc, R. L.; Gearing, R. P.; Bovee, T. D.; Siegall, C. B.; Francisco, J. A.; Wahl, A. F.; Meyer, D. L.; Senter, P. D. Development of Potent Monoclonal Antibody Auristatin Conjugates for Cancer Therapy. *Nat. Biotechnol.* **2003**, *21* (7), 778–785.
- (92) Doronina, S. O.; Mendelsohn, B. A.; Bovee, T. D.; Cervený, C. G.; Alley, S. C.; Meyer, D. L.; Oflazoglu, E.; Toki, B. E.; Sanderson, R. J.; Zabinski, R. F.; Wahl, A. F.; Senter, P. D. Enhanced Activity of Monomethylauristatin F through Monoclonal Antibody Delivery : Effects of Linker Technology on Efficacy and Toxicity. *Bioconjug. Chem.* **2006**, *17* (1), 114–124.
- (93) Maderna, A.; Leverett, C. A. Recent Advances in the Development of New Auristatins : Structural Modifications and Application in Antibody Drug Conjugates. *Mol. Pharm.* **2015**, *12*, 1798–1812.
- (94) Maderna, A.; Doroski, M.; Subramanyam, C.; Porte, A.; Leverett, C.; Vetelino, B. C.; Cheng, Z.; Risley, H.; Parris, K.; Pandit, J.; Varghese, A. H.; Shanker, S.; Song, C.; Sukuru, S. C. K.; Farley, K. A.; Wagenaar, M. M.; Shapiro, M. J.; Musto, S.; Lam, M.; Loganzo, F.; Donnell, C. J. O. Discovery of Cytotoxic Dolastatin 10 Analogs with N-Terminal Modifications. *J. Med. Chem.* **2014**, *57* (24), 10527–

- 10543.
- (95) Senter, P. D.; Sievers, E. L. The Discovery and Development of Brentuximab Vedotin for Use in Relapsed Hodgkin Lymphoma and Systemic Anaplastic Large Cell Lymphoma. *Nat. Biotechnol.* **2012**, *30* (7), 631–637.
- (96) Li, F.; Emmerton, K. K.; Jonas, M.; Zhang, X.; Miyamoto, J. B.; Setter, J. R.; Nicholas, N. D.; Okeley, N. M.; Lyon, R. P.; Benjamin, D. R.; Law, C. Intracellular Released Payload In Fl Uences Potency and Bystander-Killing Effects of Antibody-Drug Conjugates in Preclinical Models. *Cancer Res.* **2016**, *76* (9), 2710–2719.
- (97) Kovtun, Y. V; Audette, C. A.; Ye, Y.; Xie, H.; Ruberti, M. F.; Phinney, S. J.; Leece, B. A.; Chittenden, T.; Bla, W. A.; Goldmacher, V. S. Antibody-Drug Conjugates Designed to Eradicate Tumors with Homogeneous and Heterogeneous Expression of the Target Antigen. *Cancer Res.* **2006**, *66* (6), 3214–3221.
- (98) Ogitani, Y.; Hagihara, K.; Oitate, M.; Naito, H.; Agatsuma, T. Bystander Killing Effect of DS-8201a , a Novel Anti-Human Epidermal Growth Factor Receptor 2 Antibody – Drug Conjugate , in Tumors with Human Epidermal Growth Factor Receptor 2 Heterogeneity. *Cancer Sci.* **2016**, *107* (7), 1039–1046.
- (99) Kupchan, M. S.; Sigel, C. W.; Guttman, L. J.; Restive, R. J.; Bryan, R. F. Maytansine, a Novel Antileukemic Ansa Macrolide from *Maytenus Ovatus*. *J. Am. Chem. Soc.* **1972**, *94* (4), 1354–1356.
- (100) Widdison, W. C.; Wilhelm, S. D.; Cavanagh, E. E.; Whiteman, K. R.; Leece, B. A.; Kovtun, Y.; Goldmacher, V. S.; Xie, H.; Steeves, R. M.; Lutz, R. J.; Zhao, R.; Wang, L.; Bla, W. A. Semisynthetic Maytansine Analogues for the Targeted Treatment of Cancer. *J. Med. Chem.* **2006**, *49* (14), 4392–4408.
- (101) Erickson, H. K.; Phillips, G. D. L.; Leipold, D. D.; Provenzano, C. A.; Mai, E.; Johnson, H. A.; Gunter, B.; Audette, C. A.; Gupta, M.; Pinkas, J.; Tibbitts, J. The Effect of Different Linkers on Target Cell Catabolism and Pharmacokinetics / Pharmacodynamics of Trastuzumab Maytansinoid Conjugates. *Mol. Cancer Ther.* **2012**, *11* (5), 1133–1142.
- (102) Moore, K. N.; Martin, L. P.; Malley, D. M. O.; Matulonis, U. A.; Konner, J. A.; Raymond, P.; Bauer, T. M.; Ruiz-soto, R.; Birrer, M. J. Safety and Activity of Mirvetuximab Soravtansine (IMGN853), a Folate Receptor Alpha–Targeting Antibody–Drug Conjugate, in Platinum-Resistant Ovarian, Fallopian Tube, or Primary Peritoneal Cancer : A Phase I Expansion Study. *J. Clin. Oncol.* **2022**, *35* (10), 1112–1118.

- (103) Socinski, M. A.; Kaye, F. J.; Spigel, D. R.; Kudrik, F. J.; Ponce, S.; Ellis, P. M.; Majem, M.; Lorigan, P.; Gandhi, L.; Gutierrez, M. E.; Nepert, D.; Corral, J.; Ares, L. P. Antibody-Drug Conjugate Lorvotuzumab Mertansine (IMG901) in Combination With Carboplatin / Etoposide in Small-Cell Lung Cancer Patients With Extensive-Stage Disease. *Clin. Lung Cancer* **2017**, *18* (1), 68-76.e2.
- (104) Ribrag, V.; Dupuis, J.; Tilly, H.; Morschhauser, F.; Laine, F.; Houot, R.; Haioun, C.; Copie, C.; Varga, A.; Lambert, J.; Hatteville, L.; Ziti-Ijjic, S.; Caron, A.; Payrard, S.; Coif, B. A Dose-Escalation Study of SAR3419 , an Anti-CD19 Antibody Maytansinoid Conjugate , Administered by Intravenous Infusion Once Weekly in Patients with Relapsed / Refractory B-Cell Non-Hodgkin Lymphoma. *Clin. Cancer Res.* **2013**, *20* (1), 213–220.
- (105) Trail, P. A.; Dubowchik, G. M.; Lowinger, T. B. Antibody Drug Conjugates for Treatment of Breast Cancer : Novel Targets and Diverse Approaches in ADC Design. *Pharmacol. Ther.* **2018**, *181*, 126–142.
- (106) Nejadmoghaddam, M.; Minai-tehrani, A.; Ghahremanzadeh, R. Antibody-Drug Conjugates : Possibilities and Challenges. *Avicenna J. Med. Biotechnol.* **2019**, *11* (1).
- (107) Maise, W. M.; Lechevalier, M. P.; Lechevalier, H. A.; Korshalla, J.; Kuck, N.; Fantini, A.; Wildey, M. J.; Greenstein, T.; Greenstein, M. CALICHEAMICINS, A NOVEL FAMILY OF ANTITUMOR ANTIBIOTICS: TAXONOMY, FERMENTATION AND BIOLOGICAL PROPERTIES. *J. Antibiot. (Tokyo).* **1989**, *42* (4), 558–563.
- (108) Choy, N.; Blanco, B.; Wen, J.; Krishan, A.; Russell, K. C. Photochemical and Thermal Bergman Cyclization of a Pyrimidine Enediynol and Enediynone. *Org. Lett.* **2000**, *2* (24), 3761–3764.
- (109) Jones, R. R.; Bergman, R. G. P-Benzyne. Generation as an Intermediate in a Thermal Isomerization Reaction and Trapping Evidence for the 1,4-Benzenediyl Structure. *J. Am. Chem. Soc.* **1972**, *94* (2), 660–661.
- (110) Smith, A. L.; Nicolaou, K. C. The Enediyne Antibiotics. *J. Med. Chem.* **1996**, *39* (11), 2103–2117.
- (111) Li, F.; Jiang, T.; Li, Q.; Ling, X. Camptothecin (CPT) and Its Derivatives Are Known to Target Topoisomerase I (Top1) as Their Mechanism of Action : Did We Miss Something in CPT Analogue Molecular Targets for Treating Human Disease Such as Cancer ? *Am J Cancer Res* **2017**, *7* (12), 2350–2394.
- (112) Wani, M. C.; Nicholas, A. W.; Wall, M. E. Plant Antitumor Agents. Resolution of a Key Tricyclic Synthone, 5'(R5)-1,5-Dioxo-5'-Ethyl-5'-Hydroxy-2' H,5' H,6' H-6'-

- Oxopyrano[3',4'-f]-Tetrahydro- Indolizine: Total Synthesis and Antitumor Activity of 20(S)- and 20(R)-Camptothecin. *J. Med. Chem.* **1987**, *30* (12), 2317–2319.
- (113) Nakada, T.; Masuda, T.; Naito, H.; Yoshida, M.; Ashida, S.; Morita, K.; Miyazaki, H.; Kasuya, Y.; Ogitani, Y.; Yamaguchi, J.; Abe, Y.; Honda, T. Bioorganic & Medicinal Chemistry Letters Novel Antibody Drug Conjugates Containing Exatecan Derivative-Based Cytotoxic Payloads. *Bioorg. Med. Chem. Lett.* **2016**, *26* (6), 1542–1545.
- (114) Ogitani, Y.; Aida, T.; Hagihara, K.; Yamaguchi, J.; Ishii, C.; Harada, N.; Soma, M.; Okamoto, H.; Oitate, M.; Arakawa, S.; Hirai, T.; Atsumi, R.; Nakada, T.; Hayakawa, I.; Abe, Y.; Agatsuma, T. DS-8201a , A Novel HER2-Targeting ADC with a Novel DNA Topoisomerase I Inhibitor , Demonstrates a Promising Antitumor Ef Fi Cacy with Differentiation from T-DM1. *Clin. Cancer Res.* **2016**, *22* (20), 5097–5108.
- (115) Nakada, T.; Sugihara, K.; Jikoh, T.; Abe, Y.; Agatsuma, T. Drug Discovery : Recent Progress and the Future The Latest Research and Development into the Antibody – Drug for HER2 Cancer Therapy. *Chem. Pharm. Bull.* **2019**, *67* (3), 173–185.
- (116) Bardia, A.; Mayer, I. A.; Diamond, J. R.; Moroosse, R. L.; Isakoff, S. J.; Alexander, N.; Shah, N. C.; Shaughnessy, J. O.; Kalinsky, K.; Guarino, M.; Abramson, V.; Tolaney, S. M.; Berlin, J.; Messersmith, W. A.; Ocean, A. J.; Wegener, W. A.; Maliakal, P.; Sharkey, R. M.; Govindan, S. V; Goldenberg, D. M.; Vahdat, L. T. Efficacy and Safety of Anti-Trop-2 Antibody Drug Conjugate Sacituzumab Govitecan (IMMU-132) in Heavily Pretreated Patients With Metastatic Triple-Negative Breast Cancer. *J. Clin. Oncol.* **2017**, *35* (19), 2141–2148.
- (117) Zhao, H.; Lee, C.; Sai, P.; Choe, Y. H.; Boro, M.; Pendri, A.; Guan, S.; Greenwald, R. B. 20- O -Acylcamptothecin Derivatives : Evidence for Lactone Stabilization. *J. Org. Chem.* **2000**, *65* (15), 4601–4606.
- (118) Cardillo, T. M.; Govindan, S. V; Sharkey, R. M.; Trisal, P.; Arrojo, R.; Liu, D.; Rossi, E. A.; Chang, C.; Goldenberg, D. M. Sacituzumab Govitecan (IMMU-132), an Anti-Trop-2/SN-38 Antibody – Drug Conjugate: Characterization and E Ffi Cacy in Pancreatic, Gastric, and Other Cancers. *Bioconjug. Chem.* **2015**, *26*, 919–931.
- (119) Goldenberg, D. M.; Cardillo, T. M.; Govindan, S. V; Edmund, A.; Sharkey, R. M. Trop-2 Is a Novel Target for Solid Cancer Therapy with Sacituzumab Govitecan (IMMU-132), an Antibody-Drug Conjugate (ADC). *Oncotarget* **2015**, *6* (26), 22496–22512.

- (120) Leimgruber, W.; Stefanovic, V.; Schenker, F.; Karr, A.; Berger, J. Isolation and Characterization of Anthramycin, a New Antitumor Antibiotic. *J. Am. Chem. Soc.* **1965**, *87* (24), 5791–5793.
- (121) Thurston, D. E.; Bose, D. S. Synthesis of DNA-Interactive Pyrrolo[2,1-c][1,4]Benzodiazepines. *Chem. Rev.* **1994**, *94*, 433–465.
- (122) Sutherland, M. S. K.; Walter, R. B.; Jeffrey, S. C.; Burke, P. J.; Yu, C.; Kostner, H.; Stone, I.; Ryan, M. C.; Sussman, D.; Lyon, R. P.; Zeng, W.; Harrington, K. H.; Klussman, K.; Westendorf, L.; Meyer, D.; Bernstein, I. D.; Senter, P. D.; Benjamin, D. R.; Drachman, J. G.; Mcearchern, J. A. SGN-CD33A : A Novel CD33-Targeting Antibody – Drug Conjugate Using a Pyrrolobenzodiazepine Dimer Is Active in Models of Drug-Resistant AML. *Blood* **2013**, *122* (8), 1455–1463.
- (123) Gregson, S. J.; Masterson, L. A.; Wei, B.; Pillow, T. H.; Spencer, S. D.; Kang, G.; Yu, S.; Raab, H.; Li, G.; Phillips, G. D. L.; Gunzner-toste, J.; Sa, B. S.; Ohri, R.; Darwish, M.; Kozak, K. R.; Cruz-chuh, J.; Polson, A.; Flygare, J. A.; Howard, P. W. Pyrrolobenzodiazepine Dimer Antibody – Drug Conjugates: Synthesis and Evaluation of Noncleavable Drug-Linkers. *J. Med. Chem.* **2017**, *60*, 9490–9507.
- (124) Gymnopoulos, M.; Betancourt, O.; Blot, V.; Fujita, R.; Galvan, D.; Lieu, V.; Nguyen, S.; Snedden, J.; Stewart, C.; Villicana, J.; Wojciak, J.; Wong, E.; Pardo, R.; Patel, N.; Hooge, F. D.; Vijayakrishnan, B.; Barry, C.; Hartley, J. A.; Howard, P. W.; Newman, R.; Coronella, J. TR1801-ADC : A Highly Potent CMet Antibody – Drug Conjugate with High Activity in Patient-Derived Xenograft Models of Solid Tumors. *Mol. Oncol.* **2020**, *14*, 54–68.
- (125) Miller, M. L.; Fishkin, N. E.; Li, W.; Whiteman, K. R.; Kovtun, Y.; Reid, E. E.; Archer, K. E.; Maloney, E. K.; Audette, C. A.; Mayo, M. F.; Wilhelm, A.; Modafferi, H. A.; Singh, R.; Pinkas, J.; Goldmacher, V.; Lambert, J. M.; Chari, R. V. J. A New Class of Antibody–Drug Conjugates with Potent DNA Alkylating Activity. *Mol. Cancer Ther.* **2016**, *15* (8), 1870–1878.
- (126) Morgensztern, D.; Besse, B.; Greillier, L.; Santana-davila, R.; Ready, N.; Hann, C. L.; Glisson, B. S.; Farago, A. F.; Dowlati, A. Efficacy and Safety of Rovalpituzumab Tesirine in Third-Line and Beyond Patients with DLL3-Expressing, Relapsed / Refractory Small-Cell Lung Cancer : Results From the Phase II TRINITY Study. *Clin. Cancer Res.* **2019**, *25* (23), 6958–6966.
- (127) Kahl, B. S.; Hamadani, M.; Radford, J.; Carlo-stella, C.; Caimi, P.; Reid, E.; Feingold, J. M.; Ardesna, K. M.; Solh, M.; Heffner, L. T.; Ungar, D.; He, S.; Boni, J.; Havenith, K.; Connor, O. A. O. A Phase I Study of ADCT-402 (Loncastuximab Tesirine), a Novel Pyrrolobenzodiazepine-Based Antibody – Drug Conjugate , in Relapsed / Refractory B-Cell Non-Hodgkin Lymphoma. *Clin. Cancer Res.*

- 2020**, 25 (23), 6986–6994.
- (128) Boger, D. L.; Ishizaki, T.; Wysocki, R. J.; Munklc, S. A. Total Synthesis and Evaluation of (±)-N-(Te/"f-Butyloxycarbonyl)-CBI, (±)-CBI-CDPI,, and (±)-CBI-CDPI2: CC-1065 Functional Agents Incorporating the Equivalent 1,2,9,9a-Tetrahydrocycloprop[1,2-c]Benz[1,2-e]Indol-4- One (CBI) Left-Hand Subuni. *J. Am. Chem. Soc.* **1989**, 111, 6461–6463.
- (129) Spijker, H. J.; Groot, F. M. H. De; Lee, M. M. C. Van Der; Ubink, R.; Dobbelsteen, D. J. Van Den; Egging, D. F.; Dokter, W. H. A.; Verheijden, G. F. M.; Lemmens, J. M.; Timmers, C. M.; Beusker, P. H. Design, Synthesis, and Evaluation of Linker-Duocarmycin Payloads: Toward Selection of HER2-Targeting Antibody – Drug Conjugate SYD985. *Mol. Pharm.* **2015**, 12, 1813–1835.
- (130) Nadal-serrano, M.; Morancho, B.; Escriv, S.; Bernad, C.; Luque, A.; Escorihuela, M.; Peg, V.; Dijcks, F. A.; Dokter, W. H. A.; Cort, J.; Saura, C. The Second Generation Antibody-Drug Conjugate SYD985 Overcomes Resistances to T-DM1. *Cancers (Basel)*. **2020**, 12, 670.
- (131) Lee, M. M. C. Van Der; Groothuis, P. G.; Ubink, R.; Van, M. A. J.; Beusker, P. H.; Goedings, P.; Verheijden, G. F. M.; Lemmens, J. M.; Timmers, M.; Dokter, W. H. A. The Preclinical Pro Fi Le of the Duocarmycin-Based HER2-Targeting ADC SYD985 Predicts for Clinical Bene Fi t in Low HER2-Expressing Breast Cancers. *Mol. Cancer Ther.* **2015**, 14 (3), 692–703.
- (132) Garcia, J.; Costa, V. M.; Carvalho, A.; Baptista, P.; de Pinho, P. G.; de Lourdes Bastos, M.; Carvalho, F. Amanita Phalloides Poisoning: Mechanisms of Toxicity and Treatment. *Food Chem. Toxicol.* **2015**, 86, 41–55.
- (133) Letschert, K.; Faulstich, H.; Keller, D.; Keppler, D. Molecular Characterization and Inhibition of Amanitin Uptake into Human Hepatocytes. *Toxicol. Sci.* **2006**, 91 (1), 140–149.
- (134) Lutz, C.; Simon, W.; Werner-Simon, S.; Pahl, A.; Müller, C. Total Synthesis of α - and β -Amanitin. *Angew. Chemie - Int. Ed.* **2020**, 59 (28), 11390–11393.
- (135) Matinkhoo, K.; Pryyma, A.; Todorovic, M.; Patrick, B. O.; Perrin, D. M. Synthesis of the Death-Cap Mushroom Toxin α -Amanitin. *J. Am. Chem. Soc.* **2018**, 140 (21), 6513–6517.
- (136) Danielczyk, A.; Stahn, R.; Faulstich, D.; Löffler, A.; Märten, A.; Karsten, U.; Goletz, S. PankoMab: A Potent New Generation Anti-Tumour MUC1 Antibody. *Cancer Immunol. Immunother.* **2006**, 55 (11), 1337–1347.

- (137) Moldenhauer, G.; Salnikov, A. V.; Lüttgau, S.; Herr, I.; Anderl, J.; Faulstich, H. Therapeutic Potential of Amanitin-Conjugated Anti-Epithelial Cell Adhesion Molecule Monoclonal Antibody against Pancreatic Carcinoma. *J. Natl. Cancer Inst.* **2012**, *104* (8), 622–634.
- (138) Pahl, A.; Lutz, C.; Hechler, T. Amanitins and Their Development as a Payload for Antibody-Drug Conjugates. *Drug Discov. Today Technol.* **2018**, *30*, 85–89.
- (139) Neumann, C. S.; Olivas, K. C.; Anderson, M. E.; Cochran, J. H.; Jin, S.; Li, F.; Loftus, L. V.; Meyer, D. W.; Neale, J.; Nix, J. C.; Pittman, P. G.; Simmons, J. K.; Ulrich, M. L.; Waight, A. B.; Wong, A.; Zaval, M. C.; Zeng, W.; Lyon, R. P.; Senter, P. D. Targeted Delivery of Cytotoxic NAMPT Inhibitors Using Antibody-Drug Conjugates. *Mol. Cancer Ther.* **2018**, *17* (12), 2633–2642.
- (140) Karpov, A. S.; Abrams, T.; Clark, S.; Raikar, A.; D'Alessio, J. A.; Dillon, M. P.; Gesner, T. G.; Jones, D.; Lacaud, M.; Mallet, W.; Martyniuk, P.; Meredith, E.; Mohseni, M.; Nieto-Oberhuber, C. M.; Palacios, D.; Perruccio, F.; Piizzi, G.; Zurini, M.; Bialucha, C. U. Nicotinamide Phosphoribosyltransferase Inhibitor as a Novel Payload for Antibody-Drug Conjugates. *ACS Med. Chem. Lett.* **2018**, *9* (8), 838–842.
- (141) Böhnke, N.; Berger, M.; Griebenow, N.; Rottmann, A.; Erkelenz, M.; Hammer, S.; Berndt, S.; Günther, J.; Wengner, A. M.; Stelte-ludwig, B.; Mahlert, C.; Greven, S.; Dietz, L.; Jörißen, H.; Barak, N.; Bömer, U.; Hillig, R. C.; Eberspaecher, U.; Weiske, J.; Giese, A.; Mumberg, D.; Nising, C. F.; Weinmann, H.; Sommer, A. A Novel NAMPT Inhibitor-Based Antibody – Drug Conjugate Payload Class for Cancer Therapy. *Bioconjug. Chem.* **2022**.
- (142) Neumann, C. S.; Olivas, K. Targeted Delivery of Nicotinamide Adenine Dinucleotide Salvage Pathway Inhibitors. WO 2018/075600 A1, 2018.
- (143) BOHNKE, N.; GRIEBENOW, N.; SOMMER, A.; HAMMER, S.; BERNDT, S.; STELTE-LUDWIG, B.; BEIER, R.; MAHLERT, C.; GREVEN, S.; GIESE, A.; GLTNHER, J.; BARAK, N.; BOMER, U.; DIETZ, L.; JORISSEN, H.; ERKELENZ, M.; ROTTMANN, A.; WENGER, Antje, M.; FERNANDEZ-MON- TALVAN, Amaury, E. Antibody Drug Conjugates (ADCS) with NAMPT Inhibitors. WO 2021/013693 A1, 2021.
- (144) Ravasco, J. M. J. M.; Faustino, H.; Trindade, A.; Gois, P. M. P. Bioconjugation with Maleimides: A Useful Tool for Chemical Biology. *Chem. - A Eur. J.* **2019**, *25* (1), 43–59.
- (145) Climent, T.; Gonzalez-Luque, R.; Merchan, M. Theoretical Analysis of the Excited States in Maleimide. *J. Phys. Chem. A* **2003**, *107*, 6995–7003.

- (146) Northrop, B. H.; Frayne, S. H.; Choudhary, U. Thiol-Maleimide “Click” Chemistry: Evaluating the Influence of Solvent, Initiator, and Thiol on the Reaction Mechanism, Kinetics, and Selectivity. *Polym. Chem.* **2015**, *6*, 3415–3430.
- (147) Koniev, O.; Wagner, A. Developments and Recent Advancements in the Field of Endogenous Amino Acid Selective Bond. *Chem. Soc. Rev.* **2015**, *44*, 5495–5551.
- (148) Frayne, S. H.; Murthy, R. R.; Northrop, B. H. Investigation and Demonstration of Catalyst/Initiator-Driven Selectivity in Thiol-Michael Reactions. *J. Org. Chem.* **2017**, *82*, 7946–7956.
- (149) Tumey, L. N.; Charati, M.; He, T.; Sousa, E.; Ma, D.; Han, X.; Clark, T.; Casavant, J.; Loganzo, F.; Barletta, F.; Lucas, J.; Graziani, E. I. Mild Method for Succinimide Hydrolysis on ADCs: Impact on ADC Potency, Stability, Exposure, and Efficacy. *Bioconjug. Chem.* **2014**, *25*, 1871–1880.
- (150) Cal, P. M. S. D.; Bernardes, G. J. L.; Gois, P. M. P. Cysteine-Selective Reactions for Antibody Conjugation. *Angew. Chemie - Int. Ed.* **2014**, *53*, 10585–10587.
- (151) Christie, R. J.; Fleming, R.; Bezabeh, B.; Woods, R.; Mao, S.; Harper, J.; Joseph, A.; Wang, Q.; Xu, Z. Q.; Wu, H.; Gao, C.; Dimasi, N. Stabilization of Cysteine-Linked Antibody Drug Conjugates with N-Aryl Maleimides. *J. Control. Release* **2015**, *220*, 660–670.
- (152) Lyon, R. P.; Setter, J. R.; Bovee, T. D.; Doronina, S. O.; Hunter, J. H.; Anderson, M. E.; Balasubramanian, C. L.; Duniho, S. M.; Leiske, C. I.; Li, F.; Senter, P. D. Self-Hydrolyzing Maleimides Improve the Stability and Pharmacological Properties of Antibody-Drug Conjugates. *Nat. Biotechnol.* **2014**, *32* (10), 1059–1062.
- (153) Kislukhin, A. A.; Higginson, C. J.; Hong, V. P.; Finn, M. G. Degradable Conjugates from Oxanorbornadiene Reagents. *J. Am. Chem. Soc.* **2012**, *134* (14), 6491–6497.
- (154) Higginson, C. J.; Eno, M. R.; Khan, S.; Cameron, M. D.; Finn, M. G. Albumin-Oxanorbornadiene Conjugates Formed Ex Vivo for the Extended Circulation of Hydrophilic Cargo. *ACS Chem. Biol.* **2016**.
- (155) Gil De Montes, E.; Jiménez-Moreno, E.; Oliveira, B. L.; Navo, C. D.; Cal, P. M. S. D.; Jim, G.; Robina, I.; Moreno-vargas, A. J.; Bernardes, G. J. L. Azabicyclic Vinyl Sulfones for Residue-Specific Dual Protein Labelling. *Chem. Sci.* **2019**, *10*, 4515–4522.

- (156) Stewart, J. A.; Piligian, B. F.; Rundell, S. R.; Swarts, B. M. A Trifunctional Cyclooctyne for Modifying Azide- Labeled Biomolecules with Photocrosslinking and Affinity Tags. *Chem. Commun.* **2015**, *51*, 17600–17603.
- (157) Gil de Montes, E.; Istrate, A.; Navo, C. D.; Jiménez-Moreno, E.; Hoyt, E. A.; Corzana, F.; Robina, I.; Jiménez-Osés, G.; Moreno-Vargas, A. J.; Bernardes, G. J. L. Stable Pyrrole-Linked Bioconjugates through Tetrazine-Triggered Azanorbornadiene Fragmentation. *Angew. Chemie* **2020**, *132* (15), 6255–6259.
- (158) Rappoport, Z. Nucleophilic Vinylic Substitution. A Single- or a Multi-Step Process? *Acc. Chem. Res.* **1981**, *14*, 7–15.
- (159) Chiba, S.; Ando, K.; Narasaka, K. Concerted Nucleophilic Substitution Reactions at Vinylic Carbons. *Synlett* **2009**, *16*, 2549–2564.
- (160) Bernasconi, C. F.; Rappoport, Z. Recent Advances in Our Mechanistic Understanding of SNV Reactions. *Acc. Chem. Res.* **2009**, *42* (8), 993–1003.
- (161) Zong, Y.; Ma, Q.; Tsui, G. C. Nucleophilic Vinylic Substitution (SNV) of Trisubstituted Monofluoroalkenes for the Synthesis of Stereodefined Trisubstituted Alkenes and Divinyl Ethers. *Org. Lett.* **2021**, *23*, 6169–6173.
- (162) Nandi, C. G.; Arvidsson, P. I. Sulfonylimidamides : Synthesis and Applications in Preparative Organic Chemistry. *Adv. Synth. Catal.* **2018**, *360*, 2976–3001.
- (163) Chen, Z.; Trudell, M. L. A SIMPLIFIED METHOD FOR THE PREPARATION OF ETHYNYL P-TOLYL SULFONE AND ETHYNYL PHENYL SULFONE. *Synth. Commun.* **1994**, *24* (21), 3149–3155.
- (164) Zhang, C.; Ballay II, C. J.; Trudell, M. L. 2-Bromoethynyl Aryl Sulfones as Versatile Dienophiles: A Formal Synthesis of Epibatidine. *J. Chem. Soc. - Perkin Trans. 1* **1999**, 675–676.
- (165) Klika Škopić, M.; Willems, S.; Wagner, B.; Schieven, J.; Krause, N.; Brunschweiler, A. Exploration of a Au(i)-Mediated Three-Component Reaction for the Synthesis of DNA-Tagged Highly Substituted Spiroheterocycles. *Org. Biomol. Chem.* **2017**, *15* (40), 8648–8654.
- (166) Kang, J. H.; Yu, S. W.; Lee, H. Y.; Mi An, K.; Cho, H. A NEW PEPTIDE DEFORMYLASE INHIBITOR COMPOUND AND MANUFACTURING PROCESS THEREOF. US20100168421A1, 2010.
- (167) Atkinson, B. N.; Chhatwal, A. R.; Lomax, H. V.; Walton, J. W.; Williams, J. M. J. Transamidation of Primary Amides with Amines Catalyzed by Zirconocene Dichloride. *Chem. Commun.* **2012**, *48* (95), 11626–11628.

-
- (168) Sociali, G.; Grozio, A.; Caffa, I.; Schuster, S.; Becherini, P.; Damonte, P.; Sturla, L.; Fresia, C.; Passalacqua, M.; Mazzola, F.; Raffaelli, N.; Garten, A.; Kiess, W.; Cea, M.; Nencioni, A.; Bruzzone, S. SIRT6 Deacetylase Activity Regulates NAMPT Activity and NAD(P)(H) Pools in Cancer Cells. *FASEB J.* **2019**, *33*, 3704–3717.
- (169) Zhang, R.; Qin, Y.; Lv, X.; Wang, P.; Xu, T.; Zhang, L.; Miao, C. A Fluorometric Assay for High-Throughput Screening Targeting Nicotinamide Phosphoribosyltransferase. *Anal. Biochem.* **2011**, *412*, 18–25.
- (170) Rongvaux, A.; Andris, F.; Gool, V.; Leo, O. Reconstructing Eukaryotic NAD Metabolism. *BioEssays* **2003**, *25*, 683–690.